Modelling of hydrophilic pervaporation systems

Cilian A. Ó Súilleabháin
B.Eng. (Chem), M.A., Chartered Engineer

Dissertation Submitted for the Award of Doctor of Philosophy

School of Biotechnology
Dublin City University

Supervisors:
Dr. Greg Foley
Dr. Jenny Lawler
Dr. Ciarán Fagan

September 2019

I hereby certify that this material, which I now submit for assessment on the programme of study leading to the award of Doctor of Philosophy is entirely my own work, and that I have exercised reasonable care to ensure that the work is original, and does not to the best of my knowledge breach any law of copyright, and has not been taken from the work of others save and to the extent that such work has been cited and acknowledged within the text of my work.

Signed:  11 September 2019 ID No.: 14211032

Acknowledgements

I wish to thank Dr. Greg Foley for accepting me as a PhD. Student. He has provided positive and flexible support throughout the period of my research.

Thanks also to my employer, Cork Institute of Technology for funding the research and reducing my teaching workload for a period of four years so as to facilitate the research.

Finally, thanks to Catherine for her patience and support over the past years.

Publications and Presentations

Peer reviewed journal publications:

Ó Súilleabháin, C., Foley, G., (2015) 'Engineering of pervaporation systems: Exact and approximate expressions for the average flux during alcohol dehydration by single-pass pervaporation', *Sep. Purif. Technol.* 152, pp. 160–163. doi: 10.1016/j.seppur.2015.08.021

Ó Súilleabháin, C., Foley, G., (2018) 'A simple model for pervaporation design' *Chem. Eng. Ed*., accepted for publication.

Oral presentations at conferences:

Ó Súilleabháin, C., Foley, G. (2016) '*Engineering of pervaporation systems: modelling of dehydration modules, including recycles*', Advanced Membranes VII, Cork, Ireland 16th September.

Ó Súilleabháin, C., Foley, G. (2017) '*Engineering of pervaporation systems: modelling of dehydration modules, including recycles*' 5th Intl. Scientific Conference on Pervaporation, Vapor Permeation and Membrane Distillation, Torun, Poland, 22nd June.

Ó Súilleabháin, C., Foley, G. (2019) '*A novel single pervaporation metric: the pervaporation membrane index*' 6th Intl. Scientific Conference on Pervaporation, Vapor Permeation and Membrane Distillation, Torun, Poland, 14-17th May.

Poster presentation

Ó Súilleabháin, C., Foley, G., (2014) '*Activation energy for permeation – feasibility for industrial pervaporation*' 4th Intl. Scientific Conference on Pervaporation, Vapor Permeation and Membrane Distillation, Torun, Poland, 21st June.

Table of Contents

List of Abbreviations

ABE	Acetone-butanol-ethanol
CFD	Computational fluid dynamics
E_j	Apparent activation energy of pervaporation
EtOH	Ethanol
IPA	Isopropanol
MFLI	Membrane flash index
NF	Nano filtration
PMI	Pervaporation membrane index
PMDS	Polydimethylsiloxane
PAN	Polyacrylo-nitrile
PSI	Pervaporation separation index
PVA	Polyvinyl alcohol
Re	Reynolds number
RO	Reverse osmosis
THF	Tetrahydrofuran
UF	Ultrafiltration
US EPA	United States Environmental Protection Agency
VLE	Vapour liquid equilibrium

List of Tables

List of figures

Abstract

Cilian A. Ó Súilleabháin
Modelling of hydrophilic pervaporation systems

This computational study focuses on the application of pervaporation for the removal of low concentrations of water from organic solvents. A classic chemical engineering approach is employed using mass and energy balances combined with an empirical expression for flux, to address a number of important problems in the area of pervaporation design and analysis.

For both composition-independent and composition-dependent fluxes, expressions are obtained for the ideal average flux, and hence the ideal membrane area, of single-stage adiabatic pervaporation membrane modules. These expressions which take the form of integrals are then approximated by easy-to-use shortcut methods suitable for rapid conceptual design calculations. Ideal isothermal pervaporation modules are analysed. The actual module efficiency of an industrial-scale pervaporation system is determined.

The range of economically feasible values of the activation energy is established. This allows the full range of typical industrial operating conditions to be determined thereby allowing validation of shortcut methods.

Novel equations are developed for determining feed flowrate and composition as functions of recycle. The optimisation of multi-stage systems is addressed and isothermal pervaporation, a limiting case of multi-stage adiabatic operation, is modelled.

Permeate composition is assumed to be constant within a module: this assumption is usually only valid for water concentrations greater than 2 wt%. The models developed assume ideal behaviour and do not allow for concentration polarisation, temperature polarisation or poor flow distribution.

Novel performance metrics for pervaporation modules are proposed. The performance of industrial-scale systems is analysed. Finally, a novel metric, the Pervaporation Membrane Index (PMI) is proposed: this metric gives appropriate weighting to flux and separation.

Areas requiring further research are identified including the analysis of industrial systems, the use of multiple types of membrane within a single system and optimisation of multi-stage pervaporation systems.

Nomenclature

A = membrane area (m^2)

A_{total} = the total membrane area required for a separation

c_p = specific heat of a liquid (kJ/kg.K)

c_{po} = specific heat of the liquid outlet stream (kJ/kg.K)

c_{ps} = specific heat of the liquid supply stream (kJ/kg.K)

C = the ratio of the recycle and outlet stream mass flowrates (-)

D_i = the membrane diffusion coefficient of component i (cm^2/s)

EF = enrichment factor (-)

Ei = the exponential integral

E_j = the apparent activation energy of the permeation flux (kJ/kmol)

E_j^{max} = the maximum feasible value of the activation energy (kJ/kmol)

h_o = the enthalpy per unit mass of the outlet stream (kJ/kg)

h_s = the enthalpy per unit mass of supply stream (kJ/kg)

h_v = the local enthalpy per unit mass of vapour (kJ/kg)

$_i$ = the preferentially permeating component (-)

$_j$ = the less preferentially permeating component (-)

j_i = molar flux of component i (cm^3(STP)/cm^2.s)

J = total permeate flux (kg/h.m^2)

J_{av} = the average flux within a module (kg/h.m^2)

J_f = the flux at the feed temperature (kg/h.m^2)

J_o = the maximum possible permeate flux for a given liquid composition (i.e. the flux as $T \rightarrow \infty$), (kg/h.m^2)

J_r = the flux at the retenate concentration and temperature (kg/h.m^2)

J_{reheat} = the flux at the retentate concentration and the feed temperature (kg/h.m^2)

K_i^G = the sorption coefficient of component i (cm^3(STP)/cm^3.s)

l = membrane thickness (cm)

M = the "Pervaporation Separation Modulus" (-)

$MFLI$ = the "membrane flash index" is the permeate purity obtained with pervaporation divided by that for vapour-liquid equilibrium (-)

$\dot{m}$ = the local mass flowrate of the liquid (kg/h)

m_f = initial mass of liquid in a batch system (kg)

$\dot{m}_f$ = the mass flowrate of the feed stream (kg/h)

$\dot{m}_o$ = the mass flowrate of the outlet stream leaving a recycle system (kg/h)

m_p = the mass of permeate in a batch system (kg)

$\dot{m}_p$ = the mass flowrate of permeate through the membrane (kg/h)

$\dot{m}_r$ = the mass flowrate of the liquid retentate (kg/h)

$\dot{m}_s$ = the mass flowrate of the liquid supply stream entering a recycle system (kg/h)

P_i^G = the membrane permeability of component *i* (Barrer)

P_i^G/l = permeance of component *i* (Barrer/cm)

p_{io} = partial pressure of component *i* on the feed side of the membrane (cmHg)

p_{il} = partial pressure of component *i* on permeate side of the membrane (cmHg)

PMI = the "Pervaporation Membrane Index" (kg/h.m^2)

PMI_T = the "Pervaporation Membrane Index" at temperature *T* (kg/h.m^2)

PSI = pervaporation separation index (kg/h.m^2)

Δq_{cool} = the power consumed by the cooling system (kJ/s)

Δq_{energy} = the power consumed by a pervaporation system (kJ/s)

Δq_{heat} = the power consumed by the heating system (kJ/s)

$\Delta q_{heat\ loss}$ = the heat loses from a pervaporation system (kJ/s)

Δq_{pump} = the power consumed by the pump (kJ/s)

$\Delta q_{recoverey}$ = the power recovered through use of a pre-heater (kJ/s)

Δq_s = the power required to bring the supply stream to the feed temperature (kJ/s)

Δq_{vac} = the power consumed by the vacuum system (kJ/s)

x_i = the mass fraction of component *i* in the local liquid *i* (-)

x_{ir} = the mass fraction of component *i* in liquid retentate (-)

R = the universal gas constant (kJ/kmol.K)

s_i = the mass fraction of component *i* in the supply stream to a system (-)

T = temperature (K)

T_f = the temperature of the feed stream (K)

T_r = the temperature of the retentate stream (K)

T_s = the temperature of the supply stream (K)

ΔT = the difference in temperature between the feed and the retentate (K)

t = the time taken to undertake a batch pervaporation (h)

x_{azeo} = the mass fraction at the azeotropic composition (-)

x_i = the mass fraction of component *i* in the local liquid (-)

y_i = the mass fraction of component *i* in the permeate (-)

y^D_{VLE} = the permeate mass fraction obtained with flash distillation (-)

z_i = the fraction of the feed comprised of component (-)

α_{ij} = selectivity (-)

β_{ij} = the separation factor (-)

β_{evap} = the evaporation separation factor (-)

β_{mem} = the membrane separation factor (-)

γ = the Euler-Mascheroni constant (-)

η_{elec} = the electrical energy consumed per unit mass of permeate (kJ/kg)

η_{energy} = the energy consumed per unit mass of retentate (kJ/kg)

η_{heat} = the heating energy consumed per unit mass of permeate (kJ/kg)

$\eta_{heat\ loss}$ = the heat losses per unit mass of energy consumed (-)

$\eta_{heat\ recovery}$ = the fraction of the enthalpy of the retentate stream that is recovered (-)

$\eta_{isothermal}$ = the area of an ideal isothermal module divided by the area of an ideal adiabatic module (-)

η_{module} = the average flux of a module divided by the average flux for an ideal module for a given separation (-)

η_{perm} = the energy consumed per unit mass of permeate (kJ/kg)

Introduction

Pervaporation is a process for the separation of liquid mixtures. Hot liquid feed enters a membrane module, permeate vaporises and passes through the membrane and the remaining solvent-rich liquid leaves as retentate. Most industrial systems operate adiabatically; the latent heat of vaporisation causes the liquid to cool as it passes through the module, leading to a reduction in the local flux. The most common industrial applications are the separation of the aqueous azeotropes of ethanol and isopropanol. This study focuses on hydrophilic pervaporation, i.e. the application of pervaporation for the removal of low concentrations of water from organic solvents.

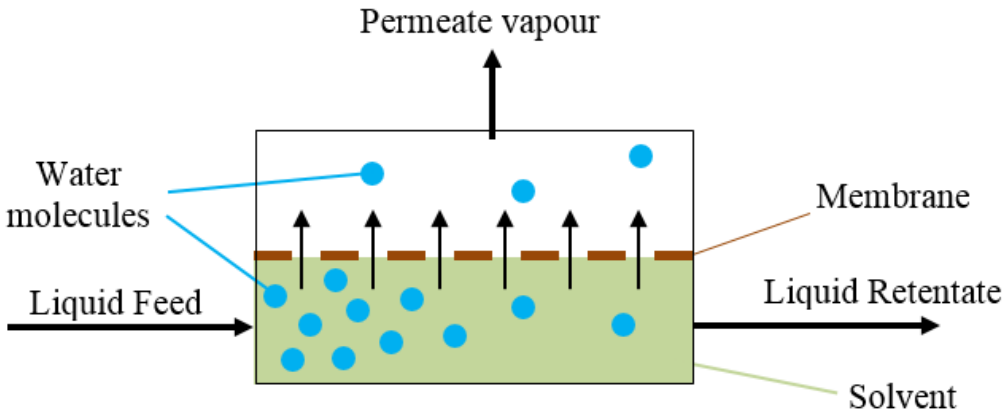

Figure 1. Schematic diagram of a pervaporation module

There is a large body of research regarding the precise mechanisms of vapour transport through pervaporation membranes. However, there has been less emphasis on chemical engineering analyses for the predictio1.n of the performance of pervaporation modules (Bausa and Marquadt, 2000; Marriott and Sørenson, 2003a; Marriott and Sørenson, 2003b; Villaleunga and Cohen, 2005; Sosa and Espinosa, 2011; Valentinyi and Mizesy, 2014; Raoufi *et al*., 2018).

Vente (2010) cites "predictability" as a barrier to the adoption of pervaporation technology by industry. This can be addressed by the development of short-cut methods for the calculation of membrane area and pervaporation system performance. Such

methods will facilitate consideration of pervaporation in process feasibility analyses and front-end design (Scharzec, Waltermann, and Skiborowski 2017); albeit that more rigorous design methods are required for the subsequent detailed design of pervaporation systems.

Ideal models of pervaporation systems are developed in this research. These models only require readily available data. Efficiency values can only be determined on the basis of the performance of ideal systems. Hence, the analytical and short-cut equations developed in this work for ideal systems provide the foundation for the development of performance metrics and design methods for industrial-scale pervaporation systems. These will facilitate the analysis of existing pervaporation systems and the design of new pervaporation systems.

A novel membrane performance metric is proposed which gives appropriate weighting to separation and flux. This will be of benefit to design engineers. It will encourage the development of membranes that perform well at industrial operating conditions.

Contribution to academic knowledge

An analytical expression for the calculation of the average flux in an ideal isothermal pervaporation module where flux is proportional to concentration is developed for the first time. This expression for ideal isothermal systems facilitates the development of efficiency metrics for adiabatic systems. A novel exact analytical expression for the time required to achieve a given separation using an ideal isothermal batch process for systems where flux is proportional to concentration is also derived.

An analytical solution for the determination of the average flux in ideal pervaporation modules where flux is independent of concentration is developed for the first time.

The novel J_r/J_{reheat} parameter is proposed which compares the retentate flux before and after reheating. The J_r/J_{reheat} parameter has been used to demonstrate that industrial operations are feasible within a limited range of combinations of E_j and $\dot{m}_p/\dot{m}_f$ ratios. This is the first time that the full range of industrial operating conditions has been determined for the dehydration of ethanol, isopropanol and other solvents. A novel simple short-cut approximation is developed that is applicable for a variety of solvents throughout the full range of industrial operating conditions for ideal adiabatic modules where flux is independent of concentration.

For the first time simple approximations are developed for ethanol and isopropanol dehydrations for ideal adiabatic modules where flux is proportional to concentration.

The effects of recycle in pervaporation systems is explored providing new insights regarding the use of recycles. Novel equations for the determination of feed concentration and feed flowrate as functions of the supply concentration and recycle ratio are developed. The potential for increased throughput in industrial systems through use of recycle is identified and explored.

The optimisation of multi-stage ideal pervaporation systems is analysed. The effect of module efficiency in relation to optimisation of multi-stage systems is explored. The

typical pattern of efficiency across multi-stage pervaporation systems has been identified for the first time.

Current metrics relating to pervaporation membranes are reviewed and are shown to be inadequate. A novel single metric for the evaluation of pervaporation membranes that gives appropriate weight to flux and separation with respect to industrial operations is proposed.

Chapter 1: Literature Review

1.1 History

Kahlenberg (1906) was the first to report pervaporation. He explained why the rate and nature of membrane separations were a function of the membrane material. In 1917 Eberlein noticed that liquid evaporated from a sealed collodion bag suspended in air (Kober, 1917). Kober discovered the selective permeation of water from aqueous solutions of albumin and toluene through a cellulose film and coined the term "pervaporation" (Kober, 2017). In 1935, Farber showed the potential for pervaporation as a separation process (Fleming and Slater, 1992). Schwob reported on the use of pervaporation for the dehydration of alcohols (Baig, 2008). Binning and his co-workers subsequently established the key principles of pervaporation during the period 1958 to 1962 (Binning *et al*., 1961; Binning *et al*., 1962).

1.2 Industrial operations

The first commercial scale pervaporation unit was installed in Brazil in 1982 by GFT Membrane Systems. It began operating the following year and was used for the dehydration of ethanol (GFT Membrane Systems GmBH, no date). The first commercial plant for the dehydration of an ester started operating in 1988 (Brüschke, 2001, p. 128). The first industrial plant where pervaporation was used to enhance ester synthesis was built in 1991 by GFT Membrane Systems GmBH for BASF (Kujawski, 2000): continuous removal of water using pervaporation was used to prevent the reaction from approaching equilibrium.

Hydrophobic pervaporation is used for the removal of solvents from wastewaters (Figoli *et al*., 2015, p. 46; Kujawa *et al*., 2015). Pervaporation of solvents from dilute aqueous solutions is the subject of ongoing research (Vatani *et al*., 2018). Applications such as the removal of chlorinated compounds from wastewater are being investigated (Ramaiah *et al*., 2013). It is used for the removal of volatile organic compounds from the washing water of gas scrubbers (Figoli *et al*., 2015, p. 44). Separation and concentration of aroma products and of food products using thermal techniques can lead to loss or damage to

aroma compounds (Babalou *et al*., 2015). Research into the use of low temperature membrane processes such as pervaporation for the purification of aroma products is ongoing, though further development is required before these applications gain widespread acceptance (Figoli *et al*., 2015, p. 50). Research into the de-alcoholisation of wine has been undertaken (Takács *et al*., 2007) but has not gained widespread acceptance industrially (Margallo *et al*., 2015). There has been research into the application of pervaporation in the production of non-alcoholic beers using commercial membranes (Magalhaes-Mendes *et al*., 2008; Paz *et al*., 2017). However, pervaporation is not widely used industrially (Brányik *et al*., 2012). Many hydrophobic pervaporation membranes are not stable at industrial conditions as impurities that reduce flux are adsorbed (Baker, 2012, p. 394).

Separation of organic-organic mixtures by pervaporation is difficult, as the species being separated have similar properties (Baker, 2012, p. 394). Furthermore, organic solutions often cause severe swelling of membranes, particular at high temperatures (Baker, 2012, p. 394). A pilot-scale separation of methanol from a methyl tert-butyl ether/isobutene mixture was reported in 1988 (Ravanchi *et al*., 2009). Pervaporation has been used to remove hydrocarbon molecules that contain sulphur from naphtha and other streams on an industrial scale since 2003 (Mortaheb *et al*., 2012). It is also used for the removal of sulphur from petrol (Kong *et al*., 2007; Lin *et al*., 2009). Membranes continue to be developed for a variety of other organic-organic separations, such as the separation of methanol from dimethyl carbonate (Kopeć *et al*., 2013).

Thermal processes such as multi-stage flash distillation continue to be used for desalination (Logan, 2015). Reverse osmosis has become the preferred option in recent decades. Use of pervaporation for desalination is now the subject of ongoing research (Ben Hamouda *et al*., 2011; Cho *et al*., 2011; Zhu *et al*. 2015; Wang *et al*., 2016b; Wang *et al*., 2017b). Membranes have been developed which are easier to make, are less susceptible to fouling, have longer lifespans and increased flux (Wang *et al*., 2017b).

Pervaporation when used for solvent recovery is typically part of a multi-step solvent recovery process (Sulzer Chemtech, 2006) or is an integral part of a hybrid distillation system (Fahmy *et al*., 2002; Baker, 2012, p. 402; Koch *et al*., 2013). Pervaporation

eliminates the need for the addition of entrainers or the use of pressure swing distillation when purifying azeotropes. As a process on its own pervaporation is not economically feasible, but in a hybrid or combined process, coupled with distillation, overall efficiency can be improved (Verhoef *et al*., 2007: Baker, 2012, p.412). Sulzer have installed over 150 alcohol dehydration units (DeltaMem AG, 2017); with a total of over 200 installed by Sulzer and its licences (Baker, 2012, p. 380). The most common industrial application is the dehydration of solvents in the chemical and pharmaceutical industries (Baker, 2012, p. 401).

1.3 Future industrial applications

Global production of bioethanol increased from 17 billion litres in 2000 to 86 billion litres in 2011 and 95 billion litres in 2017 (Ren21, 2017). Research into the production of biofuels such as isobutanol from the stalks of corn (Somerville *et al*., 2010; Minty *et al*. 2013) could see a major increase in applications of hydrophobic pervaporation (Qureshi and Ezeji, 2008; Huang *et al*., 2010). A mixture of acetone, butanol and ethanol, "ABE", is often produced in biofuel fermentation processes (Qureshi *et al*. 2001; Ni and Sun, 2009; Green, 2011; Li *et al*., 2014; Karimi *et al*., 2015). Pervaporation can be used for in-situ recovery of butanol thereby preventing inhibition of the fermentation process, (Wu *et al*., 2012; Outram *et al*., 2017). Multi-step hybrid processes that incorporate pervaporation for the separation and purification of biofuels consume less energy and have lower costs than conventional processes such as distillation (Xue, *et al*., 2014).

The development since 2008 of thermostable hybrid organo-silica membranes for the dehydration of butanols, opens up the prospect of industrial operations at 150 ^{o}C and above (Agirre *et al*., 2014).

1.4 Membrane materials

Industrial membranes usually have a separation layer that is less than 5 μm thick (Baker, 2012, p. 392). Thinner separation layers provide higher flux: however, they typically

have a lower selectivity (Samei *et al*., 2013). Asymmetric membranes comprise a single membrane component which has a dense "skin" supported by a thicker porous support layer; the variation in structure is caused by the manufacturing process (Foley, 2013, p. 9). Composite membranes comprise different materials that are bonded together (Foley, 2013, p. 10). A thin separation layer is supported by another material that provides mechanical strength with minimal reduction in flux (Samei *et al*., 2013). These are the most common type of laboratory-scale membranes as they are easier to prepare (Figoli *et al*., 2015, p. 33). Improvements to the consistency and hence the mechanical strength of support layers, reduces the occurrence of flaws in the active layer, thereby increasing the selectivity of membranes (Gladman, 2017).

A large amount of data has been published in research literature relating to the performance of membranes with thick active layers operated at low temperatures (Chapman *et al*., 2008; Vatani, Raisi and Pizuki, 2018). Many of these membranes will not withstand the higher temperatures prevalent in industrial operations (Baker, 2012, p. 392) which are outlined in section 1.15. Some data involves feed concentrations outside the range of normal industrial operating conditions (Huang *et al*., 2006; Sanz and Ghmeling, 2006). Such research is of limited value (Baker, 2012, p. 392).

The sorption of solutes in membranes is mainly a function of the chemistry; whilst diffusion depends on the size of the molecules passing through the membrane. Hydrophilic modules favour sorption of polar molecules such as water and have a high mobile selectivity, i.e. the movement of small molecules such as water is considerably faster than that of larger molecules. Materials such as polyvinyl alcohol (PVA), zeolites and chitosan have sorption selectivities that favour polar molecules (Baker, 2012, p 391). The rate of diffusion of smaller molecules through the rigid membrane structure is much faster than the rate of diffusion of larger molecules. (Baker, 2012, p 391).

In contrast, silicone rubber membranes are hydrophobic and preferentially sorp non-polar solvents. The diffusion selectivity is low, so whilst small molecules such as water diffuse faster than large molecules, the difference is limited (Baker, 2012, p 391). Other rubber membranes and polyamide-polyether-block membranes as well as polydimethylsiloxane (PMDS) membranes can also be used for hydrophobic

pervaporation (Rozicka *et al*., 2014). Sorption favours higher selectivity in both cases. However, diffusion of smaller molecules such as water is faster in both cases: this increases selectivity in the case of hydrophilic modules but reduces it in the case of hydrophobic molecules. Hence, selectivity is typically less for hydrophobic membranes than for hydrophilic membranes.

The most commonly used industrial membranes for dehydration using pervaporation are made from polymers such as polyvinyl alcohol, PVA, and chitosan (Baker, 2012, p. 392). Polymeric membranes are widely used in industry; however, they are expensive and cannot be operated at high temperatures (Chapman *et al*., 2008). They are prone to swelling which reduces selectivity. Therefore they are often cross-linked or blended to restrict swelling (Xie *et al*., 2011) with compounds such as glutaraldehyde. Semi-crystalline polymers such as poly-acrylonitrile (PAN) have also been used (Shao and Huang, 2007). Considerable research has been undertaken with regard to sodium alginate membranes (Keane and Morris, 2010); again cross linking is required to prevent swelling (Figoli *et al*., 2015, p. 30). New dehydration membranes with nanoparticles embedded in polymeric membranes are being developed; they have increased flux without loss of selectivity (Hua *et al*., 2014). The enhanced flux may result from the additional free volume in the polymer matrix caused by the incorporation of the nanoparticles (Wang *et al*., 2016a).

Inorganic membranes made from zeolites and ceramic materials have been developed (Navajas *et al*., 2002; Navajas *et al*., 2006; Chapman *et al*., 2008; Sato *et al*., 2008; Sato *et al*., 2012; Samei *et al*., 2013) and are now used in industry (Baker, 2012, p. 393). These have the potential to operate at higher temperatures, thus providing improved flux. Their rigid uniform structure makes them less prone to swelling and thus temperature has little effect on the separation factor (Figoli *et al*., 2015, p. 30). The small uniform pores ensure that small molecules diffuse much faster than large molecules. Castricum *et al*. (2008) and Vente (2010) reported the development of hybrid organo-silica membranes. Pilot trials of such membranes at temperatures of 190 ^{o}C for the dehydration of n-butanol have been successful (Van Veen *et al*., 2011).

1.5 Module types

GFT Membrane Systems GmBH developed the earliest successful plate-and-frame modules (Baker, 2012, p. 397). Liquid feed flows across a flat sheet membrane. Vapour passes through the membrane and is removed as permeate. The liquid retentate flows out of the module. Many flat sheet membranes are used in what are effectively parallel "mini-modules" which are separated by plates as illustrated in Fig. 1.1. Plate-and-frame modules are still in commercial use (Pervatech, no date; Pfizer, 2018). They are robust and have packing densities of 100-400 m^2/m^3 have been achieved (Figoli *et al*., 2015, p. 36). Industrial systems typical have membrane areas of greater than 300 m^2.

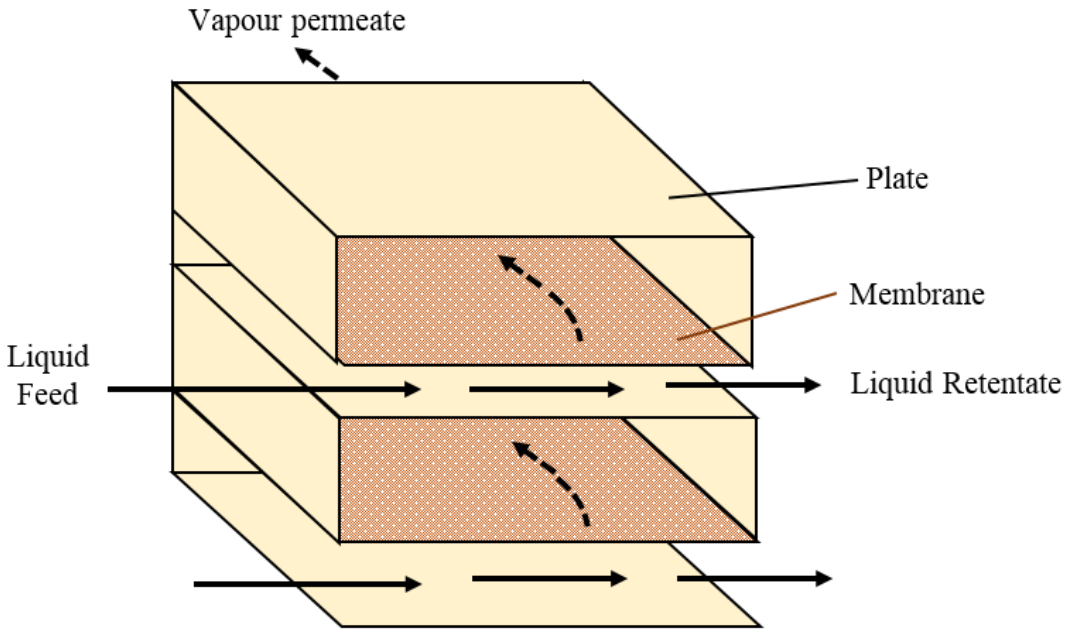

Figure 1.1 A plate and frame module

Spiral wound membranes are similar in design to plate and frame modules, except that the flat sheets wound around a core. The permeate flows inwards over the membranes to the core where it enters a perforated collection tube through which it leaves the modules as shown in Fig. 1.2. Spacers between the layers keep the membranes apart, facilitating liquid flow, increasing turbulence and thereby reducing concentration polarisation (Baker *et al*., 1997). Spiral wound membranes are widely used for other membrane technologies such as ultrafiltration, nanofiltration and reverse osmosis (Foley, 2013, p. 11) and are used in industry for hydrophobic pervaporation membranes

that remove organics from aqueous streams (Pervatech, no date). There use has been limited due to lack of adhesives that can operate with the chemicals and operating conditions prevalent in many pervaporation applications (Figoli *et al.*, 2015, p. 37). Water has a low molecular weight and therefore density is small in comparison with that of organic modules. Hence, aqueous permeate has a far higher pressure drop per unit mass flowrate within the permeate channel compared to organic molecules. Therefore spiral wound membranes are less suitable for dehydrations in comparison to hydrophobic or organic-organic pervaporation (Brüschke, 2001, p. 156).

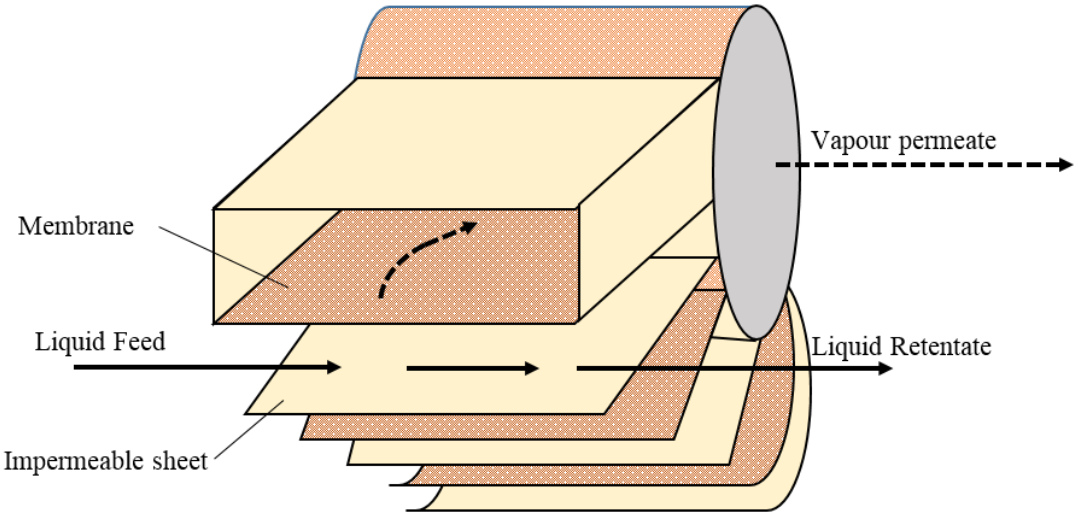

Figure 1.2 A spiral wound membrane module

The high temperatures, needed to achieve high flux, require a large pressure gradient across membranes. A thin selective layer, of up to 5 µm thickness (Baker, 2012, p. 392) is used. The thin active layer can be attached to a ceramic tubular support (Samei *et al.*, 2013). Such ceramic tubular supports are mechanically strong whilst their high porosity does not significantly reduce flux (Samei *et al.*, 2013). One or more tubes can be fitted within a module. They are the main product of Pervatech, a major supplier of pervaporation membranes (Pervatech, 2014).

Hollow fibre membrane modules are comprised of semi-permeable hollow fibres. Liquid feed flows across the outside of the fibres. Permeate passes through the wall of the fibres into the inner hollow core of the fibres. The permeate flows inside the hollow fibres and is collected at the end of the fibres as illustrated in Fig. 1.3. Modules with hollow fibre

membranes are widely used for gas separations (Baker, 2012, p. 338). They typically have higher packing densities than flat sheet modules (Santos *et al*., 2011) and tubular modules. As feed in pervaporation systems is usually clean, clogging of the membrane is not an issue. They are resistant to chemical degradation and abrasion (Shao *et al*., 2014). There are hollow fibre membranes with high pervaporation fluxes (Sukitpaneenit and Chung, 2014). Module fabrication and operation is easier than for flat sheet membranes (Sukitpaneenit and Chung, 2014). Pilot scale trials using hollow fibre membranes were reported in 1997 (Tsuyumoto *et al*., 1997). However, they are not widely used in industry for pervaporation (Zuo *et al*., 2012). The potential use of pervaporation for the dehydration of biofuels is being explored: this would require very large pervaporation units (Baker, 2012, p. 397). Hydrophobic membranes are required to remove the butanol product from fermentation broth so as to prevent the butanol concentration reaching toxic levels (Qureshi and Ezeji, 2008). The high packing density of hollow fibre membranes has led to efforts to adapt them for the pervaporation of biofuels (Baker 2012, p. 397) and for solvent dehydration (Zuo *et al*., 2012).

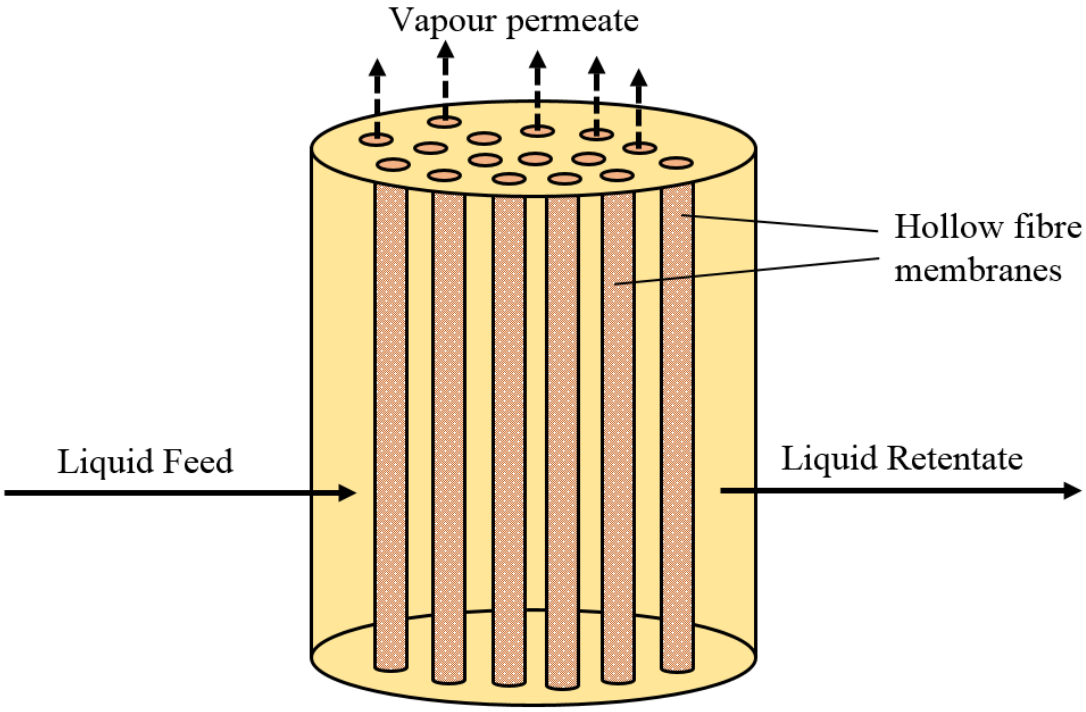

Figure 1.3 A hollow fibre membrane module

1.6 Factors affecting flux

The flux in pervaporation is usually defined as mass flux, J,

$$J \equiv \frac{\dot{m}_p}{A} \tag{1.1}$$

where: J = Permeate flux (kg/h.m^2)
$\dot{m}_p$ = mass flowrate of permeate through the membrane (kg/h)
A = membrane area (m^2)

The flux of a component is dependent on the diffusion and sorption properties of a membrane along with the difference in the partial pressure of the component across the membrane (Baker *et al*., 2010),

$$j_i = \frac{D_i K_i^G}{l}\left(p_{i_o} - p_{i_l} \right) \tag{1.2}$$

where: j_i = molar flux of component i (cm^3(STP)/cm^2.s)
D_i = the membrane diffusion coefficient of component i (cm^2/s)
K_i^G = the sorption coefficient of component i (cm^3(STP)/cm^3.s)
l = membrane thickness (cm)
p_{io} = partial pressure of component i on the feed side of the membrane (cmHg)
p_{il} = partial pressure of component i on the permeate side of the membrane (cmHg)

The diffusion and sorption coefficients both have Arrhenius-type temperature dependencies. Hence, pervaporation typically has an Arrhenius-type temperature dependency (George and Thomas, 2001). There is considerable experimental evidence of such behaviour (Feng and Huang, 1997; Adoor *et al*., 2006; Huang *et al*., 2006; Hu *et al*., 2007; Boutikos *et al*., 2014). It has also been found to be the case for industrial systems (Sato *et al*., 2008).

For most dehydration systems, flux is proportional to water concentration within the range of industrial operations (Van Veen *et al*., 2001; Gallego-Lizon *et al*., 2002; Urtiaga

et al., 2003; Van Hoof *et al*., 2004; Sommer and Melin, 2005; Cséfalvay *et al*., 2008) and the relationship is of the following form

$$J = x_i J_o e^{-E_j/RT} \tag{1.3}$$

where: x_i = the mass fraction of component *i* in the local liquid *i* (-)

E_j = the apparent activation energy of the permeation flux (kJ/kmol)

R = the universal gas constant (kJ/kmol.K)

J_o = the maximum possible permeate flux (i.e. the flux as $T \rightarrow \infty$), (kg/s.m^2)

T = Temperature (K)

There are cases where flux is independent of concentration across a range of concentrations, (Verkerk *et al*., 2001; Sommer and Melin 2005; Pera-Titus 2006; Van Hoof *et al*., 2006). In such cases Eq. (1.3) reduces to the following

$$J = J_o e^{-E_j/RT} \tag{1.4}$$

In some cases, flux is proportional to concentration at low concentrations and then gradually transitions to being independent of flux at higher concentrations (Verkerk *et al*., 2001; Sommer and Melin 2005; Van Hoof *et al*., 2006).

Many laboratory scale systems are operated isothermally. Industrial trials with isothermal membranes have been undertaken with temperatures of up to 150 ^{o}C (Van Veen, 2016). In such cases Eq. (1.3) reduces to the following

$$J = \frac{x_i}{z_i} J_f \tag{1.5}$$

where: x_i = the mass fraction of component *i* in the local liquid *i* (-)

z_i = the fraction of the feed comprised of component *i* (-)

J_f = the flux at the feed temperature (kg/s.m^2)

Flux is caused by the difference between the vapour pressure of the feed liquid and the partial pressure of the permeate vapour (Baker 2012, p. 383). Increasing the feed temperature, increases the vapour pressure and hence increases the flux. Greenlaw *et al*. (1977) showed that the pressure on the feed side of the membrane has no significant effect on the flux. Maximising the vacuum on the permeate side of the membrane, reduces the partial pressure on the permeate side thereby increasing the flux.

1.7 Separation

The separation characteristic of a membrane is usually characterised in terms of the separation factor. Huang and Xu (1988) defined the separation factor as

$$\beta_{ij} \equiv \frac{\left(y_i / y_j \right)}{\left(z_i / z_j \right)} \tag{1.6}$$

where: β_{ij} = the separation factor

z = the mass fraction in the feed

y = the mass fraction in the permeate

i = the preferentially permeating component

j = the less permeating component

The notation α_{ij} is sometimes used to denote separation factor (Chapman *et al*., 2008)

For binary systems; $y_i = 1 - y_j$ (1.7)

and $z_i = 1 - z_j$ (1.8)

The separation factor is a function of the feed composition (Kujawski, 2000). Shanahan (2010) noted the asymptotic relationship between separation factor and membrane area for a given separation. Baker (2012, p. 393) states that an increase in β_{ij} above 1,000 provides little additional benefit. There is an asymptotic relationship between the separation factor and concentration of water in the permeate stream as illustrated in Fig. 1.4. There is a similar asymptotic relationship with the mass of retentate. For a binary

system, with a given feed concentration, the relationship between separation factor and permeate concentration, Eq. (1.6) has the form

$$\beta_{ij} = k\frac{y_i}{1-y_i} \tag{1.9}$$

where k is a constant.

There are similar asymptotic relationships between separation factor and other parameters such as energy consumption per unit feed. The need for a metric that better reflects separation performance is addressed in chapter 8 of this thesis.

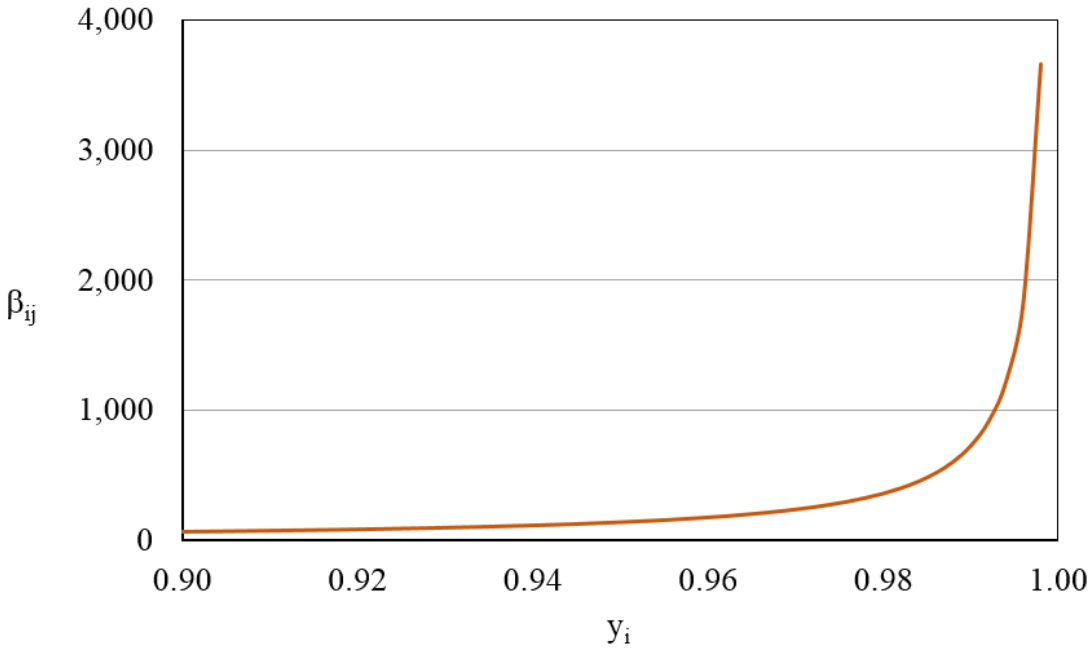

Figure 1.4 Separation factor versus permeate mass fraction for a binary system: $z_i = 12\%$.

1.8 Alternative metrics

Molar flux

During recent years, molar flux, j has been used instead of mass flux. The use of molar flux facilitates comparison with gas permeation data (Baker *et al.*, 2010).

Baker *et al*. (2010) recommend the use of membrane permeability to describe the rate of flow through pervaporation membranes. The membrane permeability is the product of the diffusion coefficient multiplied by the corresponding sorption coefficient. Some separation due to vapour liquid equilibrium usually occurs: permeability measures the additional separation that occurs because of the membrane. It is solely a function of the properties of the membrane; hence, it facilitates comparisons of data obtained at different operating conditions.

$$\mathrm{P_i^G} = j_i \frac{l}{P_{io} - p_{il}} \tag{1.10}$$

Permeability, P_i^G, is usually reported in Barrers (1 Barrer 1×10^{-10} cm^3(STP).cm/cm^2.s. cmHg).

Membrane permeance does not require knowledge of the membrane thickness (Baker *et al*., 2010). It is defined as

$$\frac{P_i^G}{l} \equiv \frac{j_i}{p_{io} - p_i} \tag{1.11}$$

Permeance is represented as P_i^G/l rather than by a single symbol (Baker *et al*., 2010; Jyoti *et al*., 2015; Wu *et al*. 2016). Much of the published literature provides data in the form of component fluxes and separation factors, as is clear from Chapman *et al*. (2008) and as stated by Baker *et al*. (2010). Some recent papers have provided permeance and permeability data (Marszałek and Kamiński, 2012; Luis *et al*., 2013; Choudhury and Ray, 2017; Xu and Chung, 2017), though selectivity continues to be widely used (Gao *et al*., 2017; Narkkun *et al*., 2017): others include both (Wang *et al*., 2017a; Yin *et al*., 2017).

The enrichment factor, *EF*, has been defined as the ratio of permeate concentration to feed concentration (Feng and Huang, 1997).

$$EF_i \equiv \frac{y_i}{z_i} \tag{1.12}$$

where: EF_i = enrichment factor (-)

z = mass fraction in the feed (-)

y = mass fraction in the permeate (-)

i = preferentially permeating component

The enrichment factor is a function of the feed composition as is the separation factor (Kujawski, 2000). Baker (1991) noted that separation can occur in the absence of a membrane due to evaporation and therefore proposed that the separation factor be comprised of two separate parameters; an evaporation separation factor and a membrane separation factor.

$$\beta_{ij} = \beta_{evap}\beta_{mem} \tag{1.13}$$

The evaporation separation factor is unity at the azeotropic composition of a mixture as no separation occurs in the absence of a membrane.

Baker *et al*. (2010) recommend the use of selectivity, α_{ij}, rather than separation factor to characterise the performance of pervaporation membranes.

$$\alpha_{ij} = \frac{P_i^G}{P_j^G} = \frac{P_i^G / l}{P_j^G / l} \tag{1.14}$$

Permeability, permeance and β_{mem} all provide performance data that is independent of operating conditions. They are useful when analysing membrane performance, including swelling and mass transfer. These parameters need to be combined with vapour liquid equilibrium (VLE) data when designing a pervaporation system, thereby adding complexity to the design process.

Most data continues to be reported in terms of flux (Chapman *et al*., 2008; Baker *et al*., 2010; Choudhray and Ray, 2017; Kujawski *et al*., 2017). Thus for the design engineer at least, it is important to formulate pervaporation design equations in terms of flux. Therefore mass fluxes are used in this thesis.

1.9 A single metric for pervaporation performance

Huang and Yeom (1990) identified the need for a single composite metric incorporating flux and separation. They proposed the pervaporation separation index (PSI)

$$PSI = J\beta_{ij} \tag{1.15}$$

where: PSI = Pervaporation Separation Index (kg/h.m^2)

J = mass flux (kg/h.m^2)

β_{ij} = separation factor (-)

The flux and separation factor may relate to any concentration and temperature.

This definition permits high PSI values even in cases where there is no separation, i.e. $\alpha_{ij} = 1$. To address this, Huang and Feng (1993) modified the definition as follows

$$PSI = J\left(\beta_{ij} - 1\right) \tag{1.16}$$

Sosa and Espinosa (2011) suggested modifying the PSI by replacing the flux with the inverse of the average area required for a given separation. As discussed section 1.7, the separation factor has been shown to be unsatisfactory due its asymptotic relationship with the membrane area required for a given separation: hence, the PSI is unsatisfactory. Whilst PSI continues to be used (Xing *et al*., 2016; Kujawski *et al*., 2017), it does not have widespread acceptance in industry as evidenced from its omission from industry-focused literature (Vente, 2010; Baker, 2012, pp. 379-416; Deltamem, 2017; Pervatech, 2018). An alternative single unified metric for membrane performance is needed that gives appropriate weight to separation and flux. Toth *et al*. (2017, pp. 72-73; Toth *et al*., 2018) proposed the Membrane Flash Index (MFLI). The MFLI compares the separation data using a membrane with the corresponding vapour-liquid equilibrium data for a flash distillation. It facilitates comparison of pervaporation with distillation. The limitations of current metrics including both the separation factor and the PSI will be discussed in chapter 8. A novel single metric will be proposed that better reflects the needs of industrial operations.

1.10 Theoretical models of pervaporation

Pore flow model.

Okada and Matsuura (1991) proposed the pore flow model. A membrane is considered as a series of parallel pores, through which liquid moves. The model involves three steps, which occur in series within each pore:

1. Liquid transport from the surface of the membrane in along the pore.
2. Evaporation of the liquid within the pore.
3. Vapour transport along the pore to the membrane surface.

Resistances-in-series model

(Jiraratananon *et al*. 2002) proposed the resistance-in-series model. The model involves a number of steps, which occur in series:

1. Transport through the liquid boundary layer.
2. Sorption onto the active layer of the membrane.
3. Diffusion of liquid through the active layer of the membrane.
4. Desorption from the active layer.
5. Transport of vapours through the support layers of the membrane.
6. Transport though the vapour boundary layer.

Jiraratananon *et al*. (2002) state that resistance within the liquid boundary layer is negligible. However, resistance in the liquid phase boundary layer can be significant as shown by the work of Vane *et al*. (1999) with dynamic modules. Sommer *et al*. (2005) have shown that concentration and temperature polarisation in the liquid phase boundary layer can significantly reduce flux, particularly where flux is high as can occur with the high temperatures used in industrial systems. As vacuum is usually applied, resistance due to desorption and resistance in the vapour phase are negligible. Thus the key resistances are in the liquid boundary layer, sorption onto the active layer of the membrane and diffusion of liquid through the active layer of the membrane.

The Solution-diffusion model

The solution-diffusion model assumes that liquid dissolves in the membrane material and then diffuses through the membrane down a concentration difference before

desorption at the vapour side of the membrane (Feng and Huang, 1997). Separation is achieved because the components dissolve at different rates (Kahlenberg, 1906) and diffuse at different rates (Wijmans and Baker, 1995). Diffusion across the membrane occurs by permeating molecules jumping from micro-cavity to micro-cavity within the polymer. Random movements of the polymer molecules cause the micro-cavities to be created and to disappear over time. Smaller molecules can enter both large and small micro-cavities and so have more opportunities to move. Hence, they diffuse faster than large molecules (Baker 2012, p. 20). The following equation applies

$$J_i = \frac{D_i K_i^G}{l}\left(p_{io} - p_i\right) \tag{1.17}$$

where: J_i = the mass flux of component i (kg/h.m^2)

D_i = the membrane diffusion coefficient of component i (cm^2/s)

K_i^G = the sorption coefficient of component i (cm^3(STP)/cm^3.cmHg)

Eq. (1.10) can be written as follows (Wijmans and Baker, 1995)

$$J_i = \frac{P_i^G}{l}\left(p_{io} - p_{il}\right) \tag{1.18}$$

The average pore length is proportional to the thickness of the membrane so that in all three models the resistance to flow within the membrane is proportional to the thickness of the membrane's active layer.

The pore flow model is appropriate to membranes where there are larger permanent cavities through which permeant molecules can pass: whilst the solution-diffusion model is more appropriate for membranes with smaller gaps, which open up on a transient basis (Wijmans and Baker, 1995). Industrial pervaporation membranes are generally in this latter category and the solution-diffusion model is more widely accepted (Crespo and Brazinha, 2015, p. 6).

1.11 Concentration polarisation and temperature polarisation

Concentration polarisation reduces flux and selectivity in membrane systems. The process is often modelled on the basis of a boundary layer at the feed side of the

membrane. The liquid mixture travels from the bulk fluid through the boundary layer to the membrane. The solute preferentially permeates the membrane, leaving concentrated solvent at the feed-side surface of the membrane with a correspondingly low concentration of solute at the upstream membrane surface as illustrated in Fig. 1.5. Solute travelling towards the membrane has to displace this solvent so as to reach the membrane surface; whilst the solvent diffuses back to the bulk liquid. However, for this diffusion to occur there needs to be a sufficiently large concentration gradient. The higher the flux the greater the level of concentration polarisation, as there is a greater flow of solute through the boundary layer. Concentration polarisation is a function of temperature, flowrate, feed channel dimensions, diffusion coefficient and module design (Baker, 2012, p.181). Greater bulk fluid velocity leads to greater turbulence and a reduction in the thickness of the boundary layer, leading to a greater concentration gradient per unit thickness of boundary layer. This leads to more rapid diffusion of the solvent back to the bulk fluid and thereby reduces concentration polarisation. Tubular, plate-and-frame and tube-side hollow-fibre modules have greater flow velocities and hence lower boundary layer thicknesses as compared with hollow-fibre modules with shell-side feed. The concentration of the solute rises across the membrane due to the separation that occurs within the membrane. There is no concentration gradient on the downstream side of pervaporation membranes as the flowrate of all the components is proportional to their respective concentrations. The permeate concentration of the solute is higher on the downstream side of the membrane.

The vaporisation of permeate requires considerable latent heat, which causes a reduction in the temperature of the liquid at the membrane surface as compared with the bulk fluid. This phenomenon, known as temperature polarisation, can be significant in systems with high flux as the temperature drop is greater (Sommer *et al.*, 2005). There is a temperature gradient as illustrated in Fig. 1.6. This is due to the flow of heat from the hot bulk liquid towards the cold membrane surface and due to the backflow of cold solvent from the membrane surface to the bulk liquid. The temperature drops across the membrane due the vaporisation occurring within the membrane. The temperature of the permeate vapour is lower on the downstream side of the membrane due to the vaporisation that occurs across the membrane.

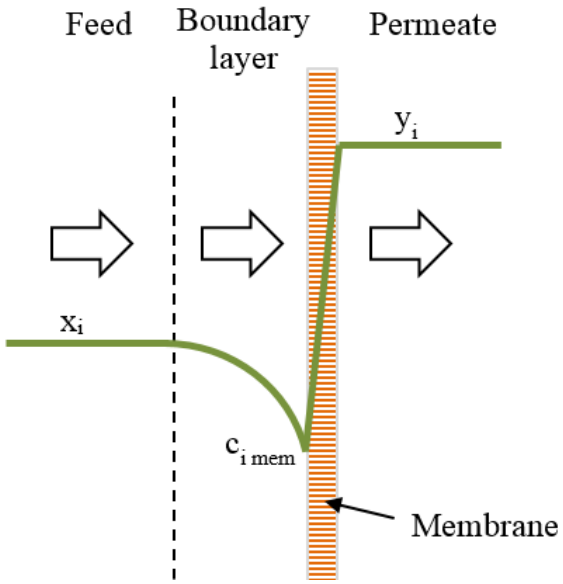

Figure 1.5 Concentration profile of water where concentration polarisation occurs: x_i is the concentration of water in the bulk feed, $c_{i\,mem}$ is the concentration at the upstream face of the membrane and y_i is the concentration of water in the permeate vapour.

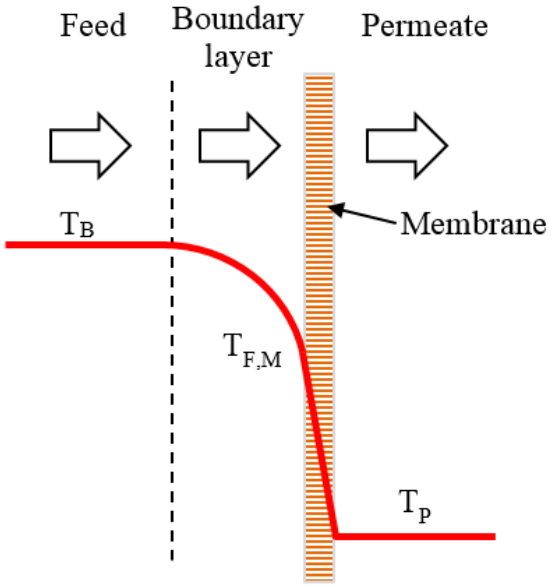

Figure 1.6 Temperature profile where temperature polarisation occurs: T_B is the temperature of the bulk liquid feed, $T_{F,M}$ is the temperature in the boundary layer and the membrane and T_P is the permeate temperature.

Concentration and temperature polarisation are significant for industrial systems as they typically operate at higher temperatures, with correspondingly higher fluxes, than those typical of laboratory-scale trials (Sommer *et al.*, 2005). Whilst, the higher temperatures lead to a reduction in the liquid viscosity, this is outweighed by the increase in flux.

1.12 Module designs

Adiabatic modules

In industrial dehydration systems the liquid feed is typically heated prior to passing through an adiabatic module. Permeate requires latent heat to evaporate; this causes the remaining liquid to become cooler. As the liquid becomes cooler the rate of pervaporation decreases. For larger systems involving continuous single-pass operation, reheaters are used between pervaporation stages (Baker, 2012, p. 395). Baker (2012, p. 402) states that 3 to 5 stages are typical. However, there are commercial systems where the liquid has been heated 9 times in (Sulzer, 2016): giving permeate-feed ratios of < 2% for IPA and < 1% for ethanol, with temperature drops of no more than 5 ^{o}C within a module. Different numbers of modules may be used for each stage (Schleger *et al*., 2004). Often a single heater with condensing steam is used to heat multiple stages as shown in Fig. 1.6 (Sander and Soukup, 1988; Smitha *et al*., 2004).

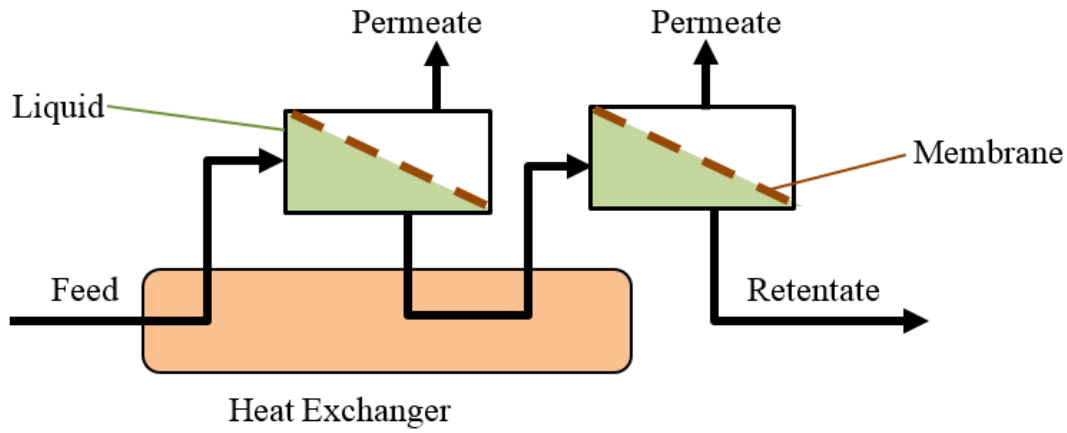

Figure 1.7 Adiabatic pervaporation module with single heater for multiple stages.

An alternative design has been developed where tubular modules are housed in a shell-and-tube type housing. Liquid retentate is reheated in a chamber within the rear-end head as illustrated in Fig. 1.7 (Brüschke *et al*., 2010; Baker, 2012, p. 398). Inadequate frequency of reheating leads to low flux and excessive membrane area, whilst over frequent reheating leads to extra piping, pumping and heat exchanger costs. These add significantly to the complexity and cost of industrial systems (Baker, 2012, p. 395).

There is a need for a design heuristic for optimisation of the frequency of reheating. This is addressed in chapters four and five.

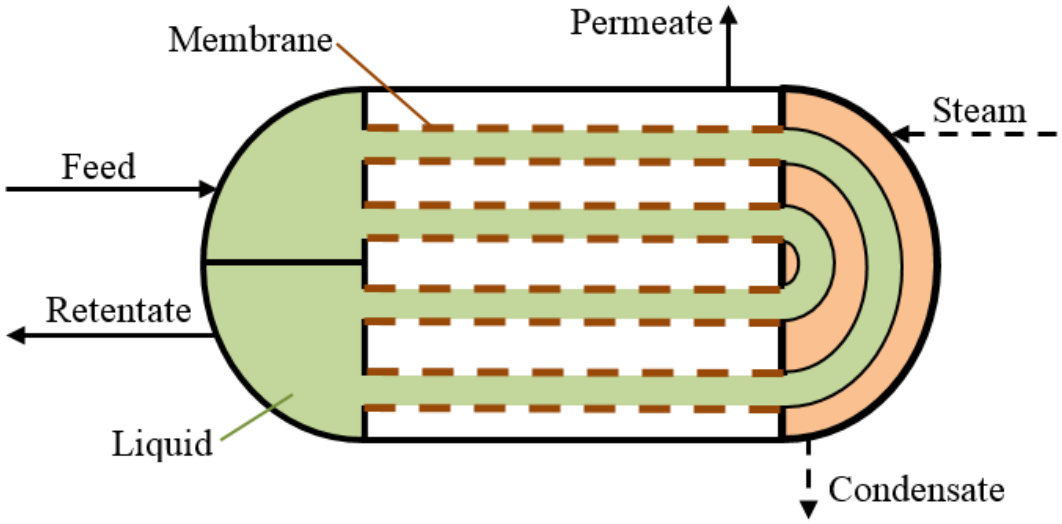

Figure 1.8 Adiabatic pervaporation module with reheating in the rear-end head

Isothermal modules

Isothermal designs incorporate heating within the membrane module so as to prevent a reduction of flux. The Sulzer SMS concept module shown in Fig. 1.8 has tubular modules surrounded by hot fluid which heats the liquid feed in the annuli of the membrane modules (Wynn, 2000; Brüschke, 2001, p. 158). Industrial trials with isothermal membranes are being undertaken with temperatures of up to 150 ^{o}C (Van Veen, 2016).

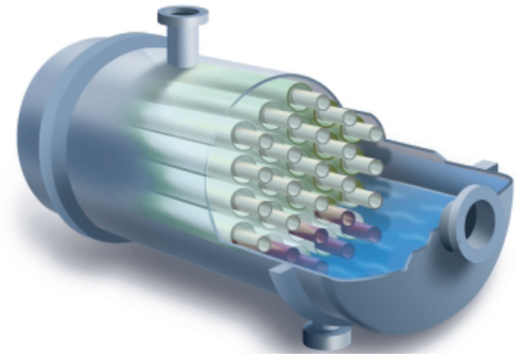

Figure 1.9 Sulzer SMS isothermal pervaporation module (Wynn 2000).

Use of partially vaporised feed has been suggested (Fontalvo *et al*., 2006a; Fontalvo *et al*., 2010). This would reduce the amount of material being vaporised, thereby reducing

the temperature drop and increasing the average flux. It can also reduce concentration and temperature polarisation (Fontalvo *et al*., 2006a; Fontalvo *et al*., 2006b).

Sweep gas modules.

In sweep gas modules a non-condensable gas flows along the permeate side of the membrane as illustrated in Fig. 1.9 (Kujawski and Krajewski, 2004). This reduces the permeate concentration thereby increasing the rate of mass transfer. However, it requires more work on the part of the vacuum pump and a larger condenser area. This approach could be used where the permeate stream is being incinerated (Baker, 2012, p. 400). Lipnizki and Field (2001) concluded that vacuum was more economical than sweep gas. Industrial units typically start up using a vacuum pump (Crespo and Brazinha, 2015, p. 13) and then proceed with vacuum obtained through condensation of the permeate at low temperatures, as this is more economical (Baker, 2012, p. 398).

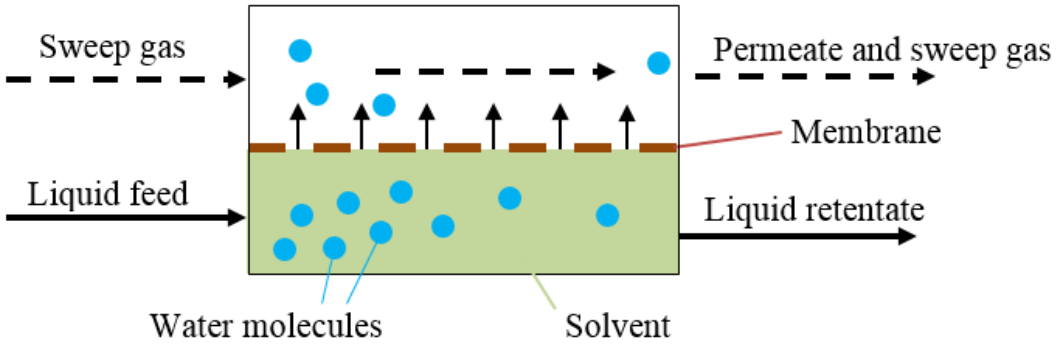

Figure 1.10 Adiabatic pervaporation module with sweep gas

Pervaporation within a distillation column

Leon and Fontalvo (2018) have proposed the inclusion of a pervaporation membrane inside a distillation column. Mathematical modelling indicates that this will allow the separation of the acetone-water-isopropanol azeotropic mixture.

Dynamic modules

Favre (2003) describes laboratory scale units with stirrers. Agitation of the liquid leads to a reduction in the thickness of the boundary layer at the membrane surface, thereby leading to increased flux. Alternatively, an entire module can be vibrated: Vane *et al*. (1999) reported up to 10-fold increases in mass transfer rates with such a system. They

used a motor with an eccentric drive attached to a torsion spring to agitate the module as illustrated in Fig. 1.10. A later paper, noted that cost is a major drawback for such systems (Vane and Alvarez, 2005): this approach has not met with commercial success.

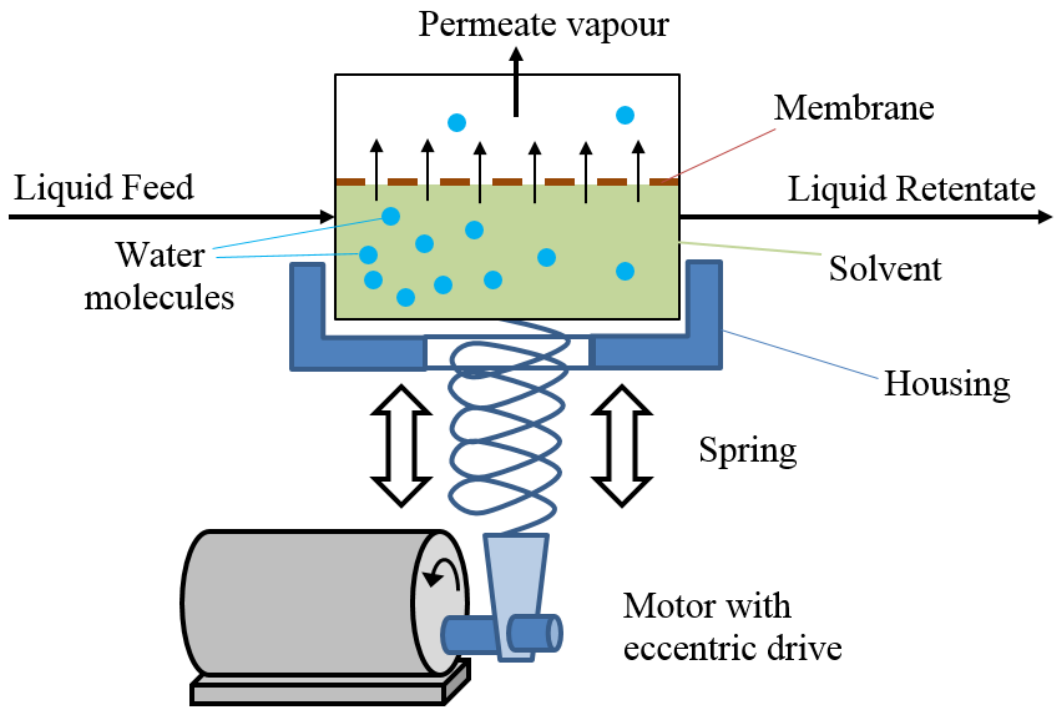

Figure 1.11 Dynamic pervaporation module, with eccentric drive motor and torsion spring.

1.13 Solvents for which pervaporation is practicable for dehydration.

Distillation can be used to dehydrate solvents that are less volatile than water. Solvents that are immiscible in water can often be separated using decanters or by distillation combined with a decanter to separate water from the distillate. Hence, hydrophilic pervaporation is typically used in industry to purify solvents which are miscible in water and which either form azeotropes with water or which are more volatile than water. Ethanol and isopropanol are the solvents for which pervaporation is most commonly used (Baker 2012, p. 401). This is reflected in the pervaporation literature (Chapman *et al.*, 2008). The following solvents are also candidates for hydrophilic pervaporation: acetone, THF, n-propanol and n-butanol (Huang *et al.*, 2010). Pervaporation can be

used for a variety of other solvents including acetonitrile, dimethylformamide, dioxin and xylene (Pervatech, no date).

Approximately US$30 million worth of pervaporation plant is installed each year, (Baker, 2012, p. 401). The adoption of pervaporation on an industrial scale has been slow due to the high capital cost of modules (Baig, 2008) and due to the limited number of solvents for which its use is economically advantageous (Pervatech, no date). The perception by end-users of a lack of predictability (Vente, 2010) acts as a barrier to adoption of pervaporation. He notes the lack of a "predictive tool". The provision of simple equations for the sizing of ideal hydrophilic pervaporation modules furnishes the first steps towards addressing this need.

1.14 Industrial operating conditions

Pervaporation is often combined with distillation in hybrid distillation-pervaporation systems (Vente, 2010; Baker, 2012, p. 410). An example of a system used for the dehydration of isopropanol (IPA) is shown in Fig. 1.11. Distillation is used to obtain distillate that is close to the azeotropic composition. Some of the distillate is returned to the column as reflux and hydrophilic pervaporation is used to reduce the water concentration of the remainder to less than 1% w/w. Such systems are more economic for the industrial separation of aqueous azeotropes (Luis and Van der Bruggen, 2015) than either distillation or pervaporation alone.

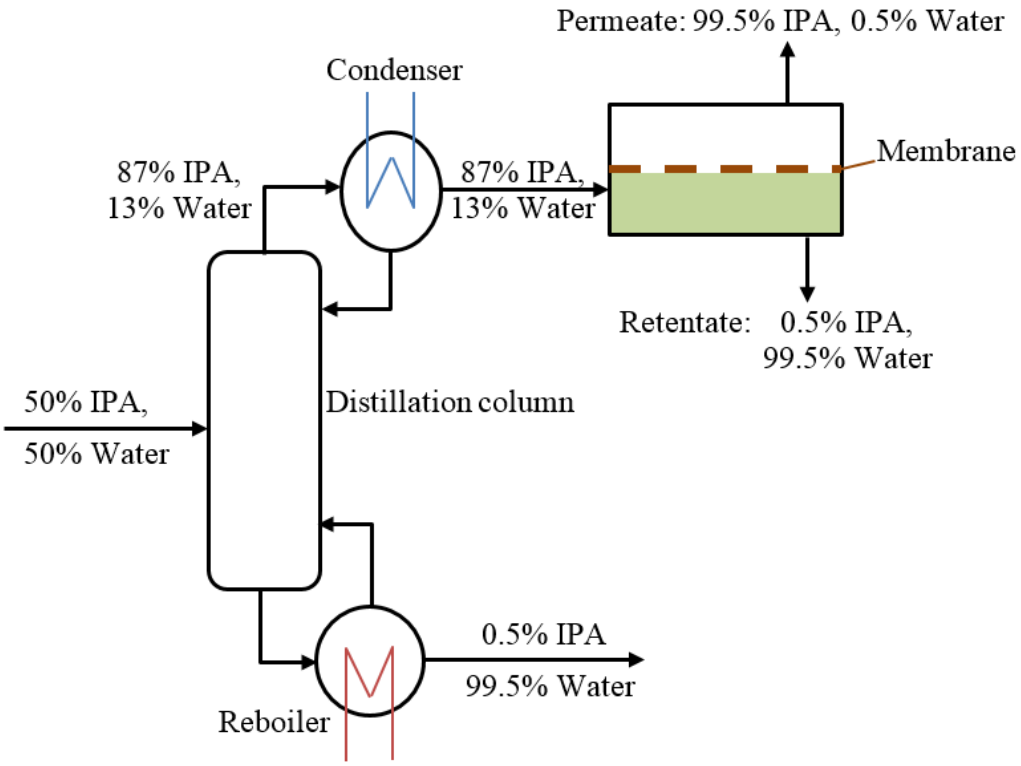

Figure 1.12 Hybrid distillation-pervaporation system for dehydration of IPA.

Feed compositions of <10% water in ethanol (Sommer & Melin, 2004; Huang *et al.*, 2008, Vente, 2010) and < 16% water in IPA are typical (Van Hoof *et al.*, 2004). Baker (2012, p. 395) states that permeate-feed ratios of 3-5% are typical for pervaporation modules. However, many units now incorporate heating, so that there multiple stages within a single module unit, each with a permeate-feed ratio of < 2% (Pfizer, 2018). Furthermore, as flux is proportional to concentration, and as standard equally-sized membrane modules are often used, the permeate-feed ratios for the later stages of such systems, where concentrations are low, are often less than 1%. Thus it is more accurate to state that permeate-feed ratios of up to 5% are used.

Across such a limited concentration range, the permeate composition can be taken to be independent of liquid composition for many commercial membranes (Verkerk *et al.*, 2001; Gallego-Lizon, *et al.*, 2002; Urtiaga *et al.*, 2003; Van Hoof *et al.*, 2004; Pera-Titus *et al.*, 2006; Koczka *et al.*, 2007; Cséfalvay *et al.*, 2008; Niemistö *et al.*, 2013; Boutikos *et al.*, 2014; Koch and Górak, 2014; Kujawski *et al.*, 2017; Kanse, Dawande and Dhanke, 2018; Schmitz *et al.*, 2018; Thiess *et al.*, 2018; Yave, 2019) although there are exceptions (Kujawski *et al.*, 2017). Many commercial membranes have permeate

compositions of greater than 99% (Verkerk *et al*., 2001; Urtiaga *et al*., 2003; Van Hoof *et al*., 2004; Sommer and Melin, 2005; Pera-Titus *et al*, 2006; Koch and Górak, 2014; Klinov *et al*., 2017; Schmitz *et al*., 2018; Yave, 2019): in such cases the permeate composition cannot vary significantly. As variations in permeate concentration within a module are usually not significant, it is reasonable to consider permeate composition to be constant. This simplifies the analysis and modelling of module performance. This is a key assumption that facilitates the modelling of pervaporation systems in this work. Permeate concentration typically plateaus at feed concentrations of between 0.6% and 5% water. Some manufacturers of commercial membranes have focused on increasing the permeate concentration at low water concentrations in recent years (Gladman, 2017).

Industrial solvent dehydration systems normally operate with feed temperatures in the range 105 ºC to 130 ºC (Baker, 2012, p. 402). Sato *et al*. (2012) reported industrial-scale trials for the dehydration of methyl pyrrolidone using zeolite membranes at temperatures of 90ºC to 130ºC. Ethanol has been dehydrated at 150 ºC using sweep gas (Navajas *et al*. 2002; Navajas *et al*. 2006); though this process has not proven to be commercially viable (Baker, 2012, p.400). There have been long-term trials where n-butanol was dehydrated at 150 ºC using hybrid silica membranes (Castricum *et al*., 2008; Kreiter *et al*, 2008; Vente, 2010). Pilot trials at 190 ºC for the dehydration of n-butanol with hybrid organo-silica membranes showed no initial decline in either flux or selectivity (Van Veen *et al*., 2011). Industrial scale trials with isothermal membranes were undertaken at temperatures of up to 150 ºC (Van Veen, 2016). Higher temperatures necessitate high pressures. The boiling pressures of ethanol and isopropanol at 150 ºC are 9.8 and 8.6 bar absolute respectively, whereas n-butanol boils at 2.8 bar at 150 ºC (Yaws, 1999, pp. 159-184). Many systems use steam heating. Saturated steam at 3 bar gauge has a temperature of 143.6 ºC. This is a typical maximum operating temperature. The temperatures at which pervaporation is undertaken in industrial systems are often limited due to the higher costs and additional hazards associated with high-pressure equipment. However, the high boiling temperature of n-butanol allows it to be separated at higher temperatures without the need for high pressures.

1.15 Activation energy of industrial membranes

The most common industrial application of pervaporation is for the dehydration of ethanol and IPA (Baker, 2012, p. 401). Industrial systems normally operate with feed temperatures in the range 100-130 ^{o}C (Baker 2012, pp. 392, 402). As stated in sections 1.12 and 1.14 permeate-feed ratios of up to 5% are used with the corresponding temperature drop in an adiabatic module, ΔT, i.e., $(T_f - T_r)$ being up to 30 K (Baker, 2012, p. 395). Feed compositions of <10% water in ethanol (Sommer & Melin, 2004; Huang *et al*., 2008, Vente, 2010) and < 16% water in IPA are typical (Van Hoof *et al*., 2004).

E_j values for commercial membranes for the dehydration of ethanol and isopropanol are typically in the range 19,000 - 63,000 kJ/kmol, (Van Veen *et al*., 2001; Gallego-Lizon *et al*., 2002; Casado *et al*., 2005; Qiao *et al*., 2005; Huang *et al*., 2006; Sanz and Ghmeling, 2006; Cséfalvay *et al*., 2008; Koch and Górak, 2014). Values as low as 8,600 kJ/kmol for isopropanol dehydrations (Sommer and Melin, 2005) and as high as 81,300 kJ/kmol for the dehydration of 2,2,3,3-tetrafluoropropan-1-ol have been reported (Kujawski *et al*., 2017). High E_j values lead to large reductions in flux within modules. A method for determining the maximum feasible E_j values is proposed using the novel J_r/J_{reheat} ratio in a chapter five. This is the ratio between the flux of the retentate, J_r, and the flux of the retentate after reheating to the feed temperature, J_{reheat}. This will complete the identification of the full range of industrial operating conditions allowing empirical equations to be developed for the modelling of pervaporation modules for industrial systems.

1.16 Recycles

A portion of the retentate can be recycled to the inlet of the preheater as illustrated in Fig. 1.12. This increases the mass flowrate of liquid through the module reducing the temperature drop per unit mass of retentate, thereby increasing the average temperature and average flux (Santoso *et al*., 2012). However, dilution of the feed often significantly counter-acts the increased flux (Santoso *et al*., 2012). The greater the reduction in feed concentration, the less the benefit of a recycle: furthermore, a recycle can reduce

performance in some circumstances (Santoso *et al*., 2012). They modelled recycles for ethanol and IPA dehydrations and found that recycles led to increased flux when the feed water concentration and the E_j values were both high.

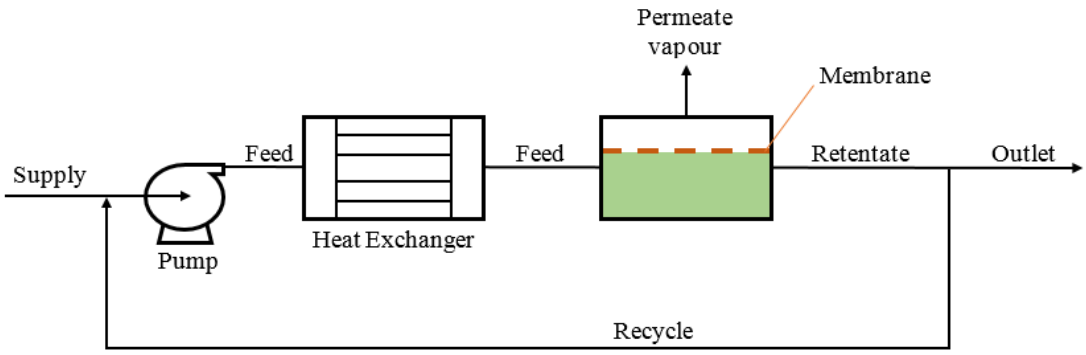

Figure 1.13 Adiabatic pervaporation module with recycle

Tsuyumoto *et al*. (1997), reported the results of a pilot study using industrial-scale equipment where a recycle was used in an ethanol dehydration with a supply concentration of 6%. A recycle on the first stage with its higher water concentration did improve performance, whilst the use of a recycle for the second stage had little effect as the increase in flux due to the higher average temperature was negated by the reduction in flux caused by the lower water concentration. Marriott and Sørensen (2003b) developed a model for optimising the use of a recycle for the same feed conditions; they found that use of a recycle did not significantly change the outlet concentration. Santoso *et al*. (2012) modelled recycles for both ethanol and IPA dehydrations. They found that recycles were of benefit when both the concentration of the water in the feed and the apparent activation energy of pervaporation, E_j, were high. They also found that the greater the reduction in feed concentration, the less the benefit of a recycle.

There are algebraic equations for the calculation of flowrate and composition of the feed to a plug flow reactor with recycle (Levenspiel, 1999): similar equations are developed for pervaporation modules with local recycle in a chapter six. The effect of recycles on throughput, whilst maintaining a constant retentate composition, has not been explored. The effect of a recycle on energy consumption in pervaporation systems needs to be reviewed: these issues are reviewed in chapter six.

1.17 Models of adiabatic pervaporation

In adiabatic systems, the latent heat of vaporisation causes the liquid to cool as it passes through the module, leading to a reduction in the local flux.

Previous approaches to the modelling of pervaporation systems have focused on operating conditions, thermodynamic properties of the fluids, and solute-membrane properties such as diffusivity. The complexity of these models is such that numerical solutions are often required (Bausa and Marquardt, 2000; Marriott and Sorensen, 2003b; Villaleunga and Cohen, 2005; Sosa and Espinosa, 2011; Valentinyi and Mizsey, 2014; Raoufi *et al*., 2018). Villaleunga and Cohen (2005) developed a numerical model of pervaporation for a rectangular plate-and-frame module using coupled Navier–Stokes equations combined with convection-diffusion equations for the component concentrations. Baig (2008) used one-dimensional finite element analysis to model steady state flow through a membrane module. He described the application of the same technique to a batch process, where the temperature drops over time: the temperature versus time profile is similar to the temperature versus residence time of the steady flow model. Computational fluid dynamics, CFD, using finite element analysis has been used to model pervaporation modules (Liu *et al*., 2015). ChemCad software has also been used to simulate pervaporation systems based on the solution-diffusion model (Valentinyi and Mizsey, 2014). Aspen software has also been used (Sommer and Melin, 2004: Van Veen and Pex, 2006; Verhoef *et al*., 2007). Hybrid systems have also been modelled (Sosa and Espinosa, 2011).

Adiabatic endothermic plug flow chemical reactors have been modelled using analytical expressions (Douglas and Eagleton, 1962). Such reactors are akin to plug flow pervaporation: the reaction rate has an Arrhenius relationship with temperature as does flux in pervaporation system. The temperature in such reactors drops as the reaction proceeds. However, pervaporation involves a reduction in the mass of the liquid within a module. This research aims to develop models of ideal adiabatic pervaporation modules.

Flux is independent of feed concentration in some cases: the average flux for such modules is determined analytically. By combining the appropriate mass and energy

balances, an exact analytical expression for the membrane area required to produce a certain mass flowrate of permeate, for systems where flux is independent of liquid concentration, is developed in chapter 3. The range of industrial operating conditions for all relevant parameters "the envelope of industrial operating conditions" is identified. Empirical short-cut equations are developed for the average flux in ideal modules where flux is independent of feed concentration.

Typically, flux is proportional to the water concentration in the liquid phase within the range of concentrations used in industrial applications. Empirical short-cut equations are developed for the average flux in ideal modules where flux is proportional to feed concentration for both ethanol and isopropanol dehydrations in chapter 4.

1.18 Isothermal pervaporation

Industrial systems typically use a series of adiabatic stages with inter-stage heaters which heat the liquid retentate to the feed temperature. Large systems may have a number of parallel modules in a stage. The temperature drop within the stages can be reduced by having a larger number of smaller stages with more frequent re-heating. This leads to an increase in the average operating temperature and consequently an increase in the average flux. In the limit, there would be isothermal operation were there an infinite number of stages. Hence, the development in chapter 2 of exact analytical equations for determining the area of ideal isothermal modules facilitates the analysis of multi-stage systems.

1.19 Models of isothermal pervaporation

Brüschke, (2001, p. 137) states that the membrane area for an ideal isothermal pervaporation module with pure permeate where flux is proportional to liquid concentration can be computed using Eq. (1.16) when the concentrations do not change significantly

$$A = \frac{\dot{m}_f}{J_f / z_i} ln \frac{z_i}{x_i} \tag{1.19}$$

where: A = membrane area (m^2)

$\dot{m}_f$ = the feed flowrate (kg/h)

J_f = the flux at the feed conditions (kg/h.m^2)

z_i = the mass fraction of component *i* in the feed

x_i = the mass fraction of component *i* in the retentate

Brüschke's approximation gives errors of less than 2%, when the retentate composition is 1%, and the feed contains up to 9% water. However, at higher feed compositions, or with higher retentate compositions (even with low $\dot{m}_p/\dot{m}_f$ ratios) the errors are substantial. The equation is analysed in chapter 2. An exact analytical expression is derived for the average flux in isothermal pervaporation modules where flux is proportional to concentration. It is applicable for both pure permeate and for the more general case, where the permeate stream contains solvent.

1.20 Module efficiency

An ideal pervaporation module would have no heat losses and the temperature at any given point would be maximised leading to optimum flux. Ideally, there would be perfect plug flow, with an identical velocity profile across the module and no back-mixing or variation in velocity across channels, albeit that the mass flowrate of the liquid decreases as permeation occurs. The temperature profile of the liquid would be uniform.

An ideal model does not predict actual performance. It does however, give the minimum possible membrane area for a given separation, thereby providing a measure against which the actual performance of pervaporation modules can be assessed. Such an approach is used in other fields, e.g. distillation (McCabe and Thiele, 1925). Sommer *et al*. (2005) proposed an average module efficiency, defined as the actual flux divided by the ideal flux in the absence of any transport resistances. This incorporates inefficiencies due to heat losses as well as those caused by poor flow patterns, pressure drop, temperature polarisation and concentration polarisation. It is akin to the "Murphree Efficiency" in distillation (Murphree, 1925). It permits module performance to be assessed independently of the membrane being used.

The actual membrane area required to achieve a particular separation will be larger than that predicted by an ideal plug flow model. Average flux in a module can be up to 50% less than for an ideal system (Sommer *et al*., 2005). Computational Fluid Dynamics, CFD, models of the temperature distribution within pervaporation modules have been shown to be accurate and confirm results in relation to temperature polarisation (Van der Gulik *et al*., 2002). Fouling can also reduce performance; this is an issue where membranes are in contact with fermentation broths (Dubreuil, *et al*., 2013): however, this is usually not a significant issue for solvent dehydration applications.

Mass transfer on the upstream side of membranes has been found to be rate-limiting for hollow fibre membranes by a number of authors including Crowder and Gooding (1997) and Cussler and Crowder (1998). Baker *et al*. (1997) noted that this could occur even where turbulence is high. Witte *et al*. (2000) modelled high-flux pervaporation membranes. They concluded that tubular modules perform better than standard plate-and-frame arrangements. The effect of concentration polarisation and temperature polarisation on module efficiency has been modelled for isothermal annular-duct type modules (Sommer *et al*., 2005).

Bausa and Marquadt (2000) calculated membrane area by adding 25% to the area required for isothermal operation: this implies a cumulative isothermal efficiency and concentration/temperature polarisation efficiency of 80%. This was based on temperature drops of 10 ^{o}C. This is less than the isothermal efficiency for ideal modules with a ΔT of 10 ^{o}C and so is not feasible. Sosa and Espinosa (2011) assumed an efficiency of 100%. Variations in efficiency within modules and across pervaporation systems are considered in chapter eight.

Turbulence can be achieved through the use of a two-phase feed by partial vaporisation, leading to substantial increase in the module efficiency and substantial reductions in the membrane area (Fontalvo *et al*., 2006a; Fontalvo *et al*., 2006b).

Models of ideal adiabatic plug flow modules provide a standard against which the actual performance of pervaporation modules can be compared. Such models allow modules

of different designs, dimensions and differing operating conditions to be compared. To date there has been limited research as regards the performance of different module designs. Much of this research comprises theoretical models (Karlsson and Tragardh, 1996; Cussler and Crowder, 1998; Witte *et al*., 2000; Sommer *et al*., 2002; Van der Gulik *et al*., 2002) or laboratory scale experiments (Crowder and Gooding, 1997). Sommer *et al*. (2005) modelled isothermal modules, however, such systems are only beginning to be used industrially. There is little data regarding the actual module efficiency of industrial-scale systems. Further research is needed to determine the typical efficiency of industrial pervaporation modules and to develop straightforward methods for the prediction of module efficiency.

1.21 Optimisation of multi-stage adiabatic pervaporation systems

Tsuyumoto *et al*. (1997) operated a 7-stage system whose first two stages had double the membrane area of the later stages. Systems with equal temperature drops have been modelled (Sosa and Espinosa, 2011). However, having an equal temperature drop in each stage requires a different membrane area in each stage; this is not practical for industrial scale plate-and-frame modules as standard size modules are the norm. Use of standard-sized modules is typical for industrial-scale tubular and hollow fibre membranes. Systems with stages of equal size have been modelled: some authors have considered both approaches (Sander and Soukup, 1988; Bausa and Marquadt, 2000). Marriott and Sørenson (2003b) used stages with varying numbers of standard-sized modules: overall area was minimised when the later stages were larger.

An alternative approach is to design systems such that the reduction in water content in each stage is equal, i.e. have an equal concentration gradient in each stage. This approach is considered in chapter 7. Various system layouts are reviewed across the envelope of industrial operating conditions and compared with the minimum possible membrane area for adiabatic multi-stage pervaporation systems where flux is proportional to water concentration. The effect of module efficiency is also considered.

1.22 Progression from previous research

There is a large body of research regarding the precise mechanisms of vapour transport through pervaporation membranes. However, there has been less emphasis on chemical engineering analyses for the prediction of the performance of pervaporation modules (Bausa and Marquadt, 2000; Marriott and Sørenson, 2003a; Marriott and Sørenson, 2003b; Villaleunga and Cohen, 2005; Sosa and Espinosa, 2011; Valentinyi and Mizesy, 2014; Raoufi *et al*., 2018). Vente (2010) cites "predictability" as a barrier to the adoption of pervaporation technology by industry. This is addressed by the development of analytical and short-cut methods for the calculation of membrane area for ideal pervaporation systems for most of the conditions encountered in industrial hydrophilic pervaporation systems, including isothermal pervaporation modules and adiabatic pervaporation modules.

Baker (2012) outlined the range of temperatures and concentrations found in typical hydrophilic pervaporation systems. In this thesis the range of values of the activation energy, E_j, that are feasible in industrial systems is determined. This is the final parameter whose industrial operating range needed to be determined. This allows short-cut approximations to be developed in this thesis that are accurate for the full range of industrial operating conditions.

Santoso *et al*. (2012) analysed the application of recycles to pervaporation systems. This analysis is extended in this work by the development of equations for the calculation of feed flowrate and feed composition for pervaporation systems with local recycle. These equations are analogous to equations for plug flow reactors with recycle (Levenspiel, 1999). Santoso *et al*. (2012) modelled the application of recycles to pervaporation systems whose flux was proportional to concentration. In this thesis a similar analysis is undertaken for systems where flux is independent of concentration.

There is significant literature regarding the performance of pervaporation membranes at laboratory scale. However, considerably less data has been published regarding the performance and energy consumption of industrial-scale pervaporation systems (Sander and Soukup, 1988; Tsuyumoto *et al*., 1997; Kujawski, 2000; Morigami *et al*., 2001; Marriott and Sørenson, 2003b). A limited number of performance metrics have been

proposed in the past including “module efficiency” by Sommer *et al*. (2005) and energy efficiency (Nagy *et al*., 2015). In this thesis the existing performance metrics are reviewed and new performance metrics are proposed. The limited literature data is analysed using these metrics. This is the first time that such data for multiples systems has been compared.

A number of authors have modelled multi-stage pervaporation systems using a variety of approaches such as equally sized modules and modules with equal temperature drops (Sander and Soukup, 1988; Bausa and Marquadt, 2000; Marriott and Sørenson, 2003b; Sosa and Espinosa, 2011). One of the benefits of the short-cut methods developed in this thesis is that they provide an easy route to multi-stage process optimisation. The data provided by Tsuyumoto *et al*. (1997) regarding an industrial-scale system is analysed. In this thesis a multi-stage system with modules using a variety of membranes is modelled for the first time. Sommer *et al*. (2005) modelled the performance of a single isothermal module and provided curves of module efficiency as a function of flux and Reynolds Number. These results were used to determine the efficiency profile of a multi-stage pervaporation system at typical industrial conditions in this thesis.

The ’Pervaporation Separation Index’, *PSI*, is the most commonly used single metric that combines flux and separation characteristics. A number of authors have outlined its inadequacy (Sosa and Espinosa, 2011; Baker, 2012; Toth *et al*., 2018). Commonly used flux and pervaporation metrics are reviewed in this thesis and an alternative metric is proposed that addresses the inadequacies of the PSI by giving appropriate weighting to flux and separation.

Chapter 2: Research Methodology

2.1 Context

Pervaporation has been used commercially since 1982. Sulzer and its licensees had installed over 200 alcohol dehydration units by 2012 (Baker, 2012, p.380). Pervaporation is now a mature and reliable technology for the dehydration of alcohols. It provides significant cost and energy savings in co1.mparison to conventional distillation processes (Scharzec *et al*., 2017). However, there is considerable scope for further implementation of pervaporation.

Previous approaches to the modelling of pervaporation systems have focussed on operating conditions, thermodynamic properties of the solution and solute-membrane properties such as diffusivity. The complexity of these models is such that numerical solutions are often required (Bausa and Marquadt, 2000; Marriott and Sorenson, 2003; Villaleunga and Cohen, 2005; Sosa and Espinosa, 2011; Valentinyi and Mizsey, 2014): e.g. Santoso *et al*. (2012) modelled a pervaporation system using both a microscopic model for the local diffusion rate combined with a macroscopic model of the membrane pervaporation unit. Engineers in manufacturing industry and in design houses who are unfamiliar with pervaporation are reluctant to undertake complex modelling due to the technical competence and the time required. Scharzec *et al*. (2017) suggested that the low level of adoption of the technology is due to the lack of suitable design methodologies. Such methodologies would facilitate consideration of pervaporation during conceptual design of a process. This echoes Vente's statement that end-users are concerned about a lack of "predictability" as regards pervaporation (Vente, 2010): he noted the lack of a "predictive tool".

The lack of simple models of pervaporation systems may also encourage the perception among some potential users and designers that pervaporation is not a mature technology. Operating plants and design houses are reluctant to commit large amounts of capital on what is perceived to be a novel technology as they believe that there is a risk that it will not perform as designed. They are reluctant to be completely dependent on equipment suppliers as regards predicting the performance of significant items of capital equipment (Lynch, 2019). The simple methodologies developed in this thesis go a long way to

providing methods for the sizing of pervaporation equipment using simple algebraic equations: this will allow operating plants and design houses to validate the designs of equipment suppliers, thereby reducing the perceived risk as regards the performance of pervaporation systems when installed.

In 2019, ECN, suppliers of HyBSi membranes provided an Aspen© software tool on their website that predicts the performance of pervaporation tools (ECN, no date). DeltaMem another major supplier of pervaporation systems, expressed an interest in providing simple equations and methodologies for the sizing of pervaporation systems for use by clients during conceptual design (Gladman, 2018). Such methodologies would need to use readily available data if they are to be widely implemented.

The development of simple models allows quantitative problems relating to pervaporation design and performance to be incorporated in university courses. This should increase the profile of pervaporation and thereby increase its adoption by industry.

2.2 Ideal Models

Sommer *et al*. (2005) defined a "module efficiency" for pervaporation modules as being the theoretical minimum membrane area for a module compared to that for an actual module with the same operating conditions. The approach taken in this research is to develop models of ideal pervaporation systems. The membrane area required for an ideal module combined with the "module efficiency" can then be used to determine the actual membrane area required for a given separation. A similar approach using a "column efficiency" is sometimes used in distillation design.

Ideal models are independent of the membrane material and so allow the performance of pervaporation modules and multi-stage systems to be analysed. Ideal models are needed to determine the actual efficiency of pervaporation systems: thereby allowing the effects of parameters such as module type (e.g. flat sheet, spiral wound etc.), module layout, flow patterns and Reynolds Number to be ascertained. This will facilitate

comparisons between different types of modules and the optimisation of the design of pervaporation systems and their operating conditions.

2.3 Selection of research topics

The use of isothermal pervaporation in industrial applications has been increasing since 2016 (Van Veen, 2016). The majority of industrial pervaporation systems are comprised of multiple adiabatic modules in series. The greater the number of stages with inter-stage reheaters, the higher the average temperature and average flux of a system: isothermal operation is equivalent to the limiting case of an infinite number of adiabatic stages. Hence, the average flux in an ideal isothermal module provides a baseline for the analysis of multi-stage adiabatic pervaporation systems. An exact analytical expression is derived for the area of isothermal pervaporation modules where flux is proportional to concentration and for systems where flux is proportional to the square root of the water concentration in the liquid phase. A short-cut approximation is developed for the latter. An exact analytical expression is derived for time as a function of retentate concentration for ideal batch isothermal operations: it will facilitate accurate analysis of data from laboratory-scale tests.

There are systems where the flux is independent of liquid concentration across a range of concentrations. Flux typically has an Arrhenius-type relationship with temperature. Modelling of such systems allows the effects of varying temperature within adiabatic modules to be analysed. An exact analytical solution is derived for the calculation of the ideal average flux in such modules. A simple approximation is developed that is applicable across the full range of industrial operating conditions: it is applicable for the dehydration of many solvents.

The majority of industrial pervaporation modules operate adiabatically and their flux is proportional to concentration. A simple empirical expression was developed that is accurate for ethanol and isopropanol dehydrations across the full range of industrial operating conditions.

The literature is reviewed so as to determine the range of industrial operating conditions: permeate-feed ratios as low as 1% are in fact used. The range of economically feasible activation energies, E_j, is established. This completes the establishment of the full range of industrial operating conditions for all relevant parameters: thereby enabling the short-cut approximations developed in this thesis to be validated.

Santoso *et al*. (2012) modelled the use of recycles in pervaporation systems. In this research mass balances and component balances are used to derive novel simple algebraic equations for the calculation of the feed flowrate and feed composition of recycles. This complements the ideal models of pervaporation modules in facilitating easy analysis of recycle systems. Recycle systems where flux is independent of concentration are analysed for the first time.

The approximate (yet accurate) expressions for the average flux are used to analyse multi-stage pervaporation systems. A variety of approaches to the design of multi-stage systems are analysed and recommendations for the design of such systems are provided. This work provides a basis for the analysis of multi-stage systems which should be undertaken when suitable data relating to the efficiency of industrial-scale systems becomes available.

Ideal models for the vast majority of hydrophilic pervaporation processes used in industry can now be easily undertaken using the analytical solutions and approximate methods developed in this work. This work provides a solid foundation as regards the sizing of pervaporation modules using simple algebraic equations and readily available data, albeit that further research is relating to the efficiency of industrial-scale pervaporation systems. This goes some way to addressing the need for "predictive tools" for pervaporation systems and will thus encourage the more widespread adoption of pervaporation.

Quantitative analysis of pervaporation systems during undergraduate courses can now be undertaken. This will increase the profile of pervaporation as a separation technology. The methods developed in this work address the concerns of Scharzec *et al*. (2017) and Vente (2010) regarding the lack of suitable design methodologies.

2.4 Metrics

There is very little data in the published literature relating to the performance of industrial-scale pervaporation systems. Four papers are analysed (Sander and Soukup, 1988; Tsuyumoto *et al*., 1997; Kujawski, 2000; Morigami *et al*., 2001; Marriott and Sørenson, 2003b); none included comprehensive data. For the first time the actual module efficiency of an industrial-scale pervaporation system is calculated (Tsuyumoto *et al.*, 1997). A novel energy consumption metric is proposed: the steam consumption per unit mass of permeate. This metric allows the energy efficiency of systems with varying feed concentrations and different solvents to be compared. Results for five systems are compared: this is the first time results for multiple industrial-scale operations has been compared. Other performance metrics relating to heat losses and energy recovery are also proposed. Results are calculated for the systems for which literature data was available. The metrics and the results obtained will allow design engineers to estimate the energy consumption of pervaporation systems when conducting feasibility studies. Whilst much work remains to be undertaken in respect of the collection and analysis of data from industrial pervaporation operations, the performance metrics developed in this work lay the foundation for such future research.

The *PSI* is a metric that combines flux and separation. It has an asymptotic relationship with membrane area and energy consumption per unit mass of feed. The weighting given to flux does not sufficiently reflect its commercial importance. A number of authors have either directly or implicitly criticised the *PSI* (Baker, 1991; Sosa and Espinosa, 2011; Toth *et al*., 2018). In attempting to achieve high *PSI* values, some researchers have developed membranes that have high separation factors but inadequate flux. A new metric, the Pervaporation Membrane Index, *PMI*, is proposed. It gives appropriate weighting to flux and concentration and so can be used for the selection of membranes for industrial applications. Much of the published literature relating to the development of new pervaporation membranes has little if any data at industrially relevant concentrations. As the *PMI* is a measure of the performance when the mass fraction of water in the feed is 4%, it will ensure that more data will be published at industrially relevant concentrations.

Chapter 3: Isothermal pervaporation modules.

3.1 Abstract

For the first time exact analytical expressions are derived for the average flux in an ideal isothermal pervaporation module where flux is proportional to concentration and where flux is proportional to the square root of the concentration. A similar approach was used to derive a novel exact analytical expression for time as a function of retentate concentration for ideal batch isothermal operations. Brüschke's approximation (Brüschke, 2001, p. 137) is compared to the analytical solution for an ideal isothermal pervaporation: it is shown to only be accurate for a limited range of conditions.

3.2 Introduction

The use of isothermal pervaporation in industrial applications has been increasing since 2016 (Van Veen, 2016). The majority of industrial pervaporation systems are comprised of multiple adiabatic modules in series. The greater the number of stages with inter-stage reheaters, the higher the average temperature and average flux of a system: isothermal operation is equivalent to the limiting case of an infinite number of adiabatic stages. Hence, the average flux in an ideal isothermal module provides a baseline for the analysis of multi-stage adiabatic pervaporation systems.

There are systems where flux is proportional to concentration. There are systems where the relationship between flux and concentration varies: flux being proportional to concentration at low concentrations and then changing gradually until it is independent of flux at higher concentrations as illustrated in Fig. 3.1. Thus for individual modules the flux may be proportional to concentration, independent of concentration or lie between the two. Each relationship is addressed in turn and analytical solutions for ideal modules are derived.

The average flux for systems where flux is independent of flux and that are operated isothermally is equal to the feed flux

$$J_{av} = J_f \tag{3.1}$$

where J_{av} is the average flux for a module and J_f is the flux at the feed conditions, and is therefore constant.

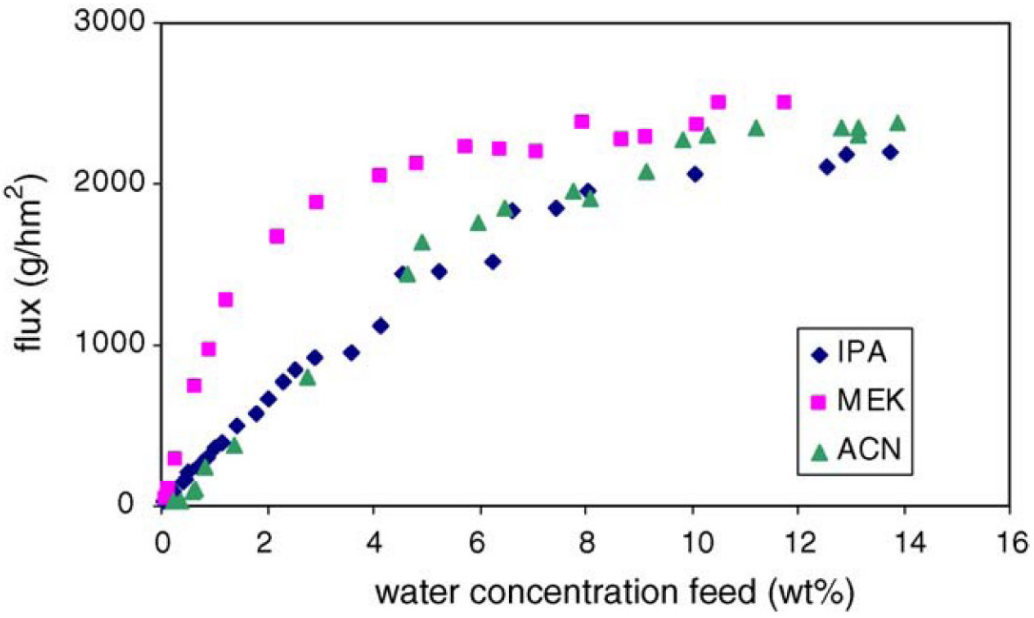

Figure 3.1 Total flux versus water concentration: dehydration with a Mitsui membrane (Van Hoof *et al*., 2006): ♦ isopropanol, ■ methyl-ethyl ketone, ▲ acetonitrile

In cases where flux is proportional to concentration, flux is typically described by an expression of the form

$$J = x_i J_0 e^{-E_j/RT} \tag{3.2}$$

where:
- x_i = the mass fraction of component i in the local liquid i (-)
- E_j = the apparent activation energy of the permeation flux (kJ/kmol)
- R = the universal gas constant (kJ/kmol.K)
- J_o = the maximum possible permeate flux (i.e. the flux as $T \rightarrow \infty$), (kg/s.m^2)
- T = Temperature (K)

The flux in such systems where flux is proportional to concentration and that are operated isothermally can be described by an expression of the form

$$J = \frac{x_i}{z_i} J_f \tag{3.3}$$

where z_i is the mass fraction of component i in the liquid feed.

Sections of the transition zone can often be modelled by equations of the following form,

$$J = \left(\frac{x_i}{z_i} \right)^n J_f \tag{3.4}$$

where n has a value between 0 and 1. A value of zero applies where flux is independent of concentration, whilst a value of unity applies where flux is proportional to concentration. No analytical solution was found for the general case of $0 \leq n \leq 1$. However, an exact analytical solution is derived for the case of $n = 0.5$. A short-cut approximation for the average flux for such systems will be developed for this case. It is applicable throughout the range of industrial operations.

$$J = \left(\frac{x_i}{z_i} \right)^{0.5} J_f \tag{3.5}$$

Batch operation

Isothermal pervaporation can be undertaken as a batch operation: feed circulates from a feed tank through a heater and a membrane module before returning the retentate to the feed tank. This continues until the required retentate concentration is achieved. The temperature of the material in the feed tank rises as retentate is returned to it. Having a feed tank full of hot solvent is neither safe nor practical on an industrial scale. Heat losses from such a tank could be significant. Batch isothermal operation is the norm for laboratory-scale pervaporations. There is minimal variation in concentration or temperature across such membrane modules at any given time; thus they effectively operate on a batch isothermal basis. An exact analytical equation is derived in this chapter for determining retentate composition as a function of time for ideal batch isothermal pervaporation.

Brüschke's approximation

Brüschke (2001, p. 137) stated that the membrane area for an ideal isothermal pervaporation module with pure permeate where flux is proportional to liquid concentration can be computed using Eq. (3.6) when the concentrations do not change significantly. The accuracy and applicability of this approximation is reviewed.

$$A = \frac{\dot{m}_f}{J_f / z_i} ln\left(\frac{z_i}{x_{ir}}\right) \tag{3.6}$$

where: $\dot{m}_f$ = the feed flowrate

x_{ir} = the mass fraction of component *i* in the liquid retentate

3.3 Model development: flux proportional to concentration

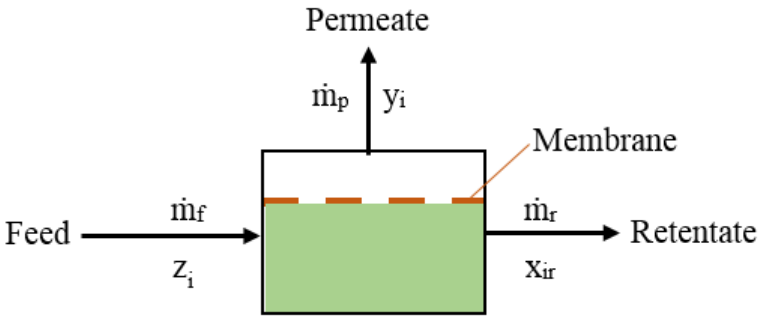

Figure 3.2 Schematic of pervaporation module

A mass balance about a pervaporation module as illustrated in Fig. 3.2 gives

$$\dot{m}_f = \dot{m}_p + \dot{m}_r \tag{3.7}$$

where $\dot{m}_p$ = mass flowrate of permeate through the membrane (kg/h)

$\dot{m}_r$ = mass flowrate of the liquid retentate (kg/h)

A component mass balance about a pervaporation module as illustrated in Fig. 3.2. gives

$$z_i \dot{m}_f = y_i \dot{m}_p + x_{ir} \dot{m}_r \tag{3.8}$$

where y_i is the mass fraction of component *i* in the permeate

Substituting for $\dot{m}_r$ gives $$z_i\dot{m}_f = y_i\dot{m}_p + x_{ir}\left(\dot{m}_f - \dot{m}_p\right) \tag{3.9}$$

Rearranging $$x_{ir} = \frac{z_i - y_i\left(\frac{\dot{m}_p}{\dot{m}_f}\right)}{1-\frac{\dot{m}_p}{\dot{m}_f}} \tag{3.10}$$

Flux in pervaporation is usually defined as mass flux,

$$J \equiv \frac{\dot{m}_p}{A} \tag{3.11}$$

where: J = Permeate flux (kg/m^2/h)

A = membrane area (m^2)

At any given location in the module

$$J = \frac{d\dot{m}_p}{dA} \tag{3.12}$$

where $\dot{m}_p$ is the permeate mass flowrate

Rearranging, $$dA = \frac{1}{J}d\dot{m}_p \tag{3.13}$$

Normalising the permeate mass flowrate by dividing across by the feed flowrate gives

$$\frac{A}{\dot{m}_f} = \int_0^{\frac{\dot{m}_p}{\dot{m}_f}} \frac{1}{J} d\left(\frac{\dot{m}_p}{\dot{m}_f}\right) \tag{3.14}$$

For isothermal pervaporation temperature does not change. Combining Eqs. (3.3) and (3.14) gives

$$\frac{A}{\dot{m}_f} = \int_0^{\frac{\dot{m}_p}{\dot{m}_f}} \frac{1}{\left(\frac{x_i}{z_i}J_f\right)} d\left(\frac{\dot{m}_p}{\dot{m}_f}\right) \tag{3.15}$$

Noting that J_f, the flux at the feed conditions, is constant and rearranging,

$$A = \frac{\dot{m}_f}{J_f} \int_0^{\frac{\dot{m}_p}{\dot{m}_f}} z_i \frac{1}{x_i} d\left(\frac{\dot{m}_p}{\dot{m}_f}\right) \tag{3.16}$$

Combining Eqs. (3.10) and (3.16),

$$A = \frac{\dot{m}_f}{J_f} \int_0^{\frac{\dot{m}_p}{\dot{m}_f}} z_i \left(\frac{1 - \frac{\dot{m}_p}{\dot{m}_f}}{z_i - y_i \left(\frac{\dot{m}_p}{\dot{m}_f}\right)} \right) d\left(\frac{\dot{m}_p}{\dot{m}_f}\right) \tag{3.17}$$

Rearranging,

$$A = \frac{\dot{m}_f}{J_f} \int_0^{\frac{\dot{m}_p}{\dot{m}_f}} \frac{1 - \frac{\dot{m}_p}{\dot{m}_f}}{1 - \frac{y_i}{z_i}\left(\frac{\dot{m}_p}{\dot{m}_f}\right)} d\left(\frac{\dot{m}_p}{\dot{m}_f}\right) \tag{3.18}$$

To simplify this expression, we let

$$u = \frac{\dot{m}_p}{\dot{m}_f} \tag{3.19}$$

therefore

$$A = \frac{\dot{m}_f}{J_f} \int_0^u \frac{1-u}{1-bu} du \tag{3.20}$$

where

$$b = \frac{y_i}{z_i} \tag{3.21}$$

From Eqs. (3.11) and (3.20) it follows that the average flux is given by,

$$J_{av} = \frac{\dot{m}_p}{A} = \frac{\dot{m}_p}{\frac{\dot{m}_f}{J_f} \int_0^u \frac{1-u}{1-bu} du} \tag{3.22}$$

therefore
$$\frac{J_{av}}{J_f} = \frac{\dot{m}_p / \dot{m}_f}{\int_0^{\frac{\dot{m}_p}{\dot{m}_f}} \frac{1-u}{1-bu}\,du} \tag{3.23}$$

Details of the integration are shown in Appendix A. The result was confirmed using both a symbolic integrator (Wolfram integrator®) and by numerical integration using the trapezoidal rule.

$$\int_0^{\frac{\dot{m}_p}{\dot{m}_f}} \frac{1\text{-}u}{1-bu}\,du = \frac{bu-(b-1)ln(1-bu)}{b^2}\Bigg|_0^{\frac{\dot{m}_p}{\dot{m}_f}} \tag{3.24}$$

therefore
$$\frac{J_{av}}{J_f} = \frac{u}{\left[\frac{bu-(b-1)ln(1-bu)}{b^2} - \frac{0-(b-1)ln(1-0)}{b^2}\right]} \tag{3.25}$$

Simplifying,
$$\frac{J_{av}}{J_f} = \frac{b^2 u}{\left[bu-(b-1)ln(1-bu)\right]} \tag{3.26}$$

Substituting for *b* and *u* gives,

$$\frac{J_{av}}{J_f} = \frac{\left(\frac{y_i}{z_i}\right)^2 \dot{m}_p / \dot{m}_f}{\left[\frac{y_i}{z_i}\left(\frac{\dot{m}_p}{\dot{m}_f}\right) - \left(\frac{y_i}{z_i}-1\right)ln\left(1-\frac{y_i}{z_i}\left(\frac{\dot{m}_p}{\dot{m}_f}\right)\right)\right]} \tag{3.27}$$

Noting that,
$$A = \frac{\dot{m}_f}{J_f}\left(\frac{\dot{m}_p / \dot{m}_f}{J_{av} / J_f}\right) \tag{3.28}$$

Hence,
$$A = \frac{\dot{m}_f}{J_f}\left(\frac{z_i}{y_i}\right)^2\left[\frac{y_i}{z_i}\left(\frac{\dot{m}_p}{\dot{m}_f}\right) - \left(\frac{y_i}{z_i}-1\right)ln\left(1-\frac{y_i}{z_i}\left(\frac{\dot{m}_p}{\dot{m}_f}\right)\right)\right] \tag{3.29}$$

Eq. (3.29) allows the ideal membrane area required for a given separation using isothermal pervaporation to be calculated for systems where flux is proportional to concentration. This simple equation only requires readily available data.

3.4 Model development: transition region

As stated previously sections of the transition zone in isothermal modules can be modelled by Eq. (3.5). Combining Eqs. (3.5) and (3.14),

$$\frac{dA}{d\dot{m}_p} = \frac{1}{\left(\frac{x_i}{z_i}\right)^{0.5} J_f} \tag{3.30}$$

Normalising the permeate flowrate by dividing across by the mass flowrate of the feed and rearranging

$$\frac{A}{\dot{m}_f} = \frac{1}{J_f} \int_0^{\frac{\dot{m}_p}{\dot{m}_f}} z_i^{0.5} \frac{1}{x_i^{0.5}} d\left(\frac{\dot{m}_p}{\dot{m}_f}\right) \tag{3.31}$$

Combining Eqs. (3.10) and (3.31) and rearranging

$$A = \frac{\dot{m}_f}{J_f} \int_0^{\frac{\dot{m}_p}{\dot{m}_f}} z_i^{0.5} \frac{1}{\left(\frac{z_i - y_i \frac{\dot{m}_p}{\dot{m}_f}}{1 - \frac{\dot{m}_p}{\dot{m}_f}}\right)^{0.5}} d\left(\frac{\dot{m}_p}{\dot{m}_f}\right) \tag{3.32}$$

Rearranging,

$$A = \frac{\dot{m}_f}{J_f} \int_0^{\frac{\dot{m}_p}{\dot{m}_f}} \left(\frac{1 - \frac{\dot{m}_p}{\dot{m}_f}}{1 - y_i / z_i \frac{\dot{m}_p}{\dot{m}_f}}\right)^{0.5} d\left(\frac{\dot{m}_p}{\dot{m}_f}\right) \tag{3.33}$$

To simplify this expression we let,

$$u = \frac{\dot{m}_p}{\dot{m}_f} \tag{3.34}$$

and

$$b = \frac{y_i}{z_i} \tag{3.35}$$

therefore

$$\frac{AJ_f}{\dot{m}_f} = \int_0^{\frac{\dot{m}_p}{\dot{m}_f}} \left(\frac{1-u}{1-bu}\right)^{0.5} d(u) \tag{3.36}$$

Carrying out the integration using a symbolic integrator (Wolfram integrator®) gives,

$$\int_0^{\frac{\dot{m}_p}{\dot{m}_f}} \left(\frac{1\text{-}u}{1-bu}\right)^{0.5} du = \frac{(b-1)\left[ln\left(\sqrt{b}\sqrt{1-bu}+b\sqrt{1-u}\right)-ln\left(\sqrt{b}\sqrt{1-bu}-b\sqrt{1-u}\right)\right]}{2b^{1.5}} - \frac{\sqrt{1-u}\sqrt{1-bu}}{b}\Bigg|_0^{\frac{\dot{m}_p}{\dot{m}_f}} \tag{3.37}$$

therefore

$$\frac{AJ_f}{\dot{m}_f} = \left\{\frac{(b-1)\left[ln\left(\sqrt{b}\sqrt{1-bu}+b\sqrt{1-u}\right)-ln\left(\sqrt{b}\sqrt{1-bu}-b\sqrt{1-u}\right)\right]}{2b^{1.5}} - \frac{\sqrt{1-u}\sqrt{1-bu}}{b}\right\}$$

$$-\left\{\frac{(b-1)\left[ln\left(\sqrt{b}+b\right)-ln\left(\sqrt{b}-b\right)\right]}{2b^{1.5}} - \frac{1}{b}\right\} \tag{3.38}$$

In section 3.7 some numerical computations are presented with this equation and regression analysis is used to derive a simple and accurate approximation for the average flux.

3.5 Batch operation

A typical batch system is illustrated in Fig. 3.3. Assuming there is little change in composition between the feed, z_i, and retentate, x_{ir}, at any moment in time, this system can be modelled as a batch process where permeate is constantly drawn from the feed tank as shown in Fig. 3.4.

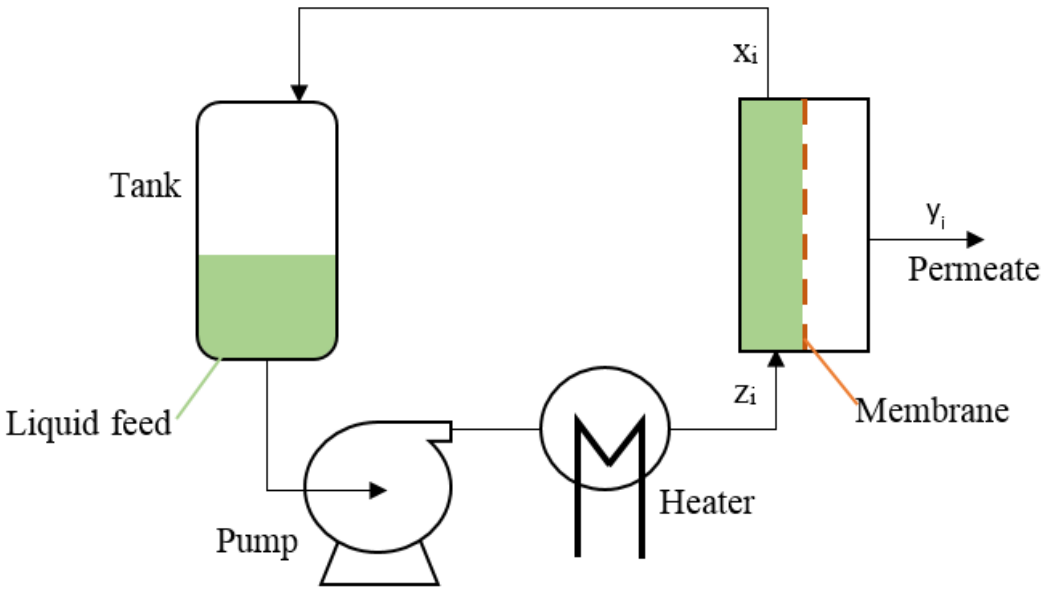

Figure 3.3 Schematic of isothermal batch pervaporation system

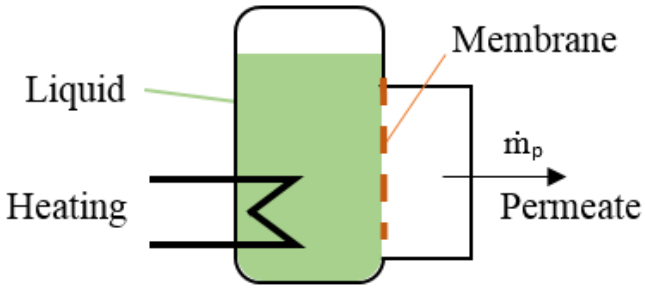

Figure 3.4 Model of isothermal batch pervaporation system.

The mass flowrate of the permeate can be described by an expression of the following form

$$\dot{m}_p = +\frac{dm_p}{dt} \tag{3.39}$$

Noting that $$\dot{m}_p = JA \tag{3.40}$$

where J is the flux and A is the membrane area

thus $$dt = \frac{1}{A}\frac{dm_p}{J} \tag{3.41}$$

For isothermal pervaporation, temperature does not change, so that combining Eqs. (3.3) and (3.41),

$$t = \frac{1}{A}\int_0^{m_p} \frac{1}{\frac{x_i}{z_i}J_f} dm_p \tag{3.42}$$

Normalising by dividing across by m_f and rearranging,

$$\frac{t}{m_f} = \frac{1}{AJ_f}\int_0^{\frac{m_p}{m_f}} z_i \frac{1}{x_i} d\left(\frac{m_p}{m_f}\right) \tag{3.43}$$

where m_f is the initial mass of liquid in the tank. Combining Eqs. (3.10) and (3.43)

$$\frac{t}{m_f} = \frac{1}{AJ_f}\int_0^{\frac{m_p}{m_f}} z_i \left(\frac{1-\frac{m_p}{m_f}}{z_i - y_i\left(\frac{m_p}{m_f}\right)}\right) d\left(\frac{m_p}{m_f}\right) \tag{3.44}$$

Rearranging, $$t = \frac{m_f}{AJ_f}\int_0^{\frac{m_p}{m_f}} \left(\frac{1-\frac{m_p}{m_f}}{1-\frac{y_i}{z_i}\left(\frac{m_p}{m_f}\right)}\right) d\left(\frac{m_p}{m_f}\right) \tag{3.45}$$

To simplify this expression, we let

$$u = \frac{m_p}{m_f} \tag{3.46}$$

therefore $$t = \frac{m_f}{AJ_f}\int_0^{\frac{m_p}{m_f}} \left(\frac{1-u}{1-bu}\right) du \tag{3.47}$$

where,
$$b = \frac{y_i}{z_i} \tag{3.48}$$

$$\int_0^{\frac{m_p}{m_f}} \frac{1\text{-}u}{1-bu}\,du = \frac{bu-(b-1)ln(1-bu)}{b^2}\Bigg|_0^{\frac{m_p}{m_f}} \tag{3.49}$$

thus
$$t = \frac{m_f}{AJ_f}\left[\frac{bu-(b-1)ln(1-bu)}{b^2}\right] \tag{3.50}$$

Substituting for b and u gives,

$$t = \frac{m_f}{AJ_f}\left[\frac{\left(\frac{m_p}{m_f}\right)\frac{y_i}{z_i} - \left(\frac{y_i}{z_i}-1\right)ln\left(1-\frac{y_i}{z_i}\left(\frac{m_p}{m_f}\right)\right)}{\left(\frac{y_i}{z_i}\right)^2}\right] \tag{3.51}$$

Rearranging
$$t = \frac{m_f}{AJ_f}\left(\frac{z_i}{y_i}\right)^2\left[\frac{y_i}{z_i}\left(\frac{m_p}{m_f}\right) - \left(\frac{y_i}{z_i}-1\right)ln\left(1-\frac{y_i}{z_i}\left(\frac{m_p}{m_f}\right)\right)\right] \tag{3.52}$$

Rearranging Eq. (3.10)
$$\frac{m_p}{m_f} = \frac{z_i - x_{ir}}{y_i - x_{ir}} \tag{3.53}$$

Substituting for m_p/m_f

$$t = \frac{m_f}{AJ_f}\left(\frac{z_i}{y_i}\right)^2\left[\frac{y_i}{z_i}\left(\frac{z_i - x_{ir}}{y_i - x_{ir}}\right) - \left(\frac{y_i}{z_i}-1\right)ln\left(1-\frac{y_i}{z_i}\left(\frac{z_i - x_{ir}}{y_i - x_{ir}}\right)\right)\right] \tag{3.54}$$

where x_{ir} is the final composition of the retentate liquid at end of the batch pervaporation run. Eq. (3.54) allows the time required for a given separation using isothermal batch pervaporation process to be calculated for systems where flux is proportional to concentration. This simple equation only requires readily available data.

3.6 Results: batch operation comparison with literature data

Much laboratory scale experimentation involves isothermal batch trials. However, whilst concentration is measured as a function of time, it is rarely published in this form. Rather, flux is calculated and presented as a function of concentration or as a function of temperature using data obtained from several isothermal trials. Accurate determination of flux during laboratory tests can be difficult as evidenced by the results obtained by Gallego-Lizon *et al*. (2002). Eq. (3.53) enables the flux at the feed conditions to be determined if the mass of the feed, the membrane area, the feed composition, retentate composition, permeate composition, and processing time are known. Use of overall and component mass balances combined with the initial and final liquid concentrations allow process data to be determined without permeate flux and concentration data.

Results for laboratory-scale isothermal batch dehydrations of ethanol at three different temperatures (Thiess *et al*., 2018) are compared with data generated using Eq. (3.52) in Fig. 3.5. Results for laboratory scale isothermal batch dehydrations of tert-butanol (Gallego-Lizon *et al*., 2002) are compared with data generated using Eq. (3.52) in Figs. 3.6 and 3.7: some of these runs appear to have been interrupted or to have been affected by a change in temperature.

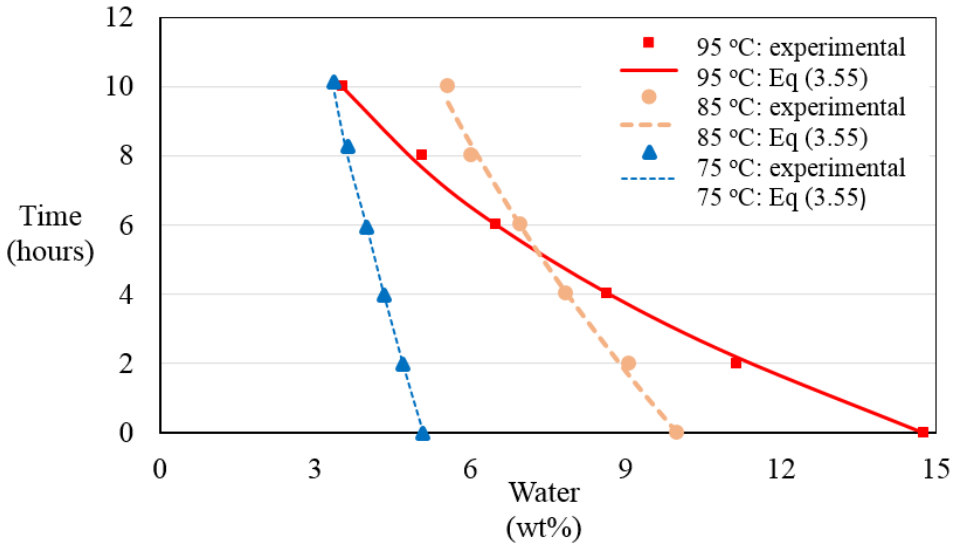

Figure 3.5 Concentration versus time, dehydrations of ethanol with a Pervap 4101™ membrane (Thiess *et al*., 2018): ▲ 75 °C, ● 85 °C and ■ 95 °C. Curves are the corresponding data generated using Eq. (3.52).

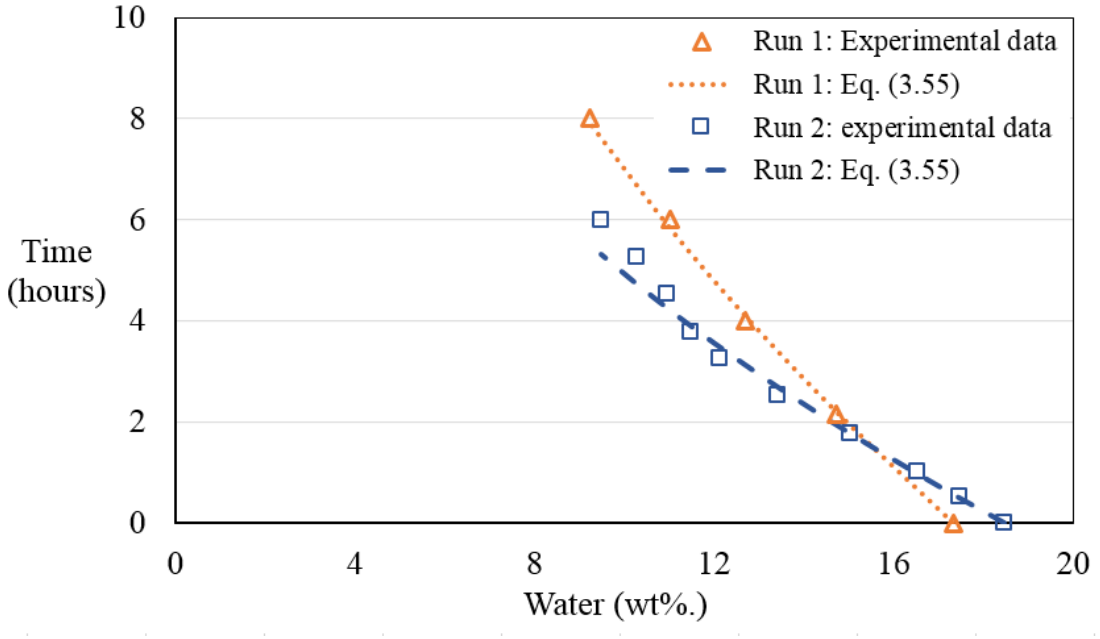

Figure 3.6 Concentration versus time, dehydration of tert-butanol with a Pervap 2510™ membrane (Gallego-Lizon *et al*., 2002). Dashed lines are data generated using Eq. (3.52). Both runs were undertaken at 60 °C.

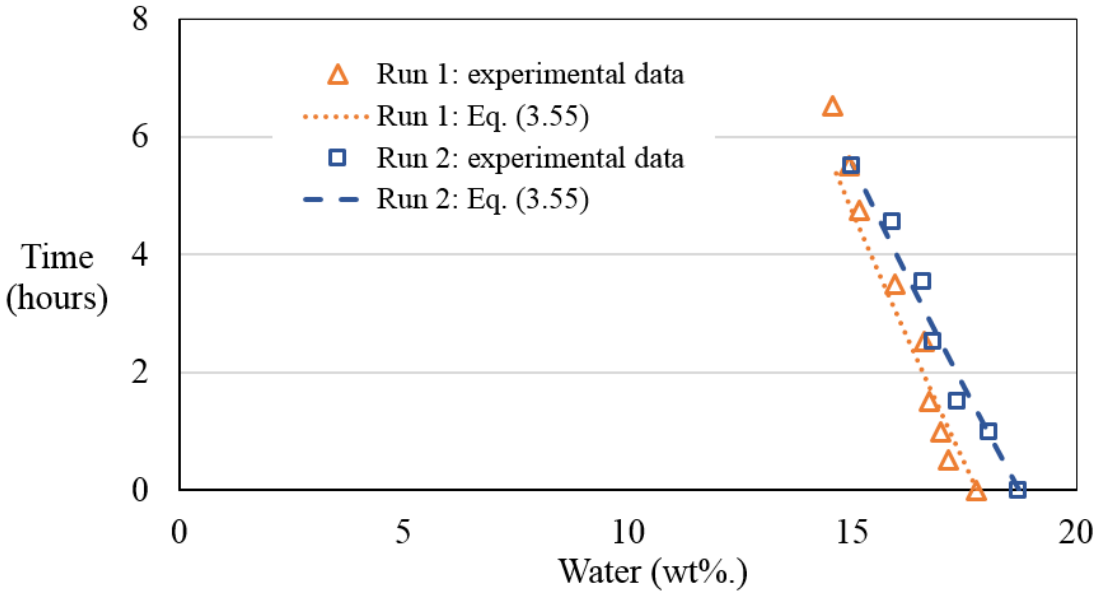

Figure 3.7 Concentration versus time, dehydration of tert-butanol using a Pervap 2202™ membrane (Gallego-Lizon *et al*., 2002). Dashed lines are data generated using Eq. (3.52). Both runs were undertaken at 60 °C.

Accurate data relating to permeate flux can be difficult to obtain, particularly for bench-scale systems. Eq. (3.54) can be rearranged to give Eq. (3.56) allowing the flux at the

feed condition to be determined without flux data. Determination of the membrane area and mass of feed is straightforward. Once the feed concentration, z_i, the permeate concentration, y_i, and the retentate concentration, xi_r at a given point in time are known the initial flux can be determined using Eq. (3.55). This provides an easier and more accurate method for determining flux from bench-scale isothermal trials than was available heretofore.

$$J_f = \frac{m_f}{\Delta t A}\left(\frac{z_i}{y_i}\right)^2\left[\frac{y_i}{z_i}\left(\frac{z_i - x_{ir}}{y_i - x_{ir}}\right) - \left(\frac{y_i}{z_i} - 1\right) ln\left(1 - \frac{y_i}{z_i}\left(\frac{z_i - x_{ir}}{y_i - x_{ir}}\right)\right)\right] \qquad (3.55)$$

Eq. (3.55) allows the flux at the initial conditions for an isothermal batch process to be calculated for systems where flux is proportional to concentration. This simple equation only requires readily available data. This will be of benefit when analysing laboratory-scale data.

3.7 Results: applicability of Brüschke's approximation

Brüschke's approximation of the area for an ideal isothermal pervaporation module with pure permeate where flux is proportional to liquid concentration can be computed using Eq. (3.6).

$$A = \frac{\dot{m}_f}{J_f / z_i} ln\left(\frac{z_i}{x_{ir}}\right) \qquad (3.6)$$

Assuming pure permeate, i.e. y_i = 1, the exact analytical expression, Eq. (3.29), simplifies to,

$$A = \frac{\dot{m}_f}{J_f}\left[\frac{\left(\frac{1}{z_i}\right)\left(\frac{\dot{m}_p}{\dot{m}_f}\right) - \left(\left(\frac{1}{z_i}\right) - 1\right) ln\left(1 - \left(\frac{1}{z_i}\right)\left(\frac{\dot{m}_p}{\dot{m}_f}\right)\right)}{\left(\frac{1}{z_i}\right)^2}\right] \qquad (3.56)$$

Rearranging,

$$A = \frac{\dot{m}_f}{J_f / z_i}\left[\frac{\dot{m}_p}{\dot{m}_f} - (1 - z_i) ln\left(1 - \frac{1}{z_i}\left(\frac{\dot{m}_p}{\dot{m}_f}\right)\right)\right] \qquad (3.57)$$

Substituting for $\dot{m}_p/\dot{m}_f$ as per Eq. (3.53)

$$A = \frac{\dot{m}_f}{J_f / z_i}\left[\left(\frac{z_i - x_{ir}}{1 - x_{ir}}\right) - (1 - z_i)\,ln\left(1 - \frac{1}{z_i}\left(\frac{z_i - x_{ir}}{1 - x_{ir}}\right)\right)\right] \quad (3.58)$$

Assuming that x_i is small and that therefore, 1-x_i, can be approximated as unity, gives,

$$A = \frac{\dot{m}_f}{J_f / z_i}\left[z_i - x_{ir} - (1 - z_i)\,ln\left(1 - \frac{z_i - x_{ir}}{z_i}\right)\right] \quad (3.59)$$

$$A = \frac{\dot{m}_f}{J_f / z_i}\left[ln\left(\frac{z_i}{x_{ir}}\right) + z_i - x_{ir} - z_i ln\left(\frac{z_i}{x_{ir}}\right)\right] \quad (3.60)$$

This has some similarities with Brüschke's approximation, Eq. (3.6). However, despite the simplifying assumption that the term, 1-$x_i \approx 1$, it nonetheless includes additional terms.

To compare Brüschke's approximation with the exact analytical expression, a realistic range of values for the parameters x_i and z_i needs to be established. Typically, a retentate composition, x_i, of 1% is desired. Feed compositions of < 10% water in ethanol (Sommer & Melin, 2004; Huang *et al*., 2008) and < 16% water in IPA are typical (Van Hoof *et al*., 2004). Permeate feed-ratios as low as 1% are used as discussed in section 1.14. Therefore the minimum feed concentration, z_i, is 2% and the maximum retentate composition, x_{ir}, is 15%. High $\dot{m}_p/\dot{m}_f$ ratios are feasible with isothermal systems, as the flux does not drop due to lower temperatures and so there is no need for inter-stage heating. Thus a module with a feed containing 16% water and retentate containing 1% water is conceivable.

Brüschke's approximation gives errors of less than 2%, when the retentate composition is 1%, and the feed contains up to 9% water. However, at higher feed compositions, or with higher retentate compositions (even with low $\dot{m}_p/\dot{m}_f$ ratios) the errors are substantial as illustrated in Fig. 3.8. Brüschke stated that his approximation was only valid for pure permeate combined with low $\dot{m}_p/\dot{m}_f$ ratios: however, it is not accurate for low $\dot{m}_p/\dot{m}_f$ ratios

when x_i is significantly greater than 1%. In contrast, the exact analytical expression is applicable for all $\dot{m}_p/\dot{m}_f$ ratios and for all retentate concentrations. Brüschke's equation is derived in Appendix B.

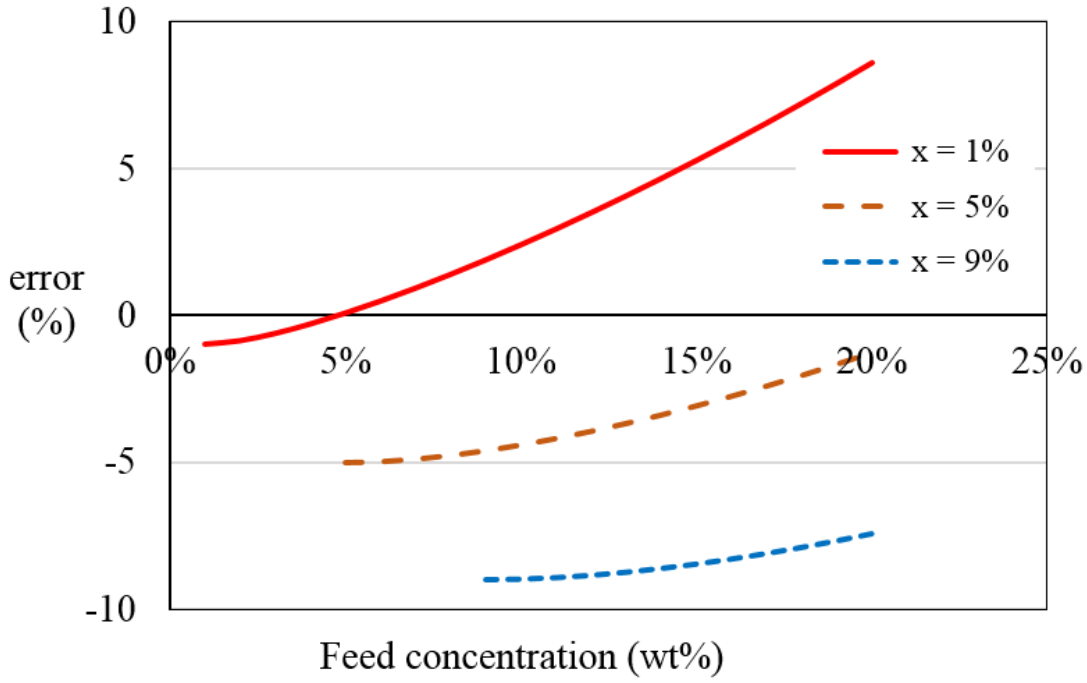

Figure 3.8 Error versus feed concentration (wt%) using Brüschke's approximation for the calculation of dimensionless area, $AJ_f/\dot{m}_f$, for x_{ir} = 1%, x_{ir} = 5% and x_{ir} = 9%.

3.8 Approximate expression for the transition region

While Eq. (3.38) poses no great computational challenges, it would be desirable to obtain a more user-friendly version of this equation.

$$\frac{AJ_f}{\dot{m}_f} = \left\{ \frac{(b-1)\left[ln\left(\sqrt{b}\sqrt{1-bu}+b\sqrt{1-u}\right) - ln\left(\sqrt{b}\sqrt{1-bu}-b\sqrt{1-u}\right)\right]}{2b^{1.5}} - \frac{\sqrt{1-u}\sqrt{1-bu}}{b} \right\}$$
$$- \left\{ \frac{(b-1)\left[ln\left(\sqrt{b}+b\right) - ln\left(\sqrt{b}-b\right)\right]}{2b^{1.5}} - \frac{1}{b} \right\} \qquad (3.38)$$

The first task in this process is to establish a realistic range of values for the parameters b and u. As discussed in section 3.7, $2\% \leq z_i \leq 16\%$. Thus assuming a permeate

concentration of at least 90% water, values of b, where $b = y_i/z_i$, will range from 5.625 to 50.0 The equation pertains to the transition zone, which is of limited range and is unlikely to extend beyond a 5% change in water concentration. Thus the maximum u value is 0.05. The permeate-feed ratio can be calculated by mass balance as in Eqs. (3.46) and (3.53),

$$u = \frac{\dot{m}_p}{\dot{m}_f} = \frac{z_i - x_i}{y_i - x_i} \tag{3.54}$$

As $1\% \le x_i \le 15\%$, this gives values of u between 0.010 and 0.152. Fig. 3.9 is a plot of J_{av} / J_f versus J_r / J_f for the full range of u and b values outlined above, i.e. the full range of industrial operating conditions for ethanol and isopropanol dehydrations. The following equation is proposed to approximate the simulated data,

$$\frac{J_{av}}{J_f} = c\left(\frac{J_r}{J_f}\right) + (1-c) \tag{3.61}$$

For c = 0.493, the maximum error is less than 0.2%, whilst for c = 0.5 the maximum error is less than 0.7%.

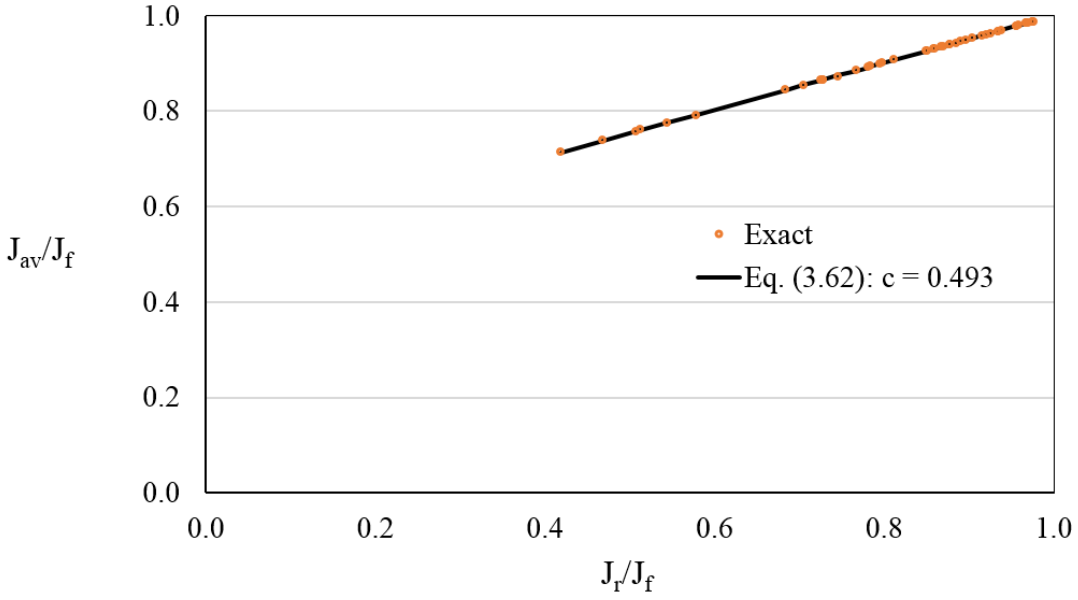

Figure 3.9 J_{av}/J_f versus J_r/J_f for industrial operating conditions. Curve denotes Eq. (3.61) with c = 0.493

Noting that $$J_{av} = \frac{\dot{m}_p}{A} \tag{3.62}$$

Combining Eqs. (3.61) and (3.62) the simplified design equation becomes,

$$A = \frac{\dot{m}_f}{J_f} \frac{\dot{m}_p / \dot{m}_f}{\left[c\frac{J_r}{J_f} + (1-c) \right]} \tag{3.63}$$

Simplifying, $$A = \frac{\dot{m}_p}{\left[cJ_r + (1-c) J_f \right]} \tag{3.64}$$

It is at the discretion of the designer as to which value of c to use. When $c = 0.5$, Eq. (3.64) reduces to

$$J_{av} = \frac{J_r + J_f}{2} \tag{3.65}$$

and Eq. (3.65) reduces to $$A = \frac{2\dot{m}_p}{\left[J_r + J_f \right]} \tag{3.66}$$

Eq. (3.66) allows the time required for a given separation using an isothermal batch pervaporation process to be calculated for systems where flux is proportional to concentration to the power of 0.5. This simple equation only requires readily available data. This equation is valid for any solvent-solute combination, at any temperature, for systems where the feed composition is no greater than 16%, the retentate composition is at least 1% and where $\dot{m}_p/\dot{m}_f \leq 5\%$.

3.9 Conclusions

An exact analytical expression for the membrane area of an ideal isothermal pervaporation module has been derived for systems where flux is proportional to concentration. This expression is applicable to all separations. An exact analytical expression for the area of isothermal pervaporation modules has been derived for

systems where flux is proportional to the square root of the water concentration in the liquid phase. This expression is applicable for all solvent-solute systems and at all temperatures. A simple approximation for this latter case has been developed for all separations with feed concentrations of up to 16% and retentate concentrations as low as 1% where $\dot{m}_p/\dot{m}_f \leq 5\%$.

An exact analytical expression has been derived for time as a function of retentate concentration for ideal isothermal operations. This expression will facilitate accurate analysis of laboratory-scale tests, including of flux at the initial feed concentration.

There are module designs where the liquid is reheated many times, with $\dot{m}_p/\dot{m}_f$ ratios ranging from as low as 1% to 5% (Baker, 2012, p. 395) or higher. The equations developed in this chapter facilitate comparison of such modules with ideal isothermal modules. The equations also facilitate comparison of multi-stage pervaporation systems with the performance of comparable isothermal pervaporation systems thereby facilitating optimisation of system designs.

Brüschke's approximation (Brüschke, 2001, p. 137) has been compared to the analytical solution for an ideal isothermal pervaporation: the approximation has been found to only be accurate for a limited range of conditions.

Chapter 4: Pervaporation where flux is independent of concentration

4.1 Abstract

Assuming a concentration-independent flux with an Arrhenius dependence on temperature, and using temperature- and composition-averaged physical properties, an exact analytical expression is derived for the average flux in an adiabatic pervaporation module. The range of feasible activation energies of permeation, E_j, is established for IPA-water and ethanol-water systems. Within this range, and over the range of typical operating conditions, a novel short-cut approximation to the exact analytical expression is derived that allows the normalised average flux to be estimated for the dehydration of many solvents.

4.2 Introduction

Hot liquid feed contacts one side of a membrane and vapour permeates through a selective membrane. In industrial systems that operate adiabatically, the latent heat of vaporisation causes the liquid to cool as it passes through the module, leading to a reduction in the local flux. This complicates somewhat the underlying mathematics of these systems and, consequently, the development of a simple and accurate method for computing the average flux as a function of feed and retentate conditions would be an important step forward in the analysis and design of pervaporation systems (Bausa and Marquardt, 2000; Marriott and Sørensen, 2003b).

While both Feng and Huang (1997) and Baker *et al*. (2010) recommend that pervaporation performance data be reported in terms of permeance, the reality remains that most data continues to be reported in terms of flux (Chapman *et al*., 2008; Baker *et al*, 2010). Thus for the design engineer at least, it is important to formulate pervaporation design equations in terms of flux. For most systems, flux is a function of both permeability and the saturated vapour pressure of the liquid. Both of these parameters have Arrhenius-type temperature dependencies (Feng and Huang, 1997) and thus the flux is typically given by an expression of the form

$$J = J_0 \mathrm{e}^{-E_j/RT} \tag{4.1}$$

where: E_j = the apparent activation energy of the permeation flux (kJ/kmol)

R = the universal gas constant (kJ/kmol.K)

J_o = the maximum possible permeate flux (i.e. the flux as T $\rightarrow \infty$), (kg/s.m^2)

T = Temperature (K)

By combining the appropriate mass and energy balances with Eq. (4.1), an expression is derived in this chapter for the membrane area required to produce a certain mass flowrate of permeate. Based on this analysis, a simple approximate expression for the average flux is derived, thus providing a straightforward methodology for pervaporation system design. This requires knowledge of the flux at the feed and retentate conditions only.

4.3 Model Development

Pervaporation flux is a function of solute concentration in many applications. However, there are some membranes for which flux is constant across a range of concentrations (Verkerk *et al*., 2001; Sommer and Melin, 2005; Pera-Titus *et al*., 2006; Van Hoof *et al*., 2006); this chapter considers such systems. Hence, it is assumed throughout this chapter, that the local flux is a function of the local temperature only and not the local concentration of the permeating solute.

Let $\dot{m}$ be the mass flowrate and let T be the temperature at a point in the channel. The heat balance can then be written in differential form as

$$d\left(\dot{m}c_pT\right) = -Jh_v dA \tag{4.2}$$

where J is the local mass flux of permeate, c_p is the local specific heat capacity, h_v is the local enthalpy per unit mass of vapour and dA represents the differential area. The relevant mass balance is

$$d\dot{m} = -JdA \tag{4.3}$$

Dividing Eq. (4.2) by Eq. (4.3) gives

$$d\left(\dot{m}c_pT\right) = h_v d\dot{m} \tag{4.4}$$

Assuming c_p is constant $$c_p T + \dot{m} c_p \frac{dT}{d\dot{m}} = h_v \tag{4.5}$$

Rearranging $$\frac{dT}{h_v - c_p T} = \frac{d\dot{m}}{\dot{m} c_p} \tag{4.6}$$

$$\int_{T_f}^{T} \frac{dT}{\frac{h_v}{c_p} - T} = \int_{\dot{m}}^{\dot{m}_f} \frac{d\dot{m}}{\dot{m}} \tag{4.7}$$

where the *f* subscript denotes the feed and the subscript *r* denotes the retenate. Assuming constant or appropriately averaged physical properties, this can be integrated to give

$$ln \frac{\left(\frac{h_v}{c_p}\right) - T_r}{\left(\frac{h_v}{c_p}\right) - T_f} = ln\left(\frac{\dot{m}_f}{\dot{m}_r}\right) \tag{4.8}$$

therefore $$T_r = \frac{h_v}{c_p} - \left(\frac{h_v}{c_p} - T_f\right)\frac{\dot{m}_f}{\dot{m}_r} \tag{4.9}$$

Rearranging Eq. (4.3) $$\frac{dA}{d\dot{m}} = \frac{-1}{J} \tag{4.10}$$

Combining Eqs. (4.1) and (4.10)

$$\frac{dA}{d\dot{m}} = \frac{-1}{J_0 e^{-E_j/RT}} \tag{4.11}$$

Combining Eqs. (4.9) and (4.11) gives

$$\frac{dA}{d\dot{m}} = -\frac{1}{J_o} e^{\frac{E_j}{R\left[\frac{h_v}{c_p} - \left(\frac{h_v}{c_p} - T_f\right)\frac{\dot{m}_f}{\dot{m}}\right]}} \tag{4.12}$$

Therefore the total area is found from computing the integral below:

$$A = \frac{1}{J_o} \int_{\dot{m}_r}^{\dot{m}_f} exp\left(\left(E_j / RT_f\right) / \left(\frac{h_v}{c_p T_f} - \left(\frac{h_v}{c_p T_f} - 1\right)\frac{\dot{m}_f}{\dot{m}}\right)\right) d\dot{m} \tag{4.13}$$

To simplify this expression, we let

$$s = \frac{\dot{m}}{\dot{m}_f} \tag{4.14}$$

therefore

$$A = \frac{\dot{m}_f}{J_0} \int_{1-\dot{m}_p/\dot{m}_f}^{1} e^{\frac{a}{b-(b-1)/s}} ds \tag{4.15}$$

where,

$$a = \frac{E_j}{RT_f} \tag{4.16}$$

and

$$b = \frac{h_v}{c_p T_f} \tag{4.17}$$

The average flux is given by

$$J_{av} = \frac{\dot{m}_p}{A} \tag{4.18}$$

Combining Eqs. (4.15) and (4.18) gives

$$J_{av} = \frac{\dot{m}_p}{\frac{\dot{m}_f}{J_o} \int_{1-\dot{m}_p/\dot{m}_f}^{1} e^{\frac{a}{b-(b-1)/s}} ds} \tag{4.19}$$

Dividing across by J_f

$$\frac{J_{av}}{J_f} = \frac{1}{J_f} \frac{\dot{m}_p}{\frac{\dot{m}_f}{J_o} \int_{1-\dot{m}_p/\dot{m}_f}^{1} e^{\frac{a}{b-(b-1)/s}} ds} \tag{4.20}$$

Noting that

$$J_f = J_0 \mathrm{e}^{-E_j/RT_f} \tag{4.21}$$

Substituting for the compound term E_j/RT_f using Eq. (4.16) gives

$$J_f = J_0 \mathrm{e}^{-a} \tag{4.22}$$

Substituting J_f in Eq. (4.20) with Eq. (4.22) gives

$$\frac{J_{av}}{J_f} = \frac{1}{J_o e^{-a}} \frac{\dot{m}_p}{\frac{\dot{m}_f}{J_o} \int_{1-\dot{m}_p/\dot{m}_f}^{1} e^{\frac{a}{b-(b-1)/s}} ds} \tag{4.23}$$

The J_o terms cancel so that

$$\frac{J_{av}}{J_f} = \frac{1}{e^{-a}} \frac{\dot{m}_p}{\dot{m}_f \int_{1-\dot{m}_p/\dot{m}_f}^{1} e^{\frac{a}{b-(b-1)/s}} ds} \tag{4.24}$$

Rearranging

$$\frac{J_{av}}{J_f} = \frac{\left(\dot{m}_p/\dot{m}_f\right) e^{a}}{\int_{1-\dot{m}_p/\dot{m}_f}^{1} e^{\frac{a}{b-(b-1)/s}} ds} \tag{4.25}$$

Carrying out the integration using a symbolic integrator (Mathematica®) gives

$$\int_{1-\dot{m}_p/\dot{m}_f}^{1} e^{\frac{a}{b-(b-1)/s}} ds = \left. \frac{b\left(b\left(s-1\right)+1\right) e^{\frac{as}{b(s-1)+1}} - a\left(b-1\right) e^{a/b} Ei\left(\frac{a\left(b-1\right)}{b\left(b\left(s-1\right)+1\right)}\right)}{b^2} \right|_{1-\dot{m}_p/\dot{m}_f}^{1} \tag{4.26}$$

therefore

$$\frac{J_{av}}{J_f} = \frac{b^2 e^{a} p}{be^{a} - a\left(b-1\right) e^{a/b} Ei\left(\frac{a\left(b-1\right)}{b}\right) - b\left(1-bp\right) e^{\frac{a(1-p)}{1-bp}} + a\left(b-1\right) e^{a/b} Ei\left(\frac{a\left(b-1\right)}{b\left(1-bp\right)}\right)} \tag{4.27}$$

where *Ei* is the Exponential Integral, a special function that has been shown to occur in the analysis of ultrafiltration systems (Foley, 2011), and *p* is defined by

$$p = \frac{\dot{m}_p}{\dot{m}_f} \tag{4.28}$$

The Exponential Integral can be computed readily with advanced computation packages but also from its series definition, Eq. (4.29) (Abramowitz, 1972) using spreadsheet software (Foley, 2011)

$$\mathrm{Ei} = \gamma + \ln|\mathrm{y}| + \sum_{n=1}^{\infty} \frac{y^n}{n!n} \tag{4.29}$$

where, γ is the Euler-Mascheroni constant. However, in cases such as this, involving a definite integral, the constant cancels and so does not affect the final calculations.

In section 4.4, some numerical computations are presented with this equation and regression analysis is used to derive a simple and accurate approximation for the average flux.

4.4 Results and Discussion

It would be desirable to obtain a more user-friendly version of Eq. (4.27), one that might be analogous to Cheryan's well-known expression for the average flux in batch ultrafiltration (Cheryan, 1998). Cheryan proposed that batch times can be accurately computed by taking the average flux to be the arithmetic mean of the initial and final fluxes, thus avoiding the need for numerical integration.

The first task in this process is to establish a realistic range of values for the parameters *a*, *b* and *p*. As discussed in section 1.14, industrial systems normally operate with feed temperatures in the range 100-130°C (Baker 2012, pp. 392,402). Baker states that the typical change in temperature, ΔT, i.e., $(T_f - T_r)$ is 15–30 K (Baker, 2012, p. 395). A permeate mass flowrate of 3 – 5 % of the feed is typical for industrial systems (Baker, 2012, p. 395) albeit that lower $\dot{m}_p/\dot{m}_f$ ratios are also used as discussed in section 1.14. Feed compositions of < 10% water in ethanol (Sommer & Melin, 2004; Huang *et al*., 2008) and < 16% water in IPA are typical (Van Hoof *et al*., 2004).

As discussed in section 1.14 it is reasonable to assume that permeate composition is constant. Feed in industrial systems flows through a series of adiabatic pervaporation modules. In order to maintain the flux in each module at sufficiently high values, the retentate is reheated to the initial feed temperature prior to entering subsequent modules. Over-frequent reheating leads to complexity; the additional cost of piping and valves

can be significant (Baker, 2012, p. 395). The optimum membrane area thus depends on the relative cost of membranes versus that of reheating equipment. Studies have suggested that a fixed temperature drop be used for each stage (Bausa and Marquardt, 2000) or that an equal membrane area be used for each stage (Bausa and Marquardt, 2000; Sosa and Espinosa, 2011). It is proposed here that a minimum J_r / J_f ratio of 0.4 be used and, on this basis, a maximum commercially feasible value of E_j can be computed. Sosa and Espinosa (2011) used fixed temperature drops with J_r / J_f ratios of greater than 0.5. J_r/J_{reheat} ratios will be discussed further in section 5.3, 5.4 5.5 an 5.6 Building on this approach, one can write

$$\frac{J_r}{J_f} = J_o e^{-\frac{E_j}{RT_r}} / J_o e^{-\frac{E_j}{RT_f}} \tag{4.30}$$

$$\frac{J_r}{J_f} = e^{-\frac{E_j}{RT_r}} / e^{-\frac{E_j}{RT_f}} \tag{4.31}$$

This expression is independent of J_0. Rearranging and applying the 0.4 criterion gives the following expression for the maximum value of E_j for industrial operations:

$$E_j^{max} = \frac{R \ ln 0.4}{\left(1/T_f - 1/T_r\right)} \tag{4.32}$$

For a given value of T_f, the retentate temperature in this equation is given by Eq. (4.9) as

$$T_r = \frac{h_v}{c_p} - \left(\frac{h_v}{c_p} - T_f\right)\frac{1}{1-p} \tag{4.33}$$

Which, for $p = 0.03$, becomes

$$T_r = \frac{h_v}{c_p} - \left(\frac{h_v}{c_p} - T_f\right)\frac{1}{1-0.03} \tag{4.34}$$

Alternatively, where latent heat data, λ, is available the following equation can be used

$$T_r = \frac{(1\text{-}p)\, c_{p1} T_f \ + 0.5p \ c_{p2} T_f \text{ - } p\lambda}{0.5p \ c_{p2} \ + \ (1\text{-}p)\, c_{p1}} \tag{4.35}$$

where: c_{p1} is the latent heat of the permeate in the liquid phase

c_{p2} is the latent heat of the retentate

Note, that if this value for T_r is such that $\Delta T > 30$ K, then

$$E_j^{max} = \frac{R \ ln 0.4}{\left(1/T_f - 1/\left(T_f - 30\right)\right)} \tag{4.36}$$

Table 4.1 Envelope of industrial operating conditions

- $J_r/J_f \geq 0.4$
- $\dot{m}_p/\dot{m}_f \leq 0.05$
- $100\,^{o}\text{C} \leq T_f \leq 130\,^{o}\text{C}$
- $y_i \geq 0.80$
- For ethanol: $z_f \leq 10\%$, for IPA: $z_f \leq 16\%$.
- 19,000 kJ/kmol $\leq E_j \leq$ 63,000 kJ/kmol.
- $T_f - T_r \leq 30\,^{o}\text{C}$

These equations establish a method for determining the maximum economically feasible value of E_j for industrial operations. In summary, the procedure for computing the average flux over a range of operating conditions using Eq. (4.27) is outlined in Table 4.2.

Table 4.2 Algorithm for generating average flux data

- For given values of T_f and feed composition, choose a value of p between 0.03 and 0.05 inclusive, and a permeate composition between 0.8 and 1.0 inclusive.
- Calculate the maximum value of E_j for these conditions. Choose a value of E_j less than or equal to this value.
- Evaluate the retentate composition by mass balance.
- Estimate a value of T_r and using this value, compute the weighted average values of h_v and c_p (Majer and Svoboda, 1985; Yaws, 1999). Iterate on Eq. (4.34) or Eq. (4.35) to obtain T_r.
- Compute J_r / J_f.
- Evaluate parameters a and b using Eqs. (4.16) and (4.17).
- Compute J_{av} / J_f using Eq. (4.27)
- Repeat for all combinations of the following parameters across the full range of industrial conditions: permeate to feed ratio *(p)*, feed composition, permeate composition, feed temperature and E_j.

Figs. 4.1 and 4.2 are plots of J_{av} / J_f versus J_r / J_f for the full range of industrial operating conditions examined for ethanol and IPA dehydration. The following equation was proposed to approximate the simulated data

$$\frac{J_{av}}{J_f} = \left(\frac{J_r}{J_f} \right)^n \tag{4.37}$$

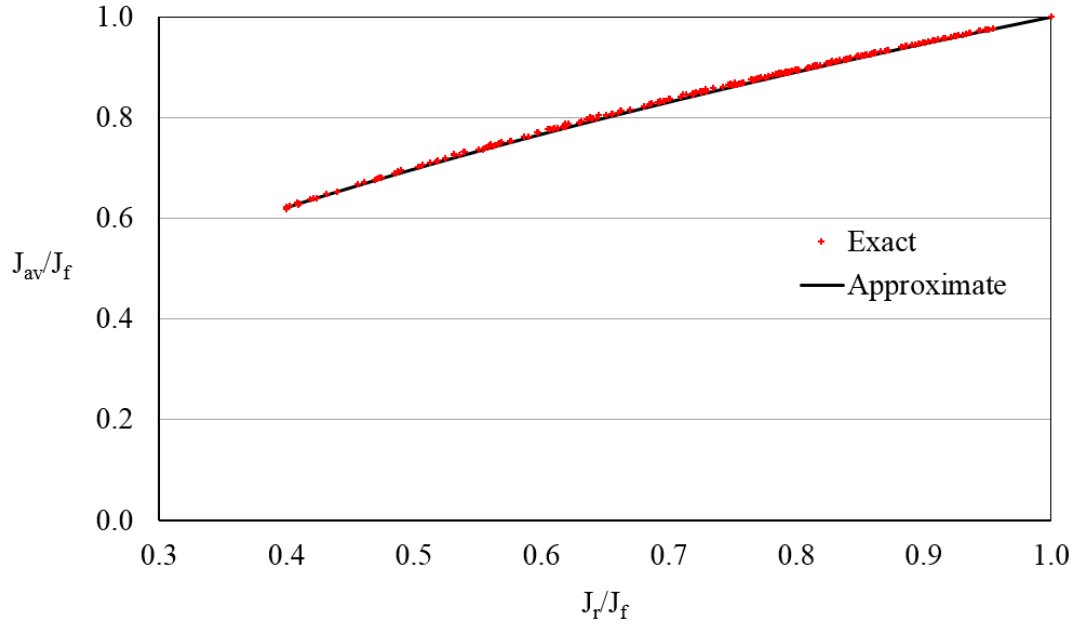

Figure 4.1. J_{av}/J_f **versus** J_r/J_f **for water-EtOH. Solid curve denotes Eq. (4.37) with n = 0.52.**

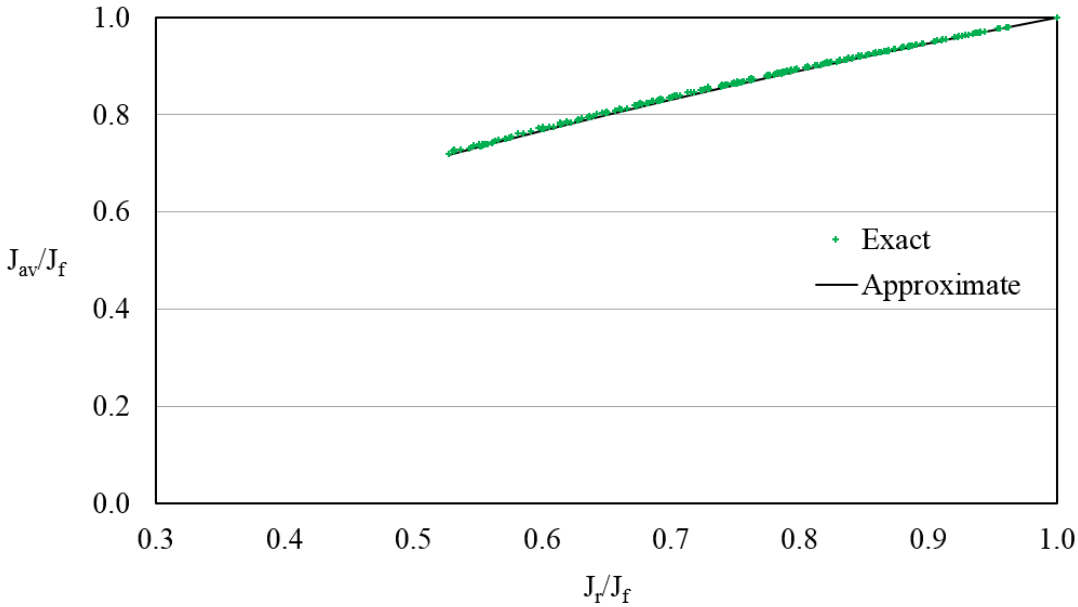

Figure 4.2. J_{av}/J_f **versus** J_r/J_f **for water-IPA. Solid curve denotes Eq. (4.37) with n = 0.52.**

Table 4.3 shows the values of *n* obtained for both solutions using different 'best-fit' criteria.

Table 4.3 Best-fit values of *n* according to various criteria

Water-ethanol	***n***	**Max Error (%)**	**Mean Error (%)**
Least squares	0.51	1.37	0.28
*Minimax	0.52	1.03	0.46
$n = 0.5$	0.50	2.31	0.33
IPA-Water	***n***	**Max Error (%)**	**Mean Error (%)**
Least squares	0.51	1.51	0.27
*Minimax	0.52	1.10	0.45
$n = 0.5$	0.50	2.44	0.32

**Minimisation of maximum error*

The average flux is equal to the permeate mass flowrate divided by the membrane area

$$J_{av} = \frac{\dot{m}_p}{A} \tag{4.18}$$

Combining Eqs. (4.30) and (4.31) the simplified design equation becomes

$$A = \frac{\dot{m}_p}{J_f}\left(\frac{J_f}{J_r}\right)^n \tag{4.38}$$

It is at the discretion of the designer as to which value of *n* to use. In summary, the steps involved in calculating the 'ideal' membrane area required for a given separation using the approximate method are outlined in Table 4.4 below

Table 4.4 Algorithm for approximate calculation of membrane area

- For a given feed, choose a membrane for which the Arrhenius flux relationship and the permeate composition are known.
- Choose a suitable feed temperature.
- Check that the E_j value is feasible using Eq. (4.36).
- Choose a desired permeate/feed ratio ensuring that $\Delta T < 30K$.
- Determine the retentate composition by mass balance and T_r by iteration as described previously.
- Calculate J_r / J_f.
- Calculate the required membrane area using Eq. (4.38).

4.5 Other solvents

The short cut equation, Eq. (4.30) with $n = 0.52$ is also valid for other solvents when T_f is between 90 °C and 130 °C and $y_i \geq 90$ wt%. The maximum error is less than 1.1% in each case. The concentrations for which it is applicable are listed in Table 4.5. The equation is valid for temperatures as high as 160 °C for the following high boiling point solvents: n-butanol, sec-butanol, tert-butanol and isobutanol as well as MIBK, cyclohexanol and ethylene glycol.

$$\frac{J_{av}}{J_f} = \left(\frac{J_r}{J_f} \right)^{0.52} \tag{4.39}$$

Table 4.5 Maximum water concentrations and maximum temperatures for which Eq. (4.39) is valid for a variety of solvents.

Solvent	**Max Conc. (wt%)**	**Max T_f (^oC)**
Water – Acetone	0 - 10%	130
Water – n-Propanol	0 - 10%	130
Water – MIBK	0 - 10%	160
Water – MEK	0 - 20%	130
Water – THF	0 - 20%	130
Water – Acetonitrile	0 - 20%	130
Water – Methanol	0 - 20%	130
Water – Cyclohexanol	0 - 20%	160
Water – Ethylene Glycol	0 - 20%	160
Water – Isobutanol	0 - 20%	160
Water – tert-Butanol	0 - 20%	160
Water – sec-Butanol	0 - 20%	160
Water – n-Butanol	0 - 20%	160

The approximate approach outlined above is simple and easy to use. It causes errors of less than 1.2% (based on the minimax criterion) for commercial operating conditions. Little data is required for the equation and such data is either readily available or easily determined. Of course, the underlying mathematical model on which Eq. (4.25) is based is itself an approximation and some form of 'efficiency factor', not unlike the column efficiency that is sometimes employed in distillation design, will ultimately be needed to compute the real area when sizing industrial systems. Such an efficiency factor is likely to be a function of module design, operating conditions and fluid properties. In that sense, the work outlined in this chapter is merely a first step towards the development of design equations that will give engineers the confidence to engage with pervaporation technology.

There are two obvious areas where the current model can be further developed. The first is to go beyond the use of averaged physical properties and to incorporate the full temperature and concentration dependence of all properties into the analysis.

4.6 Conclusions

Assuming a concentration-independent flux with an Arrhenius dependence on temperature, and using temperature- and composition-averaged physical properties, an exact analytical expression is derived for the average flux in an adiabatic, single-pass pervaporation module. For the first time the range of feasible activation energies of permeation, E_j, is established for IPA-water and ethanol-water systems. Within this range, and over the range of typical operating conditions, a novel short-cut approximation to the exact analytical expression is derived that allows the normalised average flux to be estimated for the dehydration of many solvents.

This chapter has described some early steps towards the development of easy-to-use engineering design equations for pervaporation. It complements the derivation of an analytical solution for the average flux in an ideal isothermal pervaporation systems undertaken in chapter 3.

4.7 Sample Calculation

This sample calculation determines the membrane area required for an ideal adiabatic pervaporation module where flux is independent of concentration. The flowrates and operating conditions are typical of industrial operations. The purpose of the sample calculation is to demonstrate how easily such calculations can now be done using readily available data. The membrane area calculated is typical of that for an industrial application.

A feed of 2,500 kg/h of isopropanol at 130 °C contains 15 wt% water. The permeate-feed ratio is 3%. Membrane data: E_j = 30,000 kJ/kmol.K, y_i = 0.99, J_f = 2 kg/h.m^2.

$$x_{ir} = \frac{z_i - y_i \frac{\dot{m}_p}{\dot{m}_f}}{1 - \frac{\dot{m}_p}{\dot{m}_f}} = \frac{0.15 - 0.99(0.03)}{1 - 0.03} = 0.124 \qquad \text{Eq. (3.10)}$$

Assume T_r = 385K

$$T_v = 0.5\left(T_f + T_r\right) = \left(403 + 385\right) = 394K$$

$$h_v = C_p T_v + \lambda = \left(3.446\,kJ/kg.K\right)\left(394K\right) + 2{,}123\,kJ/kg = 3{,}480\,kJ/kg$$

$$T_r = \frac{h_v}{c_p} - \left(\frac{h_v}{c_p} - T_f\right)\frac{1}{1-p} \qquad \text{Eq. (4.33)}$$

Iterate the assumed T_r until the calculated value matches the assumed value until the same result is obtained.

$$\frac{J_r}{J_f} = \frac{e^{-30{,}000/8.31435(384K)}}{e^{-30{,}000/8.3145(403K)}} = 0.645$$

$$\dot{m}_p = \left(\frac{\dot{m}_p}{\dot{m}_f}\right)\dot{m}_f = \left(0.03\right)2{,}500kg/hr = 75kg/hr$$

$$A = \frac{\dot{m}_p}{J_f}\left(\frac{J_f}{J_r}\right)^{0.52} = \frac{\left(75kg/hr\right)}{5kg/m^2.hr}\left(\frac{1}{0.645}\right)^{0.52} = 18.8m^2 \qquad \text{Eq. (4.39)}$$

Chapter 5: Sizing of modules and operating parameters for systems when the flux is proportional to liquid composition.

5.1 Abstract

Industrial pervaporation systems typically operate adiabatically. The flux is proportional to concentration and has an Arrhenius-type relationship with temperature. Multiple pervaporation stages are often used with inter-stage heaters. The range of feasible activation energies of permeation, E_j, is established for IPA-water and ethanol-water systems. Within this range, and over the range of typical operating conditions, an empirical expression for the average flux of a single-pass pervaporation module is developed for both ethanol and IPA dehydrations.

5.2 Introduction

In chapter 4 an analytical expression was developed for ideal adiabatic pervaporation systems where flux was independent of concentration. The purpose of this chapter is to extend this work to the more frequently-encountered situation of adiabatic modules where flux is proportional to water concentration, x_i, and thus flux is typically given by an expression of the form

$$J = x_i J_0 e^{-E_j/RT} \tag{5.1}$$

In such systems the vaporisation of the aqueous permeate causes the flux to decrease due to the drop in temperature caused by the latent heat and also as a result of the reduction in the water content of the liquid phase. In this chapter it is assumed, as previously, that the flux at the retentate temperature and composition will be no lower than 40% of the flux when the retentate has been reheated to the feed temperature. Application of this criterion allows the determination of the combinations of permeate-feed mass flow ratios, $\dot{m}_P/\dot{m}_F$, and maximum apparent activation energy of pervaporation, E_j, values, which are economically viable for a given system. The determination of the range of E_j values that are feasible for industrial systems completes the establishment of the range of industrial operating conditions for all operating parameters, known as the "envelope of industrial operating conditions".

5.3 J_r/J_{reheat} ratio

A typical adiabatic pervaporation system with inter-stage heating is illustrated in Fig. 5.1. In this example, both stages comprise two parallel adiabatic pervaporation modules. The feed is heated before entering the first stage. The retentate from the first stage passes through an inter-stage heater prior to entering the second stage.

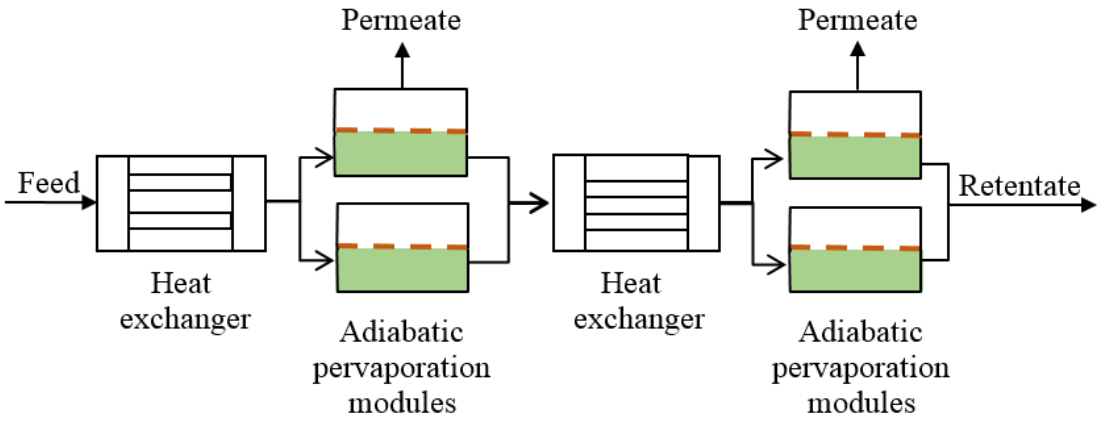

Figure 5.1 Typical pervaporation system with multiple modules in each stage.

The black dashed diagonal line in Fig. 5.2 illustrates the relationship between flux and liquid composition for an *isothermal* system where flux is proportional to concentration as per Eq. (5.1). In such cases flux is proportional to concentration.

In an *adiabatic* system, starting at the point labelled J_f (the flux at the feed conditions) at the top right of Fig. 5.2, the flux drops along the solid blue curve to point J_r (the flux at the retentate concentration and temperature), as aqueous permeate is removed. The decreasing temperature causes the reduction in flux to be greater than that for the corresponding isothermal system. Reheating the retentate to the feed temperature, causes the flux to increase from J_r up the red vertical line to point J_{reheat}. The flux has returned to the isothermal line, but is less than the feed flux, J_f, due to its reduced water content.

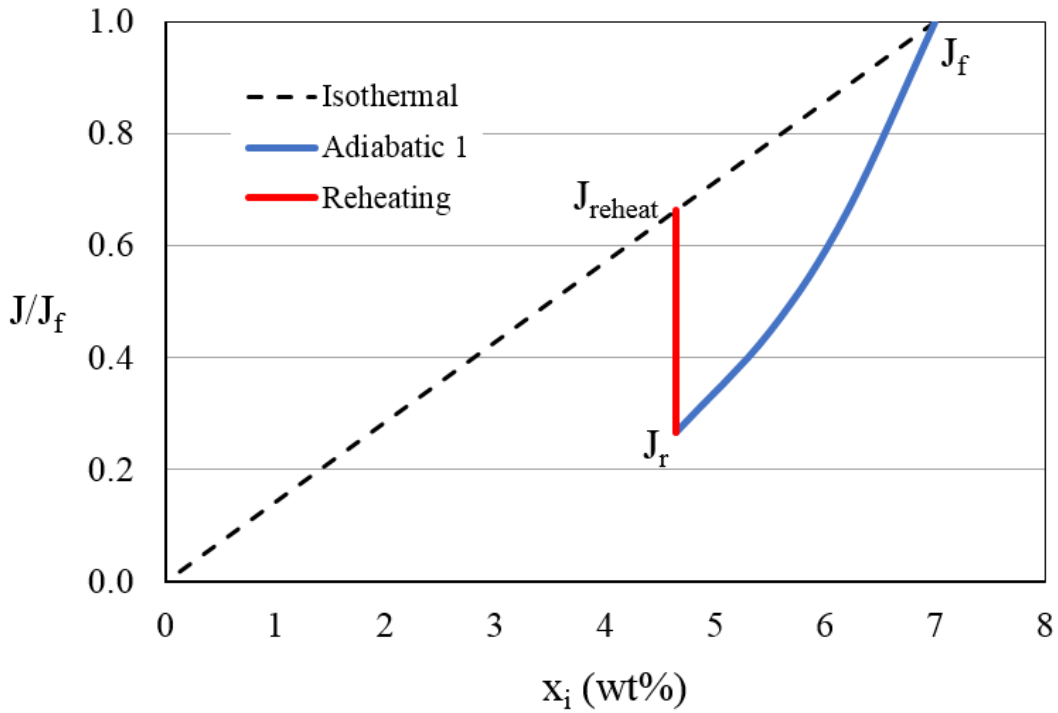

Figure 5.2 Isothermal flux, adiabatic flux and reheating for a typical multi-stage adiabatic pervaporation system where flux is proportional to concentration: isothermal flux (black dashed line), adiabatic flux (solid blue curve) and reheating (red vertical line). J/J_f vs. x_i for J_r/J_{reheat} = 0.4, flux proportional to concentration, dehydration of ethanol, E_j = 45,000 kJ/kmol, z_i = 8%, T_f = 120 °C, y_i = 95 %w/w.

As discussed in section 4.4, over-frequent reheating leads to complexity: the additional cost of piping and valves can be significant (Baker, 2012, p. 395). Insufficient frequency of reheating leads to pervaporation at low temperatures, which causes flux to be low and therefore requires excessive membrane area. The novel J_r/J_{reheat} ratio allows the minimum number of stages for a pervaporation system to be determined irrespective of the flux-concentration and flux-temperature relationships. The J_r/J_{reheat} ratio provides a rationale for the choice of temperature drop within a module: it allows for the effect of E_j on the optimum temperature drop. The $J_r/J_{reheat} \geq 0.40$ criterion allows the maximum E_j to be determined for a given system.

The composition is the same for both J_r and J_{reheat}. Hence, the J_r/J_{reheat} ratio is dependent on temperature and is independent of composition. The J_r/J_{reheat} ratio can be calculated by using Eq. (5.1) to calculate J_r and J_{reheat} respectively.

$$\frac{J_r}{J_{reheat}} = \frac{x_i J_0 e^{-E_j/RT_r}}{x_i J_0 e^{-E_j/RT_f}} \tag{5.2}$$

$$\frac{J_r}{J_{reheat}} = \frac{e^{-E_j/RT_r}}{e^{-E_j/RT_f}} \tag{5.3}$$

Simplifying,
$$\frac{R}{E_j}\ln\left(\frac{J_r}{J_{reheat}}\right) = \left(\frac{1}{T_f} - \frac{1}{T_r}\right) \tag{5.4}$$

hence,
$$T_r = \frac{1}{\frac{1}{T_f} - \frac{R}{E_j}\ln\left(\frac{J_r}{J_{reheat}}\right)} \tag{5.5}$$

thus,
$$\Delta T = T_f - \frac{1}{\frac{1}{T_f} - \frac{R}{E_j}\ln\left(\frac{J_r}{J_{reheat}}\right)} \tag{5.6}$$

A constant J_r/J_{reheat} ratio for a system leads to equal temperature drops for all stages as is evident from Eq. (5.6). E_j values for commercial membranes for the dehydration of ethanol and isopropanol are typically in the range 19,000 - 63,000 kJ/kmol as discussed in section 1.15. Baker (2012, p. 395) stated that temperature drops within a module of 15 – 25 K are typical as illustrated by the shaded area in Fig. 5.3. The curves in Fig. 5.3 show the relationship between flux and E_j at a variety of J_r/J_{reheat} ratios for a particular feed temperature. These relationships are independent of the materials being separated. Lower feed temperatures have lower ΔT values.

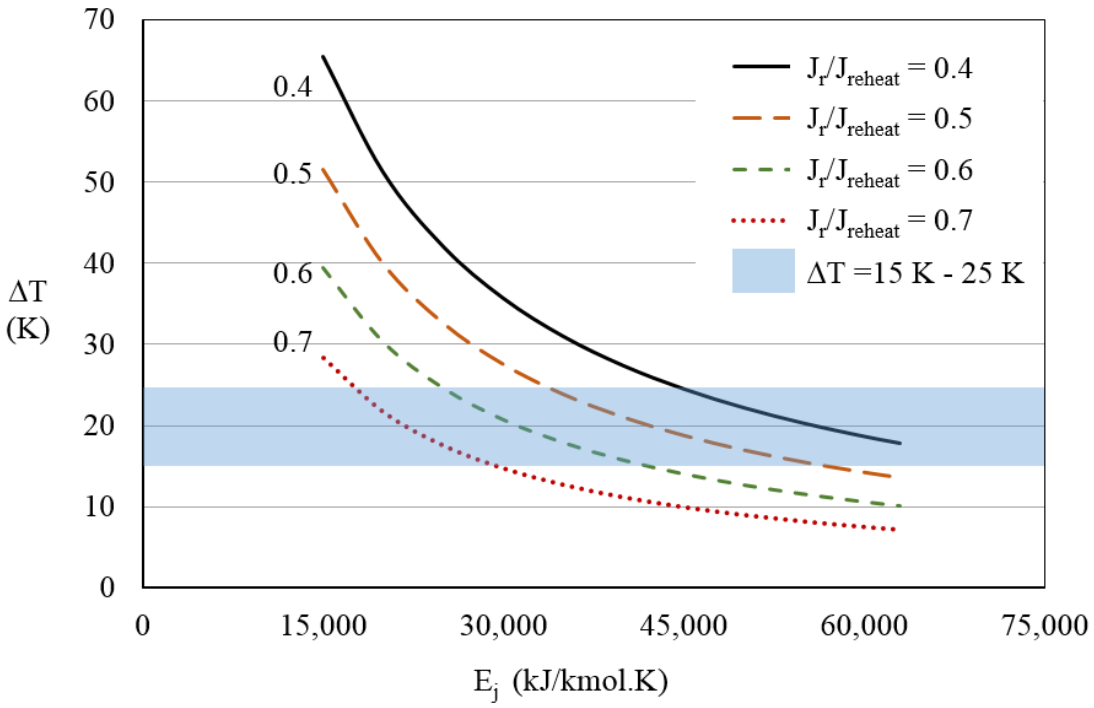

Figure 5.3 ΔT versus E_j for various J_r/J_{reheat} ratios: ethanol dehydration, T_f = 120 °C

The water content of the liquid reduces from stage to stage. Water has a considerably higher specific heat than most solvents for which pervaporation is used. Most industrial pervaporation systems have equally-sized stages: as the concentration and hence the flux reduces progressively from stage to stage, so the $\dot{m}_p/\dot{m}_f$ ratio progressively reduces from stage to stage.

A minimum J_r/J_f ratio was recommended in section 4.3 for systems where flux was independent of concentration: in such systems, J_{reheat} is equal to J_f as the change in concentration does not affect flux. The J_r/J_{reheat} criterion is a generalisation of this earlier criterion and extends the concept to systems where flux is a function of concentration: whilst also being applicable to systems where flux is independent of concentration.

5.4 Model Development

Let $\dot{m}$ be the local liquid mass flowrate in the module. Then, the differential mass balance for the liquid phase can be written

$$\frac{d\dot{m}}{dA} = -J \tag{5.7}$$

where dA is the differential area and J is the local flux which is both composition and temperature dependent. The solute balance can then be written

$$\frac{d\left(x_i\dot{m}\right)}{dA} = -Jy_i \tag{5.8}$$

where x_i is the local liquid composition and y_i represents the composition of the permeate. Permeate-feed ratios up to 5% are used in industrial systems as discussed in section 1.14. A component balance shows that even with pure aqueous permeate the water concentration in the liquid phase will vary by ≤ 5%. As discussed in section 1.14, across this limited range, the permeate composition can generally be taken to be constant and independent of x_i for commercial membranes. Using the product rule and combining Eqs. (5.7) and (5.8) gives

$$\frac{d\left(x_i\right)}{d\dot{m}} = \frac{y_i - x_i}{\dot{m}} \tag{5.9}$$

Integrating gives

$$x_i = y_i - \left(y_i - z_i\right)\frac{\dot{m}_f}{\dot{m}} \tag{5.10}$$

where: z_i = the liquid feed composition of component i.

noting that

$$A = \int_{\dot{m}_r}^{\dot{m}_f} \frac{d\dot{m}}{J} \tag{5.11}$$

where: $\dot{m}_f$ = is the mass flowrate of the feed (kg/s)

$\dot{m}_r$ = is the mass flowrate of the retentate (kg/s)

The flux in this work was assumed to be related to temperature by the Arrhenius-type expression outlined in Eq. (5.1). Hence,

$$A = \int_{\dot{m}_r}^{\dot{m}_f} \frac{d\dot{m}}{x_i J_o e^{-E_j/RT}} \tag{5.12}$$

Using Eq. (5.10) one can write

$$A = \int_{\dot{m}_r}^{\dot{m}_f} \frac{d\dot{m}}{\left[y_i - \left(y_i - z_i \right) \frac{\dot{m}_f}{\dot{m}} \right] J_o e^{-E_j / RT}} \tag{5.13}$$

In chapter 3, using a heat balance, the retentate temperature was shown to be easily calculated using the expression

$$T_r = \frac{h_v}{c_p} - \left(\frac{h_v}{c_p} - T_f \right) \frac{\dot{m}_f}{\dot{m}_r} \tag{5.14}$$

where: h_v = an average vapour enthalpy

c_p = the average specific heat

$\dot{m}_f$ = the mass flowrate of the feed

$\dot{m}_r$ = the mass flowrate of the retentate

Using Eq. (5.13) and the generalised form of Eq. (5.14) the final expression for the membrane area becomes

$$A = \int_{\dot{m}_r}^{\dot{m}_f} \frac{d\dot{m}}{\left[y_i - \left(y_i - z_i \right) \frac{\dot{m}_f}{\dot{m}} \right] J_0 \exp\left\{ -E_j / R \left(\frac{h_v}{c_p} - \left(\frac{h_v}{c_p} - T_f \right) \frac{\dot{m}_f}{\dot{m}} \right) \right\}} \tag{5.15}$$

To simplify this expression, we let

$$s = \frac{\dot{m}}{\dot{m}_f} \tag{5.16}$$

Therefore the total area is found using the integral below:

$$\frac{A J_0}{\dot{m}_f} = \int_{1-p}^{1} \frac{e^{\frac{a}{b-(b-1)/s}}}{y_i - \left(y_i - z_i \right) / s} ds \tag{5.17}$$

where p is the ratio of permeate flowrate to feed flowrate, i.e., $\dot{m}_p/\dot{m}_f$, while the parameter a is defined by

$$a = \frac{E_j}{RT_f} \tag{5.18}$$

and b is defined by $$b = \frac{h_v}{c_p T_f} \tag{5.19}$$

The dimensionless average flux in the system can now be expressed as

$$\frac{J_{av}}{J_f} = pe^a \left[\int_{1-p}^{1} \frac{e^{\frac{a}{b-(b-1)/s}}}{y_i - (y_i - z_i)/s} ds \right]^{-1} \tag{5.20}$$

Integration was attempted using symbolic integrators (WolframAlpha®; Integral-calculator.com®). However, no analytical solution was found; i.e. no algebraic equation was found for the calculation of the integral of this complex expression. It is unlikely that such an equation exists given the extensive range of integrals addressed by these two symbolic integrators. It is possible that such an expression may be derived in the future. Mass balances allow the retentate composition to be calculated as a function of the permeate-feed ratio. Integration using the trapezoidal rule was used to calculate the retentate temperature and average flux for an adiabatic module. "Data" was generated over a wide range of conditions spanning the envelope of industrial operating conditions. The "data" thus generated was used along with regression techniques to derive an empirical algebraic expression, for the average flux.

Noting that $A_{total} = \frac{\dot{m}_p}{J_{av}}$, a dimensionless membrane area can be calculated as:

$$\frac{A_{total} J_o}{\dot{m}_f} = \frac{\frac{\dot{m}_p}{\dot{m}_f}}{\frac{J_f}{J_o}\frac{J_{av}}{J_f}} \tag{5.21}$$

The membrane area for a module can be calculated

$$A_{total} = \frac{\dot{m}_f \left(\dot{m}_p / \dot{m}_f \right)}{J_f \left(J_{av} / J_f \right)} \tag{5.22}$$

The underlying differential equations are solved using integration using the trapezoidal rule. Let "*h*" be the 'increment size', i.e. some fraction of the desired ratio of permeate-feed flowrate for the module. The retentate temperature at the outlet of each increment is estimated and then solved by iteration. The inverse flux of each increment is calculated. The trapezoidal rule is used to determine the average inverse flux for the module. The average flux for the module is then calculated. In summary it can be stated that for a given system, average flux "data" can be determined using the simplified algorithm outlined in Table 4.1.

Table 5.1 Algorithm for calculation of the membrane area by integration using the trapezoidal rule.

- Note the feed composition, the permeate composition achievable with the membrane, the activation energy and the feed temperature.
- Calculate the flux and the inverse flux at the feed conditions.
- Assume a value, *h*, for the permeate-feed ratio ($\dot{m}_p/\dot{m}_f$) increments.
- Calculate the $\dot{m}_p/\dot{m}_f$ ratio for each increment, noting that the mass of liquid entering later increments decreases, leading to larger $\dot{m}_p/\dot{m}_f$ ratios for later increments.
- Use a mass balance to calculate the retentate composition for each increment.
- Assume a retentate temperature for each increment and hence calculate the average vapour temperature, the average specific heats of the feed, retentate and permeate (liquid phase) as well as the latent heat of the permeate for each increment.
- Iterate using Eq. (5.14) to determine the retentate temperature for each increment.
- Calculate the ratio of the flux at the start of the module versus the flux at the outlet of each increment, J/J_f, and calculate the inverse of this ratio J_f/J.

- Calculate the inverse of the normalised average flux for the module, J_f/J_{av}. The trapezoidal rule may be used.
- Hence, calculate the normalised average flux for the module, J_{av}/J_f.
- Calculate the J_r/J_{reheat} ratio at the outlet of each increment.
- Cease calculations when the required J_r/J_{reheat} ratio is reached, the required $\dot{m}_p/\dot{m}_f$ ratio is achieved, the required retentate composition is achieved or the maximum allowable temperature drop within the module has been reached.
- Calculate the membrane area required using Eq. (5.22).

Results were constant when 500 to 1,000 increments were used. Calculations were undertaken using varying physical properties and also with constant physical properties: module retentate temperatures differed by less than 0.2 K.

5.5 Results and Discussion

Calculation of average flux

Calculations were performed over a wide range of industrially relevant conditions. Specifically, the calculations were performed for the dehydration of ethanol and IPA solutions with a permeate purity of at least 90% water. For IPA-water, the water composition of the feed ranged from 1% to 16%, while in the case of ethanol-water, the range was 1% to 10% water. Typical industrial feed temperatures range from 105 - 130 ^oC (Baker, 2012, p. 402). Values of $\dot{m}_p/\dot{m}_f$ were as high as 5%. E_j values were greater than 15,000 kJ/kmol. It is worth noting in passing that the range of economically feasible $\dot{m}_p/\dot{m}_f$ values in any pervaporation process is a function of E_j and the solvent being dehydrated. For $J_r/J_{reheat} \geq 0.4$ and $\dot{m}_p/\dot{m}_f \geq 0.03$ the maximum E_j value was no greater than 63,000 kJ/kmol for IPA dehydrations and no greater than 52,000 kJ/kmol for ethanol dehydrations.

Constant permeate concentration.

In section 1.14 it was stated that across the limited range of liquid compositions that occur within a pervaporation module, the permeate composition can generally be taken

to be constant and independent of x_i for commercial membranes. However, there can be some variability. The robustness of the assumption was tested by varying the permeate concentration within a module and determining the affect this would have on the required module area. Calculations were conducted wherein half a module had a permeate composition 1% above the average and the remainder had a permeate composition 1% below the average. The calculated membrane area varied by no more than 0.4%. Thus the assumption was found to be robust and variations about the mean will not cause significant errors. In cases where there are greater variations, a conservative approach would be to undertake calculations using the lowest permeate concentration.

Empirical equation

Various combinations of parameters were analysed to determine whether empirical relationships could be found. Figs. 4.4a and 4.4b are plots of J_{av}/J_f versus J_r/J_{reheat} for ethanol and IPA dehydrations. The data points represent calculations based on the algorithm outlined in Table 5.1. Each curve has a particular x_{ir}/z_i ratio and includes data for combinations of feed concentrations, feed temperatures and E_j values across the full envelope of industrial operating conditions. All curves had regression values above 99.6% for equations of the form

$$\frac{J_{av}}{J_f} = g \ln\left(\frac{J_{reheat}}{J_f}\right) + h \tag{5.23}$$

where g and h are constants.

The relationship between the x_{ir}/z_i ratio and the constant g was linear in both cases. The curves in Figs. 5.4 and 5.5 represent the fit of Eq. (5.24) to the data:

$$\frac{J_{av}}{J_f} = \left[a\left(\frac{x_{ri}}{z_i}\right) + b\right] ln\left(\frac{J_r}{J_{reheat}}\right) + c\left(\frac{x_{ri}}{z_i}\right)^n + d\left(\frac{x_{ri}}{z_i}\right) + eln\left(\frac{x_{ri}}{z_i}\right) + f \tag{5.24}$$

where a, b, c, d, e, f, and n are constants.

The "$eln(x_{ir}/z_i)$" term ensures that when there is no separation (i.e. the feed and retentate compositions are equal) that the average flux is equal to the feed flux as occurs at the entrance to a membrane module.

Noting that for systems where flux is proportional to concentration, and where the retentate is reheated to the feed temperature,

$$J_{reheat} = \frac{x_{ir}}{z_i} J_f \tag{5.25}$$

hence,

$$\frac{J_r}{J_{reheat}} = \frac{z_i J_r}{x_{ri} J_f} \tag{5.26}$$

where x_{ir} is the mass fraction of the solute in the retentate.

Hence Eq. (5.24) can be rewritten

$$\frac{J_{av}}{J_f} = \left[a\left(\frac{x_{ri}}{z_i}\right) + b \right] ln\left(\frac{z_i J_r}{x_{ri} J_f}\right) + c\left(\frac{x_{ri}}{z_i}\right)^n + d\left(\frac{x_{ri}}{z_i}\right) + eln\left(\frac{x_{ri}}{z_i}\right) + f \tag{5.27}$$

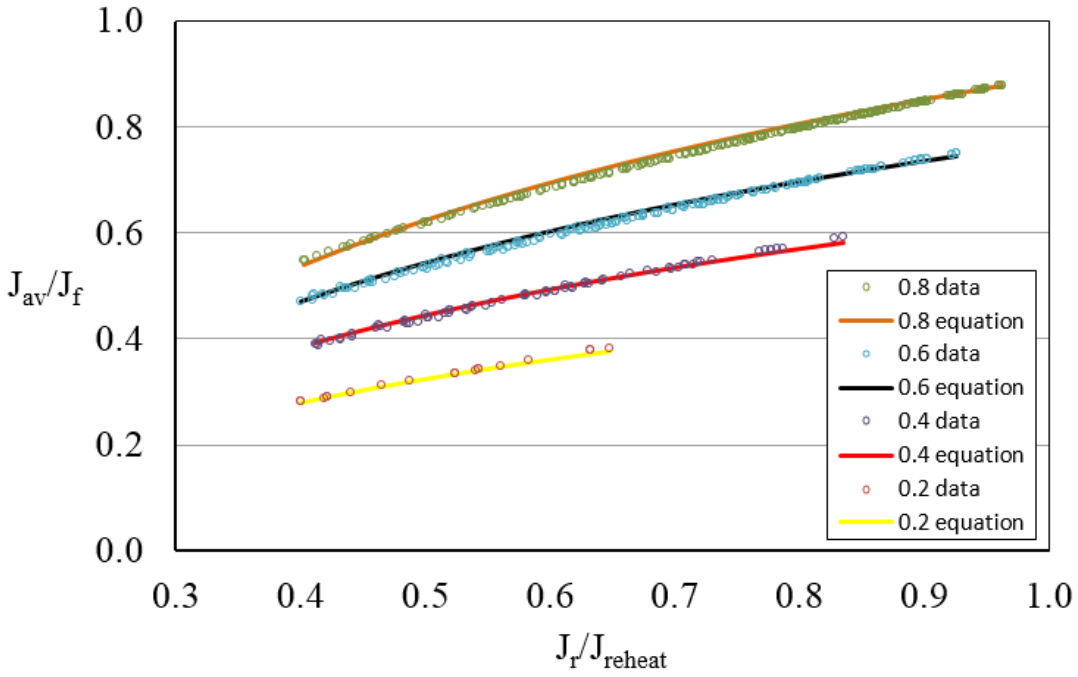

Figure 5.4 J_{av}/J_f versus J_r/J_{reheat} for water-ethanol. Solid curves denote Eq. (5.27) for values of x_{ir}/z_i of 0.2, 0.4, 0.6 and 0.8.

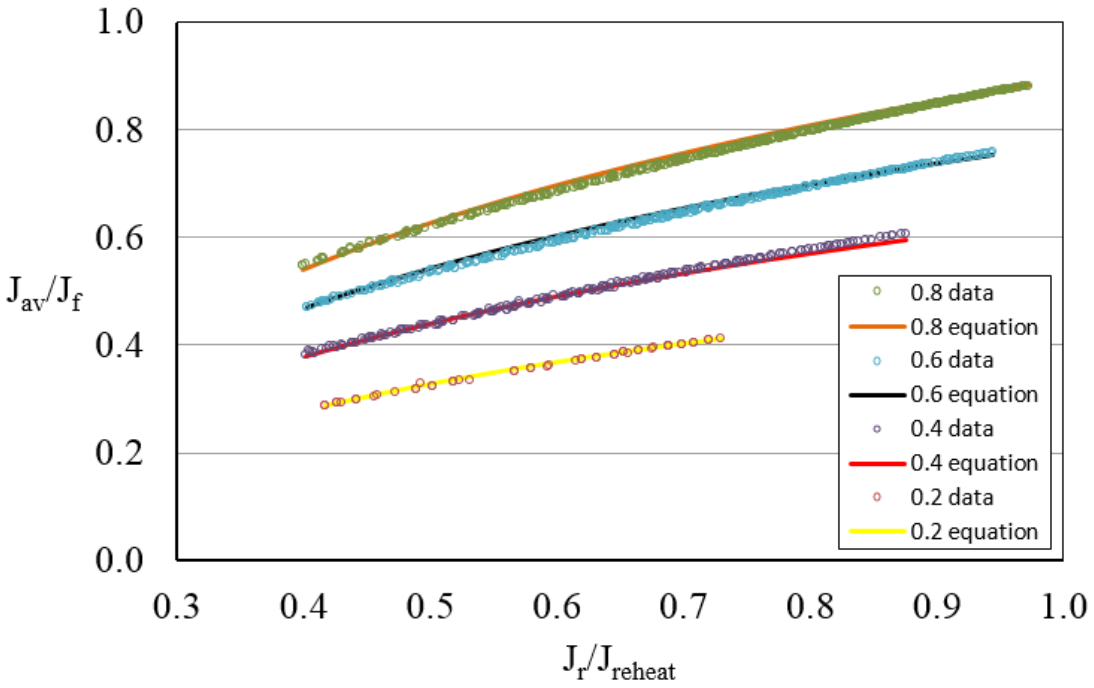

Figure 5.5 J_{av}/J_f versus J_r/J_{reheat} for water-IPA. Solid curves denote Eq. (5.27) for values of x_{ir}/z_i of 0.2, 0.4, 0.6 and 0.8.

Eq. (5.27), in particular the dependence of J_{av}/J_f on J_r/J_{reheat}, was derived by trial and error, so it is quite possible that simpler equations might be discovered in the future. The method of symbolic regression might be useful in this regard (Cai *et al.*, 2006). Symbolic regression analyses a dataset to determine the form of the relationships between the variables. No initial assumptions as to the type of relationship are required. Hence, the analysis is not affected by human bias or ignorance of possible relationships. The complexity of the correlation can be stipulated and a best-fit model is than determined using software.

Table 5.2 shows the values for the constants for both solutions. These constants were determined by minimising the maximum difference between the prediction of Eq. (5.27) and the calculation performed using the algorithm outlined in Table 5.1. The approximate approach outlined above is clearly simple and easy to use, and causes errors of less than 2.5% for water-ethanol and 2.2% for water-IPA for commercial operating conditions.

Table 5.2 Best fit values for constants for minimisation of maximum error.

Parameter	Water-ethanol	Water-IPA
a	0.3100	0.2696
b	0.1427	0.1710
c	-0.3000	-0.2620
d	0.9800	1.0260
e	0.0174	-0.0339
f	0.3200	0.2360
n	1.650	1.950
Max. error	2.4%	2.2%

Armed with Eqs. (5.22), (5.27) and the parameters in Table 5.2, a simple algorithm for computing the area of a pervaporation system presents itself and is outlined in Table 5.3.

Table 5.3 Algorithm for approximate calculation of membrane area

Choose the $\dot{m}_p/\dot{m}_f$ ratio and compute the retentate composition, x_{ir}, by mass balance.
Using an estimate of the retentate temperature, calculate the composition- and temperature-averaged physical properties. Iterate to determine the retentate temperature.
Evaluate J_{av}/J_f using Eq. (5.27).
Hence, calculate the membrane area required using Eq. (5.22).

5.6 Range of economically feasible $\dot{m}_p/\dot{m}_f$ ratios

Baker (2012, p. 395) states that current industrial practice is to have $\dot{m}_p/\dot{m}_f$ ratios between 3% and 5 % as illustrated by the shaded area in Fig. 5.6. However, systems with 9 or more equally-sized stages are used that have temperature drops of less than 5 K and $\dot{m}_p/\dot{m}_f$ ratios of less than 1% in the later stages where the low concentrations lead to low fluxes as discussed in section 1.14.

The zone of economically viable operations for a typical set of process conditions is shown in Fig. 5.6. It is the area bounded by the solid curve. E_j values for commercial membranes are typically in the range 19,000 - 65,000 kJ/kmol as outlined in section 1.15. These limits are indicated by the two vertical lines. The curve shows the $\dot{m}_p/\dot{m}_f$ ratio as a function of E_j when $J_r/J_{reheat} = 0.40$. The points on the curve were obtained by determining the $\dot{m}_p/\dot{m}_f$ ratios for a module for a given set of process conditions with a variety of E_j values such that the J_r/J_{reheat} ratio was 0.40 in each case.

A J_r/J_{reheat} ratio of less than 0.40 would require overly frequent reheating as discussed in section 5.3: thus the zone above and to the right of the curve is not economically viable. The maximum feasible $\dot{m}_p/\dot{m}_f$ ratio is a function of E_j and the J_r/J_{reheat} ratio. In the example illustrated in Fig. 5.6, $\dot{m}_p/\dot{m}_f$ ratios above 5% are economically feasible where $E_j < 33{,}000$ kJ/kmol; indeed values as high as 7.85% are feasible. Whereas, at high E_j values, the $\dot{m}_p/\dot{m}_f$ ratio is limited to less than 3%. High J_r/J_{reheat} ratios restrict the zone of economically feasible operating conditions. The exact value of the optimum J_r/J_{reheat} ratio depends on the particular equipment and system. This novel analysis indicates that the range of commercially viable operating conditions is more complex than previously understood. High E_j values may be feasible for membranes used for the later stages of pervaporation systems where concentrations, fluxes and $\dot{m}_p/\dot{m}_f$ ratios are low.

If new commercial membranes with lower E_j values are developed, higher $\dot{m}_p/\dot{m}_f$ ratios will be feasible. However, a minimum retentate temperature is required to provide an adequate temperature difference for heat transfer within the condenser so as to avoid the need for an excessively large heat transfer area. Nonetheless, $\dot{m}_p/\dot{m}_f$ ratios for individual stages are likely to be 2% or less due to the use of re-heating within pervaporation modules as discussed previously.

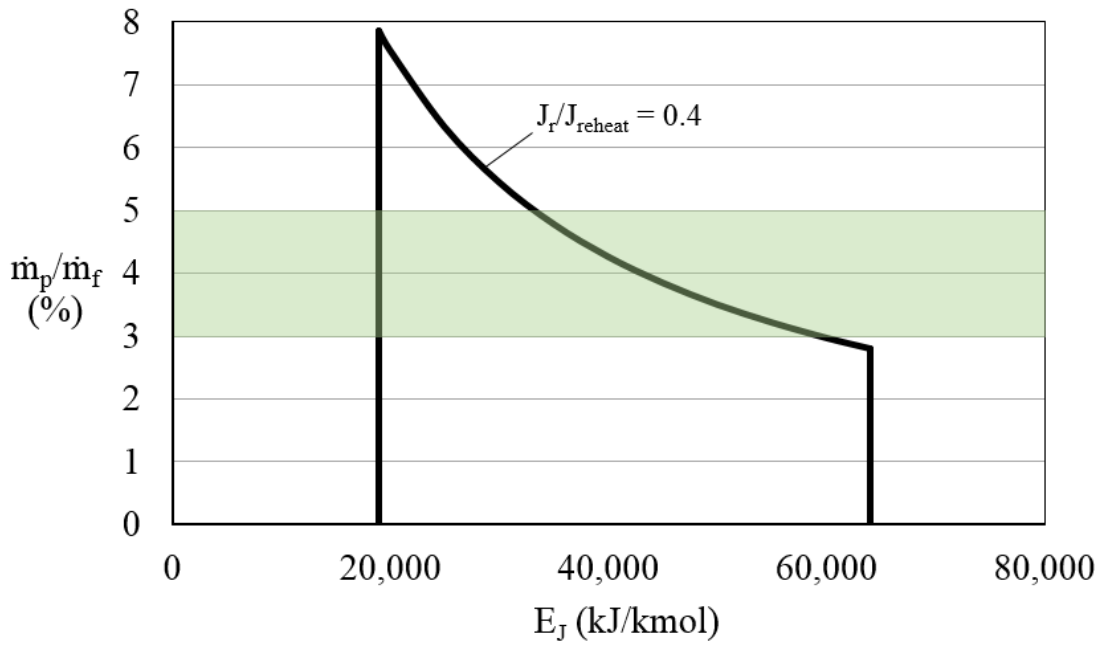

Figure 5.6 Zone of commercial operations: $\dot{m}_p/\dot{m}_f$ versus E_j for flux dehydration of IPA with proportional to concentration, z_i = 12%, T_f = 120 °C, y_i = 95% w/w. Vertical lines show limits for typical commercial membranes: E_j =19,000 to 63,000 kJ/kmol. Green shaded area is zone where permeate-feed ratio is 3% to 5% as stated by Baker (2012, p. 395)

Examples of systems with low and high E_j values are illustrated in Fig. 5.7. The curves were computed for a particular set of process conditions. The dashed curve relates to a system with E_j = 19,000 kJ/kmol: starting at point J_f at the top right of the graph, the feed concentration of 7% is reduced to 1% in a single stage, with J_r/J_{reheat} = 0.4 and a $\dot{m}_p/\dot{m}_f$ ratio of 6.36%. The solid curve corresponds to a system with E_j = 66,300 kJ/kmol: the higher E_j value leads to a more rapid decrease in flux. This necessitates three stages with two inter-stage reheaters to achieve the same final retentate purity of 1% when J_r/J_{reheat} = 0.4 for each stage, with $\dot{m}_p/\dot{m}_f$ ratios of 2.20%, 2.18% and 2.15% for each stage respectively. The $\dot{m}_p/\dot{m}_f$ ratios are progressively smaller as stated earlier in this section.

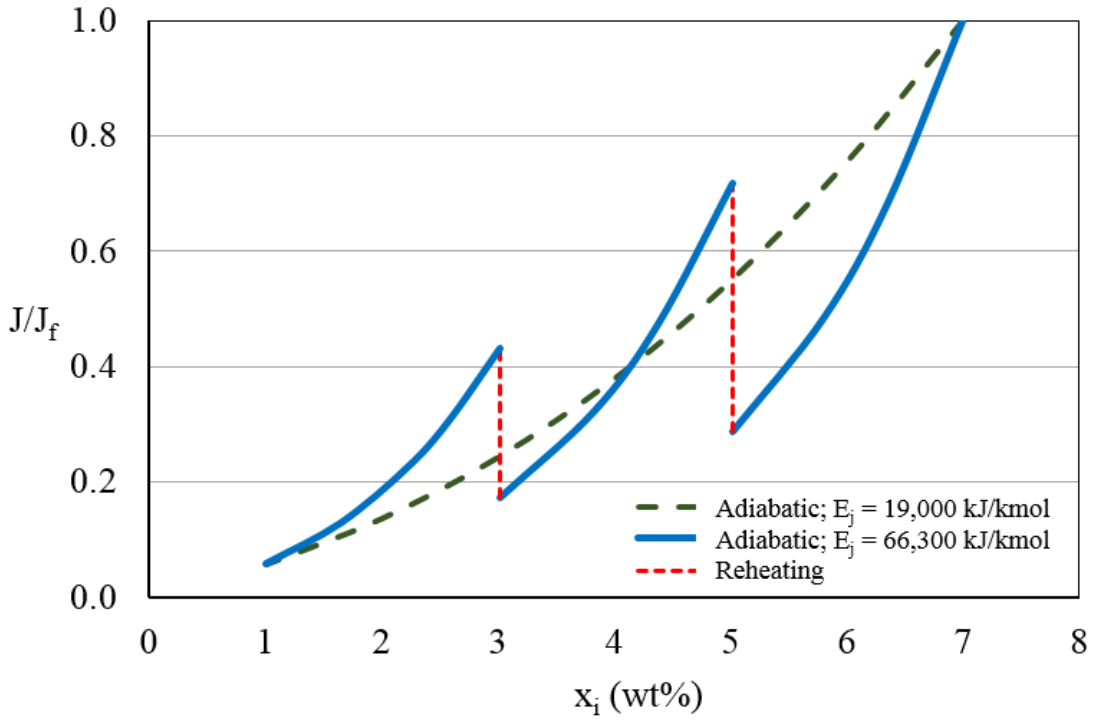

Figure 5.7 Effect of E_j on flux and concentration change across modules: J/J_f vs. x_i for J_r/J_{reheat} = 0.4, flux proportional to concentration, ethanol, z_i = 7%, y_i = 95 %, T_f = 120 °C: blue solid curve E_j = 66,300 kJ/kmol: green dashed curve E_j = 19,000 kJ/kmol.

5.7 Conclusions

In chapter 3 exact analytical expressions are derived for the average flux in an ideal isothermal pervaporation module where flux is proportional to concentration whilst in chapter 4 expressions were derived for ideal adiabatic modules where flux is independent of concentration. In this chapter an empirical expression has been developed for the average flux in an adiabatic module where flux is proportional to concentration. Together, these provide for the first time, ideal models of the modules present in industrial pervaporation systems. These ideal models predict the minimum theoretical membrane area for such systems.

An 'efficiency factor' needs to be used in conjunction with these ideal models to compute the real area when sizing industrial systems. The efficiency factor is likely to be a function of module design, operating conditions and fluid properties (Sommer *et al.*, 2005). It is discussed further in chapter 7.

The novel J_r/J_{reheat} parameter has been used to demonstrate that industrial operations are only feasible within a limited range of combinations of E_j and $\dot{m}_p/\dot{m}_f$ ratios and also that $\dot{m}_p/\dot{m}_f$ ratios greater than 5% are feasible when E_j values are low. It has shown the importance of the activation energy of the membrane as regards the performance of pervaporation systems. Determining the range of economically feasible E_j values completes the establishment of the full range of industrial operating conditions for the first time: this allows the validation of the empirical equation developed in this chapter.

This work, especially the approximate (yet accurate) expressions for the average flux, provides researchers with the tools to explore a variety of process design and analysis problems in the field of pervaporation. These include systems with recycles multi-stage adiabatic systems which are reviewed in chapter which are reviewed in chapters 6 and 8 respectively. The field of pervaporation has been opened to practicing chemical engineers as well as membrane scientists.

Chapter 6: Recycles

6.1 Abstract

Mass balances and component balances are used to derive novel simple algebraic equations for the calculation of the feed flowrate and feed composition of recycles. These equations are used to review the effect of recycle on systems where flux is proportional to concentration and for the first time to analyse recycle systems with concentration-independent flux. The effect of recycles on energy consumption in pervaporation is briefly reviewed.

6.2 Introduction

As discussed in section 1.16, in pervaporation, recycling some of the retentate to the inlet of the preheater leads to an increase in the liquid flowrate through a pervaporation module, giving a lower permeate-retentate ratio and hence a smaller temperature drop. The increased average temperature within a module leads, in principle, to increased flux (Santoso *et al*., 2012). However, recycling retentate reduces the solute concentration in the feed and when flux is an increasing function of concentration, this significantly counter-acts the increased flux (Tsuyumoto *et al*., 1997).

In this chapter equations are developed for the calculation of the feed flowrate and feed composition for pervaporation modules with local recycle. These are analogous to the algebraic equations for the calculation of feed flowrate and feed composition for plug flow reactors with recycle (Levenspiel, 1999).

Algorithms for the calculation of the membrane area of ideal modules are developed for systems where throughput is increased whilst maintaining constant retentate composition. This novel approach provides flexibility for operators of industrial systems.

6.3 Mass balance equations for recycle systems

Consider continuous pervaporation incorporating partial recycle as illustrated in Fig. 6.1.

where, C = the ratio of the recycle and outlet stream mass flowrates

$\dot{m}_f$ = the mass flowrate of the feed entering the membrane module

$\dot{m}_o$ = the mass flowrate of the outlet stream leaving the system

$\dot{m}_p$ = the mass flowrate of the permeate

$\dot{m}_r$ = the mass flowrate of the retentate leaving the membrane module

$\dot{m}_s$ = the mass flowrate of the supply stream entering the system

s_i = the water concentration in the supply stream

x_{ir} = the water concentration in the retentate

y_i = the water concentration in the permeate

z_i = the water concentration in the feed stream to the module

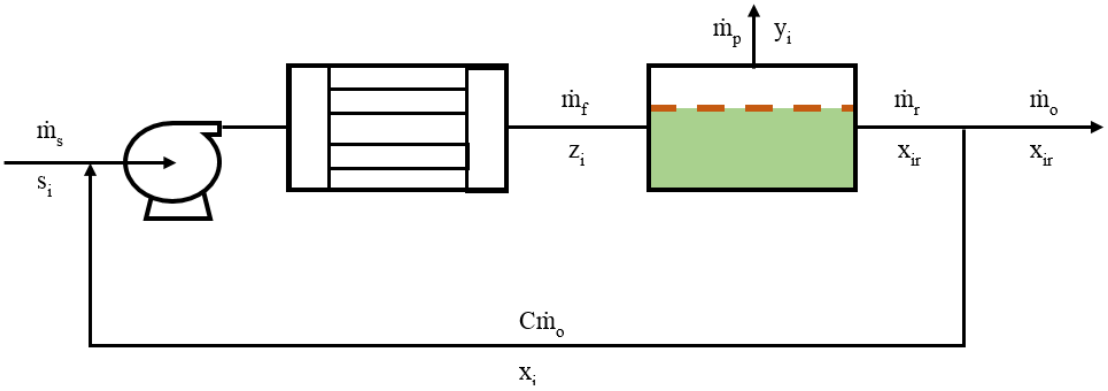

Figure 6.1 Adiabatic pervaporation module with recycle

A mass balance about the system gives

$$\dot{m}_s = \dot{m}_p + \dot{m}_o \tag{6.1}$$

A mass balance about the junction prior to the pump yields

$$\dot{m}_f = \dot{m}_s + C\dot{m}_o \tag{6.2}$$

hence

$$\frac{\dot{m}_f}{\dot{m}_s} = 1 + C\left(1 - \frac{\dot{m}_p}{\dot{m}_s}\right) \tag{6.3}$$

A mass balance around the membrane module gives

$$\dot{m}_f - \dot{m}_p = \dot{m}_r \tag{6.4}$$

hence

$$\frac{\dot{m}_r}{\dot{m}_s} = (1+C)\left(1-\frac{\dot{m}_p}{\dot{m}_s}\right) \tag{6.5}$$

Rearranging Eq. (6.5)

$$\frac{\dot{m}_p}{\dot{m}_r} = \frac{\dfrac{\dot{m}_p}{\dot{m}_s}}{\left[(1+C)\left(1-\dfrac{\dot{m}_p}{\dot{m}_s}\right)\right]} \tag{6.6}$$

Rearranging Eq. (6.4)

$$\frac{\dot{m}_p}{\dot{m}_f} = \frac{1}{1+\dfrac{1}{\dot{m}_p/\dot{m}_r}} \tag{6.7}$$

Combining Eqs. (6.6) and (6.7)

$$\frac{\dot{m}_p}{\dot{m}_f} = \frac{1}{1+\dfrac{\left[(1+C)\left(1-\dfrac{\dot{m}_p}{\dot{m}_s}\right)\right]}{\dot{m}_p/\dot{m}_s}} \tag{6.8}$$

Noting that $A = \dot{m}_p/J_{av}$ then a dimensionless membrane area can be calculated as:

$$\frac{AJ_o}{\dot{m}_s} = \frac{\dfrac{\dot{m}_p}{\dot{m}_f}}{\dfrac{J_f}{J_o}\dfrac{J_{av}}{J_f}} \tag{6.9}$$

where: A = the membrane area of the module (m^2)

J_f = the flux at feed conditions ($kg/h.m^2$)

J_o = the maximum possible permeate flux for a given liquid composition (i.e. the flux as $T \rightarrow \infty$), ($kg/s.m^2$)

J_{av} = the average flux in the module ($kg/h.m^2$)

As discussed in section 1.15 variations in permeate concentration within a module are usually not significant and so it is reasonable to consider permeate composition to be constant. A component mass balance for the system yields

$$\dot{m}_s s_i \;=\; \dot{m}_p y_i \;+\; \dot{m}_o x_{ir} \tag{6.10}$$

Rearranging allows the retentate composition, x_{ir}, to be calculated

therefore
$$x_{ir} \;=\; \frac{s_i - \dfrac{\dot{m}_p}{\dot{m}_s} y_i}{\dfrac{\dot{m}_o}{\dot{m}_s}} \tag{6.11}$$

With Eq. (6.7), this gives
$$x_{ir} \;=\; \frac{s_i - \dfrac{\dot{m}_p}{\dot{m}_s} y_i}{1 - \dfrac{\dot{m}_p}{\dot{m}_s}} \tag{6.12}$$

A component balance at the junction prior to the pump yields

$$\dot{m}_s s_i \;+\; C\dot{m}_o x_{ir} = \dot{m}_f z_i \tag{6.13}$$

With Eq. (6.3) this allows the feed concentration entering the membrane module, z_i, to be calculated as a function of the supply concentration entering the system, s_i, the recycle ratio, C, the permeate-supply ratio, $\dot{m}_p/\dot{m}_s$, and the retentate composition

$$z_i = \frac{s_i \;+\; C\left(1 - \dfrac{\dot{m}_p}{\dot{m}_s}\right) x_{ir}}{1 \;+\; C\left(1 - \dfrac{\dot{m}_p}{\dot{m}_s}\right)} \tag{6.14}$$

With Eq. (6.12) the retentate composition can be substituted so that z_i, can be calculated as a function of s_i, C, $\dot{m}_p/\dot{m}_s$, and y_i the permeate composition

$$z_i = \frac{s_i \;+\; C\left(s_i - \dfrac{\dot{m}_p}{\dot{m}_s} y_i\right)}{1 \;+\; C\left(1 - \dfrac{\dot{m}_p}{\dot{m}_s}\right)} \tag{6.15}$$

6.4 Calculation of performance for an ideal module with recycle

Calculation of the membrane area with recycle and constant supply flowrate

In chapter 3, using a heat balance, the retentate temperature, T_r, was shown to be easily calculated using the expression

$$T_r = \frac{h_v}{c_p} - \left(\frac{h_v}{c_p} - T_f \right) \frac{\dot{m}_f}{\dot{m}_r} \tag{6.16}$$

where: h_v = the average enthalpy per unit mass of vapour

c_p = the average specific heat capacity

The effect of recycle when using a module with a particular membrane area can be determined using the various mass balance relationships derived in section 6.2 combined with the algorithms detailed in chapter 4. An algorithm for the calculation of the change in the permeate-supply ratio due to recycle for a membrane module of fixed area is outlined in Table 6.1.

Table 6.1 Algorithm for calculation of flux with recycle and constant supply flowrate.

Calculate the membrane area required without a recycle using Table 3.3 in chapter 3 or Table 4.3 in chapter 4 as appropriate.
Choose a recycle ratio. Note the supply composition, the permeate composition achievable with the membrane, E_j and the feed temperature.
Assume a value for the $\dot{m}_p/\dot{m}_s$ ratio (this will usually be larger than with no recycle).
Calculate the $\dot{m}_p/\dot{m}_r$ and $\dot{m}_p/\dot{m}_f$ ratios using Eqs. (6.6) and (6.7).
Calculate the retentate and feed compositions using Eqs. (6.12) and (6.15).
Calculate J_{av}/J_f for the module using the method outlined in Table 4.3 in chapter 4.
Calculate $\dot{m}_s/AJ_o$ using Eq. (6.9)
Iterate the $\dot{m}_p/\dot{m}_s$ ratio until $\dot{m}_s/AJ_o$ equals the $\dot{m}_s/AJ_o$ value for the base case with no recycle (this involves a nested iteration of the T_r for each increment).

As A, J_o and $AJ_o/\dot{m}_s$ are the same for recycle and without recycle, hence $\dot{m}_s$ is the same for both cases. Hence, the change in flux is proportional to the $\dot{m}_p/\dot{m}_s$ ratio with recycle divided by the $\dot{m}_p/\dot{m}_s$ ratio without recycle.

Calculation of throughput with constant retentate composition

A recycle can be used to increase throughput whilst maintaining a constant retentate composition. Such an approach may be of benefit in an industrial setting in cases where the required retentate composition specification is being achieving. For a given membrane area and supply concentration, increasing the supply flowrate while maintaining constant $\dot{m}_p/\dot{m}_f$ and $\dot{m}_p/\dot{m}_s$ ratios causes the supply, output and permeate flowrates to all increase equally. It can be shown using mass balances about the system that the retentate composition is unchanged. An algorithm for the calculation of the change in throughput due to recycle for a given membrane area and retentate composition is outlined in Table 6.2.

Table 6.2 Algorithm for calculation of flux with recycle with increased throughput.

Calculate the membrane area required without a recycle using Table 3.1 in chapter 3 or Table 4.3 in chapter 4 as appropriate.
Choose a recycle ratio. Note the supply composition, the permeate composition achievable with the membrane, E_j and the feed temperature.
Use the $\dot{m}_p/\dot{m}_s$ ratio as calculated for the base case with no recycle.
Calculate the $\dot{m}_p/\dot{m}_r$ and $\dot{m}_p/\dot{m}_f$ ratios using Eqs. (6.6) and (6.7).
Calculate the retentate and feed compositions using Eqs. (6.12) and (6.15).
Calculate J_{av}/J_f for the module using the method outlined in Table 5.1 in chapter 5.
Calculate $\dot{m}_s/AJ_o$ using Eq. (6.9)

As $\dot{m}_p/\dot{m}_s$ and $\dot{m}_p/\dot{m}_f$ are constant, an increase in the supply flowrate, $\dot{m}_s$, causes a proportional increase in the feed and permeate flowrates. As A and J_o are constant, the compound factor, $\dot{m}_s/A_{total}J_o$ is proportional to $\dot{m}_s$ which is in turn proportional to the permeate flowrate. Hence, the change in flux due to use of a recycle is proportional to $\dot{m}_s/A_{total}J_o$ with recycle divided by $\dot{m}_s/A_{total}J_o$ without recycle.

6.5 Results

Variations in flux within a module

The dimensionless area, $AJ_o/\dot{m}_s$, required to achieve a given $\dot{m}_p/\dot{m}_f$ ratio can be calculated using Eq. (6.8). The corresponding J/J_f and A/A_{total}, ratios can also be determined, where A is the membrane area corresponding to the $\dot{m}_p/\dot{m}_f$ ratio and A_{total} is the membrane area of the entire module. The J/J_f ratio can be plotted as a function of the A/A_{total} ratio as illustrated in Figs 6.2 and 6.3.

Typically, flux is proportional to concentration for industrial systems. The feed temperature is unchanged when a recycle is used: however, the feed concentration is diluted and this causes a reduction in flux at the start of a module. The temperature drop is less with recycle: this leads to increased flux in the latter part of modules. At infinite recycle, the temperature and concentration remain constant throughout a module and hence flux remains constant. Examples are shown in Figs. 6.2 and 6.3 of curves of J/J_s versus A/A_{total} for recycle ratios of 0, 1, 2 and ∞ for an IPA-water system; where J_s is the flux with no recycle at the supply concentration and feed temperature. The results for total recycle ($C = \infty$) were approximated by using C = 9,999.

Effect of recycle on the flux distribution within a module

The dilution effect is greater when the water concentration in the supply stream is low. This is caused by the greater ratio between the water concentration in the supply stream and that in the recycle stream: e.g. a reduction in the feed concentration from 6% w/w to 3% w/w reduces the concentration by 50%, whereas from 15% w/w to 12% w/w the reduction is 20%. The change from reduced flux to increased flux occurs earlier for systems with higher water concentrations in the supply stream as shown in Figs. 6.2 and 6.3. Therefore at higher supply concentrations there is a proportionately larger part of the module with increased flux and a smaller proportion with reduced flux.

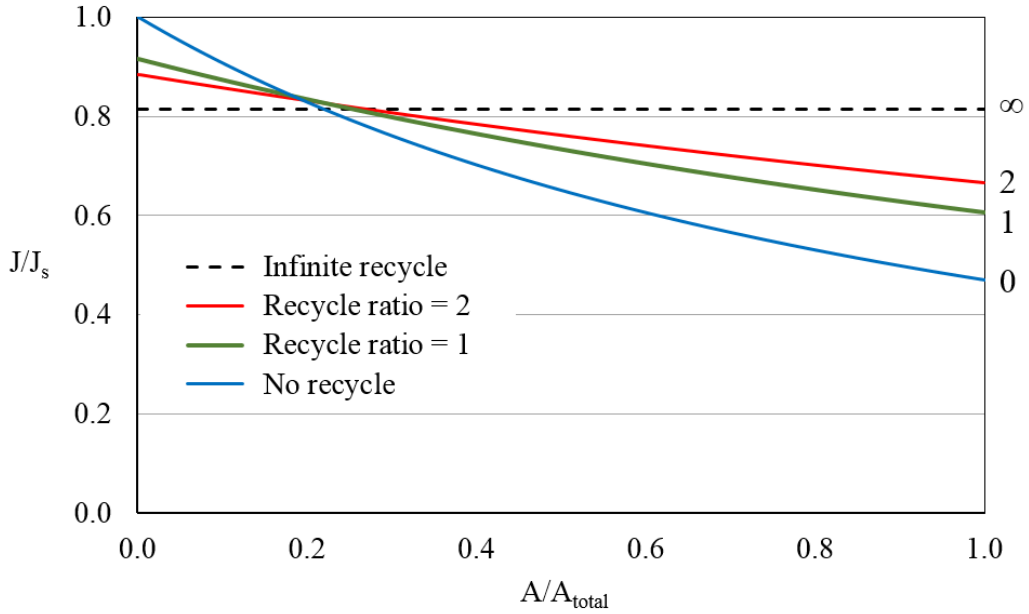

Figure 6.2 Variation in flux within an adiabatic pervaporation module, s_i = 7 wt% water. Isopropanol dehydration with flux proportional to concentration, T_f = 120 °C, y_i = 95 wt% water, E_j = 40,000 kJ/kmol and $\dot{m}_p/\dot{m}_f$ = 0.04 when there is no recycle. Recycle ratios of 0, 1 and 2 and infinity are shown. J_s is the flux at the feed temperature and supply concentration with no recycle.

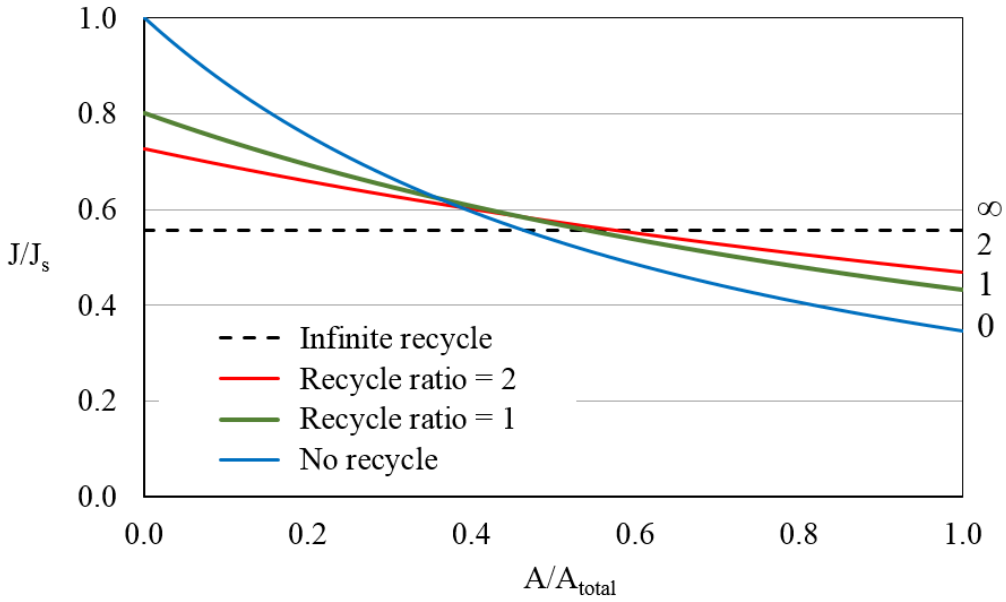

Figure 6.3 Variation in flux within an adiabatic pervaporation module, s_i = 15 wt%. Isopropanol dehydration with flux proportional to concentration, T_f = 120 °C, y_i = 95 wt% water, E_j = 40,000 kJ/kmol and $\dot{m}_p/\dot{m}_f$ = 0.04 when there is no recycle. Recycle ratios of 0, 1 and 2 and infinity are shown. J_s is the flux at the feed temperature and supply concentration with no recycle.

Effect of concentration on average flux

As previously stated, recycling reduces the solute concentration in the feed and when flux is an increasing function of concentration, this significantly counter-acts the increased flux. Fig. 6.4 illustrates the effect of the supply concentration on the increase in flux for a given recycle ratio. The greater the feed concentration the greater the increase in flux for a given recycle ratio. For a given reduction in solute concentration, the effect on the x_{ir}/z_i ratio is greater at lower supply concentrations. Consider a case where s_i = 0.10, y_i = 0.99, a $\dot{m}_p/\dot{m}_s$ ratio of 0.02 and a recycle ratio of 1. The feed concentration as calculated using Eq. (6.15) is 0.091: a reduction of 9%. In contrast, were s_i = 0.04, the feed concentration would be 0.0304: a reduction of 24%.

The increase tails off at higher water concentrations. There can be a reduction in flux when the supply concentration and E_j are both low, as illustrated in Fig. 6.4. This was noted by Santoso *et al*. (2012); however, this is due to dilution and not temperature effects, contrary to what they stated.

Effect of solvent on the change in flux due to recycle

Permeate typically comprises ≥ 90% water as discussed in section 1.14. Thus the solvent is only a minor factor as regards the latent heat of the permeate stream and values are similar whatever the solvent. The specific heats of ethanol, IPA and isobutanol at 120 ^{o}C are 2.688, 3.330 and 2.474 kJ/kg.K respectively. A smaller specific heat leads to a larger temperature drop within a module for a given permeate-feed ratio: in such cases use of a recycle leads to a commensurately greater increase in the average temperature and hence a greater increase in flux. This is evident in Figs. 6.4 and 6.5 as well as Table 6.4 where increases in flux for a given recycle ratio and combination of operating conditions are greater for ethanol as compared to IPA.

As discussed previously, recycles are of less benefit at low supply concentrations. Hence, recycles are likely to be of less benefit when dehydrating ethanol as its azeotrope contains 4% water and hence the feed composition is usually ≤ 10% as compared with IPA or isobutanol which form azeotropes at 12% and 33% water respectively.

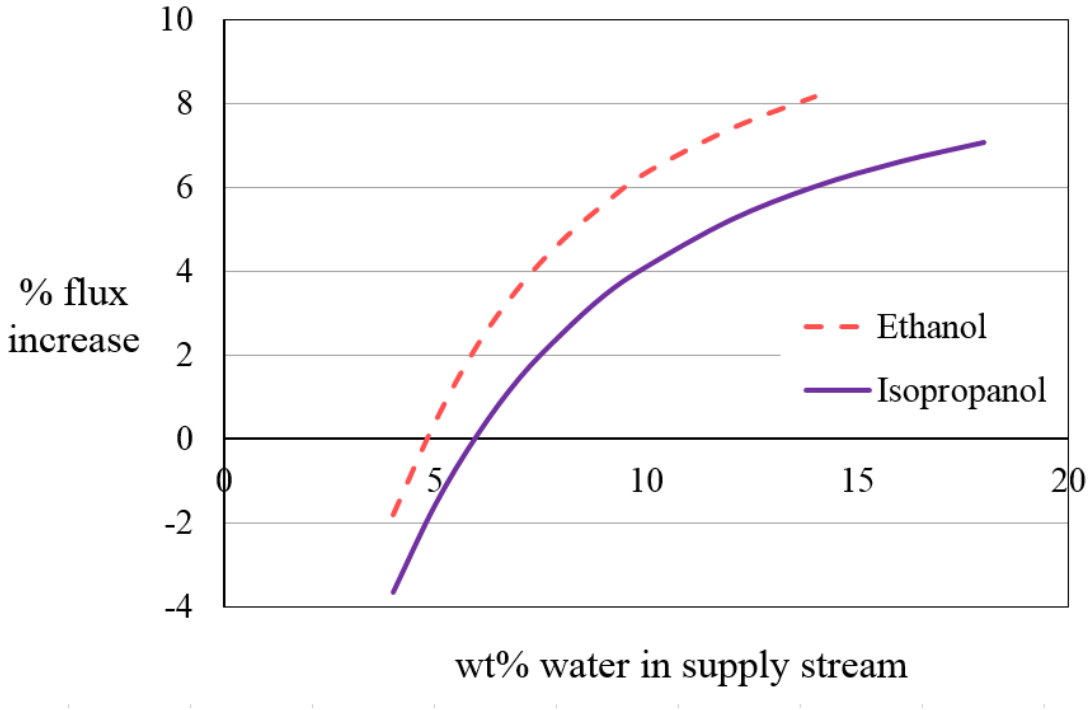

Figure 6.4 Change in flux versus feed concentration due to recycle ratio of 1.0: T_f = 120 °C, y_i = 98 wt% water, E_j = 40,000 kJ/kmol, $\dot{m}_p/\dot{m}_f$ = 0.03 when there is no recycle. Flux is proportional to concentration. Solid purple line is IPA: dashed pink line is ethanol.

Increased Recycle Ratio

Increasing the recycle ratio increases the effect of a recycle, as noted by Santoso *et al.* (2012): although the relationship is asymptotic. This is evident from the examples shown in Fig. 6.5 and Table 6.3. In cases where a recycle causes a decrease in flux, this too is more pronounced at higher recycle ratios. Santoso *et al.* (2012) reported cases where flux peaked: however, this only occurs at low concentrations and the subsequent decline at higher recycle ratios is not significant. Tsuyumoto *et al.* (1997) noted a similar result.

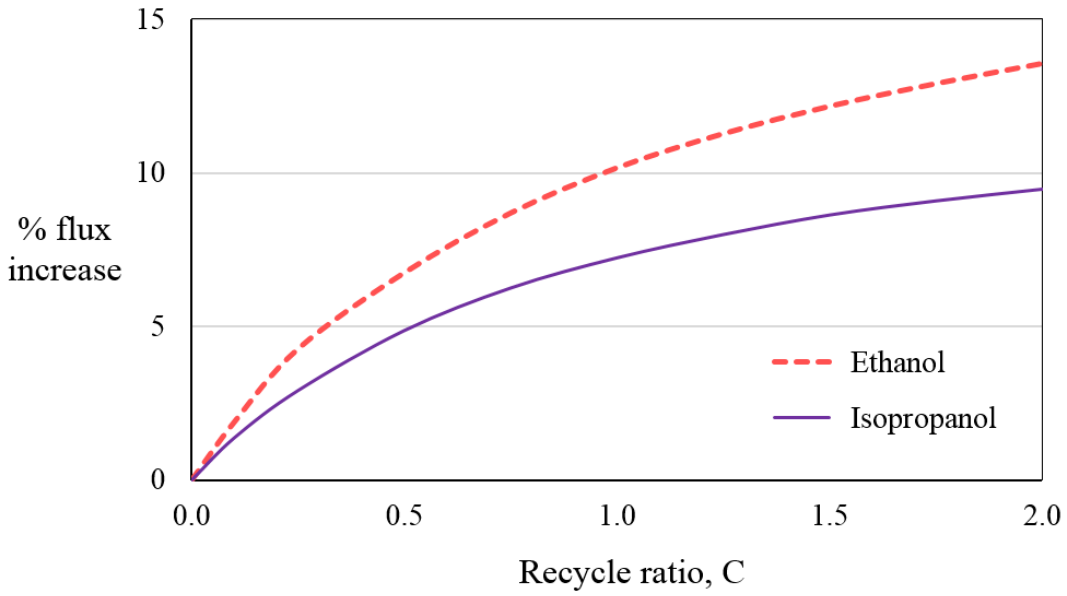

Figure 6.5 Increase in flux versus recycle ratio with flux proportional to concentration; s_i = 10% water, T_f = 120 °C, y_i = 90 wt% water and E_j of 40,000 kJ/kmol. $\dot{m}_p/\dot{m}_f$ = 0.03 when there is no recycle. Solid purple line is IPA; dashed pink line is ethanol.

Effect of operating conditions on average flux

Examples of the effect of recycle on the flux in ideal modules are shown in Table 6.3. A recycle leads to a greater increase in flux at higher $\dot{m}_p/\dot{m}_s$ ratios due to the greater temperature drop associated with increased permeate flow as is evident from a comparison of the first two rows in Table 6.3

Latent heat is greater at lower temperatures, whereas specific heat varies little with temperature: hence, the ratio of specific heat to latent heat is greater at lower temperatures, leading to larger temperature drops and greater increases in flux when a recycle is used. This is evident from a comparison of the first and third rows in Table 6.3.

The latent heat of the permeate stream is higher the greater the water concentration in the permeate stream, due to the higher latent heat of water as compared with other solvents. Thus for a given $\dot{m}_p/\dot{m}_f$ ratio, more energy is required to vaporise the permeate stream and hence, the temperature drop is greater. Thus use of recycle leads to a larger

increase in flux for systems with a higher water concentration in the permeate stream. This is evident from a comparison of the first and last rows in Table 6.3.

Table 6.3 Effects of operating conditions on flux with recycle: constant supply flowrate, Recycle ratio = 1, E_j = 40,000 kJ/kmol, s_i = 10 wt%, flux proportional to water concentration.

$\dot{m}_p/\dot{m}_s$	T_f °C	y_i	EtOH % increase $\dot{m}_p/\dot{m}_s$	IPA % increase $\dot{m}_p/\dot{m}_s$
0.030	120	0.90	10.1	7.2
0.036	120	0.90	12.0	8.6
0.030	90	0.90	14.3	10.7
0.030	120	0.98	10.3	7.4

Effect of the apparent activation energy of pervaporation on average flux

A higher E_j value leads to a greater temperature drop for a given $\dot{m}_p/\dot{m}_f$ ratio. Hence, use of a recycle causes greater flux increases in circumstances where the E_j value is high as shown in Fig. 6.6: the distance between the permeate-supply ratio curves is greater at higher E_j values. This effect was noted by Santoso *et al*. (2012). At lower feed concentrations, the curves are closer together as recycles cause a smaller increase in flux. There can even be decreases in flux as noted by Santoso *et al*. (2012). At E_j values below 25,000 kJ/kmol, use of a $\dot{m}_p/\dot{m}_s$ ratio greater than 5% without a recycle may be feasible as discussed in chapter 4: this will usually be of more benefit than use of a recycle, as the equipment is less complex.

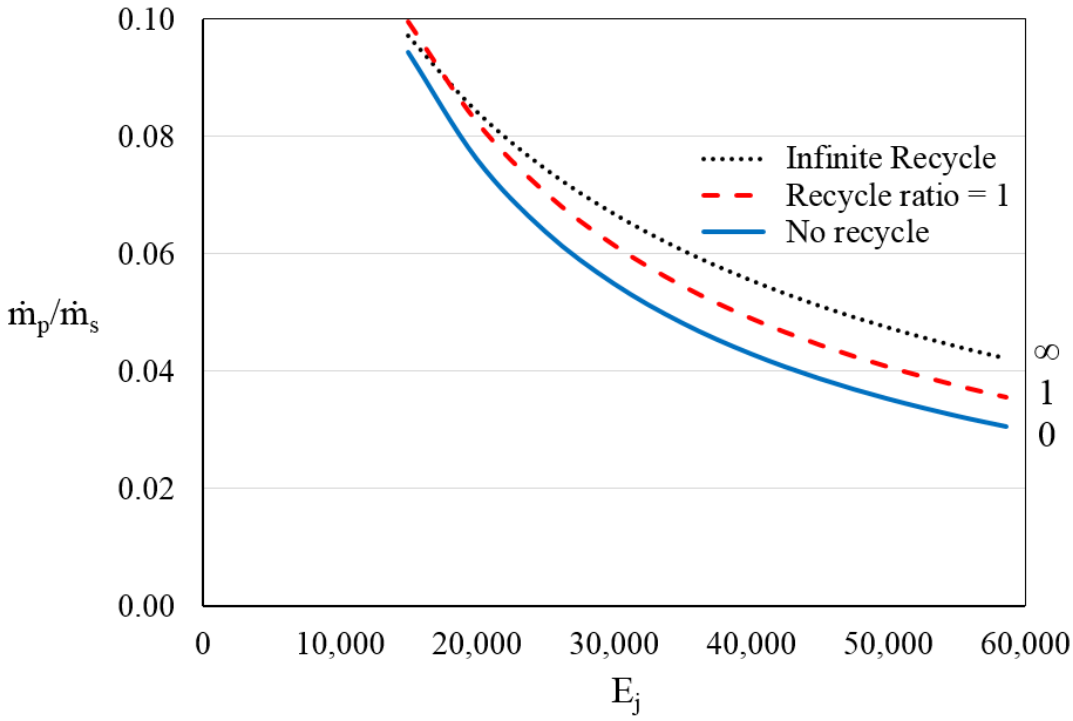

Figure 6.6 Permeate-supply ratios versus activation energy: IPA with s_i = 15%, y_i = 0.95, J_r/J_{reheat} = 0.4 with no recycle. Dotted black line is for infinite recycle. Dashed red line is for a recycle ratio of 1 and solid blue line is with no recycle.

Comparison with literature data

Tsuyumoto *et al*. (1997), reported the results of an industrial-scale ethanol dehydration: a recycle ratio of 1.79 with s_i = 6.05% water, E_j = 43,326 and T_f = 60 °C led to a 9.9% increase in flux. The modules in the system had considerable variations in membrane thickness which could have affected the results. The results are consistent with those calculated using mass balances per Eqs. (6.12) and (6.15). Calculations with the flux-concentration relationship for the system, assuming ideal behaviour using the equations developed in this chapter, predicted a 10.4% increase in flux. Marriott and Sørensen (2003b) found no significant change in the outlet concentration and flux when they modelled the above system.

Increased throughput

Increasing the supply flowrate, while maintaining a constant $\dot{m}_p/\dot{m}_s$ ratio, causes the supply flowrate, output flowrate and permeate flowrate to each increase equally, thereby keeping the retentate composition unchanged. As A and J_o are constant, the change in $\dot{m}_s/AJ_o$ is proportional to the increase in throughput. Examples of increased throughput

as a function of recycle ratio are shown in Fig. 6.7. The specific heat of ethanol is less than that of IPA, so the temperature drop and the effect of recycle are greater for ethanol as illustrated in Fig. 6.7. Use of a recycle to increase throughput does not lead to a change in the retentate concentration: hence the increase in flux is greater as compared with the corresponding use of recycle with constant feed flowrate: this is evident from a comparison of Figs. 6.5 and 6.7.

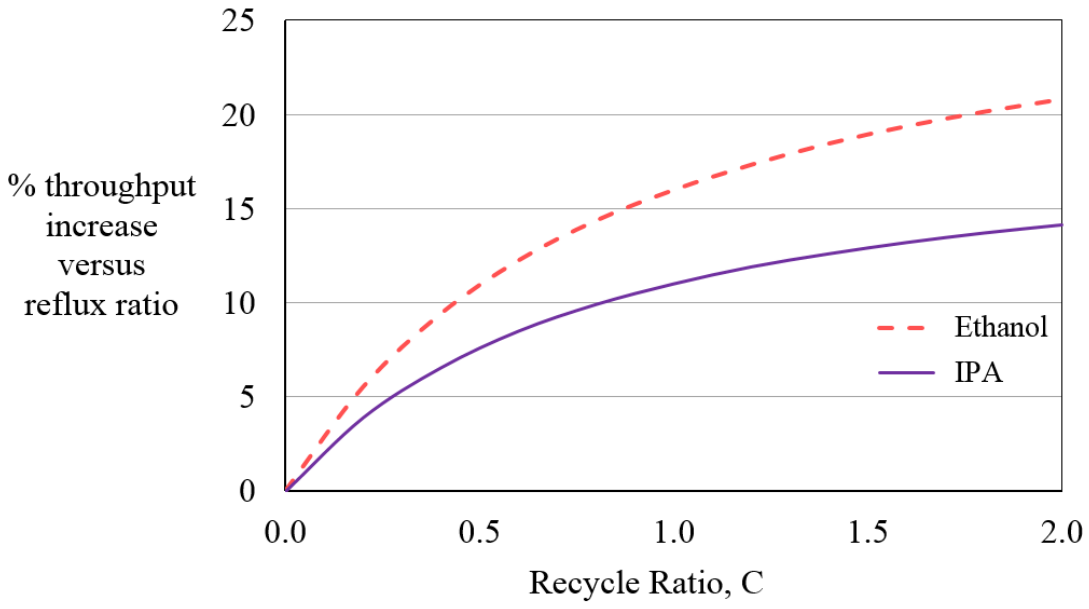

Figure 6.7 Increase in throughput vs. recycle ratio with flux proportional to concentration; s_i = 10 wt%, T_f = 120 °C, y_i = 90 wt% water, E_j = 40,000 kJ/kmol, $\dot{m}_p/\dot{m}_s$ = 0.03 when there is no recycle. Solid purple line is IPA; dashed pink line is ethanol.

At low concentrations there can be a recycle ratio that gives a maximum increase in throughput, e.g. for ethanol with 7% water, maximum throughput occurs at a recycle ratio of 10, albeit the reduction at higher recycle ratios is small. This is analogous to the maximum change in retentate concentration found by Santoso *et al.* (2012) and by Tsuyumoto *et al.* (1997) for fixed feed flowrates.

Systems where flux is independent of concentration

As discussed in chapter 3, there are membranes for which flux is constant across a range of concentrations. The effect of increased temperature within a module is not counter-acted by the dilution of the feed concentration; hence, use of a recycle leads to significant increases in flux at all concentrations. Water has a higher specific heat than ethanol or

IPA, leading to marginally greater increases in flux at low water concentrations as shown in Fig. 6.8.

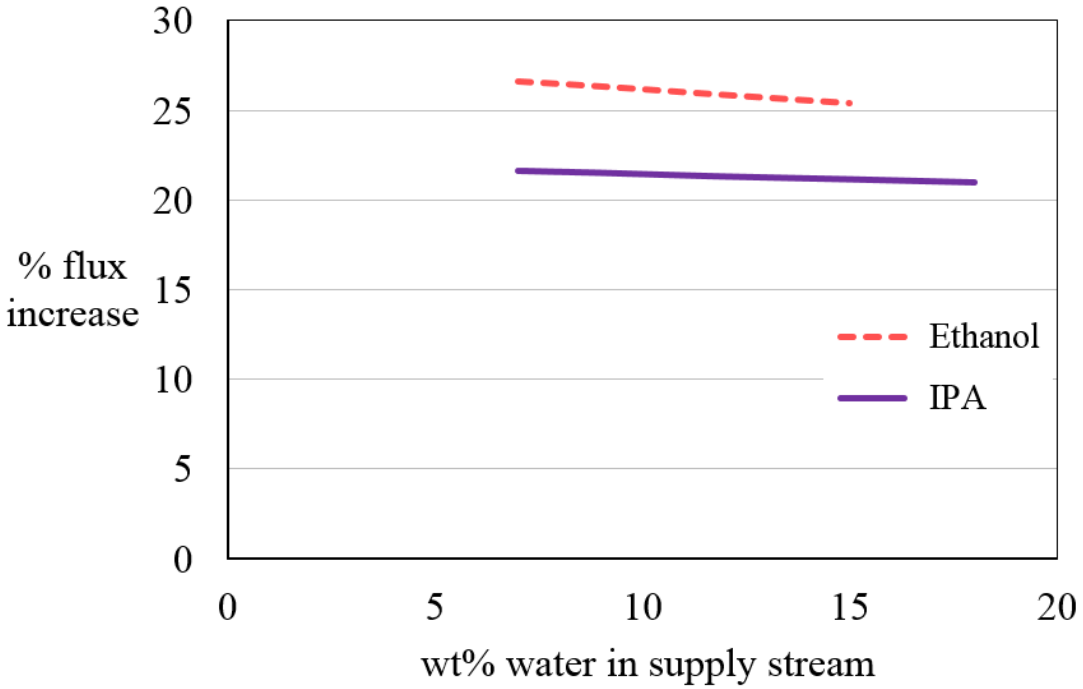

Figure 6.8 Flux versus supply concentration with concentration-independent flux: dehydration with a recycle ratio of 1.0, T_f = 120 °C, y_i = 90 wt% water, E_j = 40,000 kJ/kmol. $\dot{m}_p/\dot{m}_f$ = 0.0437 when there is no recycle. Solid purple line is IPA; dashed pink line is ethanol.

The results in Table 6.4 indicate that high $\dot{m}_p/\dot{m}_s$ ratios, low feed temperatures and high activation energies all increase the effect of recycle, whilst permeate composition has little effect: this is similar to systems where flux is proportional to concentration. The specific heat of ethanol is less than that of IPA: so the temperature drop and the effect of recycle is greater as illustrated by the examples in Table 6.4.

Table 6.4 Increase in flux for dehydrations where flux is independent of water concentration. $\dot{m}_p/\dot{m}_s$ is for base case with no recycle, s_i = 10 wt%, Recycle ratio = 1.

$\dot{m}_p/\dot{m}_s$	T_f °C	y_i	E_J kJ/kmol	EtOH % increase $\dot{m}_p/\dot{m}_s$	IPA % increase $\dot{m}_p/\dot{m}_s$
0.030	120	0.90	40,000	17.8	14.5
0.036	120	0.90	40,000	18.8	15.4
0.030	80	0.90	40,000	45.8	17.6
0.030	120	0.98	40,000	24.3	20.1
0.030	120	0.90	60,000	25.9	21.4

6.5 Energy Consumption

A key metric for solvent dehydration processes is the energy consumption per unit mass of water in the permeate stream. Energy input to the heat exchanger is a function of the heat required to bring the supply and the recycle streams to the feed temperature as illustrated in Fig. 6.9.

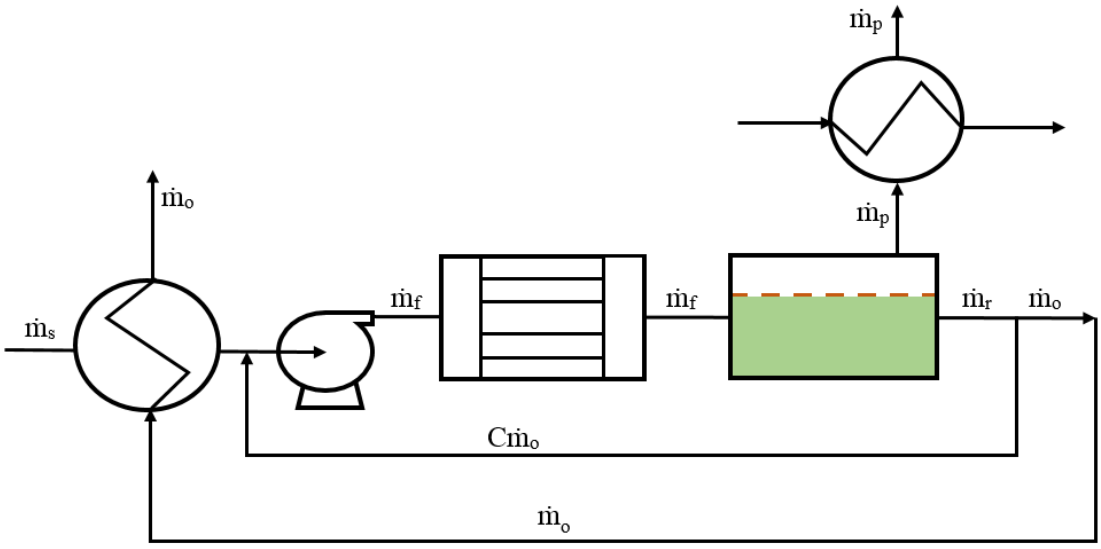

Figure 6.9 Pervaporation with recycle.

An energy balance about the heat exchanger gives

$$\Delta q = C\dot{m}_o \int_{T_r}^{T_f} c_{po} dT + \dot{m}_s \int_{T_s}^{T_f} c_{ps} dT_f \qquad (6.17)$$

where, Δq = the power required to bring the supply stream to the feed temperature.

C = the recycle ratio

$\dot{m}_o$ = the mass flowrate of the "outlet" stream leaving the system

T_r = the retentate temperature

T_f = the feed temperature $\dot{m}_s$

c_{po} = the specific heat of the outlet stream

$\dot{m}_s$ = the mass flowrate of the "supply" stream entering the system

T_s = the suppy stream temperature

c_{ps} = the specific heat of the supply stream

Whilst retentate temperature increases, the retentate mass flowrate decreases: hence, the increase in heat input is less than the increase in flux. Thus the energy consumption per unit mass of permeate decreases. For example, consider an IPA dehydration with a recycle ratio of 1.0, s_i = 10%, T_f = 120 ^{o}C, $\dot{m}_p/\dot{m}_s$ = 0.03 and: the flux increases by 14%, whilst energy consumption including that for pumping increases by 10%, leading to a net 3.9% decrease in energy consumption per unit mass of permeate.

The results are similar for single stage systems where the outlet stream is used to preheat the supply stream. The final retentate temperature is unchanged: hence, the small decrease in the mass flowrate of the retentate stream leads to a small decrease in the energy lost to the retentate stream. This is minor in terms of overall heat requirements. For the above example, with heat recovery, a recycle ratio of 1.0, leads to a 4.7% reduction in the energy consumption per unit mass of permeate.

In the case of multi-stage pervaporation systems where the retentate is reheated prior to subsequent stages, the increase in retentate temperature leads to a commensurate decrease in the heating required prior to subsequent stages. Recycles are not used in the

final stage of such systems due to the low feed concentration: so the final retentate temperature is unchanged. There is a slight increase in the permeate temperature in modules where a recycle is used, but this does not have a significant effect on the net energy consumption per unit mass of permeate.

6.7 Conclusions

A recycle may be used to achieve greater flux leading to reduced water content in the retentate. Alternatively, a recycle may be used to increase throughput. A combination of these two approaches could also be used. Such flexibility is of particular benefit in industrial systems where a pervaporation system is used to recover a variety of solvents or where there are variations in feed concentration. Kujawski (2000) noted that

> *"Flexibility with respect to part load and changing product and feed concentrations is one of the advantages of pervaporation over other separation processes."*

The novel concepts of the permeate-supply ratio $\dot{m}_p/\dot{m}_s$, and the "outlet" stream, $\dot{m}_o$, are proposed for recycle applications. They allow the development of novel algebraic equations for the calculation of the $\dot{m}_p/\dot{m}_f$ and $\dot{m}_p/\dot{m}_r$ ratios as functions of the $\dot{m}_p/\dot{m}_s$ ratio and the recycle ratio. Novel algebraic equations have been developed for the calculation of the feed and retentate compositions. These build on the work in chapters three, four and five which related to the performance of individual modules: together they facilitate calculation of the average flux for ideal modules with recycle whatever the flux-concentration-flux relationship.

The results indicate that increases in average flux can be achieved through use of recycle for industrial applications where E_j is high and where there is a high water concentration in the feed or alternatively when concentration has little or no effect on flux. Alternative module designs such as those outlined in section 1.12 with additional stages and smaller $\dot{m}_p/\dot{m}_f$ ratios, will often be more effective than use of a recycle for systems where flux is proportional to concentration.

Chapter 7: Efficiency of Pervaporation Modules and Systems.

7.1 Abstract

Existing performance metrics for pervaporation modules are reviewed and some improved metrics are proposed. Performance data relating to industrial-scale systems is analysed using these metrics. For the first time the energy efficiency of multiple industrial-scale plants is compared and the module efficiency of an adiabatic industrial-scale plant is determined.

7.2 Introduction

There is significant literature regarding the performance of pervaporation membranes at laboratory scale. There has been considerable emphasis on solute transport in pervaporation membranes as discussed in section 1.10. However, considerably less data has been published regarding the performance and energy consumption of industrial-scale pervaporation systems (Sander and Soukup, 1988; Tsuyumoto *et al*., 1997; Kujawski, 2000; Morigami *et al*., 2001; Marriott and Sørenson, 2003b). The actual energy consumption in industrial-scale systems is calculated from the limited available literature data and compared to that of ideal modules.

Energy is an important cost for pervaporation systems (Baker, 2012, p. 403), apart from some hybrid systems where much if not all of the heating occurs as part of the distillation process (Baker, 2012, p. 403). A number of novel energy efficiency metrics are developed in this chapter, including: the heat input per unit mass of permeate and also the steam consumption to permeate flow ratio. The retentate stream is often used to pre-heat the feed stream. The heat recovery efficiency can be ascertained by comparing the amount of heat recovered in a pre-heater as compared to the heat available for recovery from the retentate stream. The rate of heat loss to the environment as a proportion of the heat input is also discussed.

In this chapter an "Isothermal efficiency" is proposed: it compares the theoretical minimum membrane area for an adiabatic module to that for an isothermal module for the same separation and with the same feed temperature. This novel metric will facilitate

optimisation of the number of stages in pervaporation systems. It will allow comparison between systems, thereby facilitating the design of pervaporation systems. It can also be applied to modules which are both non-isothermal and non-adiabatic.

Sommer *et al*. (2005) defined a "module efficiency" for pervaporation modules as the theoretical minimum membrane area for a module as compared to that for an actual module with the same operating conditions. The main factors affecting module efficiency are heat losses to the environment, poor flow distribution, temperature polarisation and concentration polarisation. Heat losses to the environment reduce the liquid temperature, leading to a reduction in flux and increasing the membrane area required to achieve a given separation.

Poor flow distribution can cause zones where flow is slow allowing high levels of permeation from a proportion of the liquid passing through the module leading to low concentrations, low temperatures and low flux. The remaining liquid will have a shorter average residence time. This leads to a reduction in the average overall flux for the module.

The vaporisation of permeate as it passes through the membrane requires considerable latent heat, which causes a reduction in the temperature of the liquid at the membrane surface as compared with the bulk fluid leading to a reduction in flux: this effect is known as temperature polarisation. The solute preferentially permeates the membrane, leaving a low concentration of solute at the upstream membrane surface. This also leads to a reduction in the permeate flux: this effect is known as concentration polarisation. Both temperature polarisation and concentration polarisation are discussed in section 1.11. The high fluxes that can be achieved with modern membranes, particularly when operated at high temperatures, can lead to significant reductions in flux due to concentration and temperature polarisation (Witte *et al*., 2000; Sommer *et al*., 2005). Both these effects can be reduced by operating with turbulent flow at Reynolds Numbers $\geq$ 10,000 (Sommer *et al*., 2005).

This analysis provides an insight into the performance of industrial-scale pervaporation systems. Further research is needed to determine the typical performance of modern industrial-scale pervaporation systems.

7.3 Metrics relating to energy efficiency

Heat input

Pervaporation is undertaken at elevated temperatures so as to achieve higher flux. The feed stream is heated using a heat exchanger prior to the start of the membrane module. The heat input can be calculated by undertaking an energy balance around a pervaporation stage as illustrated by the dashed red line in Fig. 7.1.

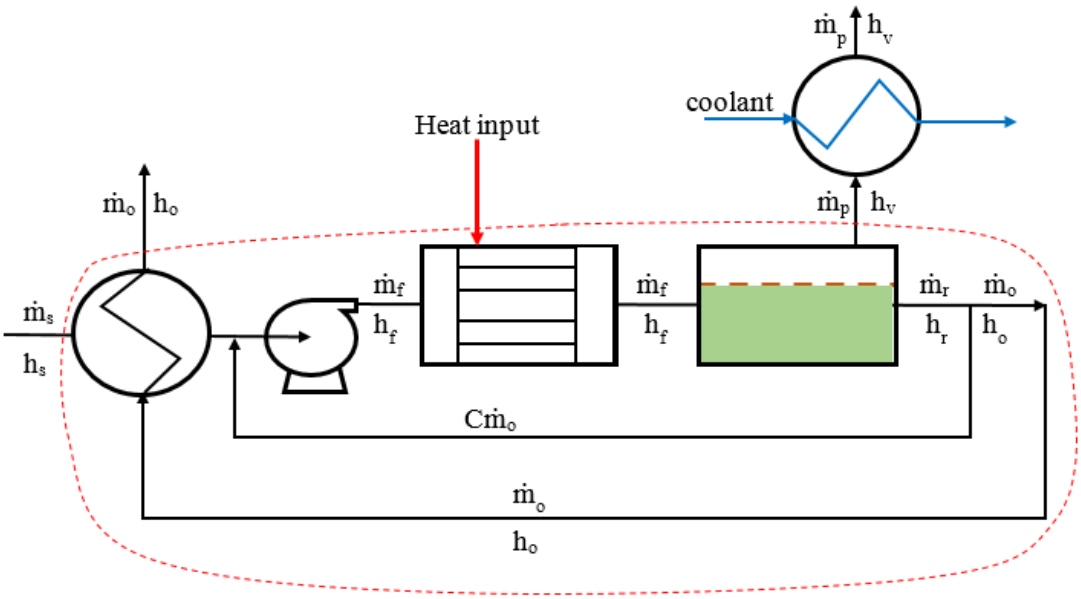

Figure 7.1 Process flow diagram of a single-stage pervaporation system

This gives the following equation

$$\Delta q_{heat} = \left(\dot{m}_p h_v + \dot{m}_o h_o\right) - \left(\dot{m}_s h_s + \Delta q_{pump}\right) \tag{7.1}$$

where Δq_{heat} the heat input per unit time via the heat exchanger

$\dot{m}_p$ the mass flowrate of the permeate stream (kg/s)

h_v the enthalpy of the permeate stream (kJ/kg)

$\dot{m}_o$ the mass flowrate of the liquid retentate leaving the system (kg/s)

h_o the enthalpy of the outlet stream (kJ/kg)

$\dot{m}_s$ the mass flowrate of the supply stream (kg/s)

h_s the enthalpy of the supply stream (kJ/kg)

Δq_{pump} the power consumed by the pump (kJ/s)

The equation is applicable to adiabatic modules, modules where heat is supplied such as isothermal modules, modules with partially vaporised feed and modules with recycles.

Eq. (7.1) can be expanded so as to be applicable to multi-stage pervaporation systems

$$\sum \Delta q_{heat} = \left(\sum \dot{m}_p h_v + \dot{m}_o h_o\right) - \left(\dot{m}_s h_s + \Sigma \Delta q_{pump}\right) \tag{7.2}$$

Energy efficiency

The energy consumed in a pervaporation system includes that used for heating the supply stream, inter-stage heating and heating within modules. The energy required for cooling, Δq_{cool}, includes energy consumed by refrigeration systems as well as any energy consumed by cooling water systems that are used to cool refrigeration systems. In systems where vacuum pumps are used during normal operations, the energy consumption of the vacuum pumps is often considerable (Baker, 2012, p. 398). Energy consumption can be calculated as follows

$$\Delta q_{energy} = \Sigma \Delta q_{heat} + \Sigma \Delta q_{pump} + \Sigma \Delta q_{cool} + \Sigma \Delta q_{vac} \tag{7.3}$$

where Δq_{energy} the energy consumption of the pervaporation system (kW)

Δq_{cool} the energy consumption of the cooling system (kW)

Δq_{vac} the energy consumption of the vacuum system (kW)

The temperature of the supply stream in hybrid systems is often considerably higher than the ambient supply temperature typical of simple pervaporation processes: indeed there may be partially vaporised feed. These factors need to be considered when comparing the performance of hybrid and conventional systems.

In systems where the product is purified retentate, such as the dehydration of ethanol, isopropanol or THF, the energy efficiency has been defined as the energy consumed per unit mass of retentate product (Nagy *et al*., 2015)

$$\eta_{energy} = \frac{\Delta q_{energy}}{\dot{m}_r} \tag{7.4}$$

Systems with high feed concentrations, require the vaporisation of more permeate per unit mass of retentate product. Thus the mass flowrate of the permeate stream is a more appropriate basis for determining energy efficiency. Systems with poor separation characteristics have a greater amount of solvent in the permeate stream and therefore a greater amount of permeate needs to be vaporised to achieve a given retentate composition: this requires additional heat input per unit mass of feed. The water concentration in the permeate stream is a function of the membrane rather than the module. Therefore the mass flowrate of the water in the permeate stream, rather than the total mass flowrate of the permeate stream is theoretically a more appropriate basis for comparison when benchmarking the performance of pervaporation modules. However, most modern commercial membranes have permeate purities of greater than 97% as discussed in section 1.14 so that use of the mass flowrate of the permeate stream is reasonable. Hence, a novel metric, the energy consumption per unit mass of permeate is proposed.

$$\eta_p = \frac{\Sigma \Delta q_{energy}}{\dot{m}_p} \tag{7.5}$$

Eq. (7.5) can be used to compare the performance of pervaporation systems with different feed concentrations and different solvents: albeit that it is an approximation as there are minor inconsistencies due to variations in latent heat caused by differences in permeate purity, solvents and operating temperatures and due to variations in the separation performance of membranes.

Steam heating usually costs less than electricity. This reflects the relative inefficiency of electricity generation and distribution (US EPA, 2013). Energy consumed in the form of electricity and energy used for heating are often presented separately (Baker, 1991; Tsuyumoto *et al*., 1997). Electricity is used for pumps, vacuum pumps and cooling

systems: it is rarely used to heat industrial-scale pervaporation systems. Electricity consumption is largely dependent on the efficiency of the electrical equipment rather than the geometry of the membrane modules. Therefore it can be useful to consider electrical energy consumption alone. An electrical efficiency, η_{elec}, is proposed

$$\eta_{elec} = \frac{\Sigma\Delta q_{pump} + \Sigma\Delta q_{cool} + \Sigma\Delta q_{vac}}{\dot{m}_p} \tag{7.6}$$

Analysis of the heat input allows the cost of heating to be considered separately. A heating efficiency, η_{heat}, is proposed

$$\eta_{heat} = \frac{\Sigma\Delta q_{heat}}{\dot{m}_p} \tag{7.7}$$

The heat input can be expressed as the mass flowrate of steam consumed. A novel metric the *"steam-permeate ratio"* is proposed: this is the ratio of the mass flowrate of the steam versus the mass flowrate of the permeate stream. As no heat is recovered from the permeate stream this ratio must be greater than unity for the aqueous permeate in hydrophilic pervaporation systems.

$$\text{Steam-Permeate Ratio} = \frac{\dot{m}_{steam}}{\dot{m}_p} \tag{7.8}$$

Heat losses

Heat losses can be calculated as follows

$$\Delta q_{heat\,loss} = \dot{m}_r h_{r\,ideal} - \dot{m}_r h_r \tag{7.9}$$

where $h_{r\ ideal}$ is the enthalpy of the retentate assuming no heat losses. This can be determined using the methods outlined in chapter 3. The retenate enthalpy, h_r, can be obtained by measuring the temperature of the retentate stream.

Heat loss as a proportion of energy consumption can be defined as follows

$$\eta_{heat\,loss} = \frac{\Delta q_{heat\,loss}}{\Delta q_{energy}} \tag{7.10}$$

Heat recovery

The energy recovered in a pre-heater, as illustrated in Fig. 7.1, can be calculated by subtracting the enthalpy of the outlet stream leaving the pre-heater from its enthalpy entering the pre-heater

$$\Delta q_{recovery} = \dot{m}_o h_r - \dot{m}_o h_o \tag{7.11}$$

The proportion of the available heat that is recovered, is a metric that facilitates design and investment decisions. Use of the supply stream to cool permeate condensers is generally not practicable, as the supply stream temperature is too high. Therefore energy can only be recovered from the outlet stream using a pre-heater. Achievement of 100% heat recovery would require an infinitely large heat exchanger to cool the outlet stream to the supply stream temperature. Higher operating temperatures lead to higher retentate temperatures and greater opportunities to recover heat from the retentate stream. The following novel definition of the heat recovery efficiency is proposed

$$\eta_{heat\ recovery} = \frac{\dot{m}_o \left(h_r - h_o \right)}{\dot{m}_o \left(h_r - h_s \right)} \tag{7.12}$$

Simplifying

$$\eta_{heat\ recovery} = \frac{\left(h_r - h_o \right)}{\left(h_r - h_s \right)} \tag{7.13}$$

In many cases, the assumption of constant physical properties over the range of temperatures encompassed by the retentate and supply streams does not lead to significant errors; so an approximation can be made with little error as shown in Eq. (7.14). This simplification is often used in relation to the coefficient of performance in refrigeration systems (Smith *et al*., 2001).

$$\eta_{heat\ recovery} = \frac{\left(T_r - T_o \right)}{\left(T_r - T_s \right)} \tag{7.14}$$

Sample calculations are shown at the end of this chapter.

7.4 Isothermal efficiency

Feed in industrial systems flows through a series of adiabatic pervaporation modules. In order to maintain the flux in each module at sufficiently high values, the retentate is reheated to the initial feed temperature prior to entering subsequent modules. Over-frequent reheating leads to complexity; the additional cost of piping and valves can be significant (Baker, 2012, p. 395). The optimum membrane area thus depends on the relative cost of membranes versus that of reheating equipment. An "Isothermal efficiency" is proposed. This compares the theoretical minimum area required for a particular separation with the theoretical minimum area required for the same separation using isothermal operation

$$\eta_{isothermal} = \frac{A_{isothermal\ ideal}}{A_{actual\ ideal}} \tag{7.15}$$

This parameter can be used when optimising the number of stages during the design of pervaporation systems or when comparing adiabatic and isothermal designs. An isothermal module has an isothermal efficiency of unity. The development of an analytical solution for the calculation of the area of isothermal modules as outlined in chapter 2 and the short-cut methods for the determination of the average flux in adiabatic modules as outlined in chapters 3 and 4 facilitate the calculation of the "isothermal efficiency".

7.5 Module efficiency

Schleger *et al*. (2004) defined a "module efficiency" for pervaporation modules as the theoretical minimum membrane area for a module as compared to that for an actual module with the same operating conditions. For an adiabatic module this can be calculated as follows

$$\eta_{module} = \frac{\text{Real flux with gradients}}{\text{Theoretical flux at bulk conditions}} \tag{7.16}$$

The module efficiency can also be defined in terms of the module area

$$\eta_{module} = \frac{A_{adiabatic\ ideal}}{A_{actual}} \tag{7.17}$$

Whereas for an isothermal module the equation is

$$\eta_{module} = \frac{A_{isothermal\ ideal}}{A_{actual}} \tag{7.18}$$

Sample calculations are shown at the end of this chapter.

7.6 Results

Electrical efficiency

The electrical energy consumption per unit permeate for a number of industrial-scale ethanol dehydrations is shown in Table 7.1. Both Kujawski (2000) and Sander and Soukup (1988) provided data for industrial operations: they are more efficient than the trials described by both Tsuyumoto *et al*. (1997) and Morigami *et al*. (2001). The energy efficiency of these latter systems may not have been optimised as they were not being operated on a long term basis. Kujawski (2000) reported the same rate of electricity consumption for an ethanol dehydration and a THF dehydration using the same equipment despite the permeate flowrate being 58% less for the THF dehydration. As a consequence the electrical consumption per unit mass of permeate is significantly higher for the THF as shown in Table 7.1.

The equipment used by Morigami *et al*. (2001) and by Tsuyumoto *et al*. (1997) used cooling water and vacuum pumps. Modern systems are more likely to use refrigeration to achieve vacuum as operating costs are considerably less (Sosa and Espinosa, 2011; Baker, 2012, p. 398). Further research is required to determine the typical electrical efficiency of modern production operations.

Table 7.1: Electric power consumption for industrial-scale dehydrations

Solvent	η_{elec} **(kJ/kg permeate)**	
Ethanol	807	Tsuyumoto *et al*. (1997)
Ethanol	525	Morigami *et al*. (2001)
Ethanol	425	Sander and Soukup (1988)
Ethanol	307	Kujawski (2000)
THF	684	Kujawski (2000)

Steam consumption

Heat consumption and recovery data (Morigami *et al*., 2001) for an industrial-scale ethanol dehydration is shown in Table 7.2. Tubular membranes were used. There were 4 stages in series. All had feed temperatures of 110 ^{o}C. The feed concentration was 10.16 wt% water and the retentate contained 0.2 wt% water. Details regarding the steam pressure were not provided: a steam pressure of 3 bar gauge was assumed as this is typical of industrial-scale equipment and would be sufficient to achieve the feed temperature. It was assumed that the condensate left the heat exchangers at the saturation temperature. The ambient temperature was 25 ^{o}C. The product was at 35 ^{o}C: so it is evident that there was heat recovery.

Heat recovery provided 27% of the heat required. Using Eq. (7.13) it can be shown that 88.2% of the available heat was recovered, whilst the corresponding figure calculated using the short-cut approximation, Eq. (7.14), was 87.6%. This illustrates the accuracy of the approximation. The permeate enthalpy accounted for 50% of the heat required. The size of the unit was estimated from the dimensions and photographs provided: this allowed the dimensions of the external surfaces to be estimated. Heat losses due to natural convection were consistent with a surface temperature of 70 ^{o}C. This is high; however, as discussed previously, it was a pilot system and insulation may have been poor as suggested by the 19% of the heat supplied that was lost to atmosphere.

Table 7.2: Heat consumption and recovery data for a pervaporation system

	kJ/kg permeate	**%**
Steam heating	2,966	73
Heat recovered	1,118	27
Heat required	4,084	
Permeate enthalpy	2,031	50
Output stream	149	4
Heat recovered	1,118	27
Heat losses	786	19

Table 7.3 shows steam consumption data for a number of industrial-scale ethanol dehydrations. The system described by Morigami *et al*. (2001) had a considerably lower steam ratio due to the use of heat recovery. The steam ratio would have been 1.88 kg steam per kg permeate had no heat recovery been applied. This is consistent with the results for Tsuyumoto *et al*. (1997) and Sander and Soukup (1988). Small plants can be inefficient (Baker, 1991, p. 164): this may explain the high steam ratio reported by Kujawski (2000).

Baker (1991, p. 164) reported a net steam consumption of 0.89 kg/kg permeate for a pervaporation system which was an integral part of a hybrid distillation-pervaporation process. The low steam consumption per unit mass of permeate was due to the feed coming directly from a distillation column at 80 ^{o}C and being fed directly to the first stage of the pervaporation unit without being heated. Furthermore, the permeate stream contained 45% ethanol whose latent heat is less than half that of water. The heat input from the steam was 27% greater than the latent heat of the permeate stream.

The THF dehydration reported by Kujawski (2000) has a very low steam ratio. It is far lower than that for the ethanol dehydration undertaken with the same equipment. The feed and retentate compositions were similar. Both solvents have azeotropes with 4 wt% water: THF boils at 66 ^{o}C as compared to 78 ^{o}C for ethanol. It is unlikely that heat

recovery was used for the THF dehydration and not used for the ethanol dehydration as the same equipment was used for both. It is not clear why there is such a significant difference in the steam ratios for the two dehydrations.

Table 7.3: Steam consumption for dehydrations

	Permeate flow (kg/h)	**Steam Ratio**
Morigami *et al*. (2001)	66.8	1.37
Morigami (without heat recovery)	66.8	1.88
Tsuyumoto *et al*. (1997)	53.3	1.88
Sander and Soukup (1988)	13.4	2.20
Kujawski (2000) ethanol dehydration	13.9	2.87
Kujawski (2000) THF dehydration	6.2	1.12

Isothermal efficiency

Examples of the relationship between the isothermal efficiency and the number of adiabatic stages used to achieve a given separation is shown in Fig. 7.2. The data shown were generated using the methods outlined in chapters 2 and 4 and relate to a theoretical ideal system. The greater the number of stages, the lower the permeate-feed ratio, the smaller the temperature drop and consequently the greater the isothermal efficiency.

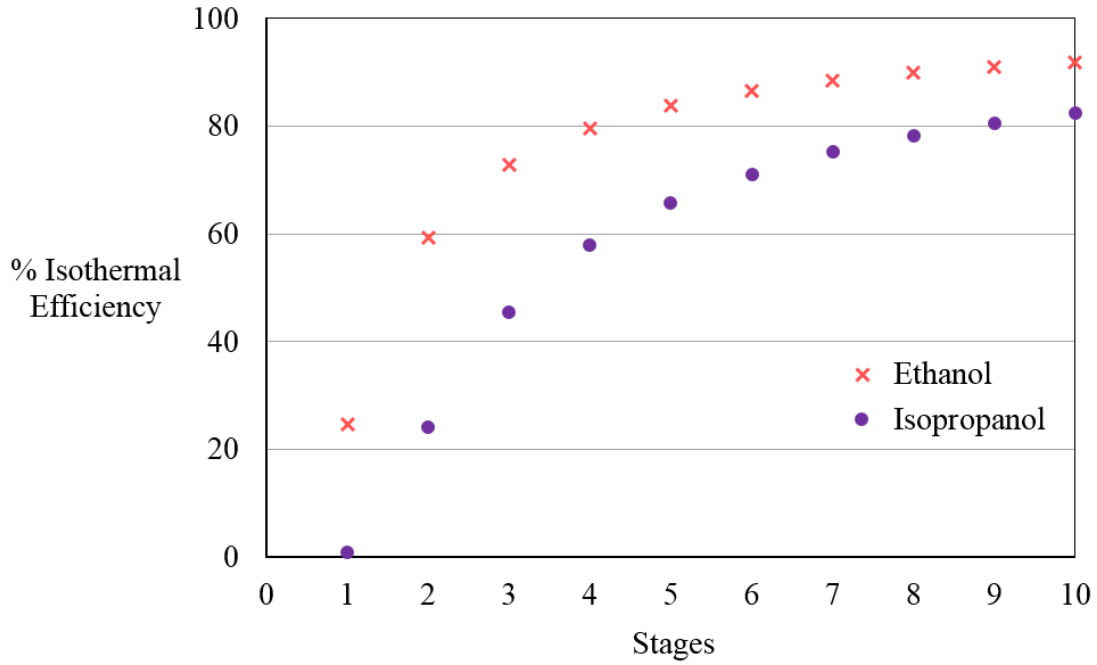

Figure 7.2 Theoretical isothermal efficiency versus number of stages, E_j = 45,400 kJ/kmol, T_f = 120 °C, y_i = 98% water: ● denotes dehydration of IPA from 15% to 0.5%; x denotes dehydration of ethanol from 6% to 0.2%.

Morigami *et al*. (2001) presented data for a 4-stage system for the industrial-scale ethanol dehydration with feed containing 10.16 wt% water. The retentate had 0.16 wt% water. Isothermal efficiencies for the various stages were calculated using the data provided: they ranged from 46% to 71%. Data from an industrial-scale unit is described by Tsuyumoto *et al*. (1997). Ethanol was dehydrated from 5.97 to 0.20 wt% water. The plant had 9 modules arranged in 7 stages, with parallel modules in each of the first two stages. Isothermal efficiencies were calculated for the various stages: they ranged from 46% to 97%. In both these examples, the isothermal efficiency was higher for later stages as they had lower water concentrations, leading to lower flux, less permeate and smaller temperature drops. Bausa and Marquadt (2000) assumed an isothermal efficiency of 80%, based on a typical 10 K temperature drop per stage for ethanol dehydrations with a permeate composition of 15 wt% water. A feed of 5.23 wt% water, could be reduced to a retentate of 1% with 4 stages each having a 10 K temperature drop. The 80% isothermal efficiency assumed would require an apparent activation energy of pervaporation of 52,630 kJ/kmol for this separation. This value is within the 19,000 to 63,000 kJ/kmol range typical of commercial membranes.

Increasing the isothermal efficiency through the incorporation of additional pervaporation stages leads to minor increases in permeate temperature and the temperature of the retentate leaving the final stage. Typically, flux is proportional to temperature, particularly at low water concentrations. Hence, the flux and temperature drop in the final stage of a multi-stage system is small, so that any change due to the additional stages will be small; furthermore a larger pre-heater can ensure the same outlet stream temperature. Thus increases in isothermal efficiency usually lead to minor increases in energy consumption. However, higher isothermal efficiency leads to increased average temperatures, increased average flux and a corresponding reduction in overall membrane area. This outweighs any minor increases in energy costs.

Module efficiency data for industrial scale equipment

Module efficiency compares the actual performance of a pervaporation module with the ideal theoretical performance of the module with an identical membrane and operating conditions.

Tsuyumoto *et al*. (1997) published data relating to the industrial scale dehydration of ethanol. The plant had 7 stages with two parallel modules in each of the first two stages. Feed was on the inside of the hollow fibre modules, with laminar flow and $Re < 40$. The results are shown in table 7.4. The data included the retentate composition from the first stage of the process as well as for the system as a whole. This allowed the module efficiency for the first stage to be calculated. The pilot-scale and industrial scale trials were at similar temperatures and concentrations: the industrial trials were undertaken at 60 ^{o}C; the pilot scale trials were undertaken at temperatures of 40 ^{o}C to 70 ^{o}C with water concentrations of 0.5% to 5.0%. There were significant variations in the thickness of the membranes in the different modules. The module efficiency was calculated on the basis that flux was inversely proportional to membrane thickness as found by Villaleunga *et al*. (2005).

Tsuyumoto *et al*. (1997) also provided data for 2 runs where recycles were used for the first stage. Data from mass balances and component balances for the junction at the entrance to the first stage did not balance when analysed using the equations relating to

recycles that were developed in chapter 5. This indicates that the data relating to the first stage was inaccurate.

There were significant variations in membrane thickness between modules. This suggests the possibility of variations in thickness within individual modules. Production of defect-free hollow fibres for pervaporation applications was challenging at that time (Liu *et al*., 2005; Zhou and Koros, 2006; Jiang *et al*., 2007).

Module efficiency values of 156-189% were calculated for the first stage for all three runs using the data from Tsuyumoto *et al*. (1997). A module efficiency of greater than 100% is not possible. Any flaws in the membrane would increase the actual flux and hence the area efficiency. The modules in the first stage had the thinnest membrane layers and were therefore the most likely to have flaws. It was stated that the two parallel modules had the same membrane thickness. However, the ethanol permeability of one was 91% higher than the other: indicating that this module had a thinner membrane than was stated or that the membrane contained flaws which allowed permeate to pass through the membrane.

The inaccurate data as evidenced by the mass balance calculations, the variations in membrane thickness between modules and the significant difference in flux for the two parallel first stage modules, which ostensibly had similar thicknesses, indicate that the high area efficiency values for the first stage can be disregarded.

As no intermediate data was provided for the remaining stages average module efficiency values were calculated for the group of stages as a whole. The feed composition entering the second module was slightly different for each of the 3 runs. The data for these later modules, gave module efficiencies of 70% - 76%. This is the first time that the actual efficiency of an industrial-scale pervaporation system has been determined. The results are consistent with the values ranging from 57% to 76% obtained by Schleger *et al*. (2004) and Sommer *et al.* (2005) when modelling the dehydration of isopropanol using a tubular isothermal module.

Table 7.4: Module efficiency of an industrial-scale pervaporation system

Stage(s)	z_i %	x_{ir} %	ΔT Average (K)	Module Efficiency %
1	5.97	2.83	31.5*	189*
1	3.72	2.55	11.4*	157*
1	3.19	2.57	6.0*	156*
2-7	2.83	0.6	1.5 - 3.5	76
2-7	2.55	0.6	1.5 - 3.0	70
2-7	2.57	0.6	1.5 - 3.0	70

Data from Tsuyumoto *et al*. (1997).

7.7 Conclusions

Novel metrics relating to energy consumption, heat recovery and isothermal efficiency of pervaporation systems have been developed which enable comparisons between systems with different solvents, varying feed concentrations and varying permeate concentrations.

For the first time the module efficiency of an industrial-scale adiabatic multi-stage process has been determined. The results are consistent with those obtained by Sommer *et al.* (2005) for an isothermal system. These results combined with the methods developed in chapters three, four and five for calculating the flux of ideal pervaporation modules, allow for the first time the actual membrane area of pervaporation systems to be estimated without the need for detailed models.

For the first time the energy efficiency of multiple industrial-scale systems is analysed in this chapter. This data along with the metrics developed in this chapter allow engineers to predict the energy consumption of actual industrial pervaporation systems for the first time. This complements the work related to the sizing of pervaporation

systems developed in chapters three, four, five and six along with the module efficiency research described in this chapter in facilitating the design of pervaporation systems.

The availability of the metrics outlined in this chapter will allow analysis and comparison of the performance of systems with varying feeds, concentrations and operating conditions as well as modules of different types and of varying geometries. This will facilitate the benchmarking of industrial systems, thereby identifying the best designs and optimum operating conditions. This will enable operators of industrial plants to identify opportunities for improvements to their systems.

It is to be hoped that the metrics and availability of industrial data will cause engineers to consider more seriously the use of pervaporation technology. Engineers will be better able to make informed decisions when choosing between separation processes.

A small number of studies have provided data regarding steam and energy consumption for pervaporation systems (Tsuyumoto *et al*., 1997; Kujawski, 2000; Morigami *et al*., 2001): there is a paucity of performance data relating to industrial pervaporation systems. The limited available data has been analysed and some initial insights into the energy efficiency and heat recovery of industrial-scale systems has been achieved. Presenting energy consumption data in the form of steam consumption per unit mass of permeate provides a useful benchmark for comparison with existing and future pervaporation systems. The module efficiency for the system described by Tsuyumoto *et al*. (1997) has been determined and it is comparable to that achieved by Schleger *et al*. (2004).

There are gaps and inconsistencies in the published data. Nowadays, cooling is used in commercial systems as the cost of operating vacuum pumps is prohibitive (Baker, 2012, p. 398). Further research is need to determine the performance of modern industrial pervaporation systems including determination of typical values of module efficiency, energy efficiency, heat recovery and steam usage per unit mass of permeate. It is anticipated that the metrics developed in this chapter will encourage such research thereby helping to address the need for industrial-scale data.

7.6 Sample calculation

The energy efficiency, heat losses and module efficiency for an ethanol dehydration are calculated assuming operating conditions typical of those for an industrial-scale pervaporation system. The purpose of the sample calculation is to demonstrate how easily such calculations can now be done using readily available data. It also shows how the actual module efficiency of a module can be determined. The results show energy consumption and module efficiency data that is typical of industrial-scale systems.

Ethanol is dehydrated in a single 60 m^2 module with no recycle. The feed flowrate is 1,000 kg/h. Feed is heated from 10 °C to 120 °C. Heat losses from the module are such that the actual retentate temperature is 93 °C. The retentate stream is used to partially heat the feed, such that the outlet stream from the pre-heater is at 30 °C. The pressure change across the feed pump is 3 bar and it has an energy efficiency of 40%. The refrigeration unit and associated utilities consume 6 kW of electricity. z_i = 6 wt%, x_{ir} = 4%, y_i = 98%, E_j = 45,030 kJ/kmol.K, J_f = 1 kg/h.m^2.

Ideal retentate temperature

$$\left(\frac{\dot{m}_p}{\dot{m}_f}\right) = \frac{z_i - x_{ir}}{y_i - x_{ir}} = \frac{0.06-0.04}{0.98-0.04} = 0.0213$$

$$\left(\frac{\dot{m}_r}{\dot{m}_f}\right) = 1 - \left(\frac{\dot{m}_p}{\dot{m}_f}\right) = 0.9787$$

$T_{r\ ideal}$ is determined by iterating an energy balance as outlined in chapter 3.

$$T_{r\ ideal} = \frac{\left(1-\frac{\dot{m}_p}{\dot{m}_f}\right)c_{p1}T_f + 0.5\left(\frac{\dot{m}_p}{\dot{m}_f}\right)c_{p2}T_f - \frac{\dot{m}_p}{\dot{m}_f}\lambda}{0.5\left(\frac{\dot{m}_p}{\dot{m}_f}\right)c_{p2} + \left(1-\frac{\dot{m}_p}{\dot{m}_f}\right)c_{p1}} \qquad \text{Eq. (4.35)}$$

Data for specific heat and latent heat for pure water and pure ethanol were calculated using equations from Yaws (1999). Averaged physical properties were used for mixtures. Calculations were undertaken using excel. The iteration converges rapidly.

$$T_{r\ ideal} = \frac{(1-0.0213)(4.190\,\text{kJ/kg.K})(393.15\,\text{K}) + 0.5(0.0213)(2.708\text{kJ/kg.K})(393.15\,\text{K}) - 0.0213(2{,}136\text{kJ/kg})}{0.5(0.0213)(2.708\text{kJ/kg.K}) + (1-0.0213)(4.190\,\text{kJ/kg.K})}$$

$T_{r\ ideal}$ = 376.28 K = 103.13 °C

Heat input

Enthalpy values calculated using h_s as datum with c_p data from Yaws (1999).

$\dot{m}_f h_s = (1{,}000 \text{ kg/h})(0 \text{ kJ/kg}) = 0 \text{ kJ/h}$

$\dot{m}_f h_f = (1{,}000 \text{ kg/h})(282.40 \text{ kJ/kg}) = 282{,}443 \text{ kJ/h}$

$\dot{m}_r h_r = (978.7 \text{ kg/h})(206.2 \text{ kJ/kg}) = 201{,}781 \text{ kJ/h}$

$\dot{m}_r h_{rideal} = (978.7 \text{ kg/h})(233.0 \text{ kJ/kg}) = 228{,}020 \text{ kJ/h}$

$\dot{m}_o h_o = (978.7 \text{ kg/h})(47.9 \text{ kJ/kg}) = 46{,}864 \text{ kJ/h}$

$$\Delta q_{heat} = \left(\dot{m}_f h_f - \dot{m}_s h_s\right) - \left(\dot{m}_r h_r - \dot{m}_o h_o\right) \qquad \text{Eq. (7.2)}$$

$$\Delta q_{heat} = (282{,}443 - 0) - (201{,}781 - 46{,}864) = 127{,}527 \text{ kJ/h}$$

Latent heat of saturated steam at 3 bar gauge = 2,134 kJ/kg

$$\dot{m}_{steam} = \frac{127{,}527 \text{ kJ/h}}{2{,}134 \text{ kJ/kg}} = 58.78 \text{ kg steam/h}$$

$$\frac{\dot{m}_{steam}}{\dot{m}_r} = \frac{58.78 \text{ kg/h}}{978.7 \text{ kg/h}} = 0.061 \text{ kg/kg}$$

$$\frac{\dot{m}_{steam}}{\dot{m}_p} = \frac{58.78 \text{ kg/h}}{21.3 \text{ kg/h}} = 2.76 \text{ kg/kg} \qquad \text{Eq. (7.5)}$$

Heat losses

$$\Delta q_{heat\,loss} = \dot{m}_r h_{r\,ideal} - \dot{m}_r h_r$$

$$\Delta q_{heat\,loss} = 228{,}020 - 201{,}781 = 26{,}236 \text{ kJ/h}$$

Heat loss as a proportion of energy consumption can be defined as follows

$$\eta_{heat\,loss} = \frac{\Delta q_{heat\,loss}}{\Delta q_{heat} + \Delta q_{pump}} = \frac{26{,}236 \text{ kJ/h}}{100{,}210 \text{ kJ/h} + 1070 \text{ kJ/h}} = 0.262 = 26.2\% \qquad \text{Eq. (7.10)}$$

Pump energy consumption

$$Q_{pump} = \frac{\dot{m}_f}{\rho_f} = \frac{(1,000\ \text{kg/h})}{(3,600\ \text{s/h})(701.1\ \text{kg/m}^3)} = 0.000\,396\ \text{m}^3/\text{s}$$

$$\Delta q_{electricity} = \frac{Q_{pump}\Delta P_{pump}}{\eta_{pump}} = \frac{(0.000396\ \text{m}^3/\text{s})(300,000\ \text{Pa})}{0.40} = 297\ \text{W} = 1,070\ \text{kJ/h}$$

The pump accounts for less than 1% of energy consumption in this example.

Ideal adiabatic area

$$J_f = z_i J_o e^{-E_j/RT_f} = 0.06(16,000,000)\,\text{e}^{45,030/8.3145(393.15\text{K})} = 1.00\ \text{kg/m}^2\text{.h}$$

$$J_r = x_i J_o e^{-E_j/RT_r} = 0.06(16,000,000)\,\text{e}^{45,030/8.3145(376.28\text{K})} = 0.36\ \text{kg/m}^2\text{.h}$$

$$J_{reheat} = x_i J_o e^{-E_j/RT_f} = 0.04(16,000,000)\,\text{e}^{45,030/8.3145(393.15\text{K})} = 0.667\ \text{kg/m}^2\text{.h}$$

$$J_r / J_{reheat} = \frac{0.359\ \text{kg/m}^2\text{.h}}{0.667\ \text{kg/m}^2\text{.h}} = 0.539$$

$$x_i / z_i = \frac{0.04}{0.06} = 0.667$$

$$\frac{J_{av}}{J_f} = \left[a\left(\frac{x_i}{z_i}\right)+b\right]ln\left(\frac{J_r}{J_{reheat}}\right)+\left[c\left(\frac{x_i}{z_i}\right)^n + d\left(\frac{x_i}{z_i}\right)+eln\left(\frac{x_i}{z_i}\right)+f\right] \qquad \text{Eq. (5.27)}$$

$$\frac{J_{av}}{J_f} = \left[0.31(0.667)+0.1427\right]ln(0.539) + \left[-0.3(0.667)^{1.65}+0.98(0.667)+0.0174ln(0.667)+0.32\right]$$

$$\frac{J_{av}}{J_f} = 0.597$$

$$A_{adiabatic\ ideal} = \frac{\dot{m}_f\left(\dot{m}_p/\dot{m}_f\right)}{J_f\left(J_{av}/J_f\right)} = \frac{1{,}000\ \text{kg/h}\,(0.0213)}{1\ \text{kg/m}^2\text{.h}\,(0.597)} = 35.68\ \text{m}^2 \qquad \text{Eq. (5.22)}$$

Module efficiency

$$\eta_{module} = \frac{A_{adiabatic\ ideal}}{A_{actual}} = \frac{35.68\ \text{m}^2}{60.00\ \text{m}^2} = 0.714 = 59.5\% \qquad \text{Eq. (7.18)}$$

Chapter 8: Optimisation of multi-stage pervaporation systems

8.1 Abstract

Ideal multi-stage systems are modelled in this chapter. Use of stages using equal membrane areas, equal temperature drops and assuming an equal feed-retentate concentration difference are compared. A novel short-cut method for the optimisation of ideal multi-stage systems is developed. The module efficiency profile of a multi-stage adiabatic system is modelled for the first time.

8.2 Introduction

One of the benefits of the approach outlined in chapters 4 and 5 is that the short-cut equations provide an easy route to multi-stage process optimisation. Systems with equal temperature drops have been modelled (Sosa and Espinosa, 2011), as have systems with stages of equal size; some authors have considered both approaches (Sander and Soukup, 1988; Bausa and Marquadt, 2000). Marriott and Sørenson (2003b) modelled a system whose stages were comprised of varying numbers of equally-sized modules. Tsuyumoto *et al*. (1997) operated a 7-stage system whose first two stages had double the membrane area of the later stages. Sander and Soukup (1998) described a system with 9 equally-sized stages. In this chapter a novel alternative approach is proposed: that systems be designed such that the reduction in water content in each stage is equal: this gives similar results to the use of equal temperature drops whilst being simpler to calculate.

8.3 Optimisation of ideal systems

Optimisation of an ideal 2-stage system

Consider where two modules in series are used for the dehydration of a 6% water-ethanol solution, the objective being a liquid product containing 1% water. Fig. 8.1 shows that there is an optimum $\dot{m}_p/\dot{m}_f$ value of the first module that leads to the lowest overall area. Fig. 8.2 provides an expanded view of the total area curve from Fig. 8.1.

Total area is minimised when the area of the first stage is less than the area of the second stage. This concurs with results for multi-stage models for the dehydration of isopropanol (Marriott and Sørenson, 2003b). The $\dot{m}_p/\dot{m}_f$ ratio of the first stage when equal areas are used is greater than that for the minimum overall area: whilst when equal temperature drops are used, it is less. Use of an equal concentration difference ($z_i - x_{ir}$) provides results similar to those achieved with equal temperature drops: the minor differences are due to variations in the specific heat caused by the changing liquid composition. Calculations using equal concentration differences are simpler than for equal temperature drops. Similar results were obtained for two-stage systems for both IPA and ethanol across the envelope of industrial operating conditions. Use of a retentate composition, x_1, that is halfway between that for equal areas and equal concentration differences, gives an overall area that is within 0.1% of the minimum overall area for applications involving ethanol and IPA throughout the envelope of industrial operating conditions. This approach provides a simple method for the optimisation of ideal multi-stage systems. The results are illustrated in Figs. 8.1 and 8.2.

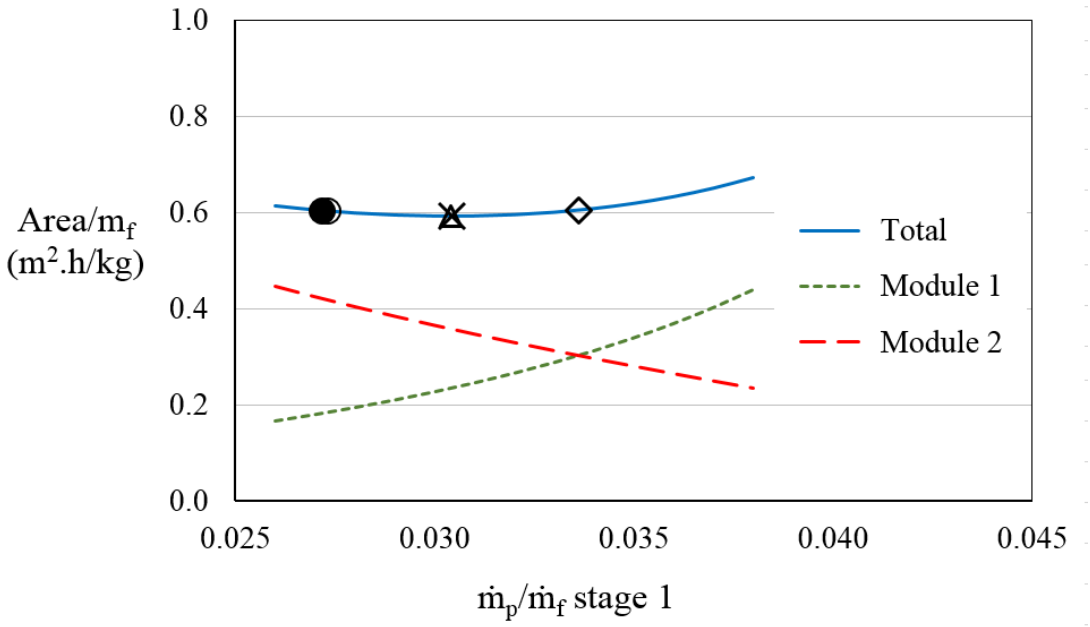

Figure 8.1 Membrane area versus permeate-feed ratio for a 2-stage system: water-ethanol, T_f = 105 °C, z_1 = 6%, x_2 = 1%, y = 0.95, E_j = 47,500 kJ/kmol, J_o = 2 ×10^7 kg/m^2. O equal ΔT for both stages, ● equal concentration gradient (z_i - x_{ir}) for both stages, Δ retentate composition halfway between that for equal areas and equal ΔT, X minimum area, ◊ equal areas.

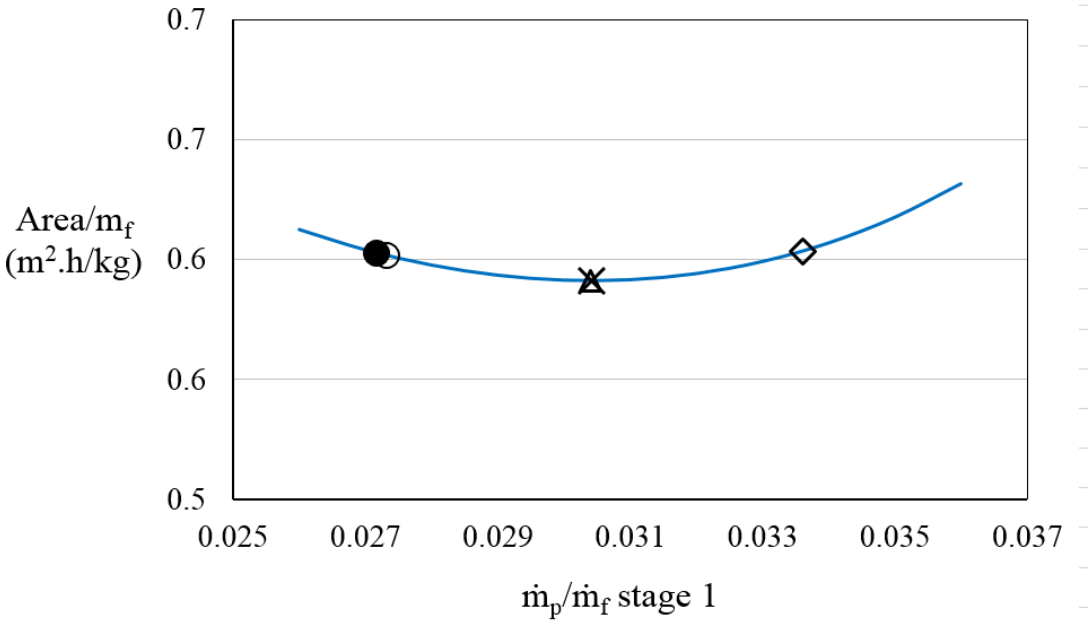

Figure 8.2 Expanded view of total membrane area curve from Fig. 8.1

Optimisation of an ideal 9-stage system

Pfizer Ireland Pharmaceuticals operate a Sulzer plate-and-frame pervaporation system with 9 equally-sized stages. Results for an ideal model of a system with similar performance characteristics are shown in Table 8.1: inefficiencies due to temperature polarisation, concentration polarisation and poor flow patterns were not considered.

Use of equal stage areas gives an overall membrane area that is similar to that when equal concentration gradients are used – albeit that the area of the individual stages are quite different. In this example, all configurations had overall areas within 2.8% of the minimum possible area. Use of retentate compositions half-way between those for equal concentration gradients and those for equal areas gave an overall membrane area that was within 0.25% of the minimum.

Typical industrial pervaporation systems use standard-sized modules. In this case use of standard-sized modules required an overall area 2.6% greater than the minimum. Similar results were obtained for IPA throughout the envelope of industrial operating conditions: with an additional area of less than 3.8% being required when equally sized modules were used in a 9-stage system. These results are consistent with those obtained for the two-stage dehydration of ethanol outlined in section 8.2.

These results indicate that use of varying membrane areas for the different stages of an ideal pervaporation system will achieve a limited reduction in overall area as compared with the use of equally-sized stages.

Use of a high flux, less selective membranes for the later stages of a multi-stage pervaporation system is briefly explored. Such an approach could significantly reduce the overall membrane area with little reduction in overall system performance.

Table 8.1 Overall membrane area per unit mass of feed for a multi-stage system: 9-stage dehydration of isopropanol, J_o = 1.9x10^8 kg/s.m^2, T_f = 100 ^{o}C, E_j, = 50,591 kJ/kmol, z_i = 15% and x_i = 1% and y_i = 99%.

Stage	Equal z_i-x_i m^2.h/kg x10^{-3}	Equal area m^2.h/kg x10^{-3}	Minimum m^2.h/kg x10^{-3}	x_i halfway m^2.h/kg x10^{-3}
1	0.0107	0.0239	0.0163	0.0163
2	0.0115	0.0239	0.0168	0.0169
3	0.0126	0.0239	0.0174	0.0174
4	0.0141	0.0239	0.0181	0.0182
5	0.0162	0.0239	0.0191	0.0192
6	0.0195	0.0239	0.0208	0.0209
7	0.0249	0.0239	0.0239	0.0239
8	0.0358	0.0239	0.0302	0.0302
9	0.0701	0.0239	0.0469	0.0470
Total	**0.2153**	**0.2148**	**0.2096**	**0.2099**
Area	102.7%	102.5%	**100.0%**	100.2%

8.4 Module efficiency in multi-stage systems

The factors affecting module efficiency were outlined in chapter 6. Sommer *et al*. (2005) analysed the performance of a module containing tubular ceramic membranes. A graph of efficiency as a function of Re and flux from their paper is shown in Fig. 8.3. Higher flux and lower Re values lead to reduced efficiency. The exact relationships are a function of module design and operating conditions. High flux leads to low levels of solute at the upstream side of the membrane causing concentration polarisation. It also causes a decrease in temperature at the membrane surface as compared with the bulk fluid. The increased turbulence associated with higher Re values reduces the thickness of the boundary layer. This increases the concentration and temperature gradients across the boundary layer, leading to more rapid mass transfer of the solute from the bulk fluid

to the membrane surface and more rapid heat transfer from the bulk fluid to the membrane surface.

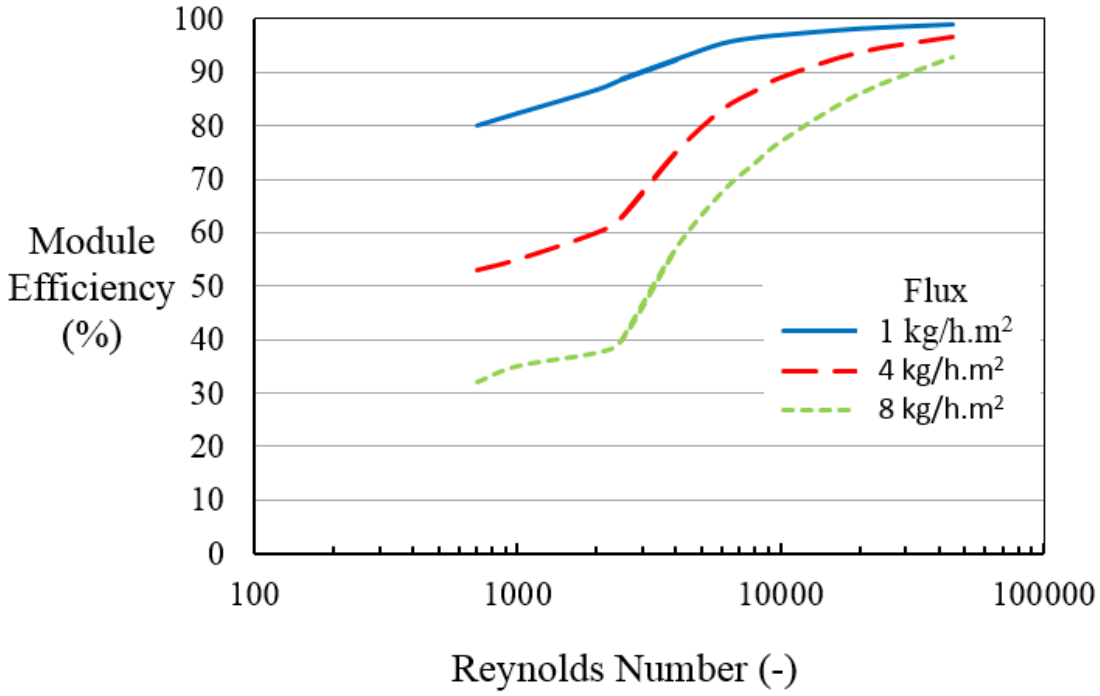

Figure 8.3. Module efficiency as a function of Reynolds Number and flux: calculated efficiency of an annular duct type technical module as a function of the Re number for permeate fluxes of 1 kg/m^2.h^{-1}, 4 kg/m^2.h^{-1} and 8 kg/m^2.h^{-1}. Graph is adapted from Sommer *et al*. (2005)

Industrial dehydrations of isopropanol typically have supply streams containing 12 - 15 % water. Normally there are multiple pervaporation stages interspersed with re-heaters; each stage has the same feed temperature. The water concentration of the feed decreases progressively from stage to stage. This leads to progressively lower liquid densities. The viscosities of water, isopropanol and ethanol are similar for temperatures between 90 ^{o}C and 130 ^{o}C: so changes in concentration do not lead to significant variations in viscosity from stage to stage. The vaporisation of permeate leads to lower mass flowrates and hence lower liquid velocities in later stages. For these reasons the Re of the feed decreases progressively from stage to stage; a drop of 13 – 21% when dehydrating isopropanol and 5 – 11% when dehydrating ethanol is typical for industrial systems. In contrast, the flux at the start of the final stage of an ideal 9-stage system for the dehydration of isopropanol is approximately 10% that of the first stage. The supply

to an ethanol dehydration typically contains 5 – 10% water. Hence, the flux for the final stage of an ideal 4-stage ethanol dehydration with equally sized stages is less than 32% that of the first stage for industrial conditions. The effect of the decreased flux usually outweighs the decrease in Re, so that the efficiency at the start of each stage increases progressively as illustrated in Fig. 8.4.

The higher temperature and higher water concentration near the start of a stage lead to higher flux and a more rapid decrease in temperature. This leads to a more pronounced increase in efficiency at the start of each stage with a progressively lower rate of increase thereafter. Reheating leads to increased flux and a decrease in efficiency notwithstanding the increase in Re as a result of decreased viscosity. Fig. 8.4 illustrates the efficiency profile of a typical multi-stage system.

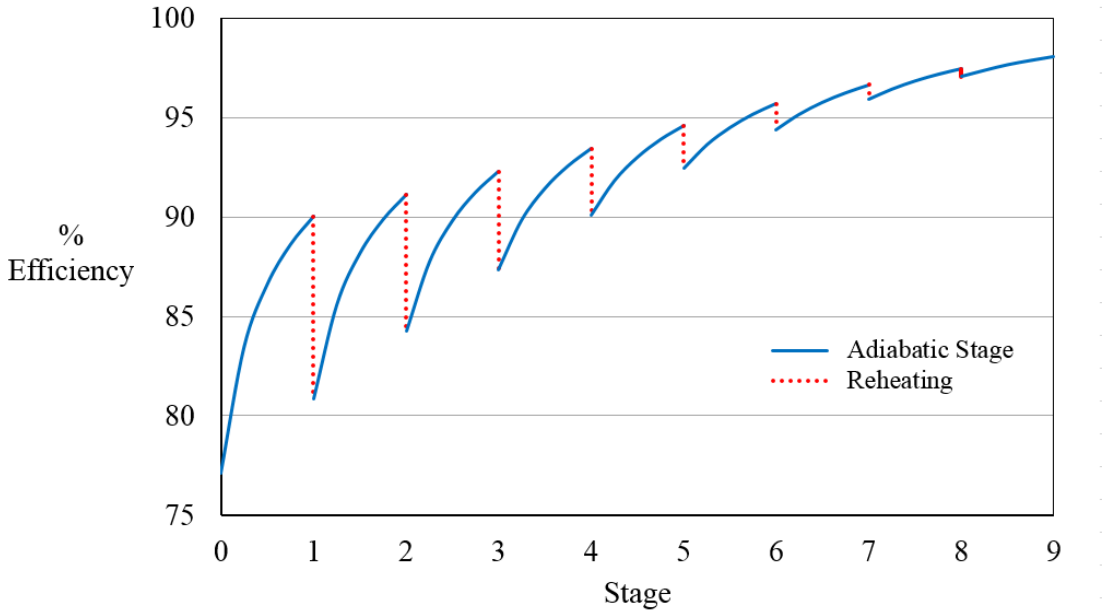

Figure 8.4: Efficiency profile for a typical multi-stage dehydration: 9 equally-sized stages. Solid blue curves are for adiabatic pervaporation, dotted red vertical lines indicate inter-stage heating. Isopropanol dehydration from 15% to 1% water.

8.5 Optimisation of multi-stage systems

Splitting flow between parallel modules reduces the flowrate through the individual modules thereby leading to reduced velocity and Re values. The curves in Fig. 8.3 indicate that a reduction in Re has a greater effect on efficiency when flux is high as occurs in earlier modules with their high water concentrations. Thus parallel modules are best used for the later stages of pervaporation systems. This is consistent with the results for models of multi-stage systems undertaken by Marriott and Sørenson (2003). Tsuyumoto *et al*. (1997) used an industrial scale system with 7 stages for the dehydration of ethanol from 6% to 1% water: the overall efficiency would have been higher had parallel modules been used for the last two stages rather than the first two stages.

8.6 Multi-stage systems with a variety of membranes

All data and models in the literature relate to systems with a single type of membrane for all stages. A novel approach is proposed wherein multiple types of membrane are used within a single multi-stage system. Use of a low-flux highly selective membrane for the early stages of a multi-stage system and a high-flux membrane with lower selectivity for the later stages reduces the required membrane area with little increase in the amount of solvent in the permeate stream as compared to use of the low-flux selective membrane throughout such a system.

Different types of membranes could be used or alternatively the same type of membrane but with a thinner active layer. Villaleunga *et al*. (2005) found that flux is inversely proportional to membrane thickness. They also found that membrane thickness has little effect on separation factor, whilst Koops *et al*. (1994) found that membrane selectivity decreased with membrane thickness below 15 μm for several membranes. Samei *et al*. (2013) found that halving the thickness of the active layer reduced the permeate concentration by 1.4 wt% at 30 °C and by 4.0 wt% at 60 °C.

An ideal 9-stage system similar to that described in Table 8.1 was modelled. The last 3 stages were assumed to have membranes whose active layer was half the thickness of the earlier membranes. The flux was assumed to double and the permeate composition to reduce from 99% to 90%. The same retentate composition was achieved with 27.0%

less membrane area, albeit with 0.4% less retenate product and an average permeate composition of 96.8% water as compared with 99.0% with the original membranes.

Existing heating and cooling arrangements should be able to accommodate such membrane changes as the permeate flowrate is low in later modules. Some membrane manufacturers are focused on increasing selectivity, particularly at low water concentrations (Delatmem, 2017). This analysis suggests that developing membranes that have higher flux at low water concentrations, even at the cost of reduced separation, would be more beneficial. There is scope for further research to ascertain the merits of such an approach.

Membranes with high activation energies could be used for the latter stages of multi-stage systems: the small amount of permeate vaporised and consequent small temperature drops would lead to reductions in flux that would not be excessive even with high activation energies.

8.7 Isothermal efficiency

In an isothermal system the temperature is constant throughout the system and the concentration decreases progressively as permeate vaporises. Thus, the number of stages and the relative size of each stage has no effect on the overall membrane area. However, running modules in parallel reduces the flowrate and velocity of the liquid in the parallel modules, thereby reducing the Re and the efficiency.

Systems that have high isothermal efficiencies approach the performance of isothermal modules and so there is little scope for the optimisation of such systems. Achievement of the optimum membrane area requires that the correct number of stages be used so as to balance the cost of membranes versus the costs associated with reheating equipment as discussed in sections 4.4 and 5.3.

8.8 Conclusions

The short-cut equations developed in chapters 2, 3, 4 and 5 facilitate the optimisation of multi-stage pervaporation systems. For systems where flux is proportional to concentration, the minimum overall membrane area is achieved by having progressively larger stages. Parallel modules are of most benefit when used for the later stages of a multi-stage pervaporation system. They can also be used to avoid excessively high pressures in systems with high throughputs. Optimising the membrane area of the various stages of a system leads to a limited reduction in the overall area, and as industrial systems are typically comprised of standard equally-sized modules, the scope for optimisation is limited. The number of stages in a system should be optimised so as to balance the cost of additional membrane area versus that of reheating equipment.

Literature data and models all relate to systems with a single type of membrane for all stages. Use of a high flux membrane with low selectivity for the latter stages of a pervaporation system has the potential to reduce the required membrane area with little additional solvent in the permeate stream for the system as a whole. The low permeate-feed ratios and consequent low temperature drops in the later stages of a pervaporation system allow membranes with high E_j values to be used without undue increases in membrane area. There is scope for research to ascertain the merits of such an approach.

In typical multi-stage adiabatic pervaporation systems where flux is proportional to concentration efficiency increases within each stages as flux declines due to the reduction in temperature and concentration and efficiency increases progressively from stage to stage as flux declines due to reduced concentration.

Further research is required so as to determine typical efficiency data for multi-stage pervaporation systems so as to allow reliable prediction of efficiency of industrial-scale systems.

Chapter 9: Engineering of pervaporation systems: A single metric for adiabatic pervaporation dehydration membranes.

9.1 Abstract

Performance metrics for pervaporation membranes are reviewed including the Pervaporation Separation Index. A novel metric, the Pervaporation Membrane Index (*PMI*) is proposed: this is the first metric that gives appropriate weighting to flux and separation.

9.2 Introduction

Performance metrics should reflect the economic value of a membrane operating in an industrial system. This facilitates membrane selection by design engineers. Metrics influence the development of membranes by material scientists: inappropriate metrics that fail to properly reflect the requirements of industrial systems encourage the development of sub-optimal membranes. Current performance metrics are reviewed in this chapter. Two novel metrics are proposed: one relates to separation and the other is a combined metric that gives appropriate weighting to both separation and flux.

Industrial dehydrations typically operate at 105 ^{o}C to 130 ^{o}C (Baker, 2012, p. 402), yet of over 140 papers relating to pervaporation membranes listed by Chapman *et al*. (2008) less than ten reported pervaporation data at temperatures greater than 80 ^{o}C. Baker (2012, p. 392) has commented that many such membranes would fail at the higher temperatures used industrially. Commercial plants typically operate with feeds of up to 10 wt% water for ethanol dehydrations and 18 wt% for IPA dehydrations. However, many research papers provide data outside these ranges. Some have little if any data within these ranges (Chen *et al*., 2001; Tsai *et al*., 2002; Xu *et al*., 2003; Wang *et al*., 2004). Higher water concentrations usually provide higher flux. In such cases the flux reported is high, but the flux at industrial operating conditions is lower.

The most widely used metric relating to separation performance is the separation factor, β_{ij}. It has an asymptotic relationship with membrane area for a given separation. This gives undue weight to minor variations in permeate purity as will be explained in this chapter. The 'Pervaporation Separation Index', *PSI*, is the most commonly used single metric that combines both flux and separation characteristics. Huang and Feng (1993) defined it as,

$$PSI = J\left(\beta_{ij} - 1\right) \tag{9.1}$$

Flux is typically a function of concentration and temperature. Sosa and Espinosa (2011) stated that the *PSI* is unsatisfactory as the performance in relation to flux is based on a single data point: i.e. at a single concentration and temperature. They suggested that the flux be redefined as the inverse of the minimum area required for a given separation: this would reflect variations in flux with concentration. It would also allow for the effect of the apparent activation energy of pervaporation, E_j.

Membranes with similar performance characteristics can have considerably different peak *PSI* values. Peak *PSI* values can occur outside the range of concentrations used industrially. Thus both the flux and the separation aspects of this common metric have been found to be unsatisfactory in recent years.

The pervaporation separation modulus is proposed as a metric of separation performance. A novel single performance metric, the Pervaporation Membrane Index, *PMI,* is proposed: it incorporates flux and separation. It is discussed in relation to membrane area, energy consumption, solvent yield and waste produced. Equations are developed that facilitate calculation of the pervaporation membrane index. The *PSI* and *PMI* values of a variety industrial membranes are compared.

These novel metrics should be of benefit to engineers when selecting membranes for process feasibility studies or when designing pervaporation systems. They should encourage researchers to develop membranes whose performance characteristics are relevant to industrial operations.

9.3 Flux metrics

There are several metrics for flux: all provide data at a single temperature and concentration. The flux in pervaporation is usually defined as mass flux, J

$$J \equiv \frac{\dot{m}_p}{A} \tag{9.2}$$

where: J = Permeate flux (kg/h.m^2)

$\dot{m}_p$ = mass flowrate of permeate through the membrane (kg/h)

A = Membrane area (m^2)

However, molar flux, j has also been used (Baker *et al*., 2010). This has units of cm^3(STP)/cm^2.s. The use of molar flux facilitates comparison with gas permeation data (Baker *et al*., 2010).

For most systems, flux is proportional to concentration within the envelope of industrial operating conditions and the following equation applies

$$J = x_i J_o e^{\frac{-E_j}{RT}} \tag{9.3}$$

where: J_o = the maximum possible permeate flux for a given liquid composition (i.e. the flux as T → ∞). (kg/h.m^2)

E_j = the activation energy of the membrane for a given system

R = the universal gas constant.

In some cases flux is independent of concentration across a range of concentrations, (Verkerk *et al*., 2001; Sommer and Melin 2005; Pera-Titus 2006; Van Hoof, Dotremont and Beukenhoudt, 2006). In such cases Eq. (9.3) reduces to the following,

$$J = J_o e^{\frac{-E_j}{RT}} \tag{9.4}$$

There are cases where flux is proportional to concentration at low concentrations and then gradually transitions to being independent of flux at higher concentrations (Verkerk

et al., 2001; Sommer and Melin 2005; Van Hoof, Dotremont and Beukenhoudt, 2006); an example is illustrated in Fig. 9.1.

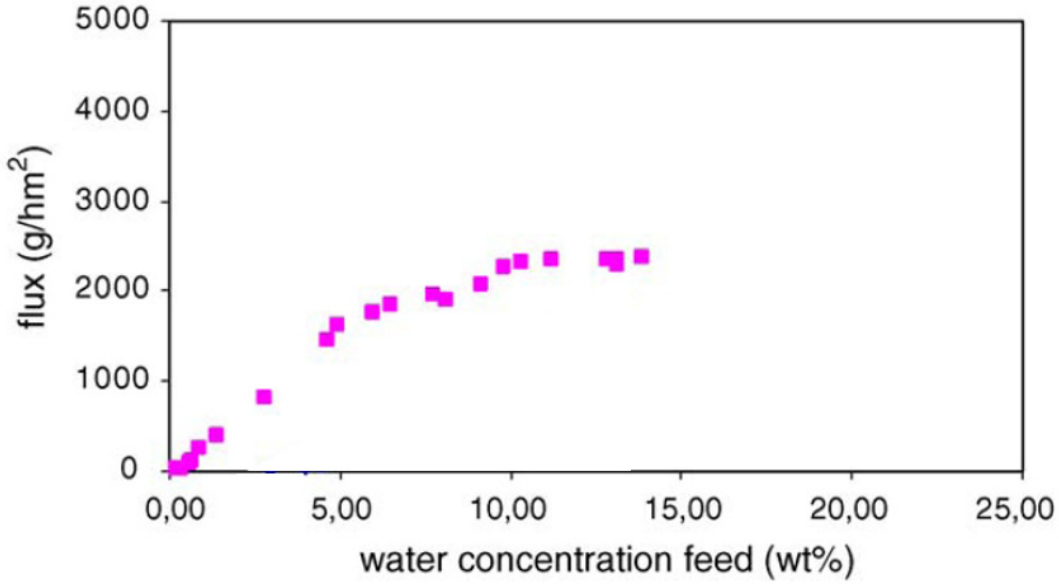

Figure 9.1 Flux versus water concentration, dehydration of MEK. Mitsui membrane. Graph from Van Hoof *et al*. (2006).

Both mass flux and molar flux provide data at specific temperatures and concentrations. Neither accounts for the effects of activation energy or the flux-concentration relationships that occur in pervaporation modules. Sosa and Espinosa (2011) stated that the *PSI* is unsatisfactory as the performance in relation to flux is based on a single data point and does not allow for variations in flux due to liquid concentration. They recommended that the *PSI* be redefined as the overall separation factor multiplied by the inverse of the minimum membrane area required to perform a given separation: in effect it should be proportional to the average flux for a given separation rather than the flux at a particular temperature and concentration. As permeate vaporises the temperature within a module decreases: a high E_j value leads to rapid reduction in flux and therefore requires a larger membrane area as compared with a similar system with a lower E_j value. The approach suggested by Sosa and Espinosa (2011) would encompass the effects of activation energy and the concentration-flux relationship. It would allow comparison of the performance of membranes for a specific separation. However, it would not facilitate comparisons when there are variations in feed composition or retentate specification.

Permeability and permeance

Baker *et al*. (2010) recommend the use of permeability to describe the rate of flow through pervaporation membranes. It is a measure of the additional separation that occurs due to the presence of a membrane; i.e. it is a function of vapour liquid equilibrium. It is solely a function of the properties of the membrane; hence, it facilitates comparisons of data obtained at different operating conditions. The most common units are Barrer (1 Barrer ≡ 1 x 10^{-10}cm^3(STP).cm/cm^2.s.cmHg).

Membrane permeance, P_i^G/l, does not require knowledge of the membrane thickness (Baker *et al*., 2010). It is typically reported using gas permeation units (gpu), (1 gpu ≡ 1 x 10^{-6}cm^3(STP)/cm^2.s.cmHg) or (1m^3.m/m^2.s.kPa = 1.33x10^8gpu):

$$\frac{P_i^G}{l} = \frac{j_i}{P_{io} - P_{il}} \tag{9.5}$$

where:

P_i^G	is the membrane permeability of component *i* (1 x 10^{-10}cm^3(STP).cm/cm^2.s.cmHg).
l	is the thickness of the membrane (cm)
j_i	is the molar flux (1 x 10^{-10}cm^3(STP).cm/cm^2.s)
p_{io}	is the partial pressure of component *i* on the feed side (cmHg)
p_{il}	is the partial pressure of component *i* on the permeate side (cmHg)

Permeability and permeance both provide performance data that is independent of the operating conditions. They are useful when analysing membrane performance, including swelling and mass transfer. However, permeability and permeance need to be combined with vapour liquid equilibrium data to determine membrane performance when designing a pervaporation system, thereby making the design process more time consuming. Provision of data in the form of permeance makes comparison with data relating to other pervaporation membranes more complex (Chapman *et al*., 2008).

9.4 Separation metrics

Permeate-feed ratios of up to 5% are typical for industrial pervaporation modules as discussed in section 1.14. Across such a limited concentration range, the permeate composition can be taken to be independent of liquid composition for many commercial membranes as discussed in section 1.14. Fig. 9.2 shows data relating to commercial membranes for the dehydration of ethanol. Fig. 9.3 shows similar data for the dehydration of IPA. Many such membranes have permeate with ≥ 99% water as discussed in section 1.14 of chapter 1: in such cases there is little scope for variation in the permeate composition. Some manufacturers of commercial membranes have focussed on improving separation, particularly at low feed concentrations rather than increasing flux (Gladman, 2017). Thus permeate purity at low water concentrations is likely to be similar to that at higher liquid concentrations. Permeate concentration typically plateaus at feed concentrations of between 0.6% and 5% water. There are exceptions as shown in Fig. 9.4 (Kujawski *et al*. 2017).

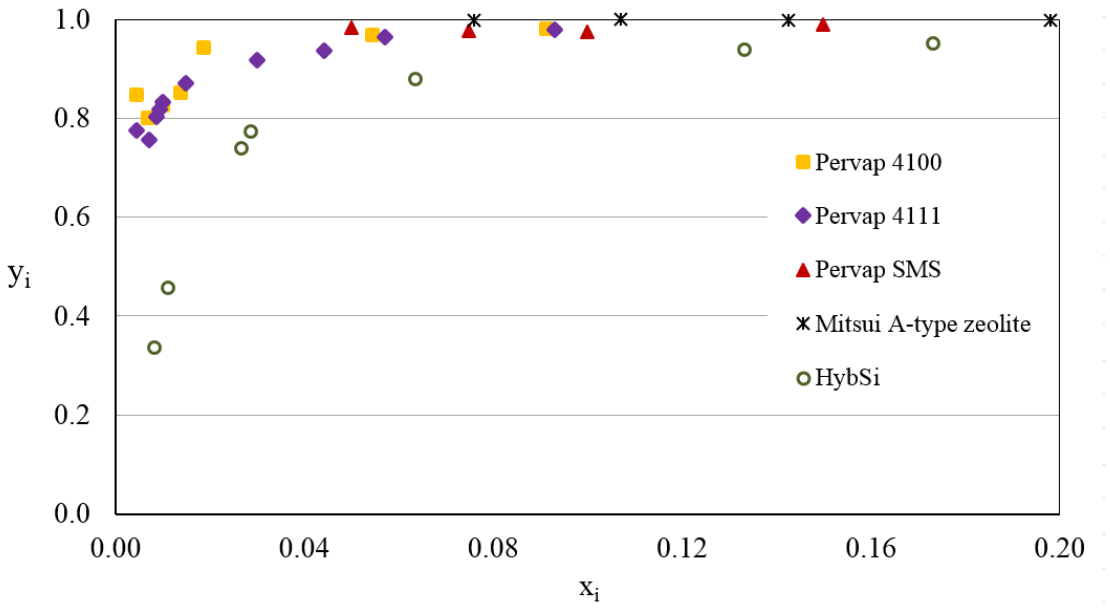

Figure 9.2 Permeate composition versus liquid composition for ethanol dehydrations using commercial membranes. ■ Pervap 4100, 98 °C, ♦ Pervap 4111, 98 °C, Niemistö *et al.* (2013); ▲ Pervap SMS, 120 °C, Ж, Mitsui A-type zeolite, 110 °C, Sommer and Melin (2005); O, HybSi 80 °C, Klinov *et al.* (2017).

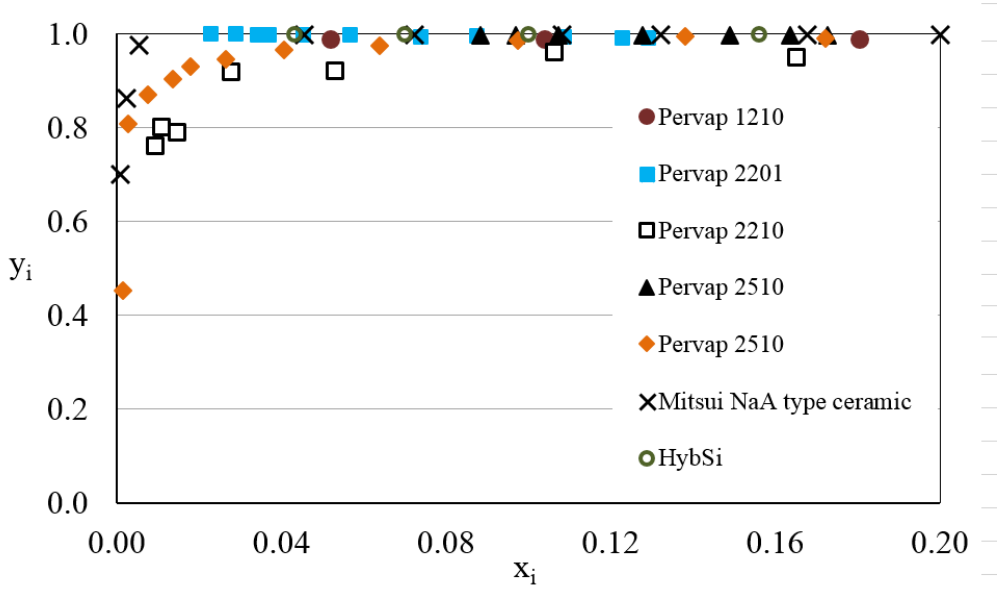

Figure 9.3. Permeate composition versus liquid composition for IPA dehydrations using commercial membranes: ● Pervap 1210, 60 ºC, Koch and Górak (2014), X Mitsui NaA type zeolite, 90 ºC, ♦ Pervap 2510, 90 ºC, Van Hoof, Dotremont and Beukenhoudt (2004): ■ Pervap 2201, 90 ºC, ▲ Pervap 2510, 100 ºC, Qiao *et al*. (2005). □ Pervap 2210, 90 ºC, Cséfalvay *et al*. (2008); O, HybSi, 80 ºC, Klinov *et al*. (2017).

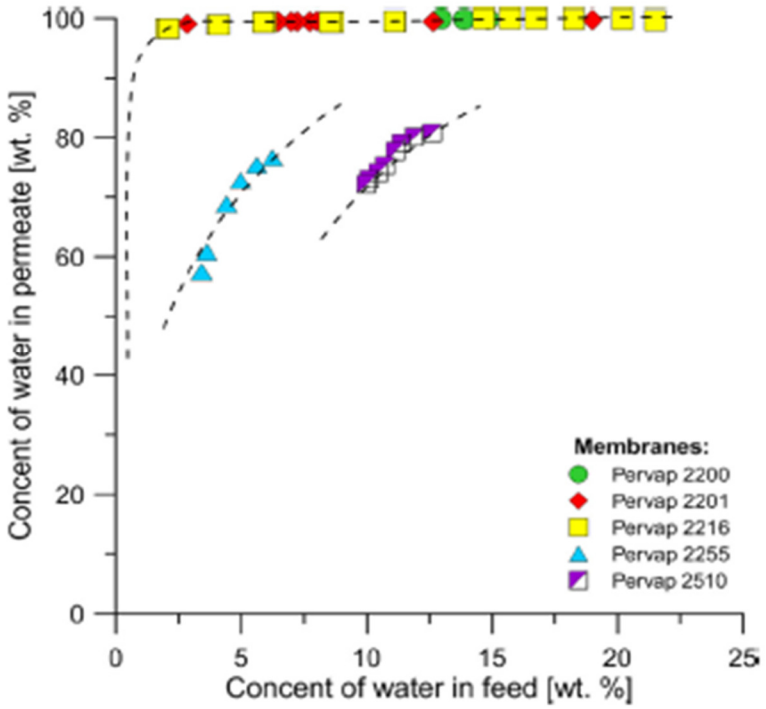

Figure 9.4. Permeate composition versus liquid composition for dehydration of 2,2,3,3-tetrafluoropropan-1-ol with commercial membranes: 70 ºC. Graph from Kujawski *et al*. (2017).

Enrichment Factor

The enrichment Factor, EF_i, has been defined as the ratio of permeate concentration to feed concentration (Feng & Huang, 1997).

$$EF_i = \frac{y_i}{z_i} \tag{9.6}$$

where: z_i = mass fraction of the solute in the feed

y_i = mass fraction of the solute in the permeate

The numerical value of enrichment depends on whether mass fractions or mol fractions are used. Typically, permeate concentration is stable and enrichment decreases with increasing feed concentration. Assuming constant permeate purity, Eq. (9.6) has the form

$$EF_i = \frac{k}{z_i} \tag{9.7}$$

where k is a constant. Typical enrichment curves are illustrated in Fig. 9.5: curves initially drop rapidly as liquid concentration increases and then tail off as the effect of the increasing denominator in Eq. (9.6) wanes. In cases where the permeate concentration rises gradually as the concentration of the water in the liquid phase increases, enrichment peaks and then drops gradually.

Peak enrichment is typically a function of the permeate concentration at a low feed concentration with the permeate concentration at higher levels being of no relevance. The peak can occur outside of normal industrial operating conditions at feed water concentrations below 1% w/w as illustrated in Fig. 9.6. Membranes with similar performance characteristics at industrial operating conditions can have significantly different enrichment values. Enrichment is not commonly used as a metric, although there are exceptions (Kaminski *et al*., 2008).

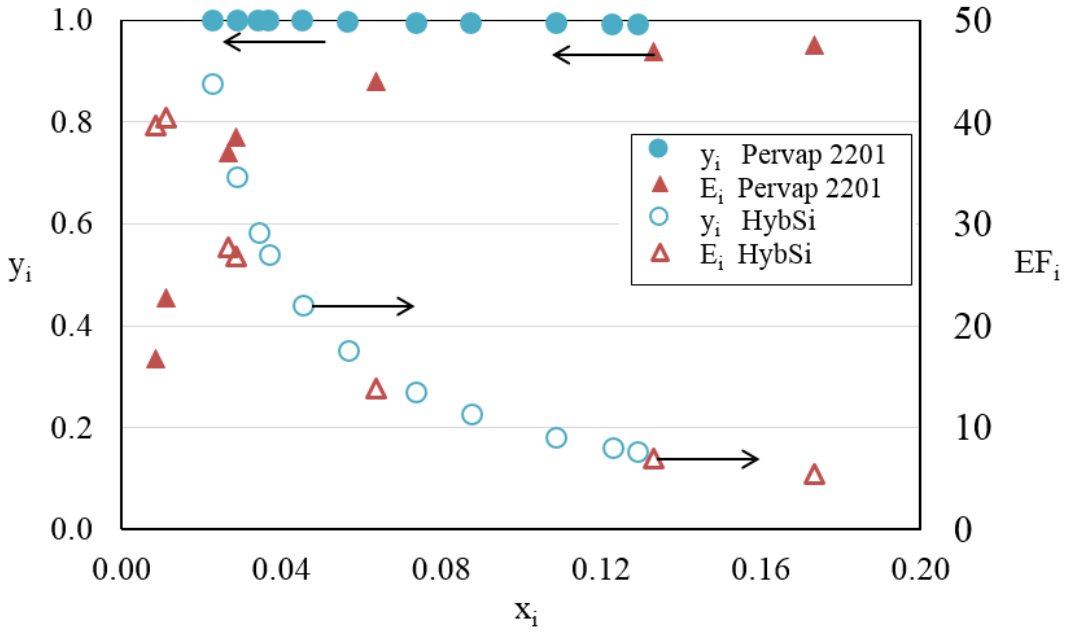

Figure 9.5. Permeate concentration and enrichment versus liquid concentration. ● dehydration of IPA at 90 °C using Pervap 2201, O are the corresponding enrichment values Qiao *et al*. (2005). ▲, dehydration of ethanol using HybSi at 80 °C, Δ are the corresponding enrichment values (Klinov *et al*. (2017).

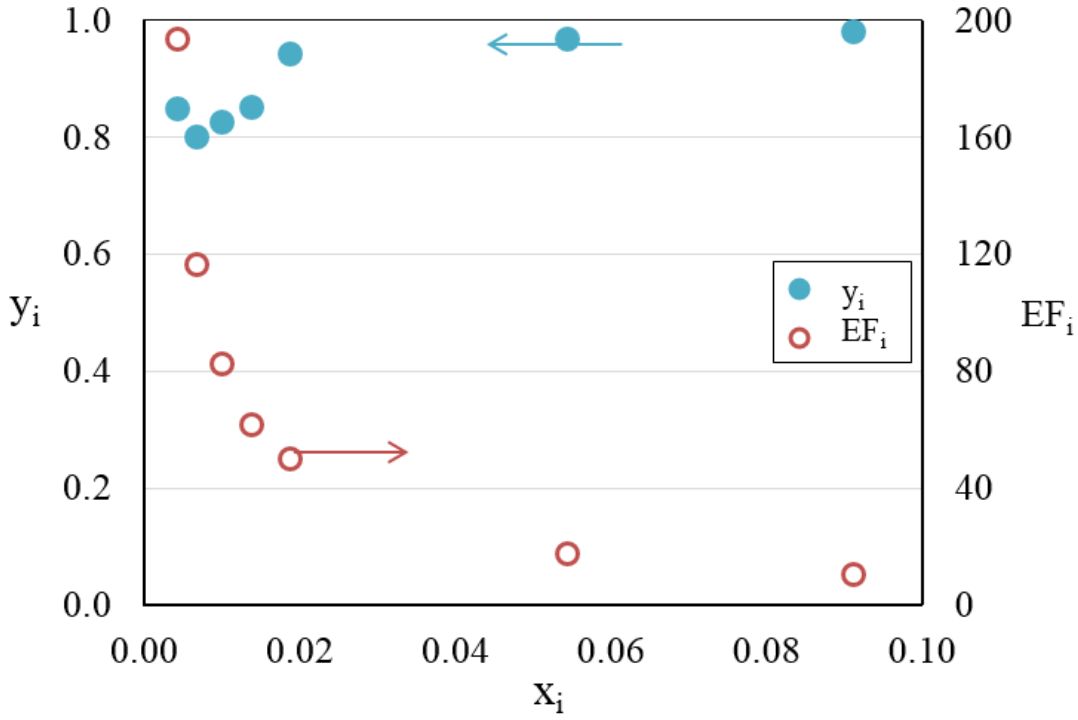

Figure 9.6. Permeate concentration and enrichment versus liquid concentration. Dehydration of ethanol at 98 °C using Pervap 4100, data from Niemistö *et al*. (2013): ● is y_i, O is EF_i.

Separation Factor

The separation characteristics of a membrane are most commonly characterised in terms of the separation factor: Chapman *et al*. (2008) include data from 140 papers with separation factor data for more than 200 membrane/solvent/solute combinations. Huang and Xu (1988) defined the separation factor as,

$$\beta_{ij} \equiv \frac{\left(y_i / y_j \right)}{\left(z_i / z_j \right)} \tag{9.8}$$

where z denotes the mass fraction in the feed

y denotes the mass fraction in the permeate

i denotes the preferentially permeating component

j denotes the less permeating component

The separation factor is a ratio of ratios. Therefore the same values are obtained irrespective of whether mass fractions or mol fractions are used. The symbol α_{ij}, has also been used for the separation factor. Analysis of the definition of the separation factor indicates that it has an asymptotic relationship with permeate purity, y_i, as noted by Nagy *et al*. (2015). As the permeate concentration plateaus, the separation factor decreases due to the effect of the increased feed concentration. Assuming constant permeate purity, the curve for binary systems has the form

$$\beta_{ij} = \frac{k}{\left(\frac{z_i}{1 - z_i} \right)} \tag{9.9}$$

Rearranging, $$\beta_{ij} = \frac{k}{z_i} - k \tag{9.10}$$

where k is a constant. The enrichment and separation factor curves are similar in shape, albeit that for a given dataset, separation factors have higher values. Peak separation factors usually occur at a low water concentrations as illustrated in Fig. 9.7. The point at which the permeate purity approaches a constant value determines the concentration

at which peak separation factor occurs. The separation factor rises rapidly to a peak and gradually declines as liquid concentration increases as shown in Fig. 9.8. In cases where the permeate concentration rises more gradually, the peak separation factor occurs at higher liquid concentrations. This typically leads to a lower peak separation value as compared with systems where plateauing occurs earlier. This is because of the effect of the greater liquid concentration, z_i, in the denominators of Eqs. (9.8) and (9.10).

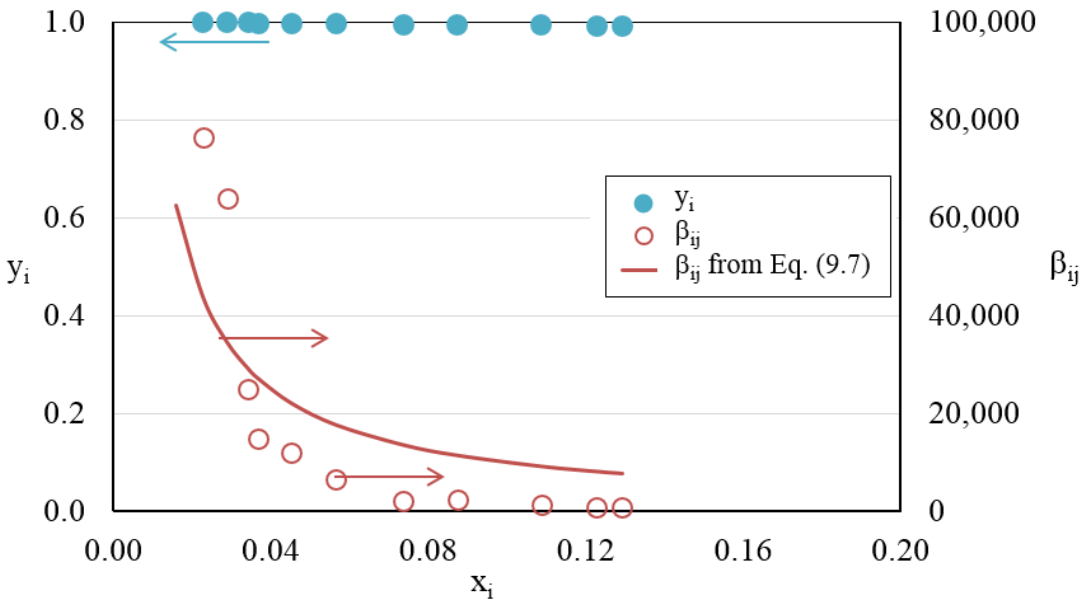

Figure 9.7 Permeate concentration and separation factor values versus liquid concentration. • permeate concentration and O are the corresponding separation factor values, dehydration of IPA at 90 °C using Pervap 2201, Qiao *et al.* (2005). Line is separation factor calculated using Eq. (9.7) with k = 10,000,000.

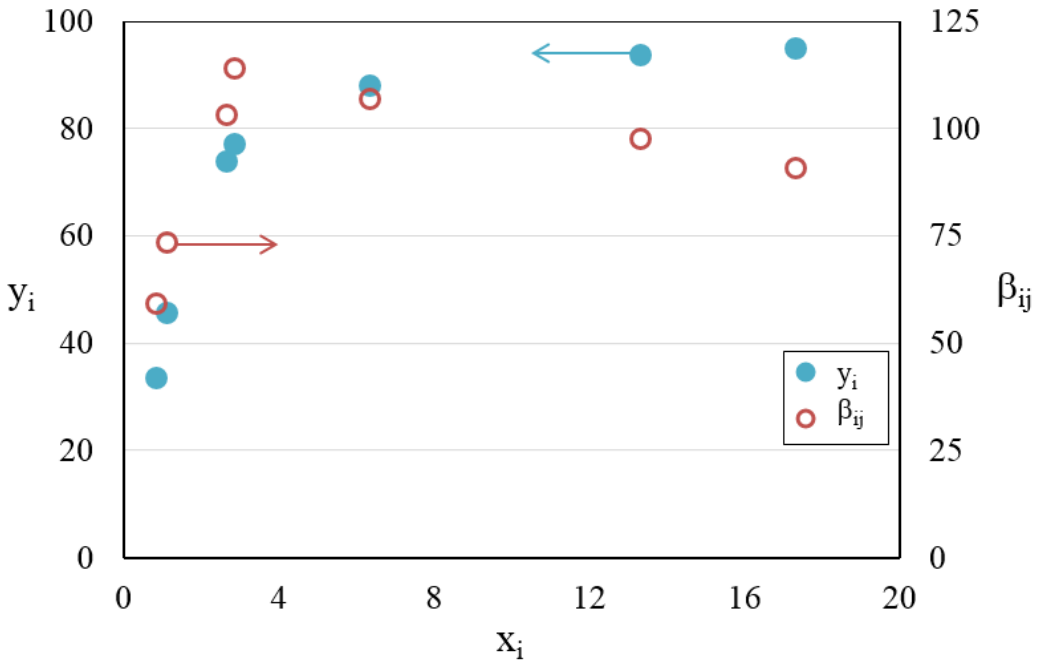

Figure 9.8 Permeate concentration and separation factor versus liquid concentration: ● permeate concentrations and O the corresponding separation factor values, dehydration of ethanol at 80 °C using HybSi membrane Klinov *et al*. (2017).

In cases where the permeate purity is greater than 98%, a small change in permeate purity can have a large impact on the proportion of solvent in the permeate stream, y_j, as shown in Eq. (9.8): this leads to a significant change in the separation factor. There can be two peaks as illustrated in Fig. 9.9. In this example, were the permeate purity at 11% water in the feed to be swapped with that at 14%, the peak separation factor would rise from 301 to 396, an increase of 32%: yet for industrial purposes there would be no significant difference in overall performance. The high levels of separation achieved by some commercial membranes in recent years, some with permeate purities greater than 99.5% (Koch and Górak, 2014; Klinov *et al*., 2017), has exacerbated this issue.

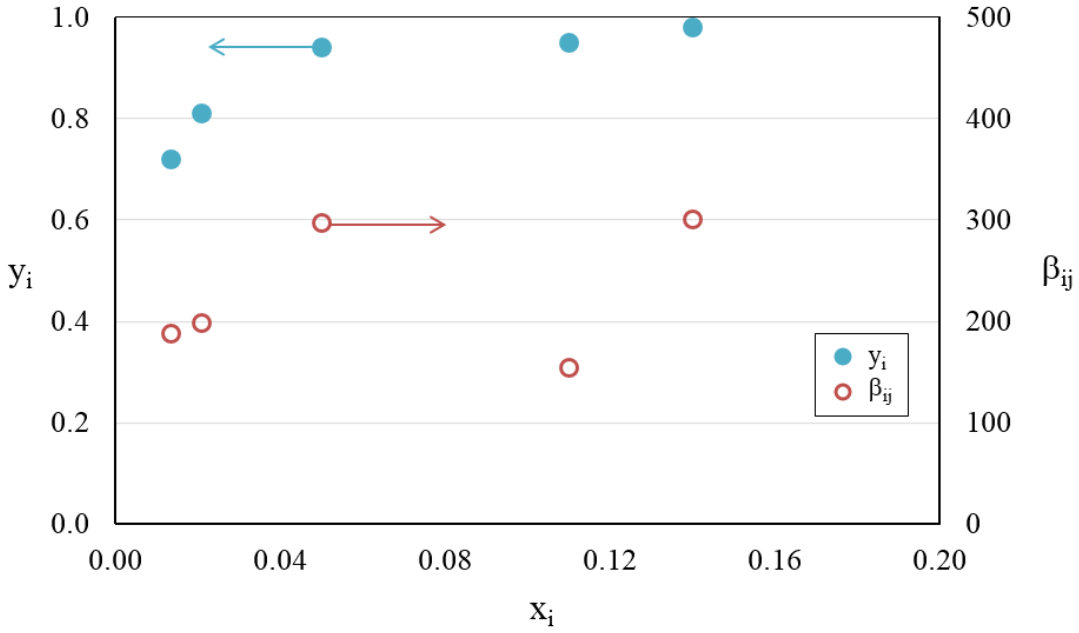

Figure 9.9 Permeate concentration and separation factor versus feed concentration: ● permeate mass fraction, O corresponding separation factor, %wt water. Calculated from IPA-water pervaporation data using Sulzer PERVAP 2210 membrane at 80 °C, Cséfalvay *et al*. (2008).

Industrial systems are normally operated at as high a temperature as is feasible so as to maximise flux. However, the peak separation factor can be higher at lower temperatures (Gallego-Lizon *et al*., 2002; Casado *et al*., 2005; Tang *et al*., 2012): in such cases the data is not relevant for industrial purposes.

Separation factor and Area

Shanahan (2010) noted the asymptotic relationship between separation factor and membrane area for a given separation. Nagy el al. (2015) noted that the separation factor had an asymptotic relationship with energy demand for a given separation. Using the calculation methods outlined in chapters 3 and 4, the membrane area per unit mass of retentate product can be calculated for a given separation. Typical data for an industrial system is shown in Fig. 9.10. Membrane area has an asymptotic relationship with β_{ij}. Baker (2012, p.393) stated that increasing the separation factor above 1,000 has little additional benefit. Increasing β_{ij} above 600 has little impact on the required area as shown in Fig. 9.5; except in cases where the feed concentration is less than 2%.

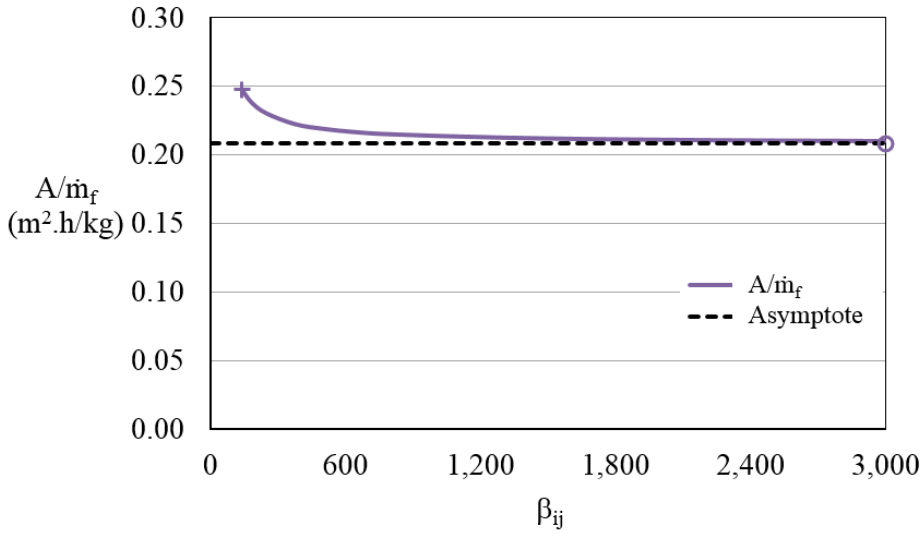

Figure 9.10 Area per unit mass of feed flowrate versus separation factor. Ethanol dehydration from 6% to 2% using Pervap 2210, T_f = 100 °C, J_o = 4.65x10^6 kg/m^2/h, E_j = 53,120 kJ/kmol: y_i = 90% is at point marked + and pure permeate is at point marked O. Horizontal line is the asymptote for pure permeate. Constants calculated from data in Huang *et al*. (2006).

There is an asymptotic relationship between the permeate-feed ratio and β_{ij}. There is also an asymptotic relationship between the permeate purity and β_{ij}. These relationships are illustrated in Fig. 9.11. Permeate is usually a waste stream: disposal costs are higher if the quantity is high and if the permeate purity is low. The latent heat of the permeate stream per unit mass of feed also has an asymptotic relationship with β_{ij}. Fig. 9.12 shows the relationship for typical industrial operating conditions. Increasing β_{ij} above 600 has little impact on these parameters.

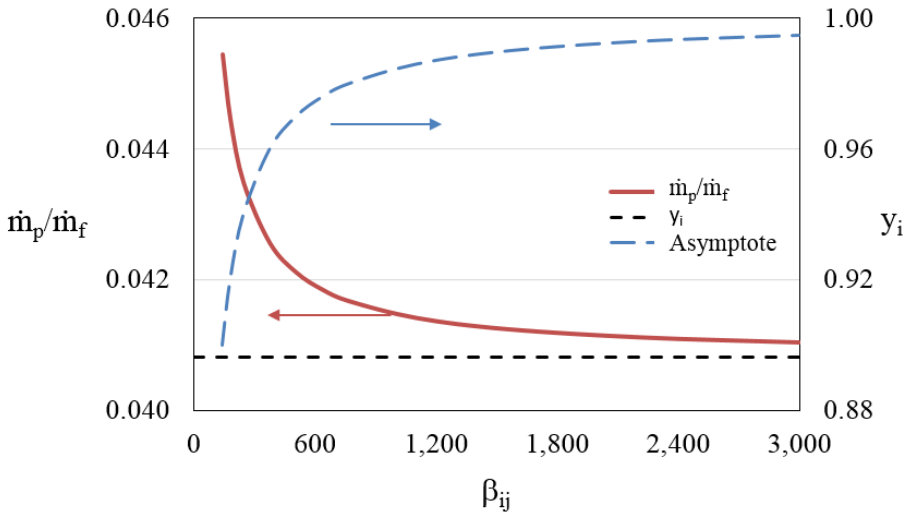

Figure 9.11 Permeate-feed ratio and corresponding permeate concentration versus separation factor, β_{ij}, for ethanol dehydration from 6% to 2% using Pervap 2210, T_f = 100 °C, J_o = 4.65x10^6 kg/m^2/h, E_j = 53,120 kJ/kmol. Dashed curve is y_i versus β_{ij} -1. Dashed horizontal line is the asymptote for pure permeate. Constants calculated from data in Huang *et al*. (2006).

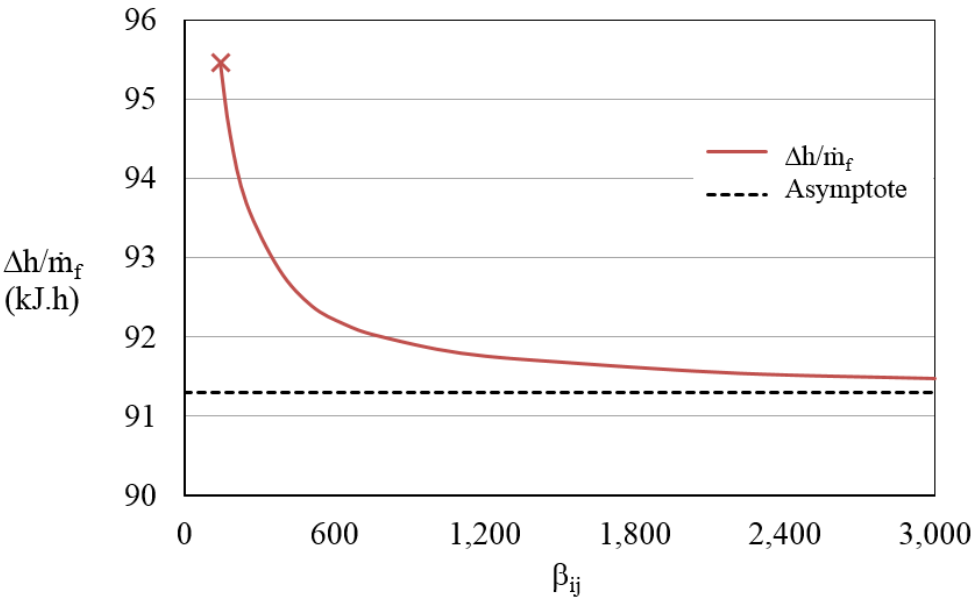

Figure 9.12 Latent heat of vapour per unit mass of feed versus separation factor. Ethanol dehydration from 6% to 2% using Pervap 2210, T_f = 100 °C, J_o = 4.65x10^6 kg/m^2/h, E_j = 53,120 kJ/kmol; y_i = 90% is at point marked X. Supply temperature of 15°C. Dashed line is the asymptote with pure permeate. Constants calculated using data from Huang *et al*. (2006).

Minor variations in permeate purity can cause arbitrary variations in the peak separation factor. Furthermore, the asymptotic relationships between β_{ij} and membrane area, permeate-retentate ratio and energy consumption per unit retentate product, also cause β_{ij} to be an unsatisfactory measure of membrane performance.

Baker (1991) noted that separation can occur in the absence of a membrane. He proposed that the separation factor be comprised of the evaporation separation factor and the membrane separation factor.

$$\beta_{ij} = \beta_{evap}\beta_{mem} \tag{9.11}$$

The evaporation separation factor is unity for azeotropes. It is less than 1.6 for ethanol and isopropanol at all points within the range of industrial operations. However, as noted by Baker (2012, p. 383), much of the published literature provides data in the form of component fluxes and separation factors.

Baker *et al*. (2010) recommend the use of selectivity, α_{ij}, rather than separation factor to characterise the performance of pervaporation membranes as shown in Eq. (9.12). Selectivity is the ratio of the permeabilities or permeances of the components. This allows pervaporation performance to be directly compared with the large body of vapour permeation data. However, it has not gained widespread acceptance. Flux and separation factor are more widely used and understood.

$$\alpha_{ij} = \frac{P_i^G}{P_j^G} = \frac{P_i^G / l}{P_j^G / l} \tag{9.12}$$

Membrane Flash Index, MFLI

Toth *et al*. (2017, pp. 72-73; Toth *et al*., 2018) proposed the Membrane Flash Index (*MFLI*). The *MFLI* compares the separation data using a membrane with the corresponding vapour-liquid equilibrium data for a flash distillation.

$$MFLI = \frac{y_i}{y_{VLE}^{D}} \tag{9.13}$$

where: $MFLI$ is the Membrane Flash Index

y_i is the permeate purity obtained with pervaporation

y_{VLE}^{D} is the permeate purity obtained with flash distillation

For a given liquid phase concentration, y_{VLE}^{D} , is constant and the *MFLI* is proportional to y_i. Hence, for a given feed concentration, the membrane area per unit retentate product has a broadly linear relationship with the *MFLI* as shown in Fig. 9.13. The $\dot{m}_p/\dot{m}_r$ ratio and the energy consumption per unit mass of retentate product also have broadly linear relationships with the *MFLI* for a given feed composition as shown in Figs 9.14 and 9.15. Thus the *MFLI* is a better measure of separation performance than the separation factor or the enrichment factor.

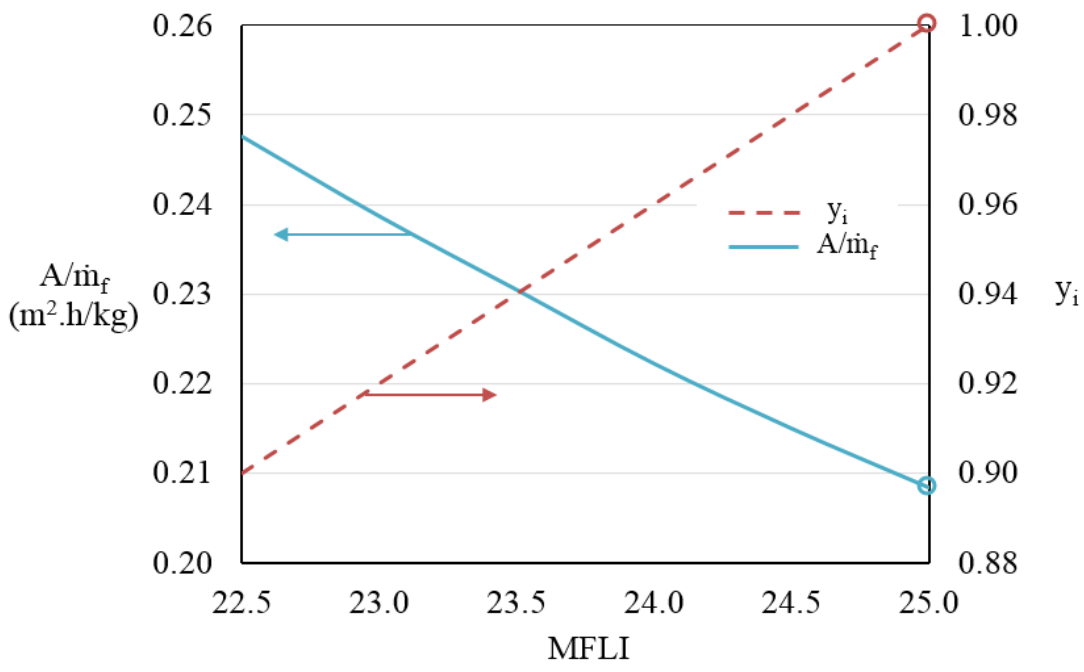

Fig. 9.13 Area per unit mass of feed and corresponding permeate concentration versus *MFLI*. Ethanol dehydration from 6% to 2% using Pervap 2210, T_f = 100 °C, J_o = 4.65x10⁶ kg/m²/h, E_j = 53,120 kJ/kmol, x_{VLE} = 4%. O denotes pure permeate. Constants calculated from data in Huang *et al.* (2006).

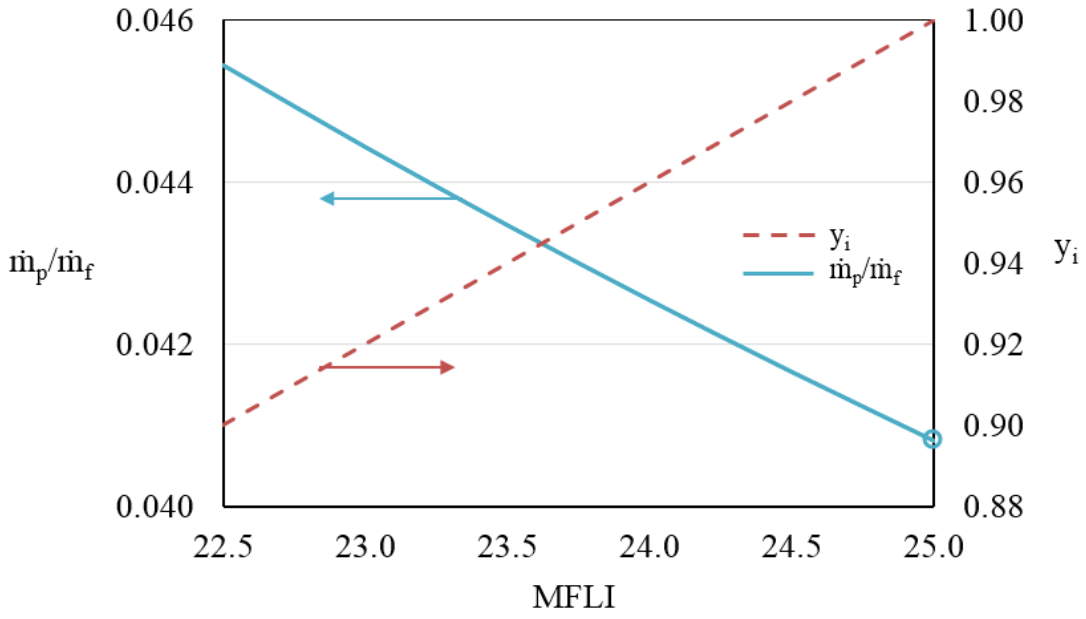

Figure 9.14 Permeate feed ratio and corresponding permeate concentration versus *MFLI*. Ethanol dehydration from 6% to 2% using Pervap 2210, T_f = 100 °C, J_o = 4.65x10^6 kg/m^2/h, E_j = 53,120 kJ/kmol, x_{VLE} = 4%. Constants calculated from data in Huang *et al.* (2006). O denotes pure permeate.

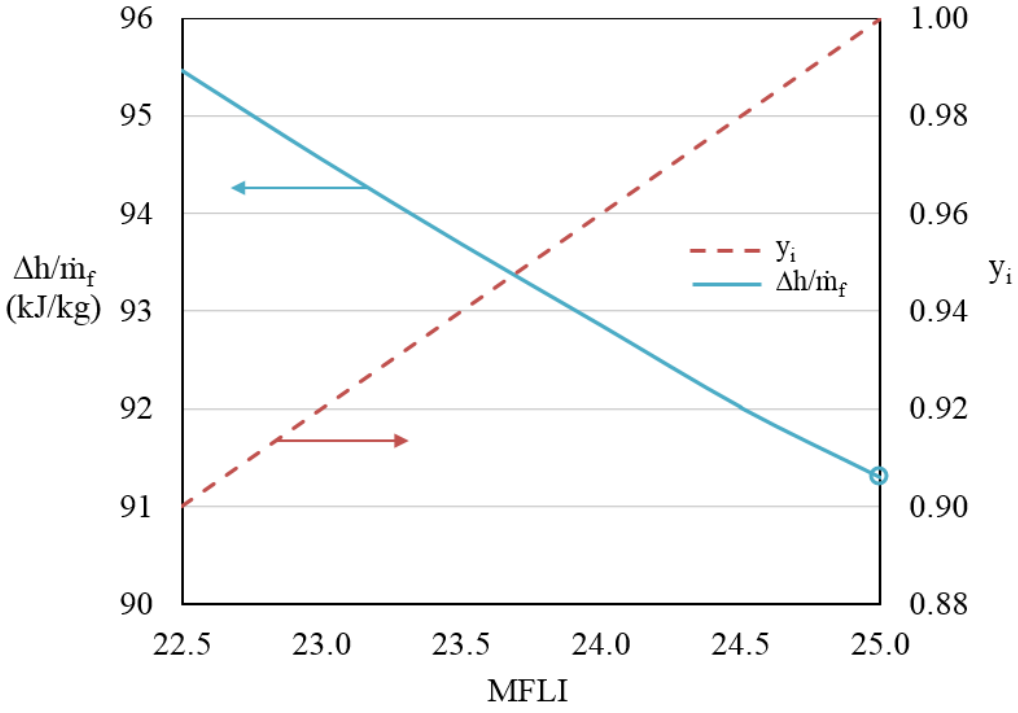

Fig. 9.15 Latent heat per unit mass of feed and corresponding permeate concentration versus *MFLI*. Ethanol dehydration from 6% to 2% using Pervap 2210, T_f = 100 °C, J_o = 4.65x10^6 kg/m^2/h, E_j = 53,120 kJ/kmol, x_{VLE} = 4%. O denotes pure permeate. Constants calculated from data in Huang *et al.* (2006).

9.5 Pervaporation Separation Index

Membrane performance is a function of both flux and separation. Huang and Yeom (1990) proposed a single combined metric, the pervaporation separation index, (*PSI*).

$$PSI = J\beta_{ij} \tag{9.14}$$

where *PSI* = Pervaporation Separation Index (kg/h.m^2)
J = mass flux (kg/h.m^2)
β_{ij} = separation factor (-)

This definition permits high *PSI* values even in cases where there is no separation, i.e. $\beta_{ij} = 1$. To address this, Huang and Feng (1993) modified the definition as follows,

$$PSI = J\left(\beta_{ij} - 1\right) \tag{9.1}$$

Flux is proportional to solute concentration for many membranes. For binary systems,

$$PSI = \mathrm{z_i} J_o \left[\frac{\left(y_i / y_j \right)}{\left(z_i / z_j \right)} - 1 \right] \tag{9.15}$$

Assuming constant permeate composition this equation has the from,

$$PSI = a - bz_i \tag{9.16}$$

where *a* and *b* are constants. *PSI* typically rises to a peak near the concentration at which the flux begins to plateau, it then declines rapidly before tailing off less sharply at higher liquid concentrations as shown in Figs 9.16 and 9.17. Peak *PSI* usually occurs at a higher concentration than peak separation factor for a given system. A more gradual rise in permeate concentration causes peak *PSI* to occur at a higher liquid concentration and this typically leads to a lower peak *PSI* value as compared with similar systems where plateauing occurs earlier. This is illustrated in Fig. 9.17. Peak *PSI* can occur outside the range of industrial operations: as shown in the example in Fig. 9.17 for an ethanol dehydration where it occurs at a liquid concentration of 18% water.

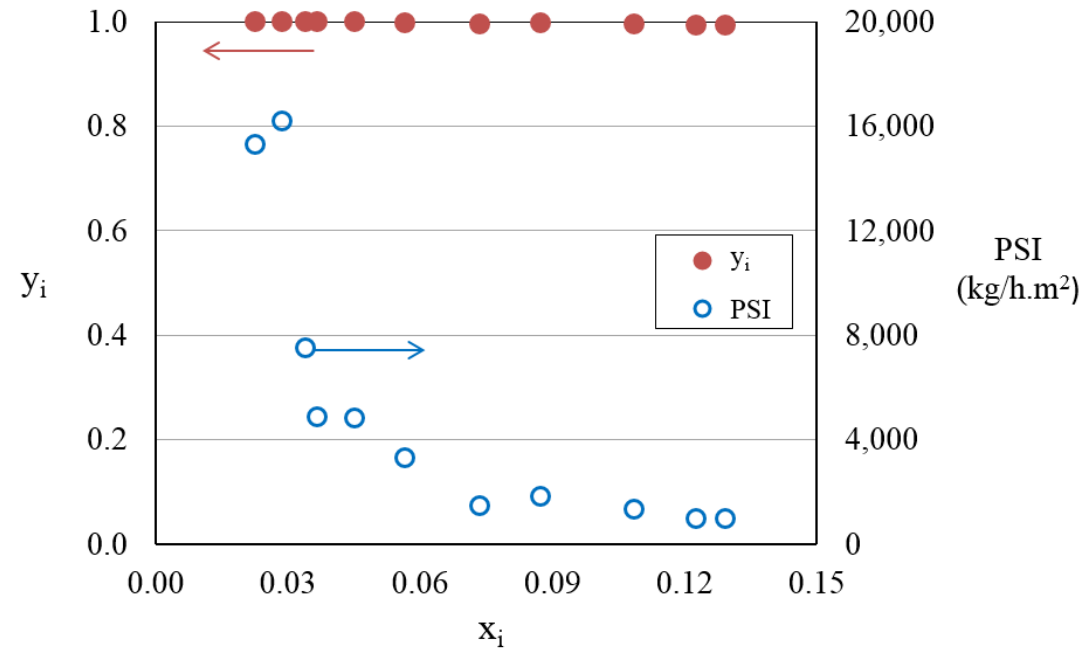

Fig. 9.16 Permeate concentration and corresponding *PSI* versus liquid concentration. ● permeate mass fraction, y_i, O is *PSI* Calculated from IPA dehydration data for Pervap 2201 membrane at 90 °C, Qiao *et al*. (2005).

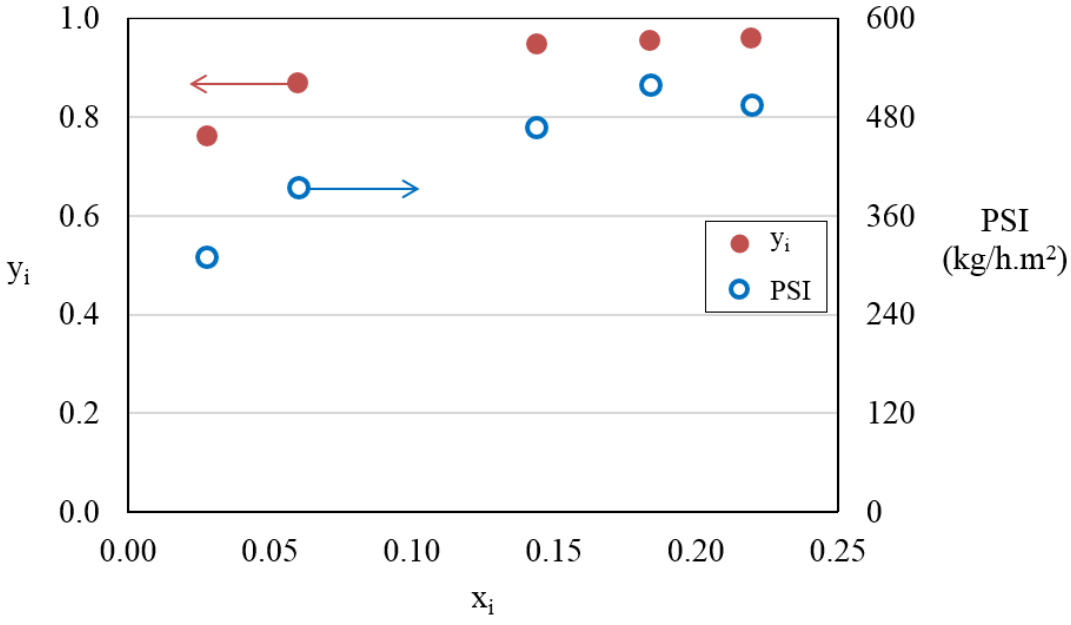

Fig. 9.17 Permeate concentration and corresponding *PSI* versus liquid concentration. ● is permeate mass fraction, y_i, O is *PSI*. Calculated from EtOH dehydration data for HybSi membrane at 80 °C, Klinov *et al*. (2017).

Values of *PSI* for commercial membranes were calculated from literature data as shown in Table 9.1. The J_{av}/J_f figures relate to dehydration of IPA from 13 to 11 wt% water.

Flux is a function of temperature, and so the value of the *PSI* is dependent on the temperature at which the experimental runs are undertaken. Trials are often undertaken at low temperatures due to the limitations of laboratory-scale equipment. Hence, published *PSI* values often fail to represent the true capabilities of membranes. *PSI* values obtained at different temperatures are not comparable.

The flux used to calculate the *PSI* is the flux value at a single combination of temperature and concentration. Thus the *PSI* neglects the effects of the activation energy. High activation energies lead to low average flux within modules as shown by the J_{av}/J_f values in Table 9.1. The average flux determines the membrane area, which is a key factor in the capital cost of pervaporation systems.

The concentration at which the flux is measured for incorporation in the *PSI* depends on the relationship between the permeate purity and liquid concentration of the membrane. Flux is often proportional to concentration. This can lead to differing *PSI* values for similar membranes.

Data relating to the performance of commercial IPA dehydration membranes is shown in Table 9.1. The β_{ij} used to calculate peak *PSI* for the Pervap 2201 is more than 4 times that for the Pervap 1210 and twice that of the HybSi membrane because the permeate purity plateaus at a lower water concentration. The separation characteristics of the membranes are similar, yet the separation factor are multiples of one another. This is reflected in the *PSI* values of the respective membranes.

The HybSi membrane has a 2% higher permeate purity than the Pervap 2510 membrane. This causes its β_{ij} of the HybSi to be 8 times greater. The average flux for the HybSi is 42% higher than that of the Pervap 2510 but the *PSI* is 10 times greater largely due to the high β_{ij} value of the HybSi membrane. Thus the *PSI* does not reflect the relative merits of membranes.

Table 9.1 Performance of commercial IPA dehydration membranes.

	T_f °C	E_j kJ/ kmol	J_{av}/J_f	J_{av} kg/ h.m^2	y_i	β_{ij}	PSI_{max} kg/ h.m^2
Pervap 2210 Cséfalvay *et al*. (2014)	90	50,591	0.613	1.157	0.980	278	692
Pervap 2201 Qiao *et al*. (2005)	90	62,800	0.559	0.738	0.997	6,828	5,988
Pervap 1210 Koch & Górak (2014)	78	64,373	0.515	0.639	0.997	1,514	2,643
Pervap 2510* Qiao *et al*. (2005)	100	45,400	0.660	2.834	0.977	294	1,151
HybSi, Klinov *et al*. (2017)	80	45,807	0.619	4.025	0.997	2,379	11,499

β_{ij} values shown are those at the concentration at which peak *PSI* occurs (not peak β_{ij})

* Qiao *et al*. (2005) and Van Hoof, *et al*. (2004) undertook isopropanol dehydrations using Pervap 2510 membranes at 70°C and 90°C. Van Hoof *et al*. (2004) report results at 70°C, these appear to be the same results as those reported by Van Hoof *et al*. (2004). The permeate purities reported are similar. However, the flux reported by Qiao *et al*. (2005) was less, whilst the E_j value was higher. The data relating to commercial membranes is used to illustrate the effects of the various metrics: hence, such inconsistencies do not affect the analysis and conclusions of this study.

Commercial membranes with permeate purities above 99.5% are now available (Koch and Górak, 2014; Klinov *et al*., 2017). At such high purities, very small increases in permeate purity can lead to large increases in separation factor and *PSI*. For example increasing the permeate purity from 99.7% to 99.8% increases both the separation factor and the *PSI* by 50%. A 50% increase in flux would be required to achieve the same increase in the *PSI*. Thus the *PSI* does not provide an appropriate balance between flux and permeate purity.

Peak *PSI* can occur outside the envelope of industrial operating conditions. The *PSI* is not a suitable metric as regards flux or separation. It does not provide appropriate

weighting to flux and separation as regards their economic value for industrial operations. It may have led some researchers to over-emphasise the importance of permeate purity to the neglect of increased flux. Other metrics have been proposed in recent years: Sosa and Espinosa (2011) suggested that the *PSI* be based on the average membrane area for a given separation, Toth *et al*. (2018) proposed the Membrane Flash Index. Table 9.2 summarises the existing pervaporation metrics. More appropriate metrics are required.

Table 9.2 Summary of current pervaporation metrics.

Metric	**Discussion**
Mass flux	Is not suitable for incorporation into a single combined metric such as the *PSI* as it does not allow for variations in flux due to concentration, temperature and apparent activation energy of pervaporation, E_j.
Molar flux	Useful for comparison with vapour permeation. Little data available. Similar issues to mass flux.
Permeability	A measure of the additional separation due to the presence of a membrane. Facilitates comparison with vapour permeation data. Needs to be combined with vapour liquid equilibrium data when designing a pervaporation module.
Permeance	Permeance = Permeability/membrane thickness. It relates to the properties of the membrane material and is independent of membrane thickness. Needs to be combined with vapour liquid equilibrium data and membrane thickness when designing a pervaporation module.
Selectivity	It is the ratio of the permeability or permeance of the components.
Enrichment	Membranes with similar industrial performance can have different enrichment values as it relates to the separation characteristics at a single concentration.
Separation factor	Minor variations in performance can lead to very different separation factor values. Asymptotic relationship with key parameters.
Membrane flash index	Compares permeate concentration with the vapour composition achievable with flash distillation. Cannot be incorporated into a combined single metric as there could be positive values even where a membrane did not cause separation to occur.
PSI	Minor variations in performance can lead to very different separation factor values. Peak *PSI* values can pertain to data outside the envelope of industrial operating conditions. Asymptotic relationship with key parameters.

9.6 Novel metrics

Flux

In this section a novel single metric is proposed. It is proportional to the average flux such that the solute content reduces from 1% w/w above, to 1% w/w below, the azeotropic composition of the solvent assuming perfect adiabatic plug flow pervaporation. A permeate composition of 90% gives a $\dot{m}_p/\dot{m}_f$ ratio of 2.30% for ethanol dehydrations and 2.53% for IPA dehydrations; with a permeate composition of 100% the corresponding values are 2.06% and 2.25%. These are within the range of permeate-feed ratios typically used in industry.

Use of an average flux is consistent with the proposal by Sosa and Espinosa (2011) that the inverse of the minimum area to perform a separation be incorporated in the *PSI*, so as to allow for the effect of the flux-concentration relationship. The capital cost of pervaporation systems is mainly a function of the membrane area. Hence, the capital cost of pervaporation systems is approximately proportional to the inverse of the average flux. Adiabatic operation is common in industry: use of an average flux ensures that the effect of activation energy is incorporated in the metric. Specifying standard feed and retentate concentrations ensures consistency and comparability of data between studies. It also ensures that data is relevant to industrial operating conditions.

For separations that do not involve an azeotrope, d_{aze} is taken to have the same value as the azeotrope of ethanol, i.e. 4 wt%. Pervaporation, in the absence of an azeotrope, is typically undertaken at low solute concentrations and so this nominal concentration reflects typical industrial operating conditions. The minimum retentate concentration of 3 wt% avoids complications regarding variations in permeate purity at low water concentrations.

Separation

A single metric needs to incorporate parameters relating to separation and flux. The metric should not have a positive value when no separation occurs or when the permeate stream contains less solute than the liquid. This was an issue with the original definition of the *PSI* (Huang and Yeom, 1990) and was subsequently addressed by Huang and

Feng (1993). The *MFLI* as proposed by Toth *et al*. (2017, pp. 72-73; Toth *et al*., 2018) indicates the separation performance of a membrane relative to vapour liquid equilibrium. However, were it to directly replace (β_{ij} -1) in the *PSI*, similar issues regarding positive values in cases where no separation occurs would arise. A novel metric, the 'Pervaporation Separation Modulus', *M*, is proposed

$$M = \left(\frac{y_i - x_{azeo}}{1 - x_{azeo}} \right) \tag{9.17}$$

where: M is the pervaporation separation modulus

x_{azeo} is the azeotropic composition

y_i is the permeate composition at the azeotropic composition

In cases where no separation occurs, the pervaporation separation modulus has a value of zero: where the permeate stream contains less solute than the liquid, it is negative. It includes a comparison between permeate purity and vapour liquid equilibrium as suggested by Toth *et al*. (2017, pp. 72-73) and Baker (1991) whilst addressing the issues identified by Huang and Feng (1993).

The Pervaporation Membrane Index

Another novel metric, the 'Pervaporation Membrane Index', *PMI* is proposed: it is defined as the average flux such that the water content reduces from 1% w/w above to 1% w/w below the azeotropic concentration, multiplied by the pervaporation separation modulus. The following equation is proposed

$$PMI = J_{av} \left(\frac{y_i - x_{azeo}}{1 - x_{azeo}} \right)^n \tag{9.18}$$

where: PMI is the pervaporation membrane index $(kg/h.m^2)^n$

J_{av} is the average flux for the standard separation $(kg/h.m^2)$

n is the index

hence $$PMI = J_{av} M^n \tag{9.19}$$

The data used for the calculation of the *PMI* is at the azeotropic composition and usually pertains to the maximum temperature that the membrane can withstand. It will encourage researchers to provide data at the concentrations and elevated temperatures used for industrial operations. The form of the equation is such that where no separation occurs the *PMI* is equal to zero and it is negative when the permeate stream contains less solute than the liquid phase.

The value of n should be such that the relative economic importance of separation relative to flux is appropriate. The results for the combination M^n can be normalised to determine the value of increased permeate purity relative to increased flux. Tables 9.3 and 9.4 show normalised values of M^n for different values of the index n for ethanol and isopropanol dehydrations.

The relative value of flux and separation depends on the application. It can vary within a single system as discussed in section 7.5, where the use of different membranes for different stages of a multi-stage pervaporation was discussed. It will vary as capital costs change relative to utility costs over the long term. However, the relative costs of many items of process equipment have changed little over several decades (Wolf, 2011, pp. 211-214). Use of a standard index allows data from different applications to be compared. The results for ethanol and IPA are similar as shown in Fig. 9.18.

The data in tables 9.3 and 9.4 show that an index value of $n = 2$ would mean that increases in permeate purity from 90% to 95% are of similar value to increases in flux of 12% to 18%. The focus of some manufacturers on increasing selectivity, particularly at low water concentrations (Delatmem, 2017) would suggest that an index value of 2 is too low. An index value of $n = 5$ would mean that increases in permeate purity from 99.0% to 99.5% are of similar value to increases in flux of 3% to 4%. The net economic gain of such an increase in permeate purity is small as is evidenced by the data illustrated in Figs. 9.13, 9.14 and 9.15. A value of $n = 3$ is recommended. However, further research involving an economic analysis of industrial systems is required to determine the most appropriate value of the index, n.

Table 9.3 Economic value of separation performance relative to flux for ethanol

y_i	n = 2	n = 3	n = 4	n = 5
0.900	1	1	1	1
0.950	1.12	1.18	1.25	1.33
0.990	1.22	1.35	1.49	1.64
0.995	1.23	1.37	1.52	1.69

Table 9.4 Economic value of separation performance relative to flux for IPA

y_i	n = 2	n = 3	n = 4	n = 5
0.900	1	1	1	1
0.950	1.13	1.22	1.31	1.40
0.990	1.24	1.39	1.55	1.73
0.995	1.26	1.41	1.59	1.78

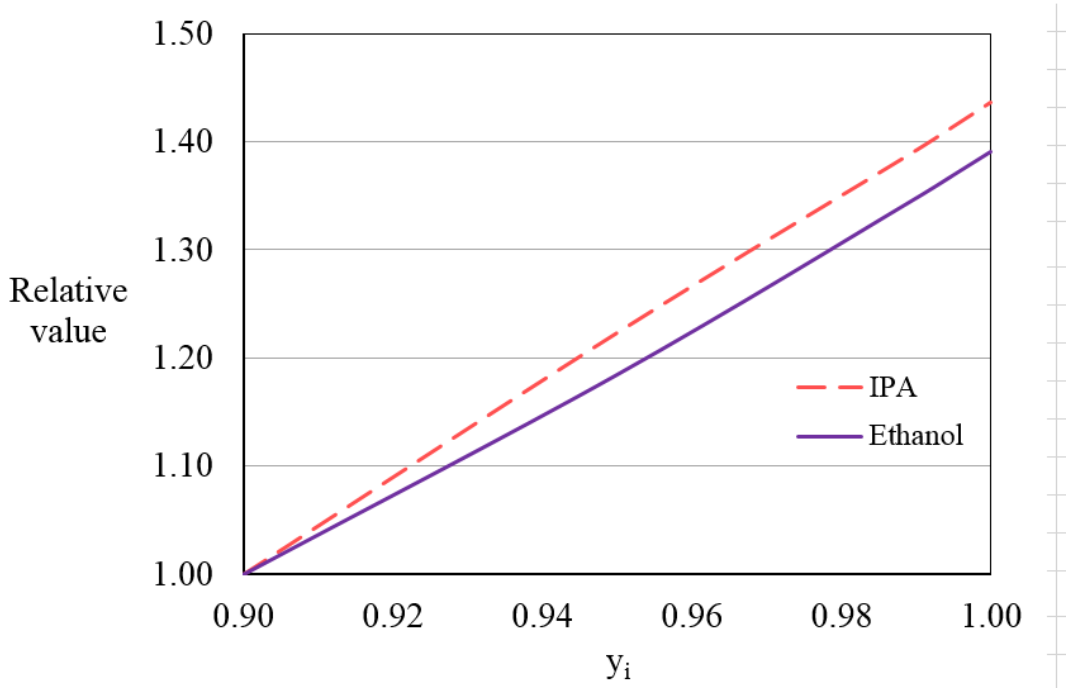

Fig. 9.18 Relative value of flux versus permeate concentration: $n = 3$

Calculation of the *PMI*

As the feed, retentate and permeate compositions are known, the $\dot{m}_p/\dot{m}_f$ ratio can be calculated.

$$\frac{\dot{m}_p}{\dot{m}_f} = \frac{z_i - x_{ir}}{y_i - x_{ir}} \tag{9.20}$$

z_i is 1 wt% more than the azeotropic composition and x_{ir} is 1 wt% less. Thus Eq. (9.20) reduces to

$$\frac{\dot{m}_p}{\dot{m}_f} = \frac{0.02}{y_i - x_{azeo} + 0.01} \tag{9.21}$$

The average flux can be calculated using the methods outlined in Table 3.1 in chapter 3 or Table 4.3 in chapter 4 as appropriate. The *PMI* can then be calculated using Eq. (9.19).

9.7 Results

Average flux

Fig. 9.19 is a plot of J_{av}/J_f versus J_r/J_f for the full range of activation energy, feed temperature and permeate conditions within the envelope of industrial operating conditions for both ethanol and IPA dehydrations with feed and retentate concentrations corresponding to the *PMI* definition. Ethanol has a lower azeotropic concentration than IPA: hence, its x_i/z_i ratio and J_r/J_f ratio values are lower.

Short cut method

The following equation approximates the simulated data for systems where flux is proportional to water concentration

$$\frac{J_{av}}{J_f} = a + b\sqrt{\frac{J_r}{J_f} + c} \tag{9.22}$$

where: J_{av} the average flux for the standard separation (kg/h.m^2)

J_f the flux at the feed conditions (kg/h.m^2)

J_r the flux at the retentate concentration and temperature (kg/h.m^2)

a, b, c are constants

The equation applies when calculating the *PMI* for both IPA and ethanol when $y_i \geq 0.90$, T_f of 363 K – 403 K, and E_j values of 15,000 to 60,000 kJ/kmol.K. It is accurate to within 0.2% for both ethanol and IPA dehydrations. Table 9.5 lists the constants for ethanol and isopropanol dehydrations and Table 9.6 outlines the algorithm for the short-cut calculation of the *PMI*.

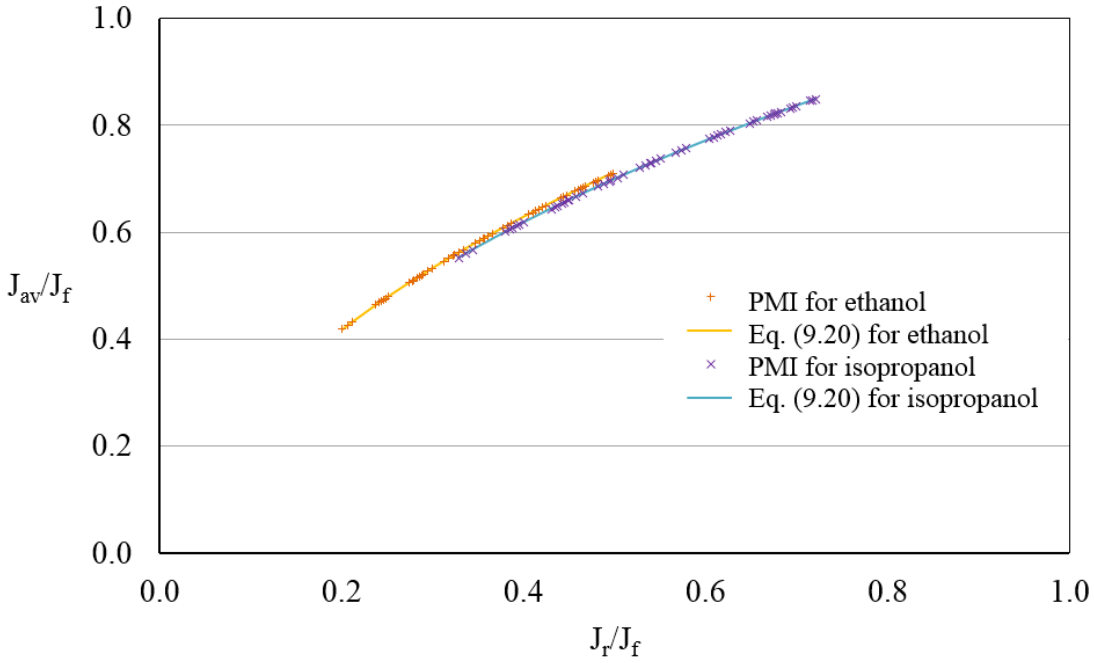

Fig. 9.19 J_{av}/J_f versus J_r/J_f for IPA and ethanol dehydrations for *PMI* conditions. The curves show the corresponding short cut equations.

Table 9.5 *PMI* equation: best fit values for minimisation of maximum error.

Parameter	Water-ethanol	Water-IPA
a	0.020	0.066
b	0.033	-0.083
c	-0.873	1.038
Max. error	0.2%	0.2%

For concentration-independent flux Eq. (9.23) can be used as outlined in chapter 3.

$$\frac{J_{av}}{J_f} = \left(\frac{J_r}{J_f} \right)^{0.52} \tag{9.23}$$

Table 9.6 Algorithm for calculation of *PMI* using short-cut method

- Note the azeotropic composition, the permeate composition, the activation energy and the feed temperature (generally the maximum temperature that the membrane can withstand).
- Calculate x_i and z_i.
- Calculate the $\dot{m}_p/\dot{m}_f$ ratio using Eq. (9.21).
- Calculate the flux at the feed temperature and composition.
- Calculate the retentate temperature.
- Calculate the flux at the retentate temperature and composition.
- Calculate the J_{av}/J_f ratio using Eq. (9.22) or Eq. (9.23) as appropriate.
- Calculate the *PMI* using Eq. (9.19)

Despite the approximations involved in calculating the retentate temperature and the J_{av}/J_f ratio, this method gives *PMI* values that are accurate to within 0.2%.

Flux

A high E_j value leads to a lower average flux and hence a lower *PMI*. A comparison calculated using data for typical industrial conditions is shown in Table 9.7. The magnitude of the *PMI* values relative to one another are independent of the feed flux.

The results relate to an IPA dehydration with flux proportional to concentration and y_i = 0.95, T_f = 120 °C, J_f = 4.0 kg/h.m^2.

Table 9.7. *PMI* and flux as a function of activation energy – IPA dehydration.

E_j (kJ/kmol)	20,000	40,000	60,000
J_{av}/J_f	0.815	0.718	0.629
PMI kg/h.m^2	2.74	2.41	2.11

Ethanol has an azeotrope at 4 wt% water, and so concentration has a greater effect on the average flux than for IPA whose azeotrope is at 12 wt%. A comparison calculated using data for typical industrial conditions is shown in Table 9.8: E_j = 40,000 kJ/kmol, y_i = 0.95, T_f = 120 °C, J_f = 4.0 kg/h.m^2. There is a minor difference in the pervaporation separation modulus, *M*, for the solvents due to the difference in azeotropic composition.

Table 9.8 Comparison of *PMI* values for IPA and ethanol dehydrations.

	IPA	Ethanol
J_{av}/J_f	0.718	0.578
x_{azeo}	0.12	0.04
M	0.839	0.852
PMI kg/h.m^2	2.41	1.97

As water permeates through a membrane, the concentration in the liquid phase reduces. This typically leads to a reduction in flux. Hence, the average flux is affected by the reduction in the water concentration. There are systems where flux is independent of concentration across a range of solute concentrations. In such cases $J_{av} = J_f$. Results for a separation with operating parameters typical of those found in industrial applications are shown in Table 9.9. There is a significant difference in the average flux and in the *PMI* values. The *PMI* is proportional to the average flux and therefore incorporates the flux-concentration relationship and the effect of activation energy, unlike the *PSI* which is based on the flux at a particular combination of temperature and concentration.

Table 9.9 Flux-concentration relationship and *PMI*; dehydration of IPA with $y_i = 0.95$, $E_j = 40{,}000$ kJ/kmol, $J_f = 4$ kg/h.m^2.

	Flux proportional to conc.	Flux independent of conc.
J_{av}/J_f	0.718	1.000
PMI kg/h.m^2	2.41	3.36

Permeate purity has a broadly linear relationship with *PMI*. Permeate purity affects the pervaporation separation modulus and indirectly affects the average flux and hence the membrane area as well as the heat required per unit mass of retentate. Membrane area is the main capital cost for pervaporation systems. The $\dot{m}_p/\dot{m}_r$ ratio and the permeate purity are proportional to the amount of waste produced and the level of solvent in the permeate waste stream respectively. Energy is the main operating cost for pervaporation systems. Examples of the relationship between *PMI* and these parameters for typical industrial conditions with permeate purity ranging from 90% to 100% are shown in Figs. 9.20, 9.21 and 9.22. Each has an approximately linear relationship with *PMI*.

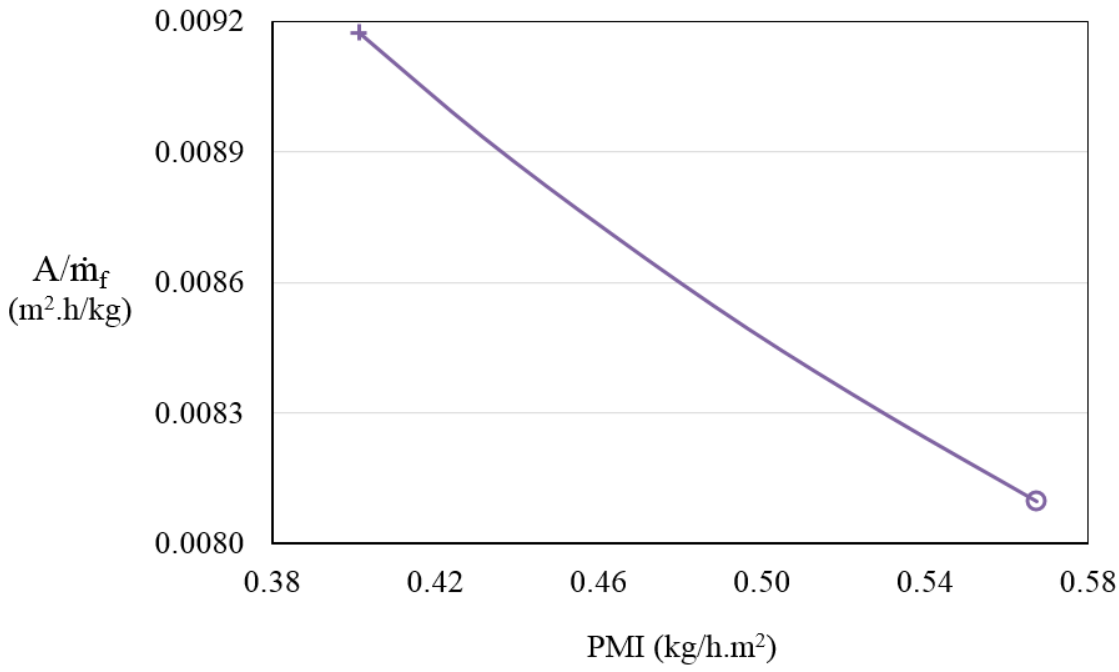

Figure 9.20 Area per unit mass of feed versus *PMI*. Ethanol dehydration with Pervap 2210, E_j = 36,620 kJ/kmol, T_f = 100 °C, J_o = 4.65x10^8 kg/m^2/h, z_i = 5%, x_{ir} = 3%. O denotes pure permeate and + denotes y_i = 0.90. Constants calculated from data in Huang *et al.* (2006).

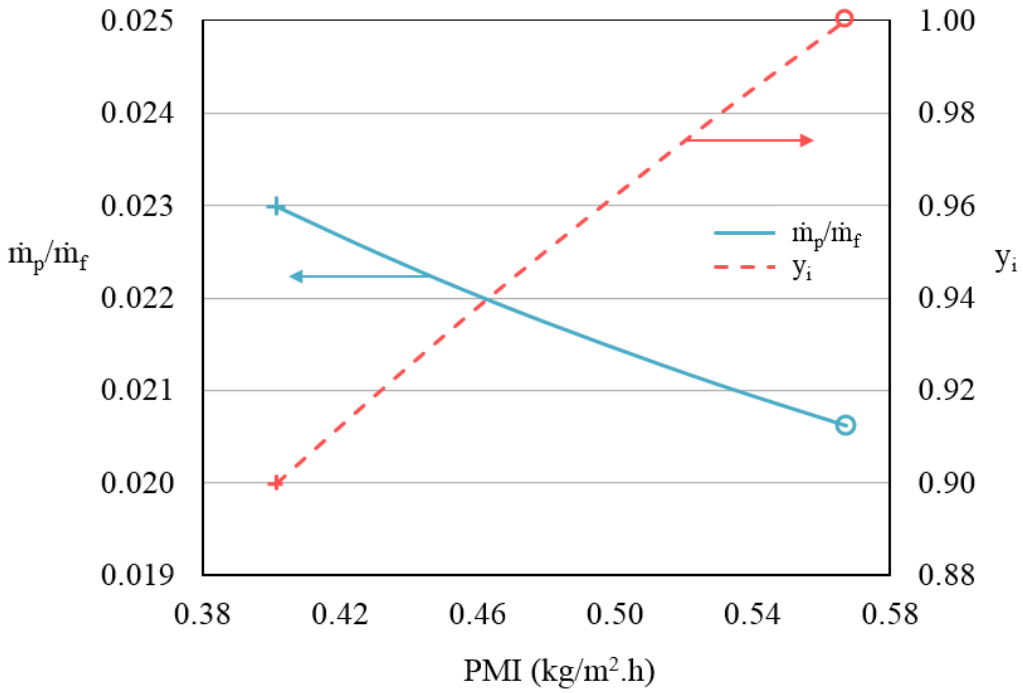

Fig. 9.21 Permeate-feed ratio and corresponding permeate concentration versus *PMI*. Ethanol dehydration with Pervap 2210, E_j = 36,620 kmol/kg, T_f = 100 °C, J_o = 12x10^6 kg/h.m^2. Dashed line is y_i versus *PMI*. O denotes pure permeate. Constants calculated from data in Huang *et al*. (2006).

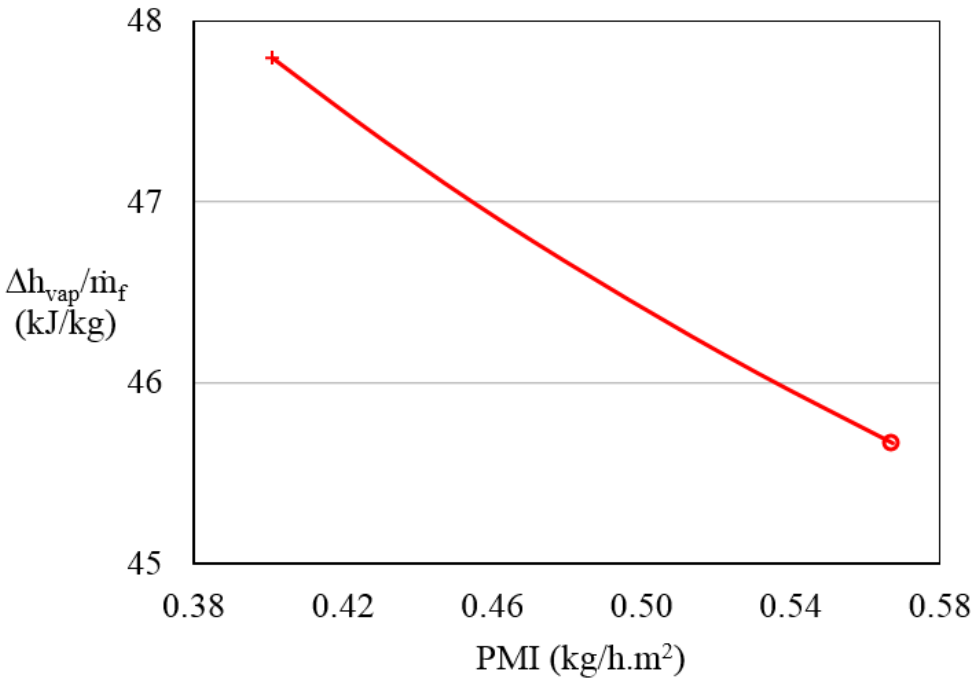

Fig. 9.22 Latent heat per unit mass of feed versus *PMI*. Ethanol dehydration with Pervap 2210, E_j = 36,620 kmol/kg, T_f = 100 °C, J_o = 12x10^6 kg/h.m^2. O denotes pure permeate and + denotes y_i = 0.9. Constants calculated from data in Huang *et al*. (2006).

9.8 Commercial membranes

Data for a number of commercial membranes are shown in Table 9.10 along with their *PMI* and *PSI* values and are illustrated in Fig. 9.23. The data in Table 9.10 are dependent on the temperatures at which the experimental data was obtained. Thus the actual performance of the membranes at industrial conditions temperatures may be significantly different. However, many membranes can fail at the high temperatures typical used in industrial applications (Baker, 2012 p. 392).

The Pervap 2201 has a similar permeate concentration at the azeotropic composition as the Pervap 1210. However, the β_{ij} of the Pervap 2201 is 4.5 times larger as permeate purity plateaus at lower liquid concentration. This causes the *PSI* to be 2.27 times larger despite the flux being only 16% higher. The 16% higher *PMI* for the Pervap 2201 better reflects the relative performance of these two membranes.

The Pervap 2510 has an average flux that is 4.4 times that of the Pervap 1210 yet it has a much lower *PSI* value. This is because the permeate purity of the Pervap 2510 is 97.7% rather than the 99.7% of the Pervap 1210. A 2% difference in permeate purity should not outweigh a four-fold increase in flux. The *PMI* gives this 2% increase in permeate purity the same weighting as a 7% increase in flux. The *PMI* for the Pervap 2510 is 4.15 times that of the Pervap 1210. This better reflects the relative economic value of the membranes.

The HybSi membrane has a 2% higher permeate purity than the Pervap 2510 membrane. This causes its β_{ij} of the HybSi to be 8 times greater. The average flux for the HybSi is 42% higher than that of the Pervap 2510. The *PSI* of the HybSi is 10 times that of the Pervap 2510 whereas the *PMI* is 52% higher: this latter figure better reflects the relative performance of the two membranes. Fig. 9.23 shows the *PMI* and *PSI* for the dehydration of IPA for a variety of commercial membranes.

The difference in E_j values causes the HybSi to have a 20% higher J_{av}/J_f ratio than the Pervap 1210. This is reflected in the *PMI* values of the respective membranes, whereas the *PSI* does not take eat effect of *Ej* values into account.

Table 9.10 *PMI* and *PSI* values for dehydration of IPA using commercial membranes.

	T_f °C	y_i	M	β_{ij}	E_j kJ/kmol	J_{av}/J_f	J_f kg/h.m^2	J_{av} kg/h.m^2	*PMI* kg/h.m^2	*PSI* kg/h.m^2
Pervap 2210 Cséfalvay *et al*., 2008	90	0.980	0.977	278	50,591	0.613	1.889	1.157	1.080	692
Pervap 2201 Qiao *et al*., 2005	90	0.997	0.997	6,828	62,800	0.559	1.319	0.738	0.731	5,988
Pervap 1210 Koch and Górak, 2014	78	0.997	0.996	1,514	64,373	0.515	1.240	0.639	0.631	2,643
Pervap 2510 Qiao *et al*., 2005	100	0.977	0.974	294	45,400	0.660	4.296	2.834	2.620	1,151
HybSi, Klinov *et al*., 2017	80	0.997	0.996	2,379	45,807	0.619	6.499	4.025	3.980	11,499

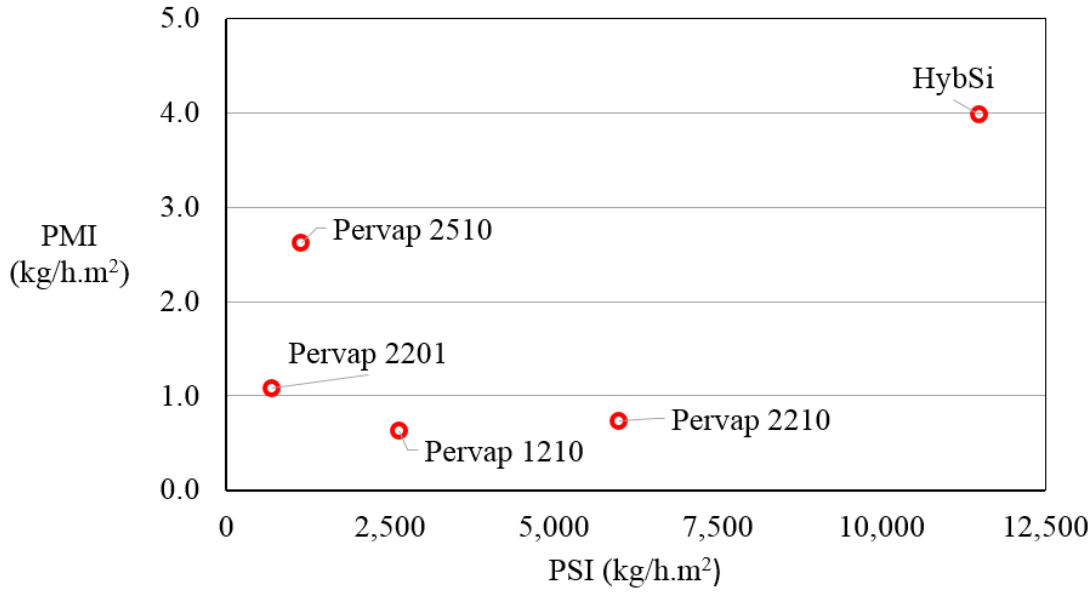

Figure 9.23 *PMI* versus *PSI* for IPA dehydrations with commercial membranes.

Some membrane manufacturers are focused on increasing selectivity, particularly at low water concentrations (Delatmem, 2017). This will lead to increased values of the *PSI* that do not reflect the actual increase in membrane performance. Achieving a permeate purity of 99% at a liquid concentration of 2% rather than 1% doubles the selection factor, albeit leading to only minor increases in the *PSI* value.

It should be noted that the flux, permeate purity and activation energy of membranes are functions of the separation being undertaken. For example the E_j for the dehydration of IPA using a Pervap 2201 membrane is 62,800 (Qiao *et al*, 2005) whereas for the dehydration of 2,2,3,3-tetrafluoropropan-1-ol the same membrane has an E_j of 81,300 kJ/kmol (Kujawski *et al*., 2017). Thus performance is dependent on the separation being undertaken as well as the type of membrane.

Temperature subscript

There are many industrial pervaporation systems where temperature is limited due to factors other than the characteristics of the membrane. These include the steam pressure available and the pressure rating of the equipment. Commercial pervaporation systems typically operate with feed temperatures of 120 ºC to 130 ºC (Baker, 2012, p. 402). Pilot trials at temperatures of up to 150 ºC using HybSi type membranes have been reported (Van Veen, 2016). The performance characteristics at temperatures above the maximum

operating temperature of the available equipment are not relevant when selecting a membrane for a particular system. Such information may lead to poor decisions. It is proposed that a subscript be used to denote the temperature to which the *PMI* figure relates. *PMI* values without a subscript refer to the highest value experimental obtained.

The *PMI* values shown in Table 9.10 are dependent on the temperatures at which the data was obtained. Corresponding results at 78 °C, PMI_{78} and 120 °C, PMI_{120}, are shown in Table 9.11. These were calculated assuming that E_j and y_i values are independent of temperature. Normally, the temperature subscript will be used for temperatures lower than the maximum for which experimental data was obtained. In this case, due to the limited availability of high temperature data, the results have been extrapolated assuming typical Arrhenius-type dependence of flux on temperature so as to illustrate the potential impact of temperature on performance. In Table 9.10 the *PMI* for the Pervap 1210 is low due to the low temperature at which data was obtained. Calculations predict a PMI_{150} of 25.1 kg/h.m^2 will be obtained from the pilot trials at 150 °C of the HybSi membrane. Such a high *PMI* value would not reflect its performance for systems whose maximum operating temperature was 120 °C. Use of a temperature subscript provides a simple means of ascertaining the relevance of data for a given application.

Table 9.11 *PMI* values at different temperatures, IPA dehydration

	E_j kJ/kmol	**T_f °C**	***PMI*** **kg/h.m^2**	***PMI*$_{78}$** **kg/h.m^2**	***PMI*$_{120}$** **kg/h.m^2**
Pervap 2210 Cséfalvay *et al*. (2014)	50,591	90	1.080	0.582	4.262
Pervap 2201 Qiao *et al*. (2005)	62,800	90	0.731	0.336	4.012
Pervap 1210 Koch & Górak, (2014)	64,373	78	0.631	0.631	7.962
Pervap 2510 Qiao *et al*. (2005)	45,400	100	2.620	0.976	5.816
HybSi, Klinov *et al*. (2017)	45,807	80	3.980	3.616	15.576

9.9 Conclusions

Current flux and separation metrics have been shown to be inadequate. The most common single combined metric, the *PSI*, does not accurately reflect the relative value of membranes as regards their performance in industrial applications. Several authors have recommend alternatives in recent years.

A novel metric, the 'Pervaporation separation modulus' relating to the separation characteristics of pervaporation membranes has been developed. A second novel metric the 'Pervaporation membrane index', *PMI*, is proposed. It gives appropriate weighting to both the flux and separation characteristics of membranes. The *PMI* incorporates the concept of a single metric for flux and separation as suggested by Huang and Yeom (1990). It has a value of zero when no separation occurs: this is similar to the approach taken by Huang and Feng (1993) when modifying the *PSI*. The *PMI* incorporates a comparison between the separation achieved using a membrane with that achieved by flash distillation: this corresponds to the β_{mem} concept outlined by Baker (1991) and the *MFLI* as suggested by Toth *et al*. (2018). Unlike the *PSI*, the *PMI* does not have an asymptotic relationship with permeate purity. An average flux is used: this is consistent with the recommendations regarding the *PSI* made by Sosa and Espinosa (2011). It thereby incorporates the effect of the E_j of the membrane and allows for the greater average flux of those rare membranes where flux is independent of concentration. The *PMI* gives appropriate weighting to the different aspects of a membrane's performance: average flux, membrane area, E_j, flux-concentration relationship, permeate-retentate ratio, separation characteristics and energy consumption.

Use of standard feed and retentate compositions ensures that *PMI* values are consistent, thereby facilitating comparisons between membranes. Standard feed and retentate compositions also ensure that data is at industrially relevant concentrations. Calculation of the *PMI* is straightforward.

Its adoption should encourage the development of membranes with an optimum balance of flux and separation characteristics at industrially relevant conditions. It should encourage researchers to develop membranes that can function at the high temperatures used in industry.

The *PMI* will be of use to engineers when selecting pervaporation membranes during process feasibility studies or when designing industrial-scale pervaporation systems.

Further research is required to ascertain whether the proposed index value of $n = 3$ for the *PMI* is an appropriate reflection of the relative economic value of flux and separation.

Chapter 10. Conclusions and suggestions for further work

10.1 Conclusions

This research examined the application of pervaporation for the removal of low concentrations of water from organic solvents. It focussed on chemical engineering analyses for the prediction of the performance of pervaporation modules. The need for short-cut methods for the calculation of the membrane area for ideal pervaporation systems using readily available data has been identified and addressed. Whilst further work in relation to module efficiency is required, substantial progress has been made in the development of short-cut methods for the calculation of membrane area.

In chapter 3, an exact analytical expression is derived for the average flux in ideal isothermal pervaporation modules where flux is proportional to concentration. Constant permeate concentration across a range of liquid concentrations is assumed. This assumption has been validated by analysis of data in peer-reviewed publications relating to commercial membranes. The analytical expression was modified so as to predict the progress of batch isothermal pervaporation operations. This provides an easier and more accurate method for determining flux from bench-scale isothermal trials than was available heretofore.

In chapter 4, an exact analytical expression is derived for the average flux in an ideal adiabatic, single-pass pervaporation module assuming a concentration-independent flux with an Arrhenius-type dependence on temperature. An envelope of industrial operating conditions is established: this is used to derive a simple approximation that is applicable for the dehydration of a variety of solvents. This derivation assumed constant physical properties: integration using the trapezoidal rule confirmed the validity of this approach.

In chapter 5, short-cut empirical expressions were developed for the calculation of the average flux for ethanol and isopropanol dehydrations for ideal adiabatic systems where flux is proportional to concentration. These are valid throughout the envelope of industrial operations.

In chapter 6, equations are developed for feed flowrate and composition as functions of recycle ratio. The impact of recycle on average flux and retentate composition for ideal systems is explored, including the use of recycle to increase throughput without changing retentate concentration. The potential of recycle for applications where concentration has a limited effect on flux is examined.

In chapter 7, metrics relating to heat losses, energy efficiency, heat recovery and isothermal efficiency are developed for pervaporation modules. The limited published data relating to the performance of industrial-scale pervaporation systems is analysed.

Short-cut methods for the calculation of the membrane area for ideal pervaporation systems were developed in chapters 2 through 5. These provide an essential foundation in the development of design methods for industrial-scale pervaporation systems. Module efficiency needs to be considered when designing pervaporation systems. In chapter 6 module efficiency values for an industrial-scale system are calculated from published data.

In chapter 8, optimisation of ideal multi-stage dehydration systems is reviewed. Minimum overall area is achieved by having successively larger areas for later stages. A novel short-cut method for minimising the area of ideal systems is presented. It was found that use of equal areas for each stage did not lead to substantial increases in overall area. The effect of module efficiency on multi-stage systems is explored.

In chapter 9, current membrane metrics relating to pervaporation membranes are reviewed and analysed. A number of authors have found current metrics relating to separation to be inadequate. A novel metric the 'Pervaporation separation modulus' is proposed.

The *PSI* encompasses both flux and separation: it is analysed and found not to accurately reflect the relative performance of different membranes. An alternative metric, the Pervaporation Membrane Index, *PMI*, is proposed. It provides appropriate weighting to flux and separation. Results for the *PSI* and *PMI* are compared for commercial membranes using published data. The development of the *PMI* should encourage

researchers to focus on the development of membranes that are suitable for industrial operations.

The ideal models and novel metrics developed in this work provide a major step towards the development of simple design methods for pervaporation systems. Assumptions in this work are justified by reference to peer-reviewed publications relating to commercial membranes and industrial-scale pervaporation systems.

This research will be of benefit to engineers working in industry, particularly those who are new to the field of pervaporation. The short-cut design methods will facilitate consideration of pervaporation in process feasibility analyses and front-end design, albeit that more rigorous design methods are required for the subsequent detailed design of pervaporation systems. The availability of such short-cut methods should increase the adoption of pervaporation in industry. The short-cut methods will also be of use for the analysis of modules and system design parameters by undergraduate students.

10.2 Suggestions for further research

In chapter 5, short cut equations were developed for the sizing of ideal adiabatic modules for the dehydration of ethanol and isopropanol for systems where flux is proportional to concentration. Further work is required to develop similar equations for the dehydration of other solvents.

In chapter 6, recycles were shown to have the potential to increase performance of pervaporation systems where flux is not significantly affected by concentration. There is scope for experimental work in relation to the use of recycles for such systems. The effect on system efficiency due to the increased flowrates, temperatures and fluxes associated with recycles needs to be analysed. The potential to increase throughput of pervaporation modules by use of recycles has been identified: experimental work is required to determine whether this will be of benefit for industrial operations.

Further work is required to determine the typical performance of modern industrial-scale pervaporation systems and hybrid pervaporation-distillation systems in relation to heat

consumption, electricity consumption, heat recovery and module efficiency. The metrics developed in chapter 7 should facilitate such research.

Simple equations have been developed that facilitate the sizing of ideal pervaporation modules. Whilst actual modules and systems are not ideal, this work provides a foundation for the design of industrial-scale pervaporation systems. Sommer *et al.* (2005) modelled the effect of concentration polarisation and temperature polarisation on module efficiency for an isothermal annular duct module. They validated their results by experiment using an isothermal module. Further work is required to determine typical module efficiencies of industrial-scale pervaporation systems, including for the adiabatic modules typical of industrial systems. Short-cut methods for determining module efficiency need to be developed.

The effect of module efficiency on the optimisation of multi-stage pervaporation systems warrants further research. In chapter 8 it was found that use of multiple types of membrane within a single pervaporation system including the use of high flux membranes with poorer separation characteristics for the final stages of pervaporation systems is an area where further research is likely to prove worthwhile. Suitable high-flux membranes capable of operating at industrial conditions need to be developed.

Results for the *PSI* and *PMI* were compared for commercial membranes using published data. Similar comparisons are required for other commercial membranes and for other membranes which show potential for industrial applications. Further research is required to ascertain whether the proposed index value of $n = 3$ for the *PMI* is an appropriate reflection of the relative economic value of flux and separation.

Research into the production of biofuels such as isobutanol from the stalks of corn (Somerville *et al.*, 2010; Minty *et al.*, 2013) could see a major increase in applications of hydrophobic and hydrophilic pervaporation (Qureshi and Ezeji, 2008; Huang *et al.*, 2010). There is scope for both experimental research and modelling of pervaporation systems for the purification of isobutanol. There is considerable ongoing research aimed at developing membranes that are suitable for the separation of Acetone-Butanol-Ethanol fermentation broths. There is considerable scope for the modelling of

pervaporation systems for the separation of the acetone, butanol and ethanol from such broths. The development of membranes that preferentially permeate individual solvents could simplify subsequent purification steps.

References

Abramowitz, M., Stegun, I.A. (eds.), (1972) *Handbook of Mathematical Functions*, New York: Dover Publications.

Adoor, S. G., Manjeshwar, L.S., Naidu, B.V.K., Sairam, M., Aminabhavi, T.M. (2006) 'Poly(vinyl alcohol)/poly(methyl methacrylate) blend membranes for pervaporation separation of water + isopropanol and water + 1,4-dioxane mixtures', *J. Membr. Sci.,* 280, pp. 594–602.

Agirre, I., Arias, P.L., Castricum, H.L., Creatore, M., ten Elshof J.E., Paradis, G.G, Ngamou, P.H.T., van Veen, H.M., Vente, J.F. (2014) 'Hybrid organosilica membranes and processes: Status and outlook', *Sep. Purif. Technol.* 121, pp. 2–12.

Babalou, A.A., Rafia, N., Ghasemzadeh, K. (2015) 'Integrated systems- involving pervaporation and applications', in Basile, A., Figoli, A., Khayet, M., (eds.) *Pervaporation, Vapour Permeation and Membrane Distillation*, Cambridge, UK: Woodhead Pub., pp. 65-86.

Baig, F.U. (2008) 'Pervaporation', in *Advanced Membrane Technology and Applications*, in Li, N.N., Fane, A.G., Ho, W.S.W., and Matsuura, T. (eds.) Hoboken, NJ: John Wiley & Sons, pp. 469-488.

Baker, R.W. (1991) 'Pervaporation', *Membrane Separation Systems: Recent Developments and Future Directions*, in Baker R.W., Cussler, E.L., Eykamp, W., Koros, W.J., Riley, R.L., Strathmann, H. (eds.) Park Ridge: Noyes Data Corporation, pp. 151-188.

Baker, R.W. (2012) *Membrane Technology and Applications.* 3rd edn. Chichester, UK: Wiley.

Baker, R.W., Wijmans, J.G., Athayde, A.L., Daniels, R., Ly, J.H., Le, M., (1997) 'The effect of concentration polarization on the separation of volatile organic compounds from water by pervaporation', *J. Membr. Sci.,* 137, pp. 159-172.

Baker, R.W., Wijmans, J.G., Huang, Y. (2010) 'Permeability, permeance and selectivity: a preferred way of reporting pervaporation performance data', *J. Membr. Sci.,* 348 (1-2), pp. 346-352.

Bausa, J., Marquardt, W. (2000) 'Shortcut design for hybrid membrane/distillation processes for the separation of non-ideal multicomponent mixtures', *Ind. Eng. Chem. Res*. 39, pp. 1658–1672.

Ben Hamouda, S., Boubakri, A., Nguyen, Q.T. Ben Amor, M. (2011) 'PEBAX membranes for water desalination by pervaporation process', *High Perform. Polym*. 23, pp. 170–173.

Binning, R.C., Jennings, J.F., Martin, E.C. (1962) *Process for removing water from organic chemicals*, US Patent 3035060, Available at: https://www.uspto.gov/patent (Accessed: 26 May 2017)

Binning, R. C., Lee, R. J., Jenning, J. F., Martin, E. C. (1961) 'Separation of liquid mixture by permeation', *Industrial and Engineering Chemistry*, 53, pp. 45– 50.

Boutikos, P., Pereira, C.S.M., Silva, V.M.T.M., Rodrigues, A.E. (2014) 'Performance evaluation of silica membrane for water–n-butanol binary mixture', *Sep. Purif. Technol.* 127, pp. 18–28.

Brányik, T., Silva, D.P. Baszczyński, M., Lehnert, R., Almeida e Silva J.B., (2012) 'A review of methods of low alcohol and alcohol-free beer production', *J. Food Eng*., 108, pp. 493-506.

Brüschke, H.E.A. (2001) in Nunes, S.P., Peinemann, K.-V. (eds.) *Membrane Technology in the Chemical Industry*, Weinheim: Wiley-VCH, pp. 127-172.

Brüschke, H.E.A., Wynn, N., Marggraff, F.K. (2010) *Membrane pipe module*, US patent 7655141. Available at: https://www.uspto.gov/patent (Accessed: 26 May 2017)

Cai, W.H., Pacheco-Vega, A., Sen, M., Yang, K.T., (2006) 'Heat transfer correlations by symbolic regression', *Int. J. Heat and Mass Transfer,* 49, pp. 4352-4359.

Casado, C., Urtiaga, A., Gorri D., Ortiz I. (2005) 'Pervaporative dehydration of organic mixtures using a commercial silica membrane Determination of kinetic parameters', *Sep. Purif. Technol*. 42, pp. 39–45.

Castricum, H.L., Sah, A., Kreiter, R., Blank, D.H.A., Vente, J.F., ten Elshof, J.E. (2008) 'Hybrid ceramic nanosieves: stabilizing nanopores with organic links', *Chem. Commun*. pp. 1103–1105.

Chapman, P.D., Oliveira, T., Livingston, A.G., Li, K. (2008) 'Membranes for the dehydration of solvents by pervaporation', *J. Membr. Sci.,* 318, pp. 5-37.

Chen, S-H., Yu, K-C. Lin, S-S., Chang, D-J., Liou, R.M. (2001) 'Pervaporation separation of water/ethanol mixture by sulfonated polysulfone membranes', *J. Membr. Sci.,* 183, pp. 29-36

Cheryan, M. (1998) *Ultrafiltration and Microfiltration Handbook*, Boca Raton: CRC Press.

Cho, C.H., Oh, K.Y., Kim, S.K., Yeo, J.G., Sharma, P. (2011) 'Pervaporative seawater desalination using NaA zeolite membrane: Mechanisms of high water flux and high salt rejection', *J. Membr. Sci.,* 371, pp. 226–238.

Choudhury, S., Ray, S.K. (2017) 'Filled copolymer membranes for pervaporative dehydration of ethanol-water mixture', *Sep. Purif. Technol*. 179, pp. 335–348.

Crespo, J.G., Brazinha, C. (2015) 'Fundamentals of pervaporation', in Basile, A., Figoli, A., Khayet, M., (eds.) *Pervaporation, Vapour Permeation and Membrane Distillation*, Cambridge, UK: Woodhead Pub., pp. 3-17.

Crowder, R.O., Cussler, E.L., (1998) Mass transfer resistances in hollow fiber pervaporation', *J. Membr. Sci*., 145, pp. 173-184.

Crowder, M.L., Gooding, C.H., (1997) 'Spiral wound, hollow fiber membrane modules: A new approach to higher mass transfer efficiency', *J. Membr. Sci*., 137, pp. 17-29.

Cséfalvay, E., Szitkai, P., Fonyó, P. (2008) 'Experimental data based modelling and simulation of isopropanol dehydration by pervaporation', *Desalination*, 229, pp. 94–108.

DeltaMem AG (2017) *DeltaMem AG*, Available at: http://www.deltamem.ch/ (Accessed: 25 May 2017)

Douglas, J.M., Eagleton, L.C. (1962) 'Analytical Solutions for some adiabatic reactor problems', *Ind. Eng. Chem.*, 1,(2) pp. 116-199.

Dubreuil, M.F.S., Vandezande, P., Van Hecke, W.H.S., Porto-Carrero, W.J., Dotremont, C.T.E. (2013) 'Study on ageing/fouling phenomena and the effect of upstream nanofiltration on in-situ product recovery of n-butanol through poly[1-(trimethylsilyl)-1-propyne] pervaporation membranes', *J. Membr. Sci.,* 447. pp. 134–143.

ECN (no date) Products and Services, Available at: https://www.hybsi.com/products-services/ (Accessed: 12 Aug 2019)

Fahmy, A., Mewes, D., Ohlrogge, K. (2002) 'On the integration of jet ejectors into hybrid dehydration processes', *J. Membr. Sci*, 196, pp. 79–84.

Favre, E., (2003) 'Temperature polarization in pervaporation', *Desalination*, 154, pp. 129-138.

Feng, X., Huang, R.Y.M. (1997) 'Liquid Separation by Membrane Pervaporation: A Review', *Ind. Eng. Chem. Res.* 36, pp. 1048-1066.

Figoli, A., Santoro, S., Galiano, F., Basile, A. (2015) 'Pervaporation membranes: preparation, characterization and application', in Basile, A., Figoli, A., Khayet, M., (eds.) *Pervaporation, Vapour Permeation and Membrane Distillation*, Cambridge, UK: Woodhead Pub., pp. 19-64.

Fleming, H.L., Slater, C.S. (1992) 'Pervaporation', in *Membrane Handbook*, Ho, W.S.W., Sirkar, K.K., (Eds.) Dordrecht, Netherlands: Kluwer Academic Publishers

Foley, G. (2011) 'Three classic ultrafiltration problems solved with the exponential integral', *Education for Chemical Engineers*, 6, e90–e96.

Foley, G. (2013) *Membrane Filtration: A Problem Solving Approach with MATLAB,* Cambridge, UK: Cambridge University Press.

Fontalvo, J., Gijsbert, M.A., Keurentjus, J.T.F., Wijers, J.G. (2010) *Pervaporation process and apparatus for carrying out same*, US patent application publication, US2010/0213125 A1, Available at: https://www.uspto.gov/patent (Accessed: 26 May 2017)

Fontalvo, J., Vorstman, M.A.G., Wijers, J.G., Keurentjes, J.T.F. (2006a) 'Heat supply and reduction of polarization effects in pervaporation by two-phase feed'**,** *J. Membr. Sci.* 279, pp. 156–164.

Fontalvo, J., Vorstman, M.A.G., Wijers, J.G., Keurentjes, J.T.F. (2006b) 'Organic–Water Mixtures by Co-Current Vapor–Liquid Pervaporation with Transverse Hollow-Fiber Membranes'**,** *J. Ind. Eng. Chem. Res.*. 45, pp. 2002-2007.

Gallego-Lizon, T., Edwards, E., Lobiundo, G., Freitas dos Santos, L. (2002) 'Dehydration of water/t-butanol mixtures by pervaporation: comparative study of commercially available polymeric, microporous silica and zeolite membranes', *J. Memb. Sci.,* 197, pp. 309–319.

Gao, L., Alberto, M., Gorgojo, P., Szekely, G., Budd, P.M. (2017) 'High-flux PIM-1/PVDF thin film composite membranes for 1-butanol/water pervaporation', *J. Membr. Sci.,* 529, pp. 207-214.

George, S.C., Thomas, S. (2001) 'Transport phenomena through polymeric systems', *Progress in Polymer Science*, 26, pp. 985-1017.

GFT Membrane Systems GmBH (no date) *History of Pervaporation*, Available at: https://gft-gmbh.com/solutions/the-history-of-pervaporation/ (Accessed: 22 Feb 2017).

Gladman, D., (2017), '*Solvent Recovery using Pervaporation and Vapour Permeation'*, [lecture], Engineers Ireland, Cork Institute of Technology, 26th Sept.

Gladman, D. (2018) Conversation with David Gladman, DeltaMem A.G., 19 June.

Green, E.M. (2011) 'Fermentative production of butanol—the industrial perspective', *Curr. Opin. Biotechnol.*, 22, pp. 1–7.

Greenlaw, F.W., Prince, W.D., Sheldon, R.A., Thompson, E.V. (1977) 'Dependence of diffuse permeation rates on upstream and downstream pressure II Two component permeant', *J. Membr. Sci.,* 2, pp. 333-348.

Hu, C., Guo, R., Li, B., Ma, X., Wu, H., Jiang, Z. (2007) 'Development of novel mordenite-filled chitosan–poly(acrylic acid) polyelectrolyte complex membranes for pervaporation dehydration of ethylene glycol aqueous solution, *J. Membr. Sci.,* 293, pp. 142–150.

Hua, D., Ong, Y.K., Wang, Y., Yang, T., Chung, T-S. (2014) 'ZIF-90/P84 mixed matrix membranes for pervaporation dehydration of isopropanol', *J. Membr. Sci.,* 453, pp. 155–167.

Huang, H-J., Ramaswamy, S., Tschirner, U.W., Ramarao, B.V. (2008) 'A review of separation technologies in current and future biorefineries', *Sep. Purif. Technol*. 62, pp. 1–21.

Huang, R.Y.M., Feng, X., (1993) 'Dehydration of isopropanol by pervaporation using aromatic polyetherimide membranes', *Sep. Sci. Technol.*, 28, (11-12), pp. 2035-2048.

Huang, R.Y.M., Xu, Y.F. (1988) 'Pervaporation separation of ethanol-water mixtures using grafted poly(acrylic acid)-nylon 6 membranes', *Eur. Poly. J.,* 24, 10, pp. 927-931

Huang, R.Y.M. Yeom, C.K. (1990) 'Pervaporation separation of aqueous mixtures using crosslinked poly (vinyl alcohol) (PVA). Part II. Permeation of ethanol–water mixtures', *J. Membr. Sci.*, 51, pp. 273–277

Huang, Y., Baker, R.W., Vane, L.M. (2010) 'Low-energy distillation-membrane separation processes', *Industrial Engineering and Chemistry Research*, 49, pp. 3760-3768

Huang, Z., Guan, H., Tan, W., Qiao, X-Y., Kulprathipanja, S. (2006) 'Pervaporation study of aqueous ethanol solution through zeolite-incorporated multilayer poly(vinyl alcohol) membranes: Effect of zeolites', *J. Membr. Sci.,* 276, pp. 260–271.

Jiang, L.Y., Chung, T-S., Rajagopalan, R. (2008) 'Dehydration of alcohols by pervaporation through polyimide Matrimid asymmetric hollow fibers with various modifications', *Chem. Eng. Sci.,* 63, pp. 204 – 216

Jiraratananon, R., Chanachai, A., Huang, R.Y.M. (2002) 'Pervaporation Dehydration of Ethanol-Water Mixtures with Chitosan / hydroxyethylcellulose (CS/HEC) Composite Membranes: II Analysis of Mass Transport', *J. Membr. Sci.,* 199, pp. 211-222.

Jyoti, G., Keshav, A., Anandkumar, J. (2015) 'Review on Pervaporation: Theory, Membrane Performance and Application to Intensification of Esterification Reaction', *J. of Eng.*, Article 927068, Available at: https://www.hindawi.com/journals/je/ (Accessed: 22 Feb 2017).

Kahlenberg, L. (1906) 'On the nature of the pressure of osmosis and the osmotic pressure with observations concerning dialysis', *J. of Physical Chemistry*, 10, pp. 141-209.

Kaminski, W. Marszalek, J., Ciolkowska, A. (2008) 'Renewable energy source—Dehydrated ethanol', *Chem. Eng. J.,* 135, pp. 95–102.

Kaminski, W., Marszalek, J., Tomczak, E. (2018) 'Water desalination by pervaporation – Comparison of energy consumption', *Desalination*, 433, pp. 89-93.

Kanse, N.G., Dawande, S.D. Dhanke, P.B., (2018), 'Effect of Feed Temperature and Solution Concentration on Pervaporation for separation of Azeotropic Mixtures', *Mater Today,* 5(2018), pp. 3541–3550.

Karimi, K., Tabatabaei, M., Horváth. I.S., Kumar, R. (2015) 'Recent trends in acetone, butanol, and ethanol (ABE) production', *Biofuel Res. J.,* 8, pp. 301-308.

Karlsson, H.O.E., Tragardh, G. (1996) 'Heat transfer in pervaporation' *J. Membr. Sci*., 119, pp. 295–306.

Keane, D., Morris M., (2010) 'Preparation of Polymer-based membranes for dehydration of ethanol by Pervaporation' STRIVE Report Series No. 50, Environmental Protection Agency, Wexford, Ireland

Klinov, A.V., Akberov, R.R., Fazlyeva, A.R., Farakhova, M.I. (2017) 'Experimental investigation and modeling through using the solution-diffusion concept of pervaporation dehydration of ethanol and isopropanol by ceramic membranes HybSi', *J. Membr. Sci*., 524, pp. 321–333.

Kober P.A. (1917) 'Pervaporation Perstillation and Percrystallisation', *J. Am. Chem. Soc.*, 39, pp. 944-978.

Koch, K., Górak, A. (2014) 'Pervaporation of binary and ternary mixtures of acetone, isopropyl alcohol and water using polymeric membranes: experimental characterisation and modelling', *Chem. Eng. Sci*. 15, pp. 95-114.

Koch, K., Sudhoff, D., Kreiß, S. Górak, A., Kreis, P. (2013) 'Optimisation-based design method for membrane-assisted separation processes', *Chem. Eng. Process. Process Intensif.* 67, pp. 2–15.

Koczka, K., Mizsey, P., Fonyo, Z. (2007) 'Rigorous modelling and optimization of hybrid separation processes based on pervaporation', *Cent. Eur. J. Chem.*, 5(4) pp. 1124–1147.

Kong, Y., Lin, L., Yang, J., Shi, D., Qu, H., Xie, K., Li, L. (2007) 'FCC gasoline desulfurization by pervaporation: Effects of gasoline components', *J. Membr. Sci.,* 293, pp. 36-43.

Koops, G.H., Nolten, J.A.M., Mulder, M.H.V., Smolders, C.A. (1994) 'Selectivity as a function of membrane thickness: Gas separation and pervaporation', *J. Appl. Polym. Sci.,* 53 (12), pp. 1639–1651.

Kopeć, R., Meller, M., Kujawski, W., Kujawa, J. (2013) 'Polyamide-6 based pervaporation membranes for organic–organic separation', *Sep. Pur. Technol*., 110, pp. 63–73.

Kreiter, R., Wolfs, D.P., Engelen, C.W.R. van Veen, H.M., Vente, J.F. (2008) 'High-temperature pervaporation performance of ceramic-supported polyimide membranes in the dehydration of alcohols', *J. Membr. Sci.,* 319, pp. 126–132.

Kujawa, J., Cerneaux, S., Kujawski, W. (2015) 'Highly hydrophobic ceramic membranes applied to the removal of volatile organic compounds in pervaporation', *Chem. Eng. J.*, 260, pp. 43–54.

Kujawski, W. (2000) 'Application of Pervaporation and Vapor Permeation in Environmental Protection', *Polish Journal of Environmental Studies,* 9(1), pp. 13-26.

Kujawski, W., Krajewski, S.R. (2004) 'Sweeping gas pervaporation with hollow-fiber ion-exchange membranes', *Desalination*, 162, pp. 129-135

Kujawski, J.K., Kujawski, W.M., Sondej, H., Jarzynka, K., Kujawska, A., Bryjak, M., Rynkowska, E., Knozowsk, K., Kujawa, J. (2017) 'Dewatering of 2,2,3,3-tetrafluoropropan-1-ol by hydrophilic pervaporation with poly(vinyl alcohol) based Pervap membranes', *Sep. Purif. Technol*., 174, pp. 520–528.

Leon J.A., Fontalvo, J., (2018) 'Tools for the Design of Hybrid Distillation-Pervaporation Columns in a Single Unit: Hybrid Rectifying - Pervaporation section' *Ind. Eng. Chem. Res.,* Just Accepted Manuscript • DOI: 10.1021/acs.iecr.8b02078 • Publication Date (Web): 16 Aug 2018

Levenspiel, O. (1999) *Chemical Reaction Engineering*, 3rd, John Wiley & Sons, New York, ISBN 047125424X

Li, J., Chen, X., Qi, B., Luo, J., Zhang, Y., Su, Y., Wan, Y. (2014) 'Efficient production of acetone–butanol–ethanol (ABE) from cassava by a fermentation–pervaporation coupled process', *Bioresour. Technol.*, 169, pp. 251–257.

Lin, L., Zhang, Y., Kong, Y. (2009) 'Recent advances in sulphur removal from gasoline by pervaporation', *Fuel,* 88, pp. 1799-1809

Linnhoff, March, (1998) *Introduction to Pinch Technology*, Available at: http://www.ou.edu/class/che-design/a-design/Introduction%20to%20Pinch%20Technology-LinhoffMarch.pdf (Accessed 19 April 2017).

Lipnizki F., Field, R.W. (1999) 'Simulation and process design of pervaporation plate-and-frame modules to recover organic compounds from waste water' *Trans. Inst. Chem. Eng.,* 77A, pp. 231-240.

Lipnizki, F., Field, R.W. (2001) 'Integration of vacuum and sweep gas PV to recover organic compounds from wastewater', *Sep. Purif. Technol*., 22-23**,** pp. 347–360.

Liu, D., Liu, G., Meng, L., Dong, Z., Huang, K., Jin, W. (2015) 'Hollow fiber modules with ceramic-supported PDMS composite membranes for pervaporation recovery of bio-butanol', *Sep. Purif. Technol.,* 146, pp. 24–32.

Liu, R., Qiao, X., Chung, T-S., (2005) 'The development of high performance P84 co-polyimide hollow fibers for pervaporation dehydration of isopropanol' *Chem. Eng. Sci.*, 60(23) pp. 6674-6686.

Liu, Y-L., Yu, C-H., Lee, K-R, Li, C-L., Lai, J-Y. (2007) 'Chitosan/poly (tetrafluoroethylene) composite membranes using in pervaporation dehydration processes', *J. Membr. Sci.,* 287, pp. 230-236

Logan, E., (2015) 'Three big fish and a shrimp', *The Chemical Engineer* (March), pp. 32-35.

Luis, P., Degrève, J., Van der Bruggen, B.V. (2013) 'Separation of methanol–n-butyl acetate mixtures by pervaporation: potential of 10 commercial membranes', *J. Membr. Sci.*, 429, pp. 1–12.

Luis, P., Van der Bruggen, B. (2015) 'Pervaporation modelling: state of the art and future trends, in Pervaporation', in Basile, A., Figoli, A., Khayet, M., (eds.) *Pervaporation, Vapour Permeation and Membrane Distillation*, Cambridge, UK: Woodhead Pub, pp. 87-105.

Lynch, A. (2019) Conversation with Annette Lynch, Pfizer, 16 May.

Magalhaes Mendes, A.M., Palma Madeira, L.M., Dias Catarino, M. (2008) Process for enriching the aroma profile of a dealcoholized beverage. European Patent Application EP20080709985, Available at: https://www.google.com/patents/EP2109372A2?cl=en (Accessed: 26 May 2017)

Majer, V., Svoboda, V. (1985) *Enthalpies of Vaporization of Organics Compounds*, *IUPAC Chemical Data Series No. 32*, Oxford: Blackwell Scientific Publications.

Margallo, M., Aldaco, R., Barceló, A., Diban, N., Ortiz, I., Irabien, A. (2015) 'Life cycle assessment of technologies for partial dealcoholisation of wines', *Sustainable Production and Consumption*, 2, pp. 29-39.

Marriott, J., Sørensen, E. (2003a) 'A general approach to modelling membrane modules', *Chem. Eng. Sci.,* 58, pp. 4975–4990.

Marriott, J., Sørensen, E. (2003b) 'The optimal design of membrane systems', *Chem. Eng. Sci.,* 58, pp. 4991–5004.

Marszałek, J., Kamiński, W.L. (2012) 'Efficiency of acetone-butanol-ethanol-water system separation by pervaporation', *Chem. and Proc. Eng.*, 33(1), pp. 131-140.

Massey, B., Ward-Smith, J., *Mechanics of Fluids* (1998) 7th edn. Cheltenham, UK: Stanley Thornes.

McCabe, W.L., Thiele, E.W. (1925) 'Graphical Design of Fractionating Columns', *Ind. Eng. Chem.*, 17, pp. 605–611.

Minty, J.J., Singer, M.E., Scholz, S.A., Bae, C.H., Ahn, J.H., Foster, C.E. Liao, J.C., Lin, X.N. (2013) 'Design and characterization of synthetic fungal-bacterial consortia for direct production of isobutanol from cellulosic biomass', *Proc. Natl. Acad. Sci. USA*, 110 (36), pp. 14592–14597.

Morigami, Y., Kondo, M., Abe, J., Kita, H., Okamoto, K. (2001) 'The first large-scale pervaporation plant using tubular-type module with zeolite NaA membrane', *Sep. Purif. Technol.,* 25, pp. 251–260.

Mortaheb, H.R., Ghaemmaghami, F., Mokhtarani, B. (2012) 'A review on removal of sulfur components from gasoline by pervaporation', *Chem. Eng. Res. Des.,* 90, pp. 409–432.

Murphree, E.V. (1925) 'Rectifying Column Calculations', *Ind. Eng. Chem.* 17(7), pp. 747–750.

Nagy, E., Mizsey, P, Hancsók, J., Boldyryev, S., Varbanov, P. (2015) 'Analysis of energy saving by combination of distillation and pervaporation for biofuel production' *Chem. Eng. and Process,* 98, pp. 86–94.

Narkkun, T., Jenwiriyakul, W., Amnuaypanich, S. (2017) 'Dehydration performance of double-network poly(vinyl alcohol) nanocomposite membranes (PVAs-DN) ', *J. Membr. Sci.,* 528, pp. 84-295.

Navajas, A., Mallada, R., Téllez, C., Coronas, J., Ménendez, M., Santamarıa, J. (2002) 'Preparation of mordenite membranes for pervaporation of water-ethanol mixtures', *Desalination,* 148, pp. 25-29.

Navajas, A., Mallada, R., Téllez, C., Coronas, J., Ménendez, M., Santamarıa, J. (2006) 'The use of post-synthetic treatments to improve the pervaporation performance of mordenite membranes', *J. Membr. Sci.,* 270, pp. 32–41.

Ni Y, Sun Z. (2009) 'Recent progress on industrial fermentative production of acetone–butanol–ethanol by Clostridium acetobutylicum in China', *Appl. Microbiol. Biotechnol.*; 83, pp. 415–423.

Niemistö, J., Pasanen, A., Hirvelä, K., Myllykoski, L., Muurinen, E., Riitta, L., Keiski, R. (2013) 'Pilot study of bioethanol dehydration with polyvinyl alcohol membranes', *J. Membr. Sci.,* 447, pp. 119–127.

O'Brien, D.J., Roth, L.H., McAloon, A.J., (2000) 'Ethanol production by continuous fermentation–pervaporation: a preliminary economic analysis' *J. Membr. Sci.,* 166, pp. 105-111.

Okada, T., Matsuura, T. (1991) 'A New Transport Model for Pervaporation', *J. Membr. Sci.,* 59, pp. 130-150.

Outram, V., Lalander, C-A., Lee, J.G.M., Davies, E.T., Harvey, A.P. (2017) 'Applied in Situ Product Recovery in ABE Fermentation', *Biotechnol. Prog.*, Vol. 00, No. 00 [Online]. Available at: http://onlinelibrary.wiley.com/doi/10.1002/btpr.2446/full (Accessed: 25 May 2017)

Paz, A., Blanco, C.A., Andrés-Iglesias C., Palacio, L., Prádanos, P., Hernández, A., (2017) 'Aroma recovery of beer flavors by pervaporation through polydimethylsiloxane membranes', *J. Food Process Eng.*; 00:e12556. [Online]. Available at: https://doi.org/10.1111/jfpe.12556 (Accessed: 25 May 2017)

Pera-Titus, M., Llorens, J., Tejero, J., Cunill, F. (2006) 'Description of the pervaporation dehydration performance of A-type zeolite membranes: A modeling approach based on the Maxwell–Stefan theory', *Catalysis Today*, 118, pp. 73–84.

Pervatech (2014) *Introduction to Pervaporation and Vapour permeation,* Available at: http://pervaporation-membranes.com/home/introduction-to-pervaporation-and-vapor-permeation/ (Accessed: 7 March 2017)

Pervatech (no date), *Modules*, Available at: http://pervaporation-membranes.com/products/modules/ (Accessed: 21 Feb 2017)

Pervatech (2018) '*Datasheet: Hybrid Silica HybSi® AR Membranes*' Available at http://pervaporation-membranes.com/wp-content/uploads/2014/04/Datasheet-Hybrid-Silica-HybSi-AR-membranes-Version-15-1-2018.pdf

Pfizer (2014) '*P&ID for Solvent recovery pervaporation plant',* Revision 34, Pfizer Ireland Pharmaceuticals Ltd., Ringaskiddy.

Pfizer (2018), site visit, Pfizer, Ringaskiddy, Ireland, 27 March.

Pratt, K.C., Wakeham, W.A. (1974) 'The mutual diffusion coefficient of binary mixtures of water and the isomers of propanol', *Proceedings of the Royal Society of London. Series A, Mathematical and Physical Sciences* 342 (1630) pp. 401-419

Qiao, X., Chunga, T-S., Guoa, W.F., Matsuura, F.T., Teoh, M.M. (2005) 'Dehydration of isopropanol and its comparison with dehydration of butanol isomers from thermodynamic and molecular aspects', *J. Membr. Sci.,* 252, pp. 37–49.

Qureshi, N, Ezeji, T.C. (2008) 'Butanol, "a superior biofuel" production from agricultural residues (renewable biomass): recent progress in technology', *Biofuels, Bioprod. Bioref.*, 2, pp. 319–330

Qureshi, N., Meagher, M.M., Huang, J., Hutkins, R.W. (2001) 'Acetone butanol ethanol (ABE) recovery by pervaporation using silicalite–silicone composite membrane from fed-batch reactor of Clostridium acetobutylicum', *J. Membr. Sci.,* 187, pp. 93–102.

Ramaiah, P., Satyasri, S., Sridhar, S., Krishnaiah, A. (2013) 'Removal of hazardous chlorinated VOCs from aqueous solutions using novel ZSM-5 loaded PDMS/PVDF composite membrane consisting of three hydrophobic layers', *Journal of Hazardous Materials*, 261, pp. 362-371.

Raoufi, N., Asadallahzadeh, M., Shirazian, S., (2018) 'Investigation into Ethanol Purification Using Polymeric Membranes and a Pervaporation Process', *Chem. Eng. Technol.*, 41(2), pp. 278–284.

Ravanchi, M.T., Kaghazchi, T, Kargari, A. (2009) 'Application of membrane separation processes in petrochemical industry: a review', *Desalination,* 235, pp. 199–244.

Rautenbach, R., Helmus, F.P. (1994) 'Some considerations on mass-transfer resistances in solution-diffusion-type membrane processes', *J. Membr, Sci.*, 87, pp. 171-181.

Ren21 (2012) '*Renewables 2011: Global Status Report'*, Paris: REN21 Renewable Energy Policy Network for the 21st Century

Ren21 (2017) '*Renewables 2017: Global Status Report'*, Paris: REN21 Renewable Energy Policy Network for the 21st Century

Rozicka, A., Niemistö, J., Keiski, R.L., Kujawski, W., (2014) 'Apparent and intrinsic properties of commercial PDMS based membranes in pervaporative removal of acetone, butanol and ethanol from binary aqueous mixtures', *J. Membr, Sci.*, 453, pp. 108-118.

Samei, M., Mohammadi, T., Asadi, A.A. (2013) 'Tubular composite PVA ceramic supported membrane for bio-ethanol production', *Chem. Eng. Res. De*s., 91, pp. 2703–2712.

Sander U., Soukup, P. (1988) 'Design and Operation of a Pervaporation Plant for ethanol dehydration', *J. Membr. Sci.,* 36, pp. 463-475.

Santos, A., Ma, W., Judd, S.J. (2011) 'Membrane bioreactors: Two decades of research and implementation', *Desalination*, 273, pp. 148–154.

Santoso, A., Cheng-Ching, Y., Ward, J.D. (2012) 'Analysis of local recycle for membrane pervaporation systems', *Ind. Eng. Chem. Res*., 51, pp. 9790-9802.

Sanz, M.T., Gmehling, J. (2006) 'Study of the Dehydration of Isopropanol by a Pervaporation - Based Hybrid Process', *Chem. Eng. Technol.* 29, pp. 473-480.

Sato, K. Sugimoto, K, Nakane, T. (2008) 'Synthesis of industrial scale NaY zeolite membranes and ethanol permeating performance in pervaporation and vapour permeation up to 130 °C and 570 kPa', *J. Membr. Sci.,* 310, pp. 161–173.

Sato, K. Sugimoto, K, Shimotsuma, N., Kikuchi, T., Kyotani, T., Kurata, T. (2012) 'Development of practically available up-scaled high-silica CHA-type zeolite membranes for industrial purpose in dehydration of N-methyl pyrrolidone solution', *J. Membr. Sci.,* 409-410, pp. 82-95.

Schäfer, T., Crespo, J.G. (2007) 'Study and optimization of the hydrodynamic upstream conditions during recovery of a complex aroma profile by pervaporation', *J. Membr. Sci*., 301, pp. 46–56.

Scharzec, B., Waltermann, T., Skiborowski, M. (2017) 'A Systematic Approach towards Synthesis and Design of Pervaporation-Assisted Separation Processes', *Chem. Ing. Tech.*, 89(11) pp. 1534–1549.

Schleger, M., Sommer, S., Melin, T. (2004) 'Module arrangement for solvent dehydration with silica membranes', *Desalination*, 163, pp. 281-286.

Schmitz, N., Breitkreuza, C.F., Ströfera, E., Burgerb, J., Hassea, H. (2018) 'Separation of water from mixtures containing formaldehyde, water, methanol, methylal, and poly(oxymethylene) dimethyl ethers by pervaporation', *J. Membr. Sci.,* 5641, pp. 806-812.

Seider, W.D., Lewin, D.R., Seader, J.D., Widagdo, S., Gani, R., Ng, K.M. (2017) *Product and Process Design Principles; Synthesis, Analysis and Evaluation.* 4th edn. Hoboken, New Jersey: Wiley.

Shanahan, D. (2010) '*Enhanced Pervaporation using a Novel Pump Configuration'*, Unpublished Master's Thesis, Cork Institute of Technology, Ireland

Shao, J., Zhan. Z., Li, J., Wang, Z., Li, K., Yan, Y. (2014) 'Zeolite NaA membranes supported on alumina hollow fibers: Effect of support resistances on pervaporation performance', *J. Membr. Sci.,* 451, pp. 10-17.

Shao, P., Huang, R.Y.M. (2007) 'Polymeric Membrane Pervaporation', *J. Membr. Sci.*, 287*,* pp. 162-179.

Sinnott, R.K. (1997) *Coulson and Richardson's Chemical Engineering, Volume 5: Chemical Engineering Design*, 2nd edn. Oxford, UK: Butterworth Heinemann.

Smith, J.M., Van Ness, H.C., Abbot, M.M. (2001), *Introduction to Chemical Engineering Thermodynamics*, 6th edn. New York, McGraw-Hill.

Smitha, B., Suhanya, D., Sridhar, S., Ramakrishna, M. (2004) 'Separation of organic-organic mixtures by pervaporation – a review', *J. Membr. Sci.,* 241, pp. 1-21.

Sommer, S., Klinkhammer, B., Melin, T. (2002) 'Integrated system design for dewatering of solvents with microporous silica membranes', *Desalination*, 149, pp. 15-21.

Sommer, S., Klinkhammer, B., Schleger, M., Melin, T. (2005) 'Performance Efficiency of Tubular Inorganic Membrane Modules for Pervaporation', *AIChE J.*, 51(1), pp. 162-177.

Sommer, S., Melin, T. (2004) 'Design and Optimization of Hybrid Separation Processes for the Dehydration of 2-Propanol and Other Organics', *Ind. Eng. Chem. Res.***,** 43, pp. 5248-5259.

Sommer, S., Melin, T. (2005) 'Influence of operation parameters on the separation of mixtures by pervaporation and vapor permeation with inorganic membranes. Part 1: Dehydration of solvents', *Chem. Eng. Sci.*, 60, pp. 4509 – 4523.

Somerville, C., Youngs, H., Taylor, C., Davis, S.C., Long, S.P. (2010) 'Feedstocks for Lignocellulosic Biofuels', *Science*, 329, pp. 790-792.

Sosa, M.A., Espinosa, J. (2011) 'Feasibility analysis of isopropanol recovery by hybrid distillation/pervaporation process with the aid of conceptual models', *Sep. Purif. Technol.*, 78, pp. 237–244.

Sukitpaneenit. P., Chung, T-S. (2014) 'Fabrication and use of hollow fiber thin film composite membranes for ethanol dehydration, *J. Mem. Sci*., 450, pp. 124–137.

Sulzer (undated) *Process description of pervaporation plant in Pfizer, Ireland Pervaporation Plant*, received 2016

Sulzer Chemtech (2006) *Membrane Technology,* Allschwil, Switzerland: Sulzer Chemtech, Ltd.

Takács, L., Vatai, G., Korány, K. (2007) 'Production of alcohol free wine by pervaporation', *J. Food Eng.,* 78, pp. 118–125.

Tang, Y., Widjojo, N., Shi, G.M., Chung, T-S, Weber, M., Maletzko, C. (2012) 'Development of flat-sheet membranes for C1–C4 alcohols dehydration via pervaporation from sulfonated polyphenylsulfone (sPPSU)', *J. Membr. Sci.,* 415-416, pp. 686-695

Thiess, H., Schmidt, A, Strube, J., (2018), Development of a Scale-up Tool for Pervaporation Processes, *Membranes*, 8 (1) 4 doi:10.3390/membranes8010004

Toth, A.J., Haaz, E., Mizsey, P., (2017) 'Novel method for evaluation of pervaporation membrane efficiency: membrane flash index (MFLI)', *Program Booklet of 5th International Conference on Pervaporation, Vapor Permeation and Membrane Distillation*, 20 -23 June, Torun, Poland, pp.72-73.

Toth, A.J., Haaz, E., Valentinyi, N., Nagy, T., Tarjani, A.J., Fozer, D., Andre, A., Mohamed, S.A.K., Solti, S., Mizsey, P., (2018) 'Selection between Separation Alternatives: Membrane Flash Index (MFLI)', *Ind. Eng. Chem. Res*. 57, pp. 11366−11373

Tsai, H.A., Hong, M.J., Huang, G.S., Wang, Y.C., Li, C.L., Lee, K.R., Lai, J.Y. (2002) 'Effect of DGDE additive on the morphology and pervaporation performances of asymmetric PSf hollow fiber membranes', *J. Membr. Sci.,* 208, pp. 233-245

Tsuyumoto, M., Teramoto, A., Meares, P. (1997) 'Dehydration of ethanol on a pilot-plant scale, using a new type of hollow-fiber membrane', *J. Membr. Sci.*, 133(1), pp. 83−94.

Urtiaga, A., Gorri, E.D., Casado C., Ortiz, I. (2003) 'Pervaporative dehydration of industrial solvents using a zeolite NaA commercial membrane', *Sep Purif. Technol.,* 32, pp. 207-213.

US EPA (2013) '*Fact Sheet: CHP as a Boiler Replacement Opportunity*', Washington D.C: U.S. Environmental Protection Agency.

Valentinyi, N., Mizsey, P. (2014) 'Comparison of pervaporation models with simulation of hybrid separation processes', *Periodica Polytechnica Chem. Eng.*, 58(1), pp. 7-14.

Van der Bruggen, B., Luis, P. (2014) 'Pervaporation as a tool in chemical engineering: a new era?' *Curr. Opin. Chem. Eng.,* 4, pp. 47-53.

Van der Gulik, G-J. S., Wijers, J.G., Keurentjes, J. T. F. (2002) 'Measurement of 2D temperature distributions in a PV membrane module using ultrasonic computer tomography and comparison with computational fluid dynamics calculations', *J. Membr. Sci.,* 204, pp. 111-124.

Van Hoof, V., Van den Abeele, L., Dotremont, C., Buekenhoudt, A., Leysen, R. (2004) 'Economic comparison between azeotropic distillation and different hybrid systems combining distillation with pervaporation for the dehydration of isopropanol', *Sep. Purif. Technol*., 37, pp. 33–49.

Van Hoof, V., Dotremont, C., Buekenhoudt, A. (2006) 'Performance of Mitsui NaA type zeolite membranes for the dehydration of organic solvents in comparison with commercial polymeric pervaporation membranes', *Sep. Purif. Technol*., 48, pp. 304–309.

Van Veen, H. (2016) *Lab and pilot scale pervaporation process for the purification of dimethyl carbonate*, [lecture], Advanced Membranes VII, Cork, Ireland, 12-16 Sept.

Van Veen, H.M., Van Delft, Y.C., Engelen, C.W.R., Pex, P.P.A.C. (2001) 'Dewatering of organics by pervaporation with silica Membranes', *Sep. Purif. Technol.*, 22-23, pp. 361-366.

Van Veen, H. M., Pex, P. P. A. C. (2006) 'Silica based membranes for water or methanol separation from organics' in *Proceedings of the International Workshop on membranes in solvent filtration*, Campus Library, Arenberg, Leuven, Belgium 23-34 March, pp. 24–30.

Van Veen, H.M., Rietkerk, M.D. Shanahan, D.P. van Tuel, M.M.A. Kreiter, R., Castricum, H.L ten Elshof, J.E. Vente, J.F. (2011) 'Pushing membrane stability boundaries with HybSi® pervaporation membranes', *J. Membr. Sci.*, 380, pp. 124–131.

Vane, L.M., Alvarez, F.R. (2005) 'Vibrating PV modules: Effect of module design on performance', *J. Membr. Sci.,* 255, pp. 213-224.

Vane, L.M., Alvarez, F.R., Giroux, E.L. (1999) 'Reduction of concentration polarization in PV using vibrating membrane module', *J. Membr. Sci.,* 153, pp. 233-241.

Vatani, M., Raisi, A., Pazuki, G. (2018) 'Pervaporation separation of ethyl acetate from aqueous solutions using ZSM-5 filled dual-layer poly(ether-block-amide)/polyethersulfone membrane', RSC Adv., 8, pp. 4713–4725.

Vente, J. (2010) *The HybSi® membrane: from research to industrial demonstration*, Presented at the NMG-Matchmaking Event, Arnhem, 22 Nov.

Verhoef, A., Degreve, J., Huybrechs, B., Van Veen, H., Pex, P. Van der Bruggen, B., (2008) 'Simulation of a hybrid pervaporation–distillation process', *Comput. Chem. Eng*. 32, pp. 1135–1146.

Verkerk, A.W., Van Male, P., Vorstman, M.A.G., Keurentjes, J.T.F. (2001) 'Description of dehydration performance of amorphous silica pervaporation membranes', *J. Membr. Sci.,* 193, pp. 227–238.

Villaluenga, J.P.G., Cohen, Y. (2005) 'Numerical model of non-isothermal pervaporation in a rectangular channel', *J. Membr. Sci.,* 260, pp. 119–130.

Villaluenga, J.P.G., Khayet, M., Godino, P., Seoane, B., Mengual J.I. (2005), 'Analysis of the membrane thickness effect on the pervaporation separation of methanol/methyl tertiary butyl ether mixtures', *Sep. Purif. Technol.,* 47, pp. 80–87.

Wang, N., Wu, T., Wang, L., Li, X., Zhao, C., Li, J., Ji, S. (2017a) 'Hyper-branched polymer composite membrane using water as solvent for separating aromatic/aliphatic hydrocarbon mixtures', *Sep. Purif. Technol*., 179, pp. 225–235

Wang, Q, Li, N., Bolto, B., Hoang, M., Xie, Z. (2016b) 'Desalination by pervaporation: A review', *Desalination* 387, pp. 46–60.

Wang, S., Wang, D.K., Smart, S., Diniz da Costa, J.C. (2017b) 'Improved stability of ethyl silicate interlayer-free membranes by the rapid thermal processing (RTP) for desalination', *Desalination*, 402, pp. 25-32.

Wang, X., Chen, J., Fang, M., Wang, T., Yu, L., Li, J. (2016a) 'ZIF-7/PDMS mixed matrix membranes for pervaporation recovery of butanol from aqueous solution', *Sep. Purif. Technol*., 163, pp. 39–47.

Wang, Y-C., Fan, S-C., Lee, K-R., Li, C-L., Huang, S-H., Tsai, H-A., Lai, J-Y. (2004) 'Polyamide/SDS-clay hybrid nanocomposite membrane application to water-ethanol mixture pervaporation separations', *J. Membr. Sci.,* 239, 219-226

Wijmans, J.G., Baker, R.W. (1995) 'The Solution – Diffusion Model: A Review', *J. Membr. Sci.,* 107, pp. 1-21.

Witte S, Günther R, Hapke J., (2000) 'Untersuchung der Eignung von Pervaporationsmodulen für Hochfluss-Membranen mittels Strömungssimulationen' *Chem-Ing-Tech*. (6) 72, pp. 613-618.

Wolf, T.E. (2011) '*Capital cost estimates – understanding analysing and evaluating'*, Charleston, South Carolina, CreateSpace**.**

Wu, H., Chen, X.P., Liu, G.P., Jiang M, Guo, T., Jin, W.Q., Wei, P., Zhu, D.W. (2012) 'Acetone–butanol–ethanol (ABE) fermentation using Clostridium acetobutylicum XY16 and in situ recovery by PDMS/ceramic composite membrane', *Bioprocess Biosystems Eng.,* 35, pp. 1057–1065.

Wu, X. M., Guo, H., Soyekwo, F., Zhang, Q.G., Lin, C.X., Liu, Q.L., Zhu, A.M. (2016) 'Pervaporation Purification of Ethylene Glycol Using the Highly Permeable PIM-1 Membrane', *J. Chem. Eng. Data*, 61, pp. 579−586.

Wynn, N. (2000) 'Pervaporation Comes of Age', *Sulzer Technical Review 3/2000*. Neunkirchen, Germany: Sulzer Chemtech.

Xing, R., Pan, F., Zhao, J., Cao, K., Gao, C., Yang, S., Liu, G., Wu, H., Jiang, Z. (2016) 'Enhancing the permeation selectivity of sodium alginate membrane by incorporating attapulgite nanorods for ethanol dehydration', *RSC Adv.,* 6, pp. 14381-14392.

Xu, Y.M., Chung, T-S. (2017) 'High-performance UiO-66/polyimide mixed matrix membranes for ethanol, isopropanol and n-butanol dehydration via pervaporation', *J. Membr. Sci.* 531, pp. 16–26.

Xu, Z-K, Dai, Q-W., Liu, Z-M., Kou, R-Q., Xu, Y-Y. (2003) 'Microporous polypropylene hollow fiber membranes Part II. Pervaporation separation of water/ethanol mixtures by the poly (acrylic acid) grafted membranes', *J. Membr. Sci.,* 214, pp. 71-81

Xue, C., Zhao, J.B., Chen, L.J., Bai, F.W., Yang, S.T., Sun, J.X. (2014) 'Integrated butanol recovery for an advanced biofuel: current state and prospects', *Appl. Microbiol. Biotechnol*. 98, pp. 3463–3474.

Yaws, C.L. (1999) *Chemical Properties Handbook*, New York: McGraw-Hill.

Yave, Y. (2019) 'Separation Performance of Improved PERVAP$_{TM}$ Membrane and its Dependence on Operating Conditions', *J. Membr. Sci.,* DOI: 10.22079/JMSR.2018 88186.1198

Yin, H. Lau, C.Y., Rozowski, M., Howard, C., Xu, Y., Lai, T., Dose, M.E., Lively, R.P., Lind, M.L. (2017) 'Free-standing ZIF-71/PDMS nanocomposite membranes for the recovery of ethanol and 1-butanol from water through pervaporation', *J. Membr. Sci.,* 529, pp. 286–292.

Zhou, F., Koros, W.J., (2006) 'Pervaporation Using Hollow-Fiber Membranes for Dehydrating Acetic Acid and Water Mixtures', *Ind. Eng. Chem. Res.*, 45, pp. 1787-1796.

Zhu, B., Myat, D.T., Shin. J-W., Na, Y-H., Moon, I-S., Connor, G., Maeda S., Morris, G., Gray, S., Duke, M., (2015) 'Application of robust MFI-type zeolite membrane for desalination of saline wastewater', *J. Membr. Sci.,* 475, pp. 167–174.

Zuo, J., Wang, Y., Peng, S., Chung, T-S. (2012) 'Molecular design of thin film composite (TFC) hollow fiber membranes for isopropanol dehydration via pervaporation', *J. Membr. Sci.,* 405–406, pp. 123– 133.

Appendix A

Integration of isothermal pervaporation equation

Integration of integral for isothermal operations.

$$\int_0^u \frac{1\text{-}u}{1-bu}\,du = \int_0^u \frac{1}{1-bu}\,du + \int_0^u \frac{-u}{1-bu}\,du$$

Simplifying the second term on the right using partial fractions:

$$\frac{1-bu}{1-bu} = \frac{1}{1-bu} + \frac{-bu}{1-bu}$$

$$1 = \frac{1}{1-bu} + \frac{-bu}{1-bu}$$

$$\frac{1}{b} = \left(\frac{1}{b}\right)\frac{1}{1-bu} + \frac{-u}{1-bu}$$

$$\frac{-u}{1-bu} = \frac{1}{b} - \left(\frac{1}{b}\right)\frac{1}{1-bu}$$

The integral can now be separated into simpler parts

$$\int_0^u \frac{1\text{-}u}{1-bu}\,du = \int_0^u \frac{1}{1-bu}\,du + \frac{1}{b}\int_0^u du - \frac{1}{b}\int_0^u \frac{1}{1-bu}\,du$$

$$\int_0^u \frac{1\text{-}u}{1-bu}\,du = \left(1-\frac{1}{b}\right)\int_0^u \frac{1}{1-bu}\,du + \frac{1}{b}\int_0^u du$$

$$\int_0^u \frac{1\text{-}u}{1-bu}\,du = \left(\frac{b-1}{b}\right)\left(\frac{1}{-b}\right)Ln\left(\frac{1-bu}{1-0}\right) + \frac{1}{b}(u-0)$$

$$\int_0^u \frac{1\text{-}u}{1-bu}\,du = -\left(\frac{b-1}{b^2}\right)Ln(1-bu) + \frac{bu}{b^2}$$

$$\int_0^u \frac{1\text{-}u}{1-bu}\,du = \frac{bu-(b-1)\,Ln(1-bu)}{b^2}$$

Appendix B

Derivation of Brüschke's equation

Introduction

The derivation of the Brüschke's equation for the area of an isothermal pervaporation module is provided in this appendix. The passage where the equation is described is shown here. (Brüschke, 2001, p.137).

> *"For small concentration changes between feed and retentate and for a first estimation of the membrane area necessary for a specified separation a simple but useful relation can be derived.*

$$A = M/t \; 1/J_0 \; ln \; (C_{feed} / C_{product}) \qquad (1)$$

here,

A	*denotes the membrane area,*
M	*the amount of feed to be treated during time t,*
J_0	*is the measured flux at a certain concentration divided by that concentration,*
C_{feed}	*the concentration of the critical component in the feed*
$C_{product}$	*the concentration of the critical component in the product*

Equation (21) assumes constant temperature of the process, infinite selectivity of the membrane (only the removed component is passing into the permeate), no loss of matter from feed to product (constant volume of the feed, or small change from feed to product concentration) and a linear relation between the concentration of the better permeable component in the feed and its flux through the membrane. As long as these limitations are kept in mind this relation is quite useful for a first estimation of membrane area for a given separation problem, especially in vapour permeation. For a given installation with fixed area of a membrane the influence of changes in one of the parameters like plant capacity (feed treated per unit of time), feed or product concentration on the on the other parameters of the plant can be estimated."

Brüschke's derivation

Flux is typically described by an expression of the form

$$J = x_i J_0 e^{-E_j/RT} \tag{2}$$

The flux in pervaporation is usually defined as mass flux,

$$J \equiv \frac{\dot{m}_p}{A} \tag{3}$$

where: J = Permeate flux (kg/m^2/h)

$\dot{m}_p$ = mass flowrate of permeate through the membrane (kg/h)

A = membrane area (m^2)

thus,
$$\frac{dA}{d\dot{m}} = \frac{-1}{J} \tag{4}$$

Combining Eqs. (2) and (4),

$$\frac{A}{\dot{m}_f} = \int_0^{\frac{\dot{m}_p}{\dot{m}_f}} \frac{-1}{x_i J_0 e^{-E_j/RT}} d\left(\frac{\dot{m}_p}{\dot{m}_f}\right) \tag{5}$$

As the system is isothermal this can be simplified to,

$$\frac{A}{\dot{m}_f} = \int_0^{\frac{\dot{m}_p}{\dot{m}_f}} \frac{-1}{x_i / z_i \, J_f} d\left(\frac{\dot{m}_p}{\dot{m}_f}\right) \tag{6}$$

Rearranging
$$A = \frac{\dot{m}_f}{J_f / z_i} \int_0^{\frac{\dot{m}_p}{\dot{m}_f}} \frac{-1}{x_i} d\left(\frac{\dot{m}_p}{\dot{m}_f}\right) \tag{7}$$

It should be noted that,
$$x_i = \frac{z_i - y_i \frac{\dot{m}_p}{\dot{m}_f}}{1 - \frac{\dot{m}_p}{\dot{m}_f}} \tag{8}$$

thus,
$$A = \frac{-\dot{m}_f}{J_f / z_i} \int_0^{\frac{m_p}{m_f}} \left(\frac{1 - \frac{\dot{m}_p}{\dot{m}_f}}{z_i - y_i \left(\frac{\dot{m}_p}{\dot{m}_f} \right)} \right) d\left(\frac{\dot{m}_p}{\dot{m}_f} \right) \tag{9}$$

Brüschke assumed that the mass flowrate of the liquid phase was constant throughout the module and that the permeate stream was comprised of pure solute, i.e. $y_i = 1$. In which case Eq. (7) reduces to

$$A = \frac{-\dot{m}_f}{J_f / z_i} \int_{z_i}^{x_i} \left(\frac{1}{z_i} \right) d\left(x_i \right)$$

Integrating,
$$A = \frac{\dot{m}_f}{J_f / z_i} Ln \frac{z_i}{x_i} \tag{10}$$

Rearranging,
$$A = \frac{M}{t} \frac{1}{J_0} Ln \left(\frac{z_i}{x_i} \right) \tag{11}$$

where, M the amount of feed to be treated during time t,

J_0 is the measured flux at a certain concentration divided by that concentration

Appendix C

Summary of equations and metrics derived

Chapter 3: isothermal pervaporation

Flux proportional to concentration:

$$A=\frac{\dot{m}_f}{J_f}\left(\frac{z_i}{y_i}\right)^2\left[\frac{y_i}{z_i}\left(\frac{\dot{m}_p}{\dot{m}_f}\right)-\left(\frac{y_i}{z_i}-1\right)ln\left(1-\frac{y_i}{z_i}\left(\frac{\dot{m}_p}{\dot{m}_f}\right)\right)\right] \tag{3.29}$$

$$t=\frac{m_f}{AJ_f}\left(\frac{z_i}{y_i}\right)^2\left[\frac{y_i}{z_i}\left(\frac{z_i-x_{ir}}{y_i-x_{ir}}\right)-\left(\frac{y_i}{z_i}-1\right)ln\left(1-\frac{y_i}{z_i}\left(\frac{z_i-x_{ir}}{y_i-x_{ir}}\right)\right)\right] \tag{3.54}$$

Flux proportional to the square root of concentration

$$\frac{AJ_f}{\dot{m}_f}=\left\{\frac{(b-1)\left[ln\left(\sqrt{b}\sqrt{1-bu}+b\sqrt{1-u}\right)-ln\left(\sqrt{b}\sqrt{1-bu}-b\sqrt{1-u}\right)\right]}{2b^{1.5}}-\frac{\sqrt{1-u}\sqrt{1-bu}}{b}\right\}$$

$$-\left\{\frac{(b-1)\left[ln\left(\sqrt{b}+b\right)-ln\left(\sqrt{b}-b\right)\right]}{2b^{1.5}}-\frac{1}{b}\right\} \tag{3.38}$$

where $u=\frac{\dot{m}_p}{\dot{m}_f}$ and $b=\frac{y_i}{z_i}$

Short-cut approximation of Eq. (3.38) $$A=\frac{2\dot{m}_p}{\left[J_r+J_f\right]} \tag{3.66}$$

Chapter 4: Adaiabatic pervaporation with flux independent of concentration

$$\frac{J_{av}}{J_f}=\frac{b^2e^a\,p}{be^a\text{-}a\left(b-1\right)e^{a/b}Ei\left(\frac{a\left(b-1\right)}{b}\right)-b\left(1-bp\right)e^{\frac{a(1-p)}{1-bp}}+a\left(b-1\right)e^{a/b}Ei\left(\frac{a\left(b-1\right)}{b\left(1-bp\right)}\right)} \tag{4.27}$$

where, $a=\frac{E_j}{RT_f}$, $b=\frac{h_v}{c_pT_f}$ and $p=\frac{\dot{m}_p}{\dot{m}_f}$

Short-cut approximation of Eq. (4.27) $$\frac{J_{av}}{J_f}=\left(\frac{J_r}{J_f}\right)^{0.52} \tag{4.38}$$

Chapter 5: Adiabatic pervaporation with flux proportional to concentration

$$\frac{J_{av}}{J_f} = \left[a\left(\frac{x_{ri}}{z_i}\right) + b \right] ln\left(\frac{z_i J_r}{x_{ri} J_f}\right) + c\left(\frac{x_{ri}}{z_i}\right)^n + d\left(\frac{x_{ri}}{z_i}\right) + eln\left(\frac{x_{ri}}{z_i}\right) + f \qquad (5.27)$$

Table 5.2 Best fit values for constants for minimisation of maximum error.

Parameter	**Water-ethanol**	**Water-IPA**
a	0.3100	0.2696
b	0.1427	0.1710
c	-0.3000	-0.2620
d	0.9800	1.0260
e	0.0174	-0.0339
f	0.3200	0.2360
n	1.650	1.950
Max. error	2.4%	2.2%

Chapter 6: recycles.

$$\frac{\dot{m}_p}{\dot{m}_f} = \frac{1}{1 + \frac{\left[(1+C)\left(1 - \frac{\dot{m}_p}{\dot{m}_s}\right) \right]}{\dot{m}_p / \dot{m}_s}} \qquad (6.8)$$

$$z_i = \frac{s_i \; + \; C\left(s_i - \frac{\dot{m}_p}{\dot{m}_s} y_i\right)}{1 \; + \; C\left(1 - \frac{\dot{m}_p}{\dot{m}_s}\right)} \qquad (6.14)$$

Chapter 7: module performance metrics

$$\eta_p = \frac{\Sigma \Delta q_{energy}}{\dot{m}_p} \tag{7.5}$$

$$\text{Steam-Permeate Ratio} = \frac{\dot{m}_{steam}}{\dot{m}_p} \tag{7.8}$$

$$\Delta q_{heat\ loss} = \dot{m}_r h_{r\ ideal} - \dot{m}_r h_r \tag{7.9}$$

$$\eta_{heat\ loss} = \frac{\Delta q_{heat\ loss}}{\Delta q_{energy}} \tag{7.10}$$

$$\eta_{isothermal} = \frac{A_{isothermal\ ideal}}{A_{actual\ ideal}} \tag{7.15}$$

$$\eta_{module} = \frac{\text{Real flux with gradients}}{\text{Theoretical flux at bulk conditions}} \tag{7.16}$$

Chapter 9: membrane metrics

$$M = \left(\frac{y_i - x_{azeo}}{1 - x_{azeo}} \right) \tag{9.17}$$

$$PMI = J_{av} \left(\frac{y_i - x_{azeo}}{1 - x_{azeo}} \right)^3 \tag{9.18}$$